A methodology to assess the movement of hydrocarbons in the subsurface and associated remediation thereof

S Roopa

orcid.org/0000-0002-3717-0578

Dissertation submitted in fulfillment of the requirements for the *Masters* degree in *Environmental Sciences with Hydrology and Geohydrology* at the North-West University

Supervisor: Prof I Dennis

Graduation May 2018

22018506

DISCLAIMER

All results, conclusions and recommendations in this dissertation are based on theoretical information and assumptions made, and therefore do not in any way reflect the contamination at the industrial site within the Durban harbour. The site was used as case study to test the numerical models.

ABSTRACT

Petroleum serves as a great source of energy, however, with such principle importance it poses a problem as a global contaminant. Hydrocarbon contamination is a huge threat to groundwater as it contains toxic substances that are insoluble in water and is referred to as the free phase. These toxins are carcinogenic and mutagenic, and have a major impact on human health and ecosystem stability. When spilled, hydrocarbons will move downward through the unsaturated zone under the influence of gravity and capillary forces, trapping small amounts in the pore spaces. Some of the components within the free phase can dissolve and move as an aqueous plume by diffusion and advection within the groundwater. There is a long term effect on ecosystems, as the insoluble free phase mass slowly decays into the aquifer making it more difficult to model and control. The net result is that some hydrocarbon fractions are transported faster than others and a contamination plume of varying intensity may spread over a large area.

The ultimate aim of this study was to develop a methodology to assess the movement and remediation of hydrocarbons in the subsurface with the use of a numerical model, to improve the management of areas contaminated by these compounds. This includes the migration and delineation of the free phase and dissolved plume. Additionally, it was necessary to simulate a number of remediation options to elevate the risk associated with the contaminant. According to the Manual for site assessment at DNAPL contaminated sites in South Africa, MODFLOW and UTCHEM can be used as a facilitator in managing and containing hydrocarbon contamination. The software package UTCHEM was therefore used to model the migration of the non-aqueous and aqueous hydrocarbon phases and surfactant and co-solvent enhanced remediation, while MODFLOW was used to facilitate the migration and extraction of the dissolved plume. The methodology was demonstrated by means of a case study of an industrial site located within the Durban harbour.

After simulating the movement and remediation of tetrachloroethene (PCE) and benzene results reflect the complexity of the problem. UTCHEM could not accurately model the migration as the generation of a working model was far too simple due to software restrictions however it was possible to simulate the change in mobility with a surfactant SDS, polymer xanthan gum, and ethanol that demonstrate trends related to literature. The proposed methodology includes a site investigation, collection of historical data, delineating and characterisation of the NAPL using non-invasive methods, chemical borehole logging, a chemical risk assessment, the modelling of the dissolved contaminated plume using MODFLOW to determine the migration and extraction of the plume, and the remediation of the free and dissolved phase using a simplified UTCHEM model in order to determine the best option for a specific site if necessary.

Key words: Petroleum, contamination, carcinogenic, mutagenic, free phase, numerical model, UTCHEM, MODFLOW, PCE, benzene, remediation.

ACKNOWLEDGEMENTS

I would like to thank the following people for their contribution to this project:

To Prof Ingrid Dennis, thank you for the opportunity, guidance, and academic freedom. It was not always easy but I am grateful that allowed me to grow as a researcher.

To Dr Rainier Dennis, thank you for technical assistance.

To my loving parents, thank you for being there and never leaving my side.

To my sister, Shriya, thank you for understanding me when no one else could.

To Prof Marthie, thank you for your support and giving me time off work whenever I needed it and for always being so considerate.

To Jessica, my friend, no one but you will ever know what we've been through. You were my inspiration even when you did not know it.

To Willie, thank you for the motivation.

To Jan Marten Huizenga and Fifi, thank you so much for checking up on me. Jan Marten, I will never forget what you've taught me.

To Nicolaus van Zweel, thank you for helping with the final editing.

To Toony, I cannot thank you enough for teaching me how to code, I could not have done this without you.

Lastly, the Almighty, this is all possible because of you. Thank you for removing all obstacles from my path. All the hardship given is as much of a gift to me as every achievement. Through you I have learnt that peace is not being in a place without noise, trouble or hard work but to be in the midst of those things and still be calm in your heart.

TABLE OF CONTENTS

DISCLAIMER ..... **I**

ABSTRACT ..... **II**

ACKNOWLEDGEMENTS ..... **IV**

TABLE OF CONTENTS ..... **V**

LIST OF TABLES ..... **X**

LIST OF FIGURES ..... **XI**

CHAPTER 1: INTRODUCTION **1**

1.1 Introduction **1**

1.2 Problem Statement **2**

1.3 Hypothesis **3**

1.4 Aims and objectives **4**

1.5 Layout **5**

CHAPTER 2: LITERATURE REVIEW **6**

2.1 Introduction **6**

2.2 Hydrocarbons **6**

2.2.1 Light non-aqueous phase liquids (LNAPLs) 7

2.2.2 Dense non aqueous phase liquids (DNAPLs) 7

2.2.3 Behaviour of NAPLs 9

2.2.4 Decomposition of hydrocarbons 12

2.2.4.1 Sorption 12
2.2.4.2 Precipitation 12
2.2.4.3 Volatilisation 13
2.2.4.4 Oxidation-Reduction 13
2.2.4.5 Biological Processes 13
2.2.4.6 Degradation Half Life 14
2.2.5 Remediation of Hydrocarbons 15
2.2.5.1 Chemical flushing 16
2.2.5.2 Chemical oxidation 17
2.2.5.3 Natural attenuation 17
2.3 Assessment procedures 18
2.3.1 Numerical modelling of hydrocarbons 26

CHAPTER 3: STUDY AREA 31
3.1 Background 31
3.2 Climate 31
3.3 Topography 32
3.4 Geology 32
3.4.1 Zululand Group 35
3.4.2 Maputaland Group 35
3.5 Geohydrology 38

CHAPTER 4: METHODOLOGY 41
4.1 Introduction 41
4.2 Data 41

4.3 Software and codes 45

4.4 Conceptual model 45

4.4.1 Boundary conditions 45

4.4.2 Topography and layer thickness 45

4.4.3 Aquifer parameters and aquifer type 47

4.4.4 Recharge 48

4.5 Numerical Model 50

4.5.1 Mesh size and layer type 50

4.5.2 Water levels and flow direction 50

4.5.3 Calibration 50

4.6 UTCHEM file 51

4.6.1 General numerical model 52

4.6.2 Simulation scenarios 53

4.6.3 Assumptions and Limitations 54

4.7 MODFLOW and MT3D 57

CHAPTER 5: RESULTS AND DISCUSSION - UTCHEM 58

5.1 Introduction 58

5.2 Simulation of the infiltration and migration of Non-Aqueous Phase Liquids 59

5.3 Simulation of the remediation of Non-Aqueous Phase Liquids 63

5.3.1 Non-aqueous phase liquids benzene and tetrachloroethylene (PCE) 63

5.3.1.1 Remediation with the use of surfactant sodium dodecyl sulphate (SDS) and polymer xanthan gum 63

5.3.1.2 Remediation with the use of surfactant sodium dodecyl sulphate (SDS) 66

5.3.1.3 Remediation with the use of polymer xanthan gum 69

5.3.1.4 Remediation with the use of surfactant sodium dodecyl sulphate (SDS) and ethanol 72

5.3.1.5 Remediation with the use of ethanol 75

5.3.1.6 Comparison of the effectiveness of different remediation fluids 78

5.3.2 Aqueous phase liquids benzene and tetrachloroethylene (PCE) 81

5.3.2.1 Remediation with the use of surfactant sodium dodecyl sulphate (SDS) and polymer xanthan gum 81

5.3.2.2 Remediation with the use of polymer xanthan gum 82

CHAPTER 6: RESULTS AND DISCUSSION - MODFLOW 87

6.1 Introduction 87

6.1.1 The distribution of aqueous benzene 87

6.1.2 The distribution of aqueous benzene after it has been extracted 88

6.1.3 The difference between UTCHEM and MODFLOW 91

CHAPTER 7: DISCUSSION - PROPOSED METHODOLOGY 94

CHAPTER 8: CONCLUSION AND RECOMMENDATIONS 101

REFERENCES 103

APPENDICES 109

Appendix A: Description of software packages capable of modelling multiphase systems 109

Appendix B: A list of existing boreholes used to calibrate the MODFLOW flow model with their coordinates and respective water levels 111

Appendix C: A list of positions used to infiltrate NAPLs in the UTCHEM model and their coordinates 113

Appendix D: A list of positions used to infiltrate NAPLs in the UTCHEM model and their coordinates 114

Appendix E: Maps illustrating the simulation results for the infiltration and migration of non-aqueous benzene 115

Appendix F: Maps illustrating the simulation results for the infiltration and migration of aqueous benzene 131

Appendix G: Maps illustrating the simulation results for the infiltration and migration of non-aqueous PCE 147

Appendix H: Appendix G: Maps illustrating the simulation results for the infiltration and migration of aqueous PCE..... 163

Appendix I: Risk Characteristics of the BTEX hydrocarbons 179

LIST OF TABLES

Table 2-1: Chemical properties of BTEX aromatic hydrocarbons, other LNAPL compounds and petroleum products (adapted from Eby, 2004)..... 8

Table 2-2: The half-life values for organic compounds during aerobic and anaerobic decomposition (Eby, 2004)..... 15

Table 2-3: Compounds used to change the chemical properties of the NAPL to enhance abstraction (adapted from Reservoir Engineering Research Program, 2000)..... 17

Table 2-4: Methods that may be used in the site assessment of NAPLs with their description, advantages, and disadvantages (adapted from Gebrekristos *et al*., 2008)..... 21

Table 3-1**:** General geological sucession of the Zululand Group (adapted from Johnson *et al.*, 2006)..... 37

Table 3-2: General geological sucession of the Maputuland Group (adapted from Mkhwanazi, 2010 & Johnson *et al.*, 2006)..... 37

Table 3-3: Physical characteristics of coastal aquifers found on the east coast of South Africa (Compiled from Campbell et al., 1992)..... 40

Table 4-1: Chemical properties of compounds used in the UTCHEM code..... 53

Table 4-2: Information regarding the concentration of each compound and the injection rate of the remediation fluid for all mobilisation simulations..... 55

LIST OF FIGURES

Figure 2-1: Diagram illustrating wettability and capillary trapping. 9

Figure 2-2: Graphic representation of the transportation of LNAPLs in a groundwater system. Adapted from Kueper et al. (2003). 11

Figure 2-3: Graphic representation of the transportation of DNAPLs in a ground water system. Adapted from Kueper et al. (2003). 11

Figure 2-4: Common organic acidic structures and their respective dissociation constants. Adapted from Eby (2004). 13

Figure 2-5: Diagrammatic representation of the framework for DNAPL site assessment as proposed in the manual for site assessment at DNAPL contaminated sites in South Africa. Adapted from Gebrekristos, *et al*. (2008)..... 20

Figure 3-1: Graph representing the average rainfall for each month for KwaZulu Natal obtained from the Department of Water and Sanitation (undated). 32

Figure 3-2: Location map and satellite image depicting the location of the industrial site (Google Earth, 2017)..... 33

Figure 3-3: Map illustrating the topography of the study area. 34

Figure 3-4: Map representing the surface geology of the study area. 36

Figure 3-5: Stratigraphic column representing the sequence of formations in the Maputuland Group with their stratigraphic thicknesses. Adapted from Mkhwanazi (2010). 38

Figure 4-1: Map illustrating the different boreholes and their location in the industrial area. 42

Figure 4-2: A scatter plot graph of the topographical heights versus the observed hydraulic heads. 43

Figure 4-3: Map illustrating the boreholes used for calibration and their location in Durban. The green outline represents the boundary of the catchment..... 44

Figure 4-4: Image illustrating the boundary conditions of the model. 46

Figure 4-5: Contour map representing the topography used in the MODFLOW model. The black outline represents catchment U60F and the Geology within it. 47

Figure 4-6: Diagrammatic representations of a cross section of the area along transect A-B. 48

Figure 4-7: Map representing the surface geology of catchment U60F. 49

Figure 4-8: Contour map illustrating the hydraulic head, flow direction and relative flow rate used in the MODFLOW model. 51

Figure 4-9: Scatter plot graph of the Initial hydraulic heads versus the simulated hydraulic heads. 52

Figure 4-10: Google Earth image of the industrial area located in the Durban harbour. 56

Figure 5-1: Maps illustrating the simulation results for the infiltration and migration of non-aqueous phase benzene and PCE. (a) Benzene in the top layer; (b) Benzene in the bottom layer; (c) PCE in the top layer; (d) PCE in the bottom layer. 60

Figure 5-2: Maps illustrating the simulation results for the infiltration and migration of aqueous phase benzene and PCE. (a) Benzene in the top layer; (b) Benzene in the bottom layer; (c) PCE in the top layer; (d) PCE in the bottom layer. 61

Figure 5-3: Map illustrating the simulation results for the infiltration and migration of non-aqueous phase benzene with vectors that represent the direction of migration. 62

Figure 5-4: Map illustrating the simulation results for the infiltration and migration of non-aqueous phase PCE with vectors that represent the direction of migration. 62

Figure 5-5: Maps illustrating the simulation results for the remediation of non-aqueous phase benzene with surfactant SDS and polymer xanthan gum. (a) Benzene without remediation; (b) Remediation using diluted SDS and xanthan gum; (c) Remediation using undiluted SDS and xanthan gum; (d) Remediation using undiluted SDS and xanthan gum and an increase in the rate of infiltration. 64

Figure 5-6: Maps illustrating the simulation results for the remediation of non-aqueous phase PCE with surfactant SDS and polymer xanthan gum. (a) PCE without remediation; (b) Remediation using diluted SDS and xanthan gum; (c) Remediation using undiluted SDS and xanthan gum; (d) Remediation using undiluted SDS and xanthan gum and an increase in the rate of infiltration..... 65

Figure 5-7: Maps illustrating the simulation results for the remediation of non-aqueous phase benzene with surfactant SDS. (a) Benzene without remediation; (b) Remediation using diluted SDS; (c) Remediation using undiluted SDS; (d) Remediation using undiluted SDS and an increase in the rate of infiltration..... 67

Figure 5-8: Maps illustrating the simulation results for the remediation of non-aqueous phase PCE with surfactant SDS. (a) PCE without remediation; (b) Remediation using diluted SDS; (c) Remediation using undiluted SDS; (d) Remediation using undiluted SDS and an increase in the rate of infiltration. 68

Figure 5-9: Maps illustrating the simulation results for the remediation of non-aqueous phase benzene with polymer xanthan gum. (a) Benzene without remediation; (b) Remediation using diluted xanthan gum; (c) Remediation using undiluted xanthan gum; (d) Remediation using undiluted xanthan gum and an increase in the rate of infiltration. 70

Figure 5-10: Maps illustrating the simulation results for the remediation of non-aqueous phase PCE with polymer xanthan gum. (a) PCE without remediation; (b) Remediation using diluted xanthan gum; (c) Remediation using undiluted xanthan gum; (d) Remediation using undiluted xanthan gum and an increase in the rate of infiltration..... 71

Figure 5-11: Maps illustrating the simulation results for the remediation of non-aqueous phase benzene with surfactant SDS and ethanol. (a) Benzene without remediation; (b) Remediation using diluted SDS and ethanol; (c) Remediation using undiluted SDS and ethanol; (d) Remediation using undiluted SDS and ethanol and an increase in the rate of infiltration. 73

Figure 5-12: Maps illustrating the simulation results for the remediation of non-aqueous phase PCE with surfactant SDS and ethanol. (a) PCE without remediation; (b) Remediation using diluted SDS and ethanol; (c)

Remediation using undiluted SDS and ethanol; (d) Remediation using undiluted SDS and ethanol and an increase in the rate of infiltration. 74

Figure 5-13: Maps illustrating the simulation results for the remediation of non-aqueous phase benzene with ethanol. (a) Benzene without remediation; (b) Remediation using diluted ethanol; (c) Remediation using undiluted ethanol; (d) Remediation using undiluted ethanol and an increase in the rate of infiltration. 76

Figure 5-14: Maps illustrating the simulation results for the remediation of non-aqueous phase PCE with ethanol. (a) PCE without remediation; (b) Remediation using diluted ethanol; (c) Remediation using undiluted ethanol; (d) Remediation using undiluted ethanol and an increase in the rate of infiltration. 77

Figure 5-15: Graphs illustrating the concentrations of non-aqueous phase benzene at different boreholes after each remediation scenario. (a) Borehole IV08; (b) borehole IV18; and (c) borehole IV24. 79

Figure 5-16: Graphs illustrating the concentrations of non-aqueous phase PCE at different boreholes after each remediation scenario. (a) Borehole IV08; (b) borehole IV18; and (c) borehole IV24. 80

Figure 5-17: Maps illustrating the simulation results for the remediation of aqueous phase benzene with surfactant SDS and polymer xanthan gum. (a) PCE without remediation; (b) Remediation using diluted SDS and xanthan gum; (c) Remediation using undiluted SDS and xanthan gum; (d) Remediation using undiluted SDS and xanthan gum and an increase in the rate of infiltration. 83

Figure 5-18: Maps illustrating the simulation results for the remediation of aqueous phase PCE with surfactant SDS and polymer xanthan gum. (a) PCE without remediation; (b) Remediation using diluted SDS and xanthan gum; (c) Remediation using undiluted SDS and xanthan gum; (d) Remediation using undiluted SDS and xanthan gum and an increase in the rate of infiltration. 84

Figure 5-19: Maps illustrating the simulation results for the remediation of aqueous phase benzene with polymer xanthan gum. (a) benzene without remediation; (b) Remediation using diluted xanthan gum; (c) Remediation using

undiluted xanthan gum; (d) Remediation using undiluted xanthan gum and an increase in the rate of infiltration. 85

Figure 5-20: Maps illustrating the simulation results for the remediation of aqueous phase PCE with polymer xanthan gum. (a) PCE without remediation; (b) Remediation using diluted xanthan gum; (c) Remediation using undiluted xanthan gum; (d) Remediation using undiluted xanthan gum and an increase in the rate of infiltration..... 86

Figure 6-1: Map illustrating the distribution of aqueous phase benzene using MODFLOW after a simulation duration of twenty years in the subsurface. 88

Figure 6-2: Line graph representing the change in concentration of aqueous benzene over the duration of 20 years measured at different boreholes located within the contaminated region. 89

Figure 6-3: Map illustrating the distribution of aqueous phase benzene in the subsurface after an extraction period of one year. 89

Figure 6-4: Line graph representing the decrease in concentration of aqueous benzene over the extraction period of one year measured at different boreholes located within the contaminated region. 90

Figure 6-5: Line graph representing the increase in concentration of aqueous benzene over the extraction period of one year measured at different boreholes located within the contaminated region. 91

Figure 6-6: Map illustrating the distribution of aqueous phase benzene after a simulation duration of one year in the top 11 m of the subsurface (MODFLOW). 92

Figure 6-7: Map illustrating the distribution of aqueous phase benzene after a simulation duration of three months in the top 11 m of the subsurface (UTCHEM)..... 92

Figure 6-8: Flow diagram representing the procedure of the proposed methodology for a site assessment and remediation evaluation. 96

CHAPTER 1: INTRODUCTION

1.1 Introduction

In the year 1989 it had been predicted that there would be a water crisis by 2025 (Falkemark, 1989) due to a lack of large fresh water bodies in South Africa. As a country with an arid and semi-arid climate, water has become a luxury in many provinces where restrictions have been put in place to reduce consumption. Stresses on the resource will unlikely make the current usage sustainable in years to come (Walmsely *et al*., 1999). Surface water is expected to become depleted in the next few decades, if not sooner (Kelbe *et al*., 2001). In order to provide for basic needs for the future, groundwater as a resource will have to play a major role. It is for this reason that groundwater integrity needs to be preserved.

With the current load on surface water, alternative resource reservoirs should become increasingly important. As the initialisation of a surface water facility is costly (a large investment is needed to build dams, storage and treatment plants and install pipelines), groundwater supplies will be the most effective alternative for the future. Limited knowledge, and operational and management expertise of groundwater however, has resulted in destruction and degradation of the resource. There is also a lack of trust in comparison to surface water that can be visibly quantified (Cobbing, 2014).

A great threat to groundwater is petroleum hydrocarbon contamination as it is not isolated to a specific area. It commonly is associated with petrol stations, petrol and diesel storage facilities, and coal tar products (Wu *et al*., 2011). When infiltration occurs in the groundwater system, it spreads into and across the saturated and unsaturated zones in a way that is difficult to contain. It collects within the unsaturated zone, along pathways, coating granular soil and rock particles and accumulates on the surface and base of aquifers, while slowly releasing dangerous soluble compounds into the aquifer (Palmer, 1992). These compounds pose a threat to biological organisms and human health as they can be carcinogenic (Wu *et al*., 2011). With increasing energy demands due to urban and industrial development, and a lack of alternative resources, it is unlikely that the problem be contained in the near future (Xu *et al.,* 2006; Zhang *et al.,* 2007). Additionally, the release of hydrocarbons in groundwater was recognised only in the 1980s as equipment could not detect relatively low concentrations. In many countries, including the United Kingdom, it was an accepted practice to spread the contaminant over the ground surface and allow it to evaporate. The lack of understanding of groundwater as a resource and the dependency on surface water bodies have resulted in the late response to petroleum contamination (Kueper *et al*., 2003).

1.2 Problem Statement

When spilled, hydrocarbons will move downward through the unsaturated zone under the influence of gravity and capillary forces, trapping small amounts in pore spaces. When it reaches the water table, it will either accumulate on the groundwater table if it is less dense than water or move into the groundwater system to a confining boundary if it is denser than water. These are referred to as light non-aqueous phase liquids (LNAPLs), and dense non-aqueous phase liquids (DNAPLs). Some of the components can dissolve in the groundwater and move as a plume of contaminated water by diffusion and advection with the groundwater (Palmer, 1992). The transport of contaminants from petroleum hydrocarbon spills needs to be described in terms of a multiphase flow system in the unsaturated zone, taking into account contaminant movement in each of the three phases: vapour, dissolved aqueous plume and non-aqueous phase liquids (NAPLs). Petroleum hydrocarbon behaviour in the subsurface is additionally complicated by the presence of multiple compounds, each with different properties. The net result is that some hydrocarbon fractions are transported faster than others and a contamination plume of varying intensity may spread over a large area (Palmer, 1992).

The Interstate Technology and Regulatory Council (ITRC) of the United States of America states that restoration within a generation has been difficult but not impossible, with few successful cases. It will require a full understanding of the site, clear remediation objectives, and knowledge of multiple remediation technologies to create an effective management plan (ITRC, 2011). Gebrekristos *et al*. (2008) have developed an extensive manual for the site assessment of areas affected by DNAPLs, however, some site assessments are not always possible due to cost and time spent on projects. Additionally, the use of modelling as a tool for assessment has not been documented extensively. The manual refers to the use of software packages MODFLOW and UTCHEM to aid understanding of current and future conditions. It is also mentioned that modelling and different codes have certain limitations and can be misleading (Gebrekristos *et al*., 2008).

The greatest issue with contaminant hydrocarbons lies in the delineation (determine the surface area and thickness) of the NAPL plume. Because its physical properties and behaviour are different from that of water, and it cannot be assumed that the mass migrates the same way other plumes do. Conventional methods used to determine groundwater flow such as pump test and flow logging would not be appropriate to assess the extent of non-aqueous phase contamination. Geophysical methods are often used to better understand the subsurface has proved to be ineffective as industrial noise at these sites is often too high. Excavation, drilling and other invasive methods tend to mobilise the NAPL and distribute it to previously

undisturbed areas which would only deepen the crisis. On the other hand, soil gas surveys and the use of an interface meter are best suited for delineation but have disadvantages. They both over estimate the size and thickness of the plume and the interface meter can only generate data where boreholes exist (Gebrekristos *et al*., 2008). All these methods will be discussed in detail at the end of Chapter 2.

The use of numerical models has been used in this field however, assessment documents retrieved do not document exactly how they have been used and what limits it may have. It is vague and unclear as there are no reference results available. The documents state that models have been used for research purposes however this is related to certain hydraulic and physical parameters and not used in an actual site assessment. When site assessments are included, the discussion of results look promising, however, the actual results and methodology is omitted entirely. This document will try and fill these gaps that exist in literature found, and exclude all methods that will generate limited data for assessment (Gebrekristos *et al.*, 2008, Reservoir Engineering Research Program, 2000, and Hulling and Weaver, 1991).

1.3 Hypothesis

As mentioned before, an assessment manual is available for areas affected by DNAPLs. Gebrekristos *et al.* (2008) concluded with an extensive flow diagram illustrating the procedure of assessment that will be discussed in detail at the end of Chapter 2. In the assessment manual, both invasive and non-invasive techniques can be conducted to provide information on the physical, chemical and hydrological characteristics of an area. The information is then conceptualised so that a numerical model can be created that best represents the environment. The numerical model is used to understand the environment and predict the fate of the groundwater based on management decisions. This research project addresses a means in which to supplement a remediation plan that allows one to, through numerical modelling, understand site dynamics and requirements in terms of movement and remediation of hydrocarbons. UTCHEM has been successfully used on sites in America, is well documented and has been proposed in the assessment manual for South African sites, as well as by the United States Environmental Protection Agency (Gebrekristos et al., 2008, Reservoir Engineering Research Program, 2000, and Hulling and Weaver, 1991). Therefore, the hypothesis states that UTCHEM can assist to assess the movement of both the free phase and dissolved plume for both DNAPLs and LNAPLs. Along with the migration, remedial options can

be simulated in order to choose the best solution to achieve objectives for management and monitoring of an area.

1.4 Aims and objectives

The aim of this study is to develop a procedural methodology to assess the movement of hydrocarbons. The methodology will be demonstrated by means of a case study of the industrial site located within the Durban harbour. Associated remediation options will be determined.

The development of a basic, sequential methodology that can be used for similar contaminated areas include the following objectives:

- Construction of a conceptual model to identify boundaries, parameters and constraints (physical, chemical and hydrological characteristic) to adequately represent the environment, to be used for the numerical model.
- Construction of a multiphase numerical model that will illustrate the migration of hydrocarbons within a shallow, primary, porous aquifer.
- Numerically model aqueous and non-aqueous phases and to simulate the extent of the plume over a fixed duration for both DNAPLs and LNAPLs.
- Simulate different remediation options to be able to make a sound decision for rehabilitation of the area of DNAPLs and LNAPLs.
- Simulate the injection of remediation fluids at varying concentrations and flow rates to determine the influence of concentration and flow rate.
- Evaluation of the difference in behaviour between DNAPLs and LNAPLs through modelling.
- Validate the movement of the dissolved aqueous plume using MODFLOW.
- Create a methodology using information from the results and from assessment manuals such as the “Manual for Site Assessment at DNAPL Contaminated Sites in South Africa”, The NAPL manual from the United Station Environmental Protection Agency, and “An illustrated handbook of DNAPL transport and fate in the subsurface” written by the Environment Agency in England and Wales.
- Lastly the advantages and disadvantages of the method will be discussed.

1.5 Layout

This dissertation provides an overview of contamination of organic compounds and a methodology that can be used to assess as well as rehabilitate affected areas. Specific aspects that will be covered include:

- Chapter 2 – Literature review
  - Information on the properties and behaviour of the contaminant.
  - An overview of the general remediation processes used for this type of problem.
  - A literature review on work that has already been conducted with regards to procedure of assessing areas affected by hydrocarbons and work done on modelling hydrocarbon contamination in groundwater
- Chapter 3 – Study area
  - A desktop study of the area used as a case study.
- Chapter 4 – Methodology
  - Data collection and processing.
  - Aquifer classification and conceptualisation.
  - Numerical and chemical modelling of the aqueous and non-aqueous phase.
  - Numerical and chemical modelling of rehabilitation options.
- Chapter 5 – Results and discussion: UTCHEM
  - Data evaluation and interpretation of information obtained through the UTCHEM software.
- Chapter 6 – Results and discussion: MODFLOW
  - Data evaluation and interpretation of information obtained through the MODFLOW software.
- Chapter 7 – Discussion of proposed methodology
  - A summary of the results obtained with reference to the objectives set out initially.
  - A compilation of knowledge obtained from results.
  - A detailed proposed methodology based on results and literature.
- Chapter 7 – Conclusion and recommendations
  - A conclusion with respect to the hypothesis.
  - A summary of the recommended methodology.
  - Recommendations for future studies.

CHAPTER 2: LITERATURE REVIEW

2.1 Introduction

Petroleum hydrocarbons are a frequent hazard to subsurface water resources. They originate from underground and surface storage tanks in and around petrol stations, airports and harbours. Even though petroleum is referred to as a single entity, it consists of a number of organic compounds with varying physical and chemical properties. Its volatility, instability and toxicity makes petroleum a difficult contaminate to eradicate (Younger, 2007).

In order to accurately model and assess the behaviour of a hydrocarbon plume in the subsurface, it is necessary to look at the theory behind the factors that influence its distribution in the subsurface. The literature review will deal with the properties of the contaminant and factors that control the distribution. The physical, chemical and biological characteristics of the subsurface become important as they are controlling factors for the migration path and rate of decomposition. Finally, the typical remediation processes will be outlined followed by a compilation of literature related to the project being conducted.

2.2 Hydrocarbons

Hydrocarbons are organic compounds that contain carbon and hydrogen. They are grouped according to the number of bonds between two carbon molecules. Alkanes have a single bond between adjacent carbons while alkenes and alkynes contain double and triple bonds respectively (Eby, 2004). It is important to identify the amount of bonds present as it gives an indication of the reactivity of the molecule. Alkanes are most stable in comparison and only react at very high temperatures. Alkanes undergo substitution, a reaction where hydrogen is replaced by atoms of another element. Alkenes and alkynes however, react more easily with other elements by addition where a single triple or double bond is broken during the process (Eby, 2004). Polycyclic aromatic hydrocarbons and NAPLs are hydrocarbon compounds that are of concern in the environment. Both are relatively insoluble and pose a threat to aquatic health (Neff, 1988).

Polycyclic aromatic hydrocarbons (PAHs) consist of fused benzene rings (Eby, 2004). Benzene rings are cyclic structures containing six carbon atoms with alternating single and double bonds.

They are commonly found on sediment and the fatty tissue of various aquatic organisms (Eby, 2004). Refined petroleum consists of a combination of alkanes, cycloalkanes, alkenes, and cycolalkenes. As the molecular weight of these liquids increase, they become more susceptible to decomposition resulting in the presence of an unstable product that has an on-going release of soluble compounds. The pollution plume is not only confined to a certain area but will continuously contaminate the aquifer (Neff, 1988).

2.2.1 Light non-aqueous phase liquids (LNAPLs)

LNAPLs are insoluble in very saline water but dissolve in fresh water. The BTEX (benzene, toluene, ethyl-benzene and xylene) aromatic compounds are examples of LNAPLs. The high solubility of benzene and toluene make these compounds a threat to drinking water as they are known to be carcinogenic (Eby, 2004). The chemical properties of the BTEX group of organic compounds are summarised in Table 2-1 along with other hydrocarbon compounds. All compounds described are less dense and more viscous in comparison to water and rapidly migrate over a large area on the surface of the groundwater system.

Additionally, MTBE (methyl tertiary butyl ether) is highly soluble petroleum associated contaminant, which has a distinct colour and odour and is problematic at very low concentrations (Younger, 2007).

Along with organic compounds, inorganic compounds sulphate (SO_4), nitrate (NO_3) and toxic metals such as cadmium (Cd), zinc (Zn), lead (Pb), nickel (Ni), chromium (Cr) and arsenic (As) are also associated with petroleum contamination (Younger, 2007).

2.2.2 Dense non aqueous phase liquids (DNAPLs)

DNAPLs include coal tar, creosote (a wood treatment oil), pesticides, transformer and insulating oils and a number of halogenated hydrocarbons that are specifically chlorinated. These include tetrachloroethene (PCE) and trichloroethene (TCE), which are slightly soluble and extremely toxic to the environment (Kueper *et al.*, 2003; Gebrekristos *et al.*, 2008).

Table 2-1: Chemical properties of BTEX aromatic hydrocarbons, other LNAPL compounds and petroleum products (adapted from Eby, 2004).

BTEX hydrocarbons	Structure	Density (g/cm^3)	Viscosity (cp)	Solubility in distilled water (ppm)	Solubility in saline water (ppm)
Water		0.998	1.14		
Benzene		0.8765	0.6468	1696	201
Toluene	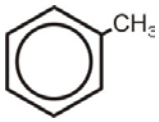	0.8669	0.58	580	50
Ethylbenzene	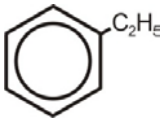	0.867	0.678	161	111
***o*-Xylene**	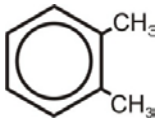	0.880	0.802	171	130
***m*-Xylene**	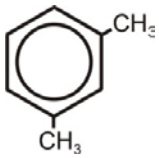	0.8642	0.608	148	106
***p*-Xylene**	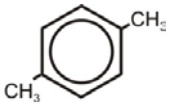	0.8610	0.663	156	111
#2 Fuel Oil		0.87 – 0.95	1.15 – 1.97		
#6 Fuel Oil		0.87 – 0.95	14.5 – 493.5		
Jet Fuel		0.75	0.83		

Densities of common DNAPLs range between 1.2 – 1.6 g/cm^3. They are denser than water and therefore exist within the saturated zone below the water table. Viscosity values are on the other hand less than that of water. This results in slow migration and accumulation in the subsurface (Kueper *et al.*, 2003).

2.2.3 Behaviour of NAPLs

When released into the environment, NAPLs will migrate down the subsurface under the force of gravity. As hydrocarbons move within the unsaturated zone, they leave a residual portion within the available porosity. If capillary forces are high enough, contaminants become trapped within this zone until there is a sufficient amount for transportation (Palmer, 1992). This can be explained by wettability. Wettability is the tendency of a fluid to adhere to a crystalline surface in the presence of another fluid that is relatively insoluble. In a multiphase system, the wetting fluid, in this case water, will coat grains and fill large pores while the non-wetting petroleum, will prefer to occupy smaller spaces where grains are in closer contact (Mercer & Cohen, 1990). This means the NAPL will fill minute pore spaces and narrow channels between grains while groundwater remains in larger pores. This phenomenon is known as capillary trapping and is illustrated in Figure 2-1.

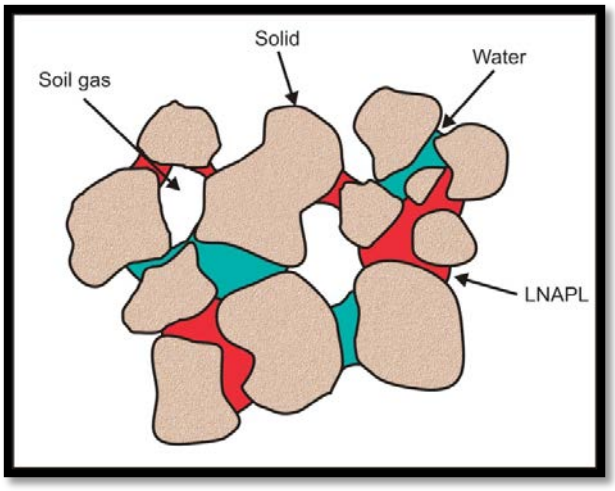

Figure 2-1: Diagram illustrating wettability and capillary trapping.

Continuous infiltration causes LNAPLs to accumulate on the surface of the groundwater table. It will accumulate along the capillary fringe and become displaced downward with additional weight creating a lens like structure. Once the combined weight exceeds the capillary pressure, it will then flow laterally on the groundwater surface (Palmer, 1992). Because DNAPLs are denser and less viscous than water, infiltration occurs with an increase in lateral migration and will cause the free phase to extend to greater depths within the saturated zone. The portion of the free phase that remains trapped between the pores is referred to as ganglia while the collective continuous mass is referred to as a pool (Kueper *et al.*, 2003).

Certain components of the NAPL are immiscible due to the differences in density and interfacial forces. These forces refer to cohesive forces between molecules of the same liquid that are greater than adhesive forces between molecules of two different liquids (Bear, 1972). This prevents the hydrocarbons from becoming emulsified in water. Emulsification does however take place on a microscopic scale. With respect to the free phase, there exists a difference in density and viscosity. As the density of the fluid increases and viscosity decreases and the relative hydraulic conductivity with respect to the liquid will alternatively decrease (Newell *et al*., undated).

The distribution of the plume is controlled by the hydraulic conductivity and the hydraulic gradient of an aquifer. Movement is dependent on gravity and therefore the pollution plume will become elongated along the hydraulic gradient. If the hydraulic conductivity is low, mobility is restricted and the plume stays relatively compact (Palmer, 1992).

Migration of both NAPLs and dissolved hydrocarbons are dependent on aquifer geology, groundwater velocity, chemical composition, and molecular weight. Natural and anthropogenic pathways have a major impact of groundwater movement. These consist of cracks, fractures, faults, dykes and sills, voids created by biological activity, and pipelines. This increases the velocity of groundwater and governs the distribution of contamination within the aquifer (Palmer, 1992).

Once the contaminant reaches the zone of saturation, a portion of the NAPLs will dissolve in water and migrate within the aquifer. These soluble substances include BTEX (Palmer, 1992), PCE and TCE (Kueper *et al.*, 2003). Transport is made possible by both advection (the process by which the movement of groundwater distributes solvents) and diffusion (occurs when a solute moves from an area of a higher concentration to that of a lower concentration). Both processes are unstable and occur at variable rates making the contamination difficult to access and control (Palmer, 1992).

Figure 2-2 and Figure 2-3 illustrates the transportation of LNAPLs and DNAPLs respectively as described above.

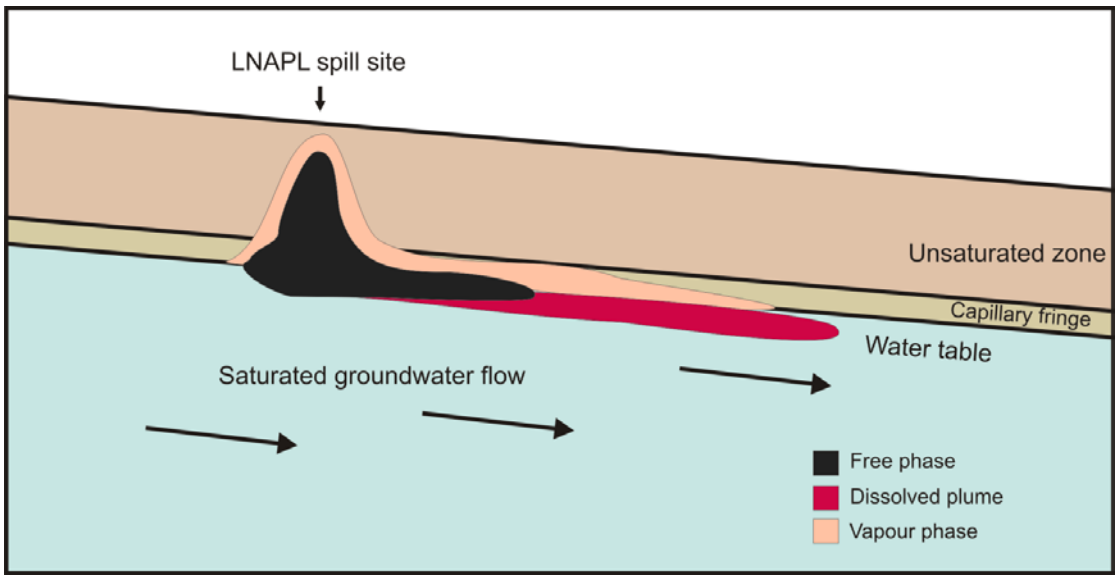

Figure 2-2: Graphic representation of the transportation of LNAPLs in a groundwater system. Adapted from Kueper et al. (2003).

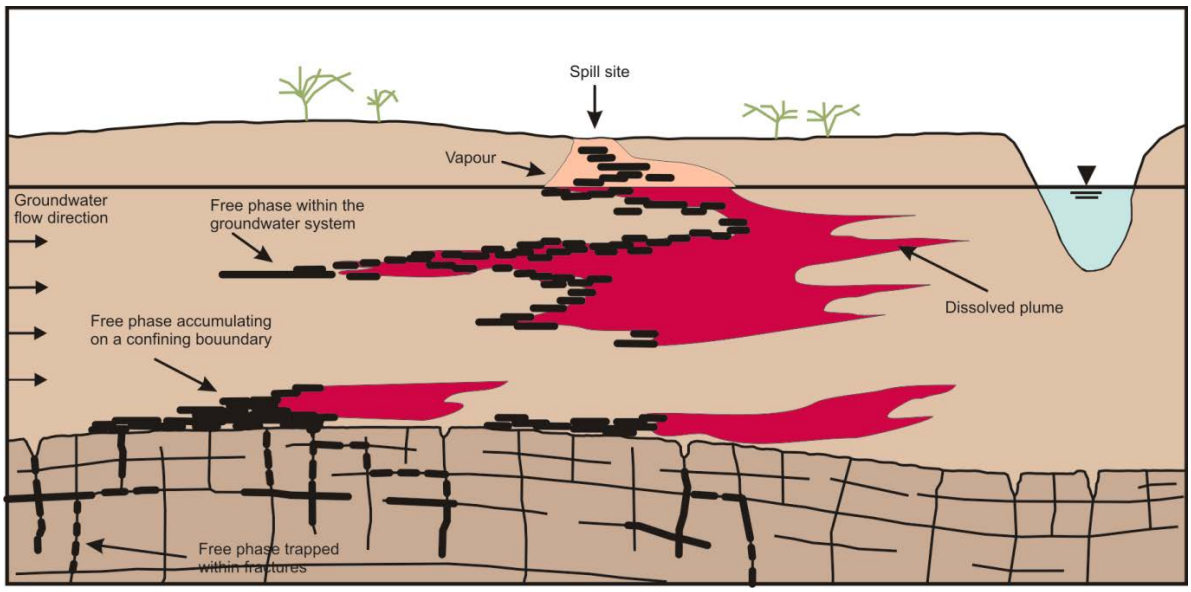

Figure 2-3: Graphic representation of the transportation of DNAPLs in a ground water system. Adapted from Kueper et al. (2003).

2.2.4 Decomposition of hydrocarbons

There are specific physical and biological processes that control the concentration of organic compounds in natural water systems. These processes act in such a way to decompose hydrocarbons and are important to determine, to aid in identifying the rate at which contaminates will be removed and dispersed in a system. Biological processes have a direct and indirect effect on disintegration of organic compounds. Physical and chemical processes include sorption, precipitation, volatilisation, and oxidation-reduction reactions and will be discussed in this section.

2.2.4.1 Sorption

Sorption is the process where various elements and compounds are attached or absorbed onto a substrate. Substrates include silicate clay minerals, carbonate, oxide and sulphide minerals, organic and humic particles as well as pre-existing particles that have organic, carbonate and oxide coatings (Eby, 2004). For adsorption to take place, the pH of the solution needs to be two units less than the dissociation constants (pK_a). The pK_a value gives an indication of how readily an organic compound will dissociate or dissolve. The lower the pK_a, the more volatile it will be. Maximum absorption occurs for this value, while maximum desorption takes places when the pK_a value is two units greater than the pH. The opposite effect is true for organic bases however, when a base is found in an acidic solution, the hydrogen ion (H^+) reacts with the hydroxide ion (OH^-) leading to ionisation instead (Eby, 2004). Figure 2-4 indicates the structure and pK_a value for different organic compounds. Oxalic and phthalic acid have two constants because both compounds have two dissociation processes.

2.2.4.2 Precipitation

Precipitation of organic compounds occurs when there is significant change in ionic strength of a solution. An increase of ionic strength decreases the solubility allowing precipitation of organic matter to take place (Eby, 2004).

Acid	Structure	pK_a
Acetic	CH_2COOH	4.9
Lactic	CH_3-CH(OH)-COOH	3.1
Oxalic	COOH-COOH	1.2, 4.2
Benzoic	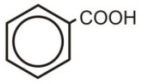	4.2
Phthalic	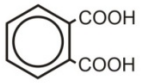	2.9, 5.5

Figure 2-4: Common organic acidic structures and their respective dissociation constants. Adapted from Eby (2004).

2.2.4.3 Volatilisation

Volatilisation refers to the process where a liquid readily changes to a vapour. Most organic compounds have a low volatility, however, certain hydrocarbons, ketones, aldehydes and esters evaporate easily. Evaporation is greater for low-molecular-weight non polar molecules such as benzene (Eby, 2004).

2.2.4.4 Oxidation-Reduction

Decomposition of organic matter is important as it reduces the amount of oxygen, in turn changing conditions from an oxidising to a reducing environment. Humic and fluvic acid found within the subsurface may act as additional reducing agents (Eby, 2004).

2.2.4.5 Biological Processes

Organic matter is removed from groundwater by consumers and decomposers. These consist of certain bacterial and fungal species. Dissolved organic carbon is then oxidised by microbial activity (Eby, 2004) and is represented by the following equation (Reservoir Engineering Research Program, 2000):

$$C_7H_8\,(dissolved\ organic\ carbon\ species) + 9O_2\,(oxygen\ from\ microbial\ activity) \rightarrow 7CO_2\,(carbon\ dioxide) + 4H_2O$$

This takes place in aerated environments such as streams, lakes, and oceans. In anaerobic conditions, decomposition still occurs with the help of an oxidising agent (Eby, 2004) represented by the reactions (Reservoir Engineering Research Program, 2000):

$$C_7H_8\,(dissolved\ organic\ carbon\ species) + 7.2NO_3^-\,(oxidising\ agent) + 7.2H^+ \rightarrow 7CO_2\,(carbon\ dioxide) + 3.6N_2\,(reduced\ compound) + 7.6H_2O$$

$$C_7H_8\,(dissolved\ organic\ carbon\ species) + 4.5SO_4^{2-}\,(oxidising\ agent) + 3H_2O \rightarrow 2.25H_2S\,(reduced\ compound) + 2.25HS^-\,(reduced\ compound) + 7HCO_3^-\,(bicarbonate) + 0.25H^+$$

$$C_7H_8\,(dissolved\ organic\ carbon\ species) + 3.6Fe^{3+}\,(oxidising\ agent) + 21H_2O \rightarrow 7HCO_3\,(bicarbonate) + 3.6Fe^{2+}\,(reduced\ compound) + 43H^+$$

The bi-products of oxidation are the much less harmful carbon dioxide (CO_3^{2-}) and bicarbonate (HCO_3^-) ions. Other types of microbial decomposition include dehalogenation, in which a halogen atom is replaced by a hydroxyl group (OH^-) (Eby, 2004). This would decrease the density of DNAPLs making them more accessible for remediation.

2.2.4.6 Degradation Half Life

Half life is defined as the length of time taken for 50 % of an organic compound to be degraded under natural conditions. The half life of substances in the soil and groundwater is dependent on the initial concentration, temperature, and whether decomposition takes place under anaerobic or aerobic conditions. Half life tends to increase with increasing concentrations and decrease with increasing temperature (Eby, 2004). Various half live values for organic compounds can be found in Table 2-2 which gives an idea of the relative rates of breakdown.

Table 2-2: The half-life values for organic compounds during aerobic and anaerobic decomposition (Eby, 2004).

	Half-Life in days			
	Aerobic decomposition		**Anaerobic decomposition**	
Compound	***Minimum***	***Maximum***	***Minimum***	***Maximum***
Napthalene	1	20	25	258
Toluene	4	22	56	210
Benzene	5	16	112	720
Xylene(s)	7	28	180	360
Tetrachloroethene	180	360	98	1653

2.2.5 Remediation of Hydrocarbons

Before the remediation process takes place, two important questions need to be addressed (Younger, 2007):

1. What will the fate of the resource be if remediation does not take place?
2. What standards should be achieved if remediation is necessary?

These two questions are important for determining the degree of contamination, future risk, and the end goal for project closure or, the beginning and end of the task. It is important to understand toxic (results in illness that may eventually lead to death) and carcinogenic (results in cancer) risks in order to create a management strategy that would eliminate these risks (Kueper *et al.*, 2003). To achieve the goals and objectives of the project, it is crucial to focus on the three areas as to how contamination can be distributed (Younger, 2007):

$$SOURCE \rightarrow PATHWAY \rightarrow RECEPTOR$$

In this case, the source are the tanks where petroleum is stored, the pathway includes the surface sediment, unsaturated zones and groundwater, and the receptor is the groundwater table, groundwater, any surface water bodies that are linked to the groundwater, aquatic species and anyone exposed to the affected water. If the contaminant is removed from the subsurface and the source still remains, there will be continuous infiltration that will have to be

re-evaluated at a later stage. The same outcome is achieved if the source and receptor are removed while the contaminant remains trapped within the unsaturated zone (Younger, 2007).

Once the base line study is complete, a remediation method needs to be identified. There are three different types of remedial technologies that are currently being utilised. They include (ITRC, 2011):

- Physical
  - eg. excavation and thermal treatment
- Chemical
  - eg. chemical flushing and chemical oxidation
- Biological treatment
  - eg. biological oxidation

For hydrocarbons, 'the pump and treat' approach is commonly used, where the contaminated groundwater is removed by means of extraction boreholes and treated on surface. When the optimum results are achieved, the water is then re-injected into the subsurface, used elsewhere or discarded into a surface water body (Younger, 2007). Because NAPLs are 'trapped' by capillary forces in pore spaces, it is difficult to extract. In-situ treatment is used to alter the chemical properties of the NAPL to increase mobility for pumping (Reservoir Engineering Research Program, 2000). This can be achieved by chemical flushing, and or, chemical oxidation (Soga *et al*., 2004)

2.2.5.1 Chemical flushing

The contaminated area is treated by injecting a surfactant, polymer, co-solvents or thermal fluid (Reservoir Engineering Research Program, 2000 & Soga *et al*., 2004) to assist in mobilising the free phase (Kueper *et al.*, 2003). Surfactants and thermal water provide a medium for NAPLs to dissolve thus decreasing the interfacial tension and reducing the capillary forces. Solubilisation, mobilisation and an increase in relative permeability are achieved therefore enhancing the recovery volumes (Reservoir Engineering Research Program, 2000 and Hulling & Weaver, 1991). Surfactants increase the viscosity of the NAPL making it easier to extract (Hulling & Weaver, 1991). There is a risk involved when using this method as the contaminant can be distributed to unaffected areas and is no longer isolated within the subsurface (Kueper *et al.*, 2003).

2.2.5.2 Chemical oxidation

Chemical oxidation takes place in the same manner as biological anaerobic decomposition. Hydrocarbon chains are broken down in the presence of an oxidising agent therefore decreasing the density and increasing the viscosity of the NAPL. The NAPL is then easily removed, while the remaining entrapped hydrocarbon can be further decomposed. Decomposition products such as organic carbon and the reduced oxidising agent, do not pose a major risk to groundwater (Eby, 2004). Compounds used for this purpose as well as chemical flushing are listed in Table 2-3.

Table 2-3: Compounds used to change the chemical properties of the NAPL to enhance abstraction (adapted from Reservoir Engineering Research Program, 2000).

Surfactant	**Oxidising agents**
Propanol, Pentanol, Hexanol, Heptanol , Ethanol	Perioxide based oxidant with a sulphate based oxidant.
2-ethyl-1-butanol	Ferric iron (Fe^{3+})
Sodium dihexyl sulphosuccinate	Nitrate (NO_3^-)
Isopropanol	Phosphate (PO_4^{3-})

2.2.5.3 Natural attenuation

Natural attenuation is the biological, chemical and physical means that result in hydrocarbons breaking down naturally in a system without anthropogenic intervention. Natural attenuation includes the processes of oxidation and biodegradation, dispersion, sorption and volatilisation.

Natural attenuation occurs at all sites but at different rates depending on biological activity, salinity and hydraulic conductivity, just to name a few. Usher *et al*. (2008) suggests that natural attenuation can solely be used as a remediation alternative if objectives can be achieved in a reasonable period of time. If this is not the case natural attenuation can be used in conjunction with chemical flushing and/or chemical oxidation (Usher *et al*., 2008).

Remediation is not always necessary. If the chemical risk is low and there is limited movement of the NAPL, in other words, if it cannot reach a water resource body, remediation should not be considered. In-stead monitored natural attenuation (MNA) is an acceptable method where the

concentration and extent of the pollution plume is measured at timely intervals. Through natural processes the risk is likely to decrease with time. If the source is not removed entirely, there will be an increase in the free phase in the groundwater system causing increases in the dissolved contaminant. If MNA is considered, the source would need to be monitored as well as the stability of the free phase (Usher *et al*., 2008).

2.3 Assessment procedures

A manual for the site assessment at DNAPL contaminated sites was written for the Water Research Commission (WRC). The purpose of the document was to compile an assessment procedure to assess DNAPLs in the subsurface with special consideration towards DNAPL properties, South African aquifer characteristics, available technology and cost-effective assessment methodologies (Gebrekristos *et al*., 2008).

A key factor that is discussed is the need for a cost effective methodology. Certain procedures discussed can become quite expensive when implemented, however, they may still be necessary to define the environment adequately and prevent misguided investigations and remedial efforts. The assessment procedure is divided into six different categories as follows (Gebrekristos *et al*., 2008):

- General site assessment – This is conducted as an initial desktop study with the use of existing information.
- Field observations – Non-invasive techniques such as geophysical investigations and invasive techniques such as borehole tests, drilling and excavation are all inclusive.
- Analysis of DNAPL, soil and water – This includes sampling, laboratory and data analysis.
- Conceptual site model – Construction of a conceptual model that best represents the environment and aids in the understanding of factors and processes that govern the migration of DNAPLs.
- Multiphase modelling – The development of a numerical model that replicates the conceptual model to help understand and interpret the environment and predict the outcome or fate of the contaminated site.
- Water quality standards and guidelines – This is related to risks associated with the contaminant and standardised concentrations that helps create a guideline for management, remediation and mitigation.

Figure 2-5 illustrates the procedure to assess a site contaminated by DNAPLs. Some methods are cost effective such as site characterisation, general site assessment, conceptualisation and modelling while others may be expensive and time consuming. Table 2-4 is a summary of all the methods documented in the manual and includes a short description of its advantages and disadvantages. In the manual, many of the methods are of no value due to major disadvantages. These include surface and aerial geophysics, test pits, drilling, pump tests, and soil and rock sampling. Geophysical methods are problematic at sites as there is often too much industrial noise to obtain meaningful results. Invasive methods such as test pits, drilling, pump test, and soil and rock sampling may disturb the free phase and cause it to migrate to uncontaminated areas within the aquifer.

An emphasis is placed on a general site assessment as it allows one to limit the amount of additional information required to create a comprehensive conceptual model used for management and modelling. Soil gas surveying, borehole logging using the interface meter, and NAPL sampling are the only methods that are directly useful for NAPL assessment (Gebrekristos *et al*., 2008). These methods can be used to determine distribution and thickness of the free phase, as well as the physical and chemical properties. Delineation using this method, however, is always an over estimation as gas can occupy a larger area than a denser liquid and the thickness of the NAPL in the borehole is always greater than in the surrounding rock or soil formation. All other methods included in the table such as down-the-hole geophysics, flow logging, video logging, tracer tests, and borehole geochemical logging can be used indirectly to determine the flow regime and chemically characterise the groundwater layers. For more information regarding each method consult the Manual for Site Assessment at DNAPL Contaminated Sites in South Africa (Gebrekristos *et al*., 2008).

The final method included in the manual is dedicated to water quality standards and guidelines. Gebrekristos *et al*. (2008) state that risk-based approaches are followed to screen trigger values and this method is consistent with strategies from the United States Environmental Protection Agency, the United Kingdom Environment Agency, and the Australian regulations (Gebrekristos *et al*., 2008, Reservoir Engineering Research Program, 2000, and Hulling & Weaver, 1991). In the document a risk assessment is defined as “an analysis that uses information about toxic substances at a site to estimate a theoretical level of risk for people/receiving environments potentially exposed to these substances”. The manual states that the risk-based methods that are generally accepted is the source-pathway-receptor approaches but there is no indication of a quantitative approach to establish wether there is a risk or not. An analytical approach needs to be applied for all sites to create a standard approach (Gebrekristos, *et al*., 2008).

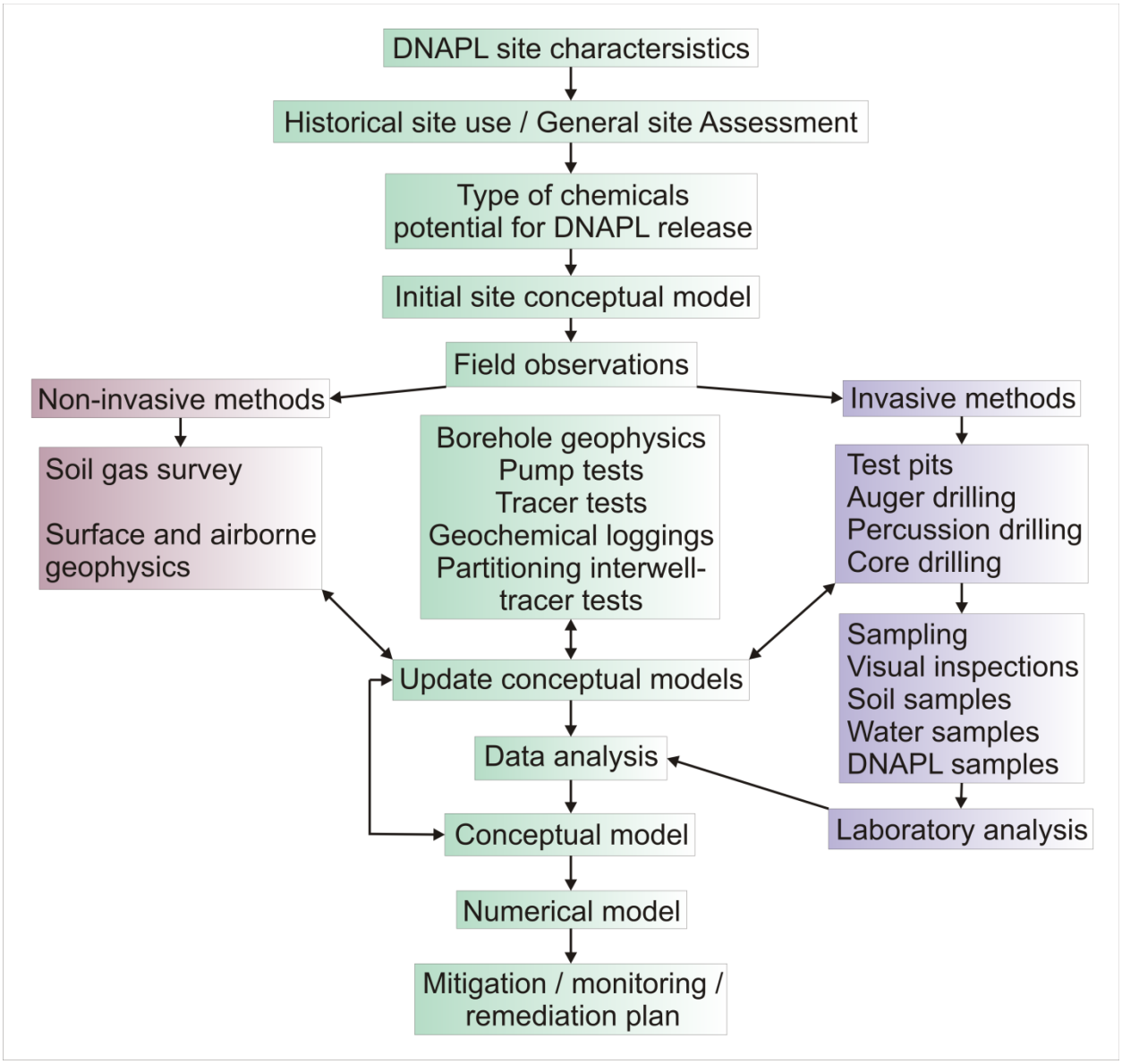

Figure 2-5: Diagrammatic representation of the framework for DNAPL site assessment as proposed in the manual for site assessment at DNAPL contaminated sites in South Africa. Adapted from Gebrekristos, *et al*. (2008).

A similar project was conducted by a group of academics from the Universities of Free State, Pretoria and Kwa-Zulu Natal for LNAPLs. The investigation procedure was similar to that of the one conducted on DNAPLs, however, emphasis is placed on a historical and field assessment, non-invasive and invasive field methods and a concise conceptual model. There is no mention of the use of a numerical model, but rather a risk assessment of the source, pathway and receptor needs to be identified before mitigation and monitoring. It was also mentioned that it is necessary to do sampling of the free phase, dissolved plume as well as the vapour emitted to the environment (Steyl *et al*., 2012).

Table 2-4: Methods that may be used in the site assessment of NAPLs with their description, advantages, and disadvantages (adapted from Gebrekristos *et al*., 2008).

Method	Description	Advantages	Disadvantages
General site assessment	-Conducted to determine whether and where NAPLs are found and released at a site. Site assessors can identify facilities and activities that may be an indicator. -Information gathered includes interviews, records of chemical purchase, waste disposed, and historical site drawings and aerial photographs	-Large amount of information can be gather from site operators, observation, historical data, and public data. -Can decrease the amount of methods needed to be conducted during the entire site assessment if information already exists. -Can create a comprehensive conceptual model of the site. Non-invasive method.	-Sometime information such as chemicals used or disposed of are limited. -Estimations and assumptions of chemical records need to be made at times.
Soil gas surveys	-A method used to identify volatile organic carbons in soil gas in the unsaturated zone. -Probes are inserted into the soil up to a depth of 3 meters and the soil gas is captured and then analysed.	-Generates extensive distribution data of the NAPL found in shallow groundwater and within the unsaturated zone. -Cost effective. -Non-invasive method.	-Contamination pools located further below the water table cannot be detected. -May become invasive if the probe intersects a NAPL pool where it can affect the distribution. -Because there is a lack of information and limited visibility, areas affected are difficult to find. -Creates a wider distribution than the actual NAPL because gas can spread over a larger area.
Surface and aerial geophysics	-Involves the identification of structural features that will control movement of the plume.	-Electromagnetic, magnetic, and resistivity methods are most suitable. -Data shows that it is possible to identify some dykes and therefore geophysics should only be used as a tool to identify geological structures when noise is limited. -Pipe lines and waste disposal pits can additional be identified. -Non- invasive method.	-Most methods are not suitable due to the local conductive overburden is South Africa. -Methods are over shadowed by noise that exists in these highly industrialised areas and the available size for surveying would be insufficient for geophysics to work.

Method	Description	Advantages	Disadvantages
Down-the-hole geophysics	-Involves lowering geophysical equipment into an existing borehole to determine characteristics at a specific depth.	- A wide variety of techniques are available. -Can be used to determine the transmissivity of the groundwater and other hydraulic parameters. -Can identify fractures, change in flow magnitude, and identify dissolved contaminates.	-Fractures may be enlarged by drilling during borehole establishment. -Field data shows that this method cannot be used to identify the presence of a NAPL layer and therefore it would have limited use in NAPL site assessment. -Fracture orientation cannot be identified and therefore flow direction cannot be determined.
Flow logging	-With the use of a flowmeter, the flow rate is measured under ambient and stressed conditions.	-Can determine the magnitude and direction of vertical flow in a borehole under ambient conditions. -The transmissivity of different fractures can be determined under stressed conditions, Important to determine flow regime, hydraulic characteristics of fractures, design well completions to reduce contamination, and for planning water sampling strategies.	-Stressed conditions used to determine the transmissivity may cause the redistribution of NAPL however, pumping or injection into a borehole is slow.
Video logging	-Used in combination with down the hole geophysics and flow logging to locate fracture flow paths and involves lowering a camera down a borehole.	-Can be used to determine well construction and to insect the borehole casing, fracture positions and orientation, and for geological profiling. -The only method that helps to determine the presence of a vertical fault that would allow contamination to reach greater depths. -Identification of NAPLS that have stained borehole walls.	-Cannot be used to determine hydraulic parameters. -Cannot be used as a quantitative method.

Method	Description	Advantages	Disadvantages
Test pits	-Involves the removal of the overburden to identify contaminated soil and delineate NAPL distribution.	-Very rapid and cost effective. -Characterise overburden. Identify contaminated areas. -Locate and examine buried structures such as storage pits and pipelines that can be the source of contamination. -Obtain soil samples for analysis.	-Limited depth and cannot be used to identify NAPLs below the overburden. -Creates potential wall stability problems. -May liberate volatile organic carbon gas. -May create a preferential path for the contaminant. -Increases the waste handling requirement for soil and NAPL that has been removed. -May create potential subsidence issues after backfilling. -Invasive, will cause redistribution of NAPL.
Drilling	-Drilling by means of an auger, percussion drilling, and core drilling to evaluate geological stratigraphy, hydrogeological parameters, and contaminant properties.	-Data collected can be used to update the conceptual model and improve site understanding.	-More than one drilling event will be necessary to characterise the site. -Invasive, will cause redistribution of NAPL to greater depths.
Pump Tests	-Involves the extraction of water from a borehole and the subsequent behaviour of the groundwater in the borehole and adjacent boreholes that allow one to calculate the aquifers hydraulic characteristics.	-Provides important hydraulic parameters needed to predict the extent of distribution of the contaminant plume.	-Invasive, will cause redistribution and mobilisation of NAPL.
Tracer tests	-A method used to determine controlling transport processes and parameters in groundwater assessment. Involves the injection of a stable tracer and monitoring the advection and dispersion of it in multiple boreholes.	-Some dyes can be analysed quick and effectively on site. Non- invasive method.	-Some tracers have very high costs for analysis. -Often the position of boreholes is not directly in the flow direction and the flow direction may change along the flow path. -Time consuming and cost intensive.

Method	Description	Advantages	Disadvantages
Visual examination of soil/rock samples	-The presence of NAPLs may be observed initially during drilling or the collection of soil and rock samples. Dark-coloured DNAPLs seen in residual pores and pools are evident. -If the DNAPL cannot be observed, screening can be done by methods such as ultraviolet (UV) fluorescence, soil-water shake tests and vapour analyses of soil samples.	-All methods (observation, UV fluorescence, soil-water shake tests, and vapour analyses of soil samples) are in expensive and if there is a successful identification, it could limit the amount of laboratory tests done to determine the presence of a NAPL.	-Invasive drilling or excavation methods are needed that may mobilise the NAPL.
Borehole logging (Geochemical logging)	-Involves the use of a multimeter probe that measures chemical parameters in a borehole at any given depth. -Chemical parameters include conductivity, pH, temperature, redox potential, and dissolved oxygen. -Helps to identify fractures that transport more saline water and dissolved contamination plumes.	-Can identify the location and delineate fractures and dissolved contaminated plumes respectively. -Can determine the redox potential and dissolved oxygen in layers that may give an indication of the amount of natural attenuation that would take place. -Used to determine hydraulic variation in a profile and in turn, the geological profile to identify migration paths. -Inexpensive. -Non-invasive method.	-As a stand-alone method, it has limited value as it cannot be used to determine the magnitude and direction of flow.
Borehole logging (Interface meter)	-An interface meter detects the boundary between air/water, air/NAPL, and NAPL and water. When lowered into a borehole it can be used to identify the interface where LNAPLs and DNAPLs exist so that the thicknesses can be calculated.	-Can be used to identify and locate the NAPL. Can be used to determine the thickness of the NAPL.	-The NAPL layer is difficult to detect when it is mixed with sediment, when it is conductive, or when it coats the probe. The thickness of the NAPL in the borehole is not related to the thickness in the surrounding formation, however, this unknown thickness can be determined if the capillary properties, borehole construction material, and NAPL properties are known.

Method	Description	Advantages	Disadvantages
NAPL, water, rock, and soil sampling	-Involves the collection of NAPL, water, rock and soil samples to be tested for physical and chemical properties.	-Chemical and physical properties of all material present in the subsurface can help reduce and contain chemical migration and determine effective remediation requirements if it is needed at contaminated sites. -Water sampling is non-invasive if water samples are obtained using a bailer.	-Invasive drilling, excavation methods, pumping techniques used to retrieve water and NAPL samples are needed and may mobilise the NAPL. -Sampling tends to disrupt the environment. -When samples have NAPLs in them, cross contamination is always a concern in these cases. -Expensive procedure.
Conceptual site models	The conceptual model is defined as a snap shot of the site ant a particular time. It combines historic data available and data collected during the site assessment to create an integrated, dynamic, site model for understanding, management, and or remediation. Because the subsurface cannot physically be seen, conceptual models are essential to any site investigation.	-Improves understanding for decision making in regards to managing and monitoring a site. -Cost effective procedure and decreases managerial costs. Effective way to incorporate all information gathered. Non- invasive method.	-It needs to be updated regularly. There should be an initial conceptual model created using historic data and assumptions. Data collected thereafter should be incorporated into the conceptual models.
Modelling	-Modelling involves transferring the conceptual model to a digital computer modelling while using numerical and analytical methods to recreate the dynamics of the site and predict future risks and simulate intervention methods.	-Improves qualitative understanding of the environment that can add value. -Used as a tool for future predictions that will aid management. -May predict the relative rate and extent of migration in the field under different conditions. -Non- invasive method.	-Time consuming. A large amount of data is required. -There are many limitations and assumptions involved and this compromises the accuracy of the results and can be misleading. -It becomes very simple and therefore cannot be used for quantitative understanding. Can be expensive.

Assessments outlined by the United States Environmental Agency and the United Kingdom Environment Agency are far less comprehensive than Gebrekristos *et al*. (2008). The United Kingdom Environment Agency states that a site assessment should include site use/site history, aerial photographs, maps, and plans, screening of soil and rock borings, laboratory analysis of soil and water samples, and borehole logging using an interface meter (Kueper *et al.*, 2003). The United States Environmental Protection Agency's site assessment documents the use of groundwater pump test analysis to determine the flow direction, soil and rock borings to determine the character of the subsurface material, water level determination, water and DNAPL sampling, and soil gas surveying. All methods mentions are briefly described in Table 2-4. An additional method included in the hydrocarbon assessment manual is the use of a cone penetrometer (a cone shaped device that is driven into the soil). The resistance generated during penetration can be used to determine the porosity and therefore the characteristics of the soil. Changes in resistance over an area can be used to delineate the free phase occupying underlying pores (Hulling & Weaver, 1991).

All in all, the documentation on field procedures are limited and those that do exist are generic. They tend to mention every field procedure as a means of assessment and this is not viable. With limited time and restrictions in budget, field procedures should be limited to acquire sufficient knowledge in a shorter amount of time.

2.3.1 Numerical modelling of hydrocarbons

In the manual for site assessment as DNAPL contaminated sites, Gebrekristos *et al.* (2008), introduced an important question: "Which is the best modelling tool/package for prediction". The answer to this is there is none. There are different software packages available, however, each one has its own advantages and disadvantages. The answer to the appropriateness of a modelling package lies in the question that needs answering or the problem that needs to be resolved. If the main aim of this project is to delineate the distribution of the free phase, a three dimensional multiphase model would be essential. This will make it easier to conceptualise the contaminated area, while a multiphase model ensures the free phase is considered as the free phase has properties that are different to that of water. In addition, because remediation has been added to this procedure, simulation of remediation options is necessary, preferably using the same package.

There are a number of software packages that accommodate multiphase environments that has not been extensively used in research. Professionals and academics seem to gravitate to

models that are more commonly used in industry as everyone is familiar with the norm. In Appendix these models are summarised, along with their abilities as well as their downfalls. From all the multiphase models included, UTCHEM is the only package that covers the following essential requirements:

- three dimensional
- multiphase
- models both LNAPLs and DNAPLs
- models an extensive range of remediation options

With that said, it is the only model that is recommended in the manual for site assessments at DNAPL contaminated sites in South Africa and the manual proposed by the United States Environmental Protection Agency.

UTCHEM has been extensively used and cited in research that will be discussed later in this dissertation. Many studies have been conducted on the transportation of hydrocarbons in groundwater. These reports focus on modelling either the LNAPL or DNAPL, while simulating biodegradation and natural attenuation within the aquifer. Other projects focus on simulating how the plume will behave with various means of rehabilitation. UTCHEM has a large number of capabilities including (Reservoir Engineering Research Program, 2000):

- Dispersion
- Dilution
- Absorption of oil, surfactant and polymers
- Capillary pressure
- Phase behaviour
- Organic biodegradation
- Multiple organic species
- Equilibrium and non-equilibrium organic dissolution in aqueous phases
- Polymer properties: shear thinning viscosity, inaccessible pore volume, permeability reduction, adsorption

The Reservoir Engineering Research Program (2000), mentions that UTCHEM has been frequently used in numerous studies to graphically demonstrate surfactant enhanced aquifer remediation (SEAR). Along with SEAR modelling, other software applications also include thermally enhanced remediation processes, the migration of radionuclides, flow and transport of NAPLS in the saturated as well as unsaturated zones, the movement of dissolved contaminates of NAPL origin, biodegradation and natural attenuation. Examples are given in the UTCHEM

technical documentation of different projects where modelling scenarios enhanced the rehabilitation design. It facilitates the uncertainties within the complex subsurface environment (Reservoir Engineering Research Program, 2000).

In research conducted by the University of Texas, two SEAR models were created at the Hill Air Force Base Operational Unit 2 located north of Salt Lake City, Utah. UTCHEM was used to determine the injection and extraction rates, amount and composition of surfactant, duration of flooding before extraction, and the concentration of contaminates in extracted effluent. The first simulation was an initial flood model to demonstrate injection and downstream extraction and to enhance the second phase of the project. UTCHEM predictions were fairly accurate when compared to field observations and therefore little changes needed to be made to the second phase model. Phase two included pre-flooding of sodium chloride (NaCl) to increase the salinity, surfactant flood, and tracer test followed by an extraction period to improve the recovery of the effluent. The second model had to be modified as the ideal organic chemical concentration was met after eighteen days and not the thirteen days predicted by the software. This is due to pumping variations that had to be made in the field. It is important to note that the model will not always be as accurate as a real life scenario but in this case the objectives were met within three weeks. There was a 99 % reduction in the contaminant concentration and field data helped improve the model to be able to determine that the maximum concentration limit of 0.005 mg/l for TCE will be achieved within 55 days of continued water flooding (Reservoir Engineering Research Program, 2000).

The second study was conducted at the Marine Corps Base Camp Lejeune in Carolina. Another SEAR model was created to approve a remediation plan. Simulations ran in UTCHEM were used to meet the following objective:

- Determine the duration of a test segment
- Determine the amount and composition of the surfactant
- Determine the design parameters such as number of boreholes, borehole location and injection and extraction rates
- Estimate the amount and composition of effluent removed from site
- Determine the amount and composition of contaminants that cannot be recovered after remediation

One hundred and fifty five varieties of surfactants were simulated in order to maximise the product options. The results obtained provided critical guidelines for the process design such as well field design, borehole abstraction rates, the frequency of sampling, analysis of effluent, and the mass and composition of effluent needed for surface treatment (Reservoir Engineering Research Program, 2000).

A number of short studies were conducted by research bodies with specific goals and objectives, including:

- Bernardez's *et al.* (2009) validation of UTCHEM with supportive laboratory experiments. The injection of surfactant Hostapur SAS-60 and two alcohols were used to recover diesel from a sand column. In both demonstrations, the physical experiment and numerical simulation, the entire diesel plume was recovered. The study additionally found that the use of equilibrium conditions leads to an underestimation of diesel migration.
- Ouyang's *et al*. (2001) simulation of the formation and migration of the micro-emulsion phase during surfactant flooding. Three simulations were modelled, surfactant flooding, the injection of a saline solution, and the addition of Calcium chloride in a high salinity environment. Results show that mobilisation of the free phase is initiated once the surfactant reaches the critical micelle concentration (CMC). It was also found that UTCHEM could be used as a tool to determine the optimal salinity needed to enhance recovery.
- Sedaghat's *et al*. (2013) prediction of recovering in a fractured medium with the use of a polymer. Micromodels were utilised for the microscopic analysis of polymer flooding and how they react in a fractured medium. Results indicate that fractures increase recovery regardless of orientation. However, the rate of recovery is significantly improved when fractures are orientated parallel to the flow direction. There was a good correlation between experimental and simulated data.
- Silva's *et al*. (2012) variable modification to improve recovery by enhancing viscosity. Again, the software was validated by experimental data. Using polymer xanthan gum increases the sweep efficiency by 90%. Other variables that are dependent for recovery include layering or strata, the position of layers and the contrast in permeability between layers.
- Liang's & Falta's (2007) remediation model using a co-solvent. UTCHEM was used to simulate a field scale test to remove a DNAL plume using ethanol. Results illustrate that when ethanol is injected, at high concentrations, the LNAPL/water/alcohol form one single mobile phase. An uncalibrated model was able to accurately predict the surfactant flooding process but the opposite was true for the removal of the free phase.
- Agaoglu's *et al*. (2012) laboratory experiments and numerical modelling of ethanol flooding at different concentrations. Physical and numerical data suggests that the greater the concentration of ethanol, the better it performs as a co-solvent for NAPL removal. Simulations were conducted repeatedly using, one–, two-, and three-dimensional models. The trend illustrates that two- and three- dimensional geometries are more accurate for reasonable modelling.

These studies are a few among many examples where UTCHEM has enhanced the remediation process. UTCHEM is a facilitator for many environmental professionals and research groups in understanding the behaviour of NAPLs in a medium that has so many uncertainties itself.

CHAPTER 3: STUDY AREA

3.1 Background

As mentioned in the introduction, the industrial site is located within the Durban harbour and will be used as a case study to develop the methodology. It is located south of the city along the eastern shore of South Africa as seen in Figure 3-2. The port was developed in the 1910s for economic growth. It became a hub for the transportation of coal and timber. To the south of the harbour, the area was reclaimed and used as an oil storage site. Due to location and favourable distance from Johannesburg, Durban's harbour became the leading port in Southern Africa (Lumby, 1992).

The port was created during World War I, after pressure for extensions and development of the railway and harbour systems were needed for increasing numbers of military vessels. In later years (1922-1923), the conversion of coal to oil powered vessels introduced the establishment for offloading and storage sites reserved within the industrial area. The second phase of development from 1924-1939 marked a time of rapid industrial growth. The Port of Durban was a major link in the import and export of sugar, wool, hides, barks, fruit, maize, fertilizer, timber, and iron-steel ware (Lumby, 1992).

Further increases in activity of passengers and ships resulted in greater oil demands and the extension of storage in the industrial site area. Even the Great Depression in the 1930s did not damper the development within these years and the Port still remained the leading shipping base for trade and tourism in the nineties (Lumby, 1992). According to an article published in the econimist in 2016, the Port of Durban is the largest in sub-Saharan Africa (Anon, 2016).

3.2 Climate

The climate of the Natal coast is characterised as subtropical. Summers and winters are both warm and very humid (Mucina *et al*., 2006) while rainfall occurs mainly throughout the warmer months from December to February. Rainfall is derived from tropical and mid-latitude weather systems. Warm moist air from the Indian Ocean is transported by advection to land where a low pressure zone exists. This creates frequent, intense cumulus convective rain over the summer months (Kelbe *et al.*, 2001).

The average minimum and maximum monthly temperatures are 5.8 ˚C and 32.6 ˚C, respectively (Mucina *et al.*, 2006), while the average annual rainfall is approximately 1000 mm/year (Jury & Melice, 2000). Figure 3-1 is a bar graph representing the amount of rain that occurs through the year. It is clear that rainfall is more significant from October to March from the figure.

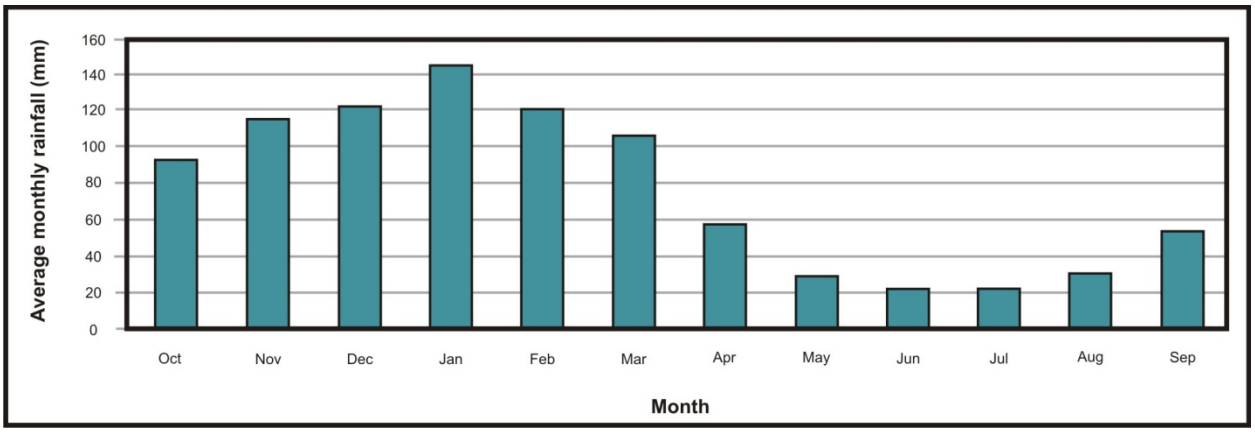

Figure 3-1: Graph representing the average rainfall for each month for KwaZulu Natal obtained from the Department of Water and Sanitation (undated).

3.3 Topography

As seen in Figure 3-3, the topography directly along the coast varies from 0 m to 250 m above sea level. The light green colour represents low lying areas whereas the dark green is representative of higher altitudes. The elongated patches represented by the dark green colour along the coastal boundary indicate steep dune formations that are typical of beach environments.

3.4 Geology

The surface geology found along the coast consists of the Maputaland sands as well as Tertiary silcrete and calcrete material transported by tidal currents and coastal winds. This alluvium forms a thin layer of unconsolidated material.

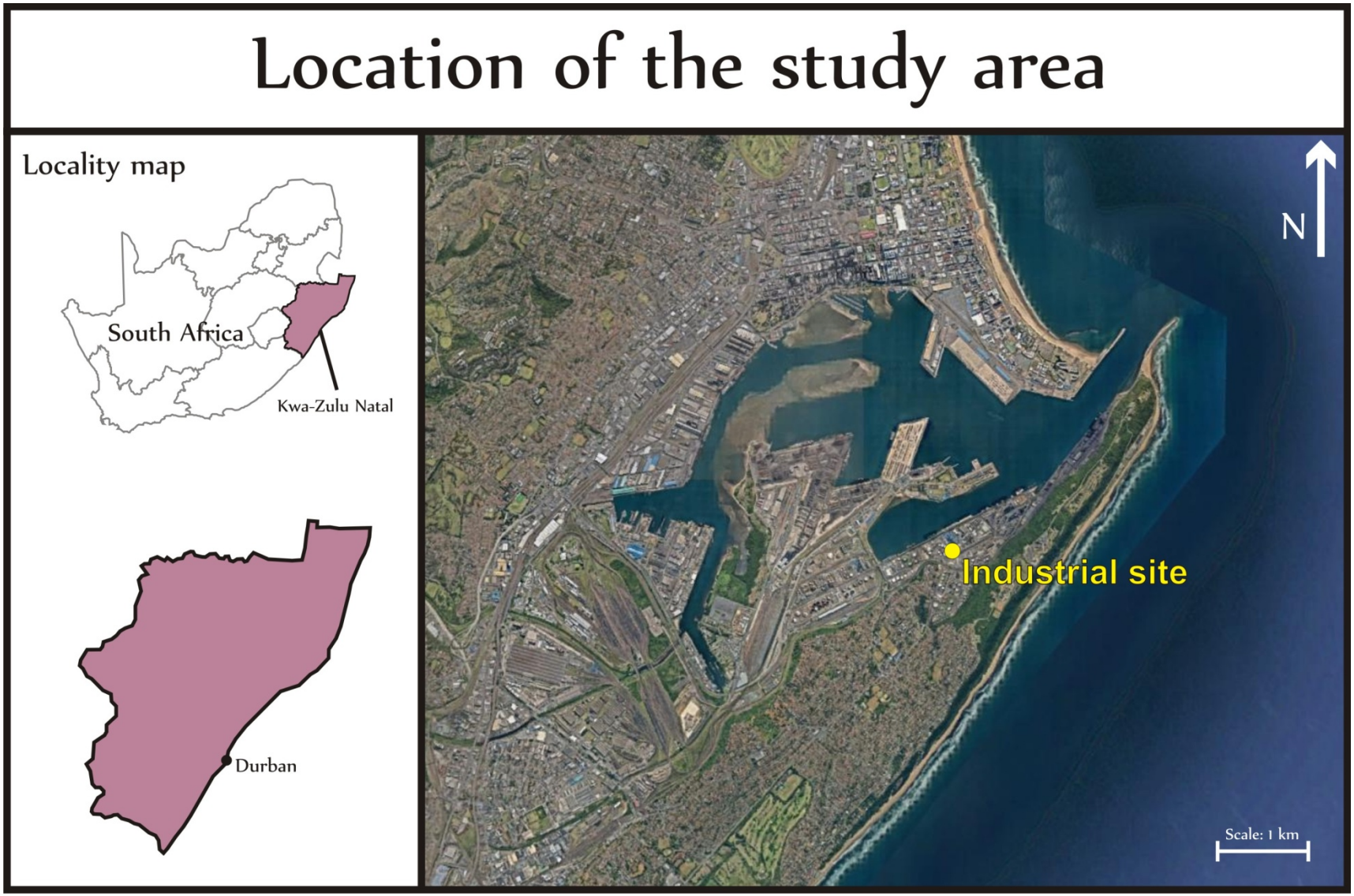

Figure 3-2: Location map and satellite image depicting the location of the industrial site (Google Earth, 2017).

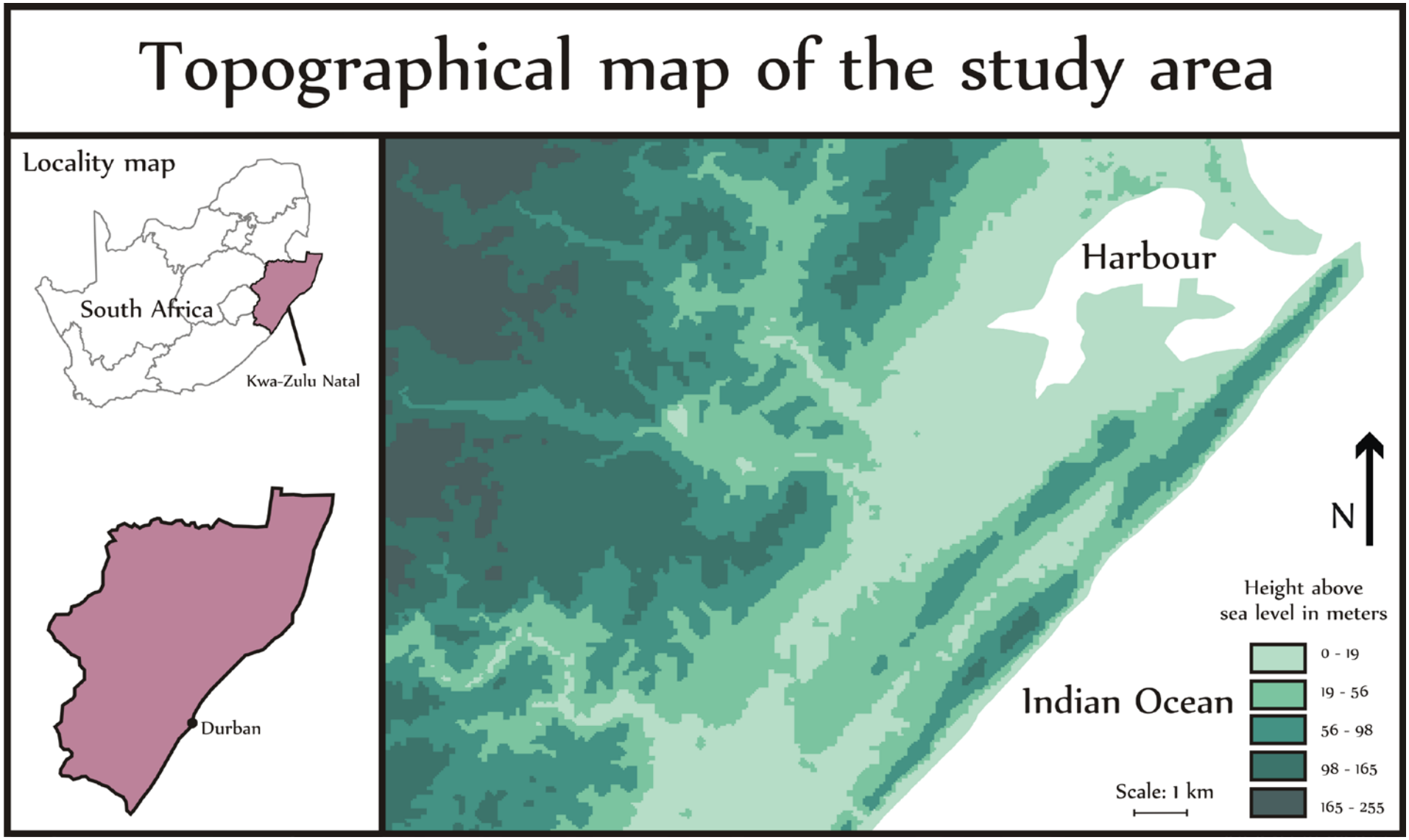

Figure 3-3: Map illustrating the topography of the study area.

Figure 3-4 is an illustration of the surface geology located in the area. There are three different types of sedimentary deposits: decalcified sand, dune sand and limestone.

The Zululand Group directly underlies the Maputaland Group and comprises of a thick sequence of Cretaceous siltstone and minor sandstone with shelly layers (Norman & Whitfield, 2006). These sequences form the main hydrological units of the shallow primary aquifer. The groups are differentiated by their pore and grain sizes. The Maputuland Group sediments have larger particles and larger void spaces while the underlying Zululand Group consists of finer clays and compacted layers. The Zululand Group is therefore an aquitard that transports groundwater at a slow rate (Thornhill & Van Vuuren, 2009).

3.4.1 Zululand Group

The Zululand Group is several hundred meters thick and dips towards the east at an angle between 1˚ and 3˚ (Dingle *et al*., 1983). These Mesozoic deposits consist of three formations, the Makatini, Mzinene, and St Lucia Formations (Johnson *et al.*, 2006). The lower sediments formed when the sea level was 100 m below the present water level and consists of beach alluvial and beach deposits. Rock types include chalky sandstone, shale and limestone (King, 1972). Above this division are rocks derived from deep marine water of the continental shelf developed when the coastal plain was beneath sea level and consists of mudstone and siltstone. The sediments are greenish grey in colour with a thin red/yellow layer half a meter in thickness (Worthington, 1978). Erosion and regression of the Zululand Group resulted in the formation of large lakes creating a basin for sediment to accumulate. This marked the beginning of the Maputaland Group (Thornhill & van Vuuren, 2009). Table 3-1 gives a detailed description of the formations of the Zululand Group.

3.4.2 Maputaland Group

The Maputaland Group consists of a number of formations formed by erosion in the glacial period. These include the Uloa, Umkwelane, Bluff, Port Dunford, Kosi Bay, Kwambonambi and Sibayi Formations.

Table 3-2 and Figure 3-5 summarises and illustrates the different formations, the time of deposition, the thickness of each layer and the type of rocks present.

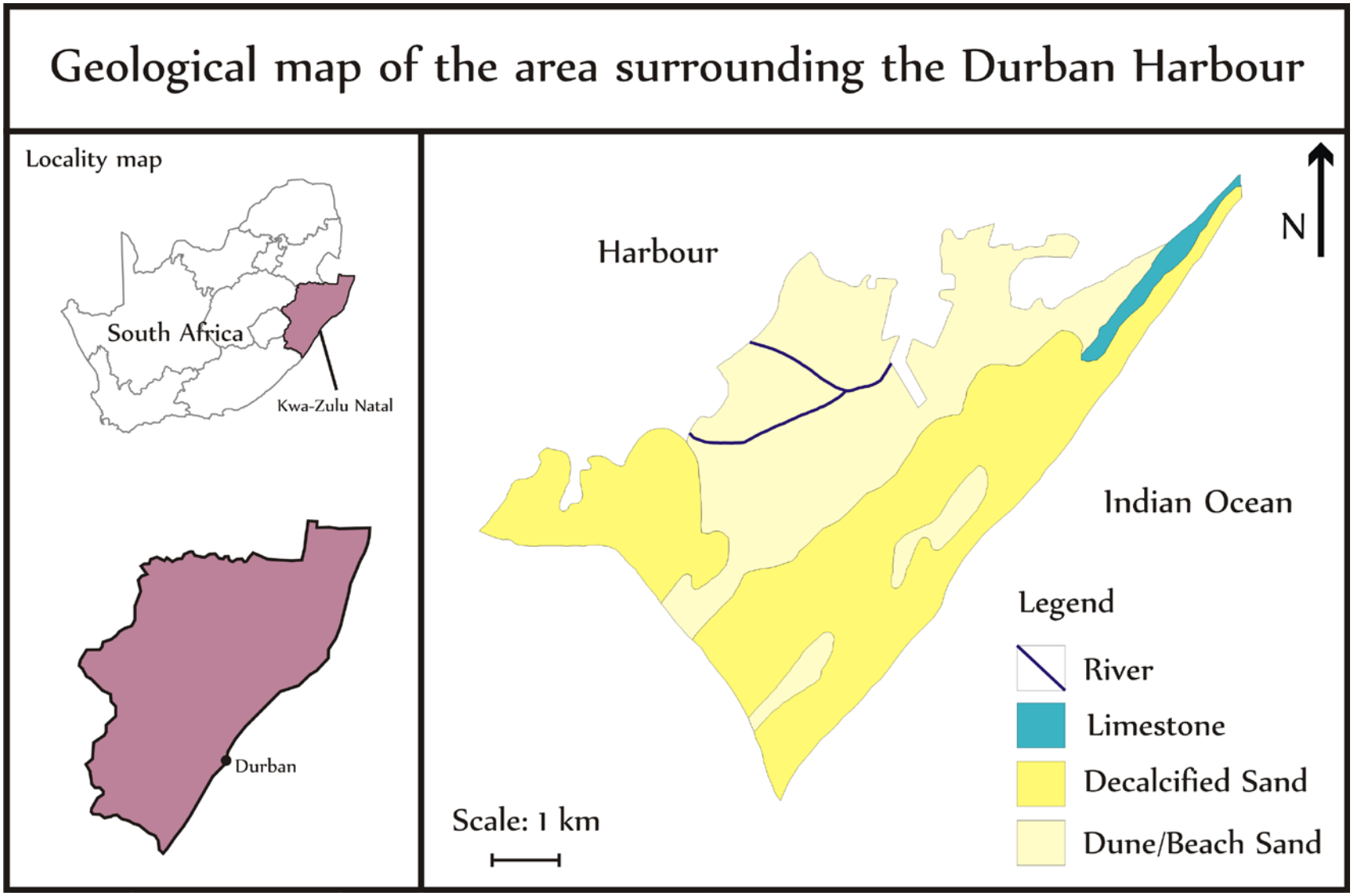

Figure 3-4: Map representing the surface geology of the study area.

Table 3-1: General geological sucession of the Zululand Group (adapted from Johnson *et al.*, 2006).

Formation	Rock types	Deposition environment	Thickness
St Lucia	Shelly glauconic sandstones, bioturbated siltstones rich in fossils	Shallow marine environments & tidal flats	7-900 m (Thickens towards the northern Zululand)
Mzinene	Glauconitic siltstones & cross-bedded sandstones rich in fossils	Shallow marine environment.	>28 m. 722 m of combined Mzinene & Makatini formations have been observed.
Makatini	Agate & volcanic fragment conglomerate, sandstone, siltstone, limestone	Braided streams & tidal flats	>80 m

Table 3-2: General geological sucession of the Maputuland Group (adapted from Mkhwanazi, 2010 & Johnson *et al.*, 2006).

Epoch	Formation	Rock types	Deposition environment	Thickness
Holocene	Sibayi	Calcareous sand Dunes rich in heavy minerals	Shoreline	<150 m
Late Pleistocene	Kwambonambi	Yellow, grey white dune sand, aeolinite, diatomite, peat. (Non-calcareous)	Marine regression, beach	±15 m
Late Pleistocene	Isipingo / Bluff	Aeolianites, calcified beach & dune deposits	Interglacial beach	<50 m
Late Pleistocene	Kosi Bay	Cross-bedded dune sand, calcarenite, carbonaceous sand.	Inland fresh water lake	Average of 45 m
Mid Pleistocene	Port Dunford	Mudstone, shale, red sandstone, beach sand.	Shallow marine	±10 m
Early Pleistocene	Umkwelane	Aeolian cross-bedded calcarenite, high clay content from weathered feldspar & mafic minerals	Shallow marine	25 m aeolianite, 5-8 m calcarenite
Miocene	Uloa	Calcareous sandstone, siltstone, conglomerate, coquina	Littoral zone on palaeoshorelines	±10 m

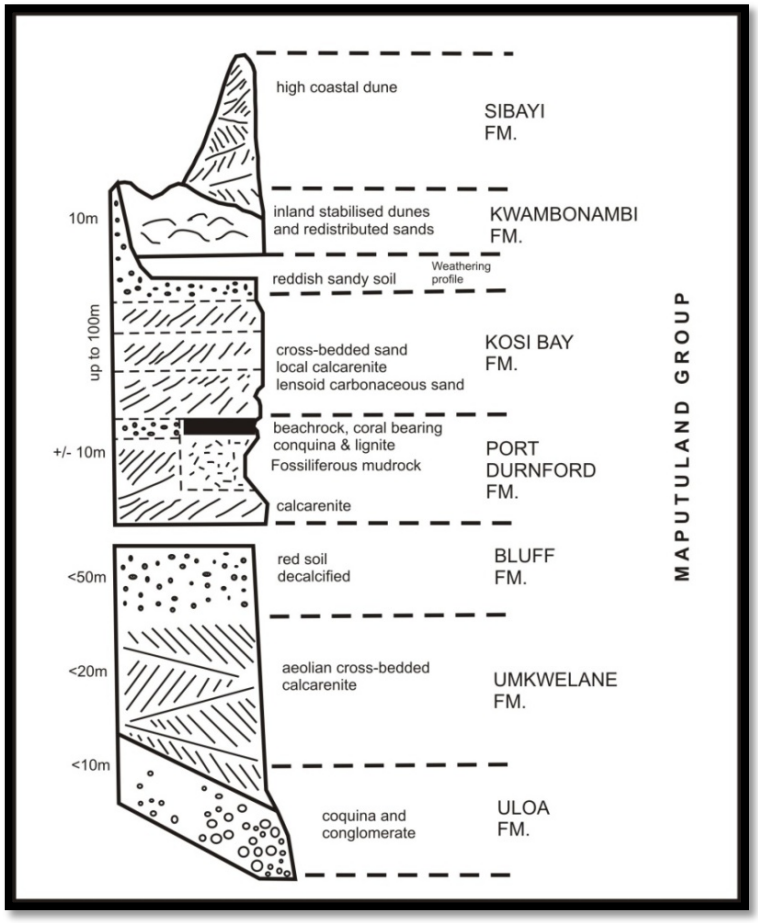

Figure 3-5: Stratigraphic column representing the sequence of formations in the Maputuland Group with their stratigraphic thicknesses. Adapted from Mkhwanazi (2010).

3.5 Geohydrology

The Zululand aquifer is the largest aquifer in South Africa and extends over the eastern coastal plain of Kwa-Zulu Natal. It is a primary aquifer where groundwater is confined to intergranular spaces of sedimentary rocks, unconsolidated material and coastal dunes (Botha & Singh, 2012). For this study area, the aquifer is classified as a coastal aquifer which is defined by Campbell *et al*. (1992), as an unconfined aquifer (the water table is under atmospheric pressure) that intersects the coastline. Coastal aquifers consist of highly transmissive material and are in direct contact with the surface environment. These characteristics make the resource extremely vulnerable to contamination. They can be used effectively for human consumption, however, over pumping may result in the intrusion of salt water making it inadequate for future use (Campbell *et al*., 1992).

According to Botha and Singh (2012), recharge of the Zululand aquifer is 5-18 % of the mean annual rainfall with moderate to good borehole yields averaging between 0.5 and 3 *l*/s. Rainfall and infiltration of surface water are the main sources of recharge for unconfined aquifer (Campbell *et al*., 1992). As much as 50 % of boreholes drilled between 20-50 meters along the costal dunes yield 2 *l*/s of water (Botha & Singh, 2012). As referenced by Campbell *et al.* (1992), the Department of Water Affairs and Forestry (1986), states that coastal aquifers in South Africa can yield between 5 and 30 % of the volume stored, however, the water supply is highly variable as it is dependent on the amount of recharge. This makes these aquifer systems sensitive to drought conditions (Campbell *et al*., 1992).

Groundwater in coastal aquifers almost always flows towards the ocean. This is due to the hydraulic gradient created through recharge inland and discharge along the coast into the ocean. This flow direction can only be reversed if the abstraction rate exceeds the total recharge. Along with the sea and other oceanic bodies, vegetation on the surface is a good indicator of groundwater discharge for example marshy areas where the water table is very close to the surface (Campbell *et al*., 1992). Discharge is most significant along the coastal boundary, and is dependent on the hydraulic gradient of the groundwater (Harvey and Odum, 1990).

Hydraulic head fluctuations in coastal aquifers are a function of the recharge, evaporation and transpiration. This is dependent on the climatic conditions and the existing vegetation. Water levels are found closer to the surface around coastlines and decrease further away from the shore. Dunes however react differently as they are very permeable. Groundwater can be found tens of meters below the surface in high dunes where plant roots are not able to reach, however, small plants may utilise water held within pores against gravitational forces (Campbell *et al*., 1992; Kelbe & Germishuyse, 2010). The depth of the water table in dunes is dependent on the permeability of the material, thickness and width of the dune. The water level will increase if the width and length of the dune is large enough or if there is an underlying impermeable boundary where groundwater can accumulate (Campbell *et al*., 1992).

The chemistry of groundwater is a function of factors such as the amount of recharge, sediment of the aquifer, residence time, and depth of the aquifer, abstraction and contamination. The salinity is dependent on salt water intrusion, evapotranspiration, salt leaching from sediment, weathering of parent material, retention of salts by plants, the retention time of the water in the aquifer and sea spray (Campbell *et al*., 1992). Bacteria on the other hand is said to be effectively filtered by sand dunes and does not pose a threat to the contamination of primary shallow aquifers (Botha & Singh, 2012).

Campbell *et al.* (1992), created a database for all coastal aquifers in South Africa using information gathered from reports from different persons and organisations. Table 3-3 summarises the geohydrological parameters relevant to sediment found in the east coast of South Africa in and around the Durban area.

Table 3-3: Physical characteristics of coastal aquifers found on the east coast of South Africa (Compiled from Campbell et al., 1992)

	Porosity (%)	**Transmissivity (m^2/d)**	**Hydraulic conductivity (m/d)**	**Yield**	**Recharge ($m^3 \times 10^6/yr$)**	**Storage coefficient**	**Rainfall (mm/yr)**
Richards Bay Recent estuaries & dune sands	20	15-20	2.5 - 16	500 $m^3/d/km^2$	0.28047	5.7×10^{-2}	900 - 1300
Lake Sibayi & Lake Kosi	10	40		12.8 l/s		1×10^{-3}	
St Lucia	20 - 50		25 - 0.10368				700 - 1300

CHAPTER 4: METHODOLOGY

4.1 Introduction

The subsurface is a complex environment and is often simplified for the purpose of understanding. It is for this reason, difficult to make decisions for rehabilitation and management options. Numerical models allow one to recreate the processes within the groundwater system to a degree of certainty. In this case they are used for two major reasons:

1. To determine whether a contaminant threatens a water body. In other words, the risk of a contaminant reaching active water resources.
2. To determine and implement the most effective rehabilitation and management plan.

A number of simulations can be conducted that will reduce the number of field trials taking into consideration all project needs and limitations. The computer generated simulation may provide a cheaper, efficient option with less on site alterations required.

In the methodology, data is captured and complied to create both a conceptual model and numerical models. The conceptual model was developed using limited data available and data found in literature. This is then used to create two numerical models.

4.2 Data

Borehole locations and water levels were received from a consultant. A total of 49 boreholes were used that can be identified in Figure 4-1. Appendix B contains a list of the boreholes with their X and Y co-ordinates. All boreholes are located within the vicinity of industrial tanks used for storage of fuel resources. The consultant had agreed to share available information (historic physical and chemical borehole data) on the study area but eventually failed to do so. Thus, additional data needed by the software was found in literature. This included recharge, precipitation, hydraulic parameters, chemical constants and chemical properties. These 49 boreholes were used initially to calibrate the model in MODFLOW, however the calibration process became difficult and a good correlation between observation and model hydraulic heads could not be achieved. For this study, the water level and topographical height showed a low correlation value of 1.65 % and this is uncommon for highly porous aquifers where the watertable is almost parallel to topography.

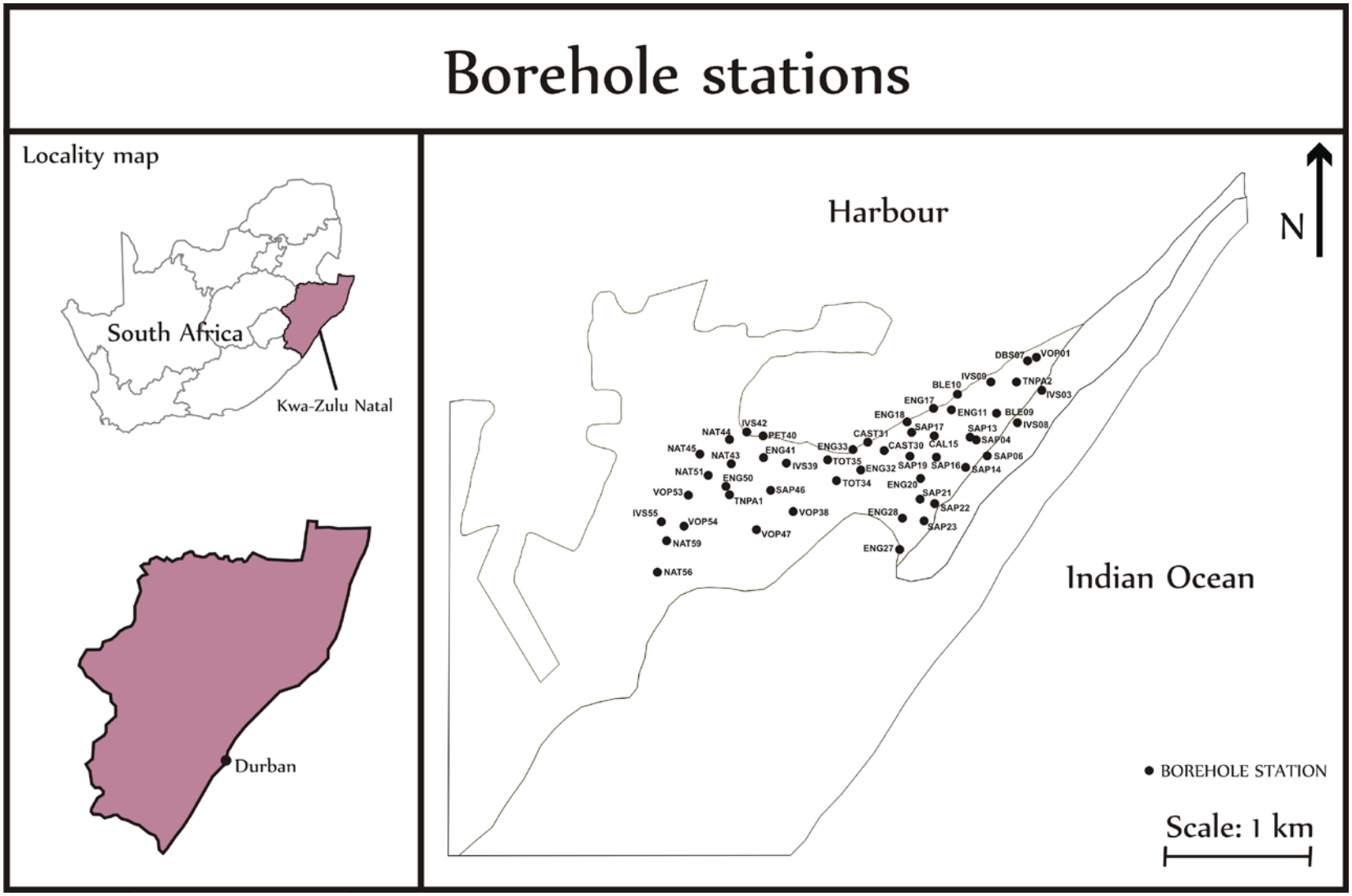

Figure 4-1: Map illustrating the different boreholes and their location in the industrial area.

The relationship between the topography and the hydraulic heads in the observation boreholes is illustrated in Figure 4-2. Milliman *et al.* (1989) states that boreholes along the coast, are often used to extract water, and maintain a constant watertable due to tidal variations, in order to reduce erosion and stabilise sediment caused by wave action. It is unclear whether the boreholes are used to extract water however this may be the reason for the distinct difference between topographical and hydraulic head values.

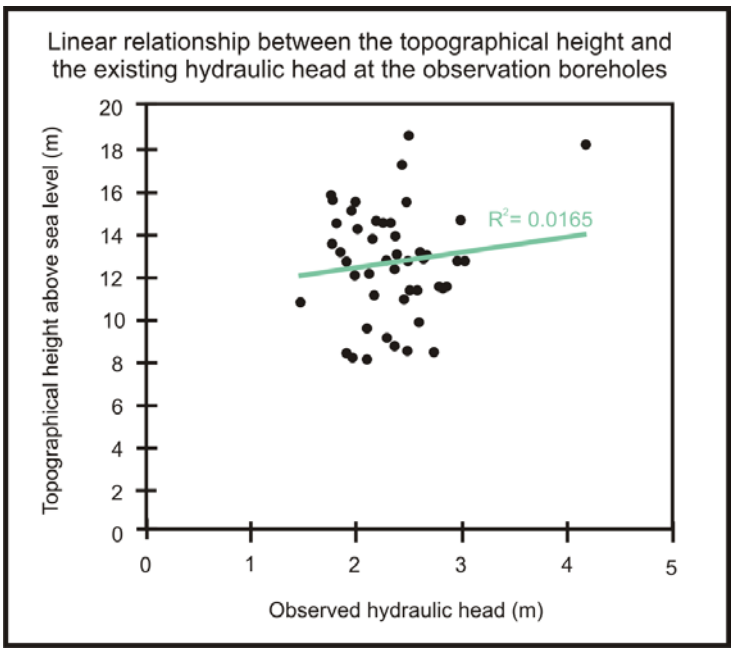

Figure 4-2: A scatter plot graph of the topographical heights versus the observed hydraulic heads.

In any environment you would need the same data that was available (borehole location and water levels) to calibrate a model. If boreholes are used in a smaller, confined area, for example in the vicinity of the storage tanks, there would be an uneven distribution of data causing the water levels to flatten. This would remain a problem if an alternative site is used and the same process would need to be followed with a larger catchment and an even distribution of boreholes. Boreholes were used over a larger area, in order to obtain more accurate water levels in the digital model. An additional 17 boreholes were obtained from consultants, The University of Kwa-Zulu Natal, and the National Groundwater Archive that spread over a larger area. None of the boreholes fall within the Bluff area closest to the shore to measure any tidal variations. These variations are ignored as both software packages used do not account for changes in tides for the calibration and validation of the model. The 17 boreholes used for calibration are plotted in the Figure 4-3, and details with regard to co-ordinates, and observed water levels, and the source of the data are shown in Appendix C.

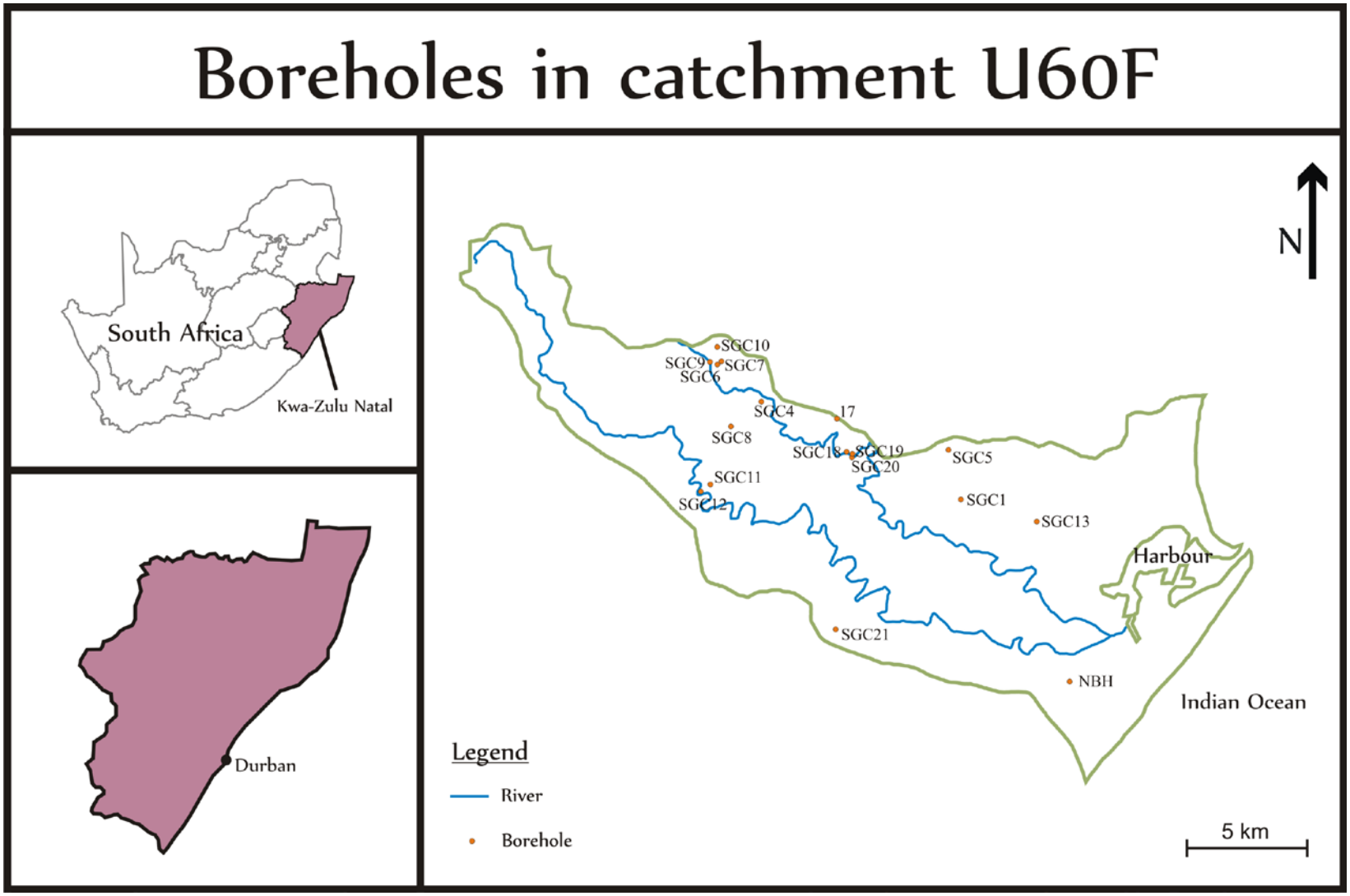

Figure 4-3: Map illustrating the boreholes used for calibration and their location in Durban. The green outline represents the boundary of the catchment

4.3 Software and codes

The initial model was set up in Processing MODFLOW 7. It has a graphical interface that is easy to use and edit. This was done to shorten the initial construction period as it is tedious to create input files for UTCHEM. Once the Processing MODFLOW model was calibrated, the physical parameters could then be transferred to the UTCHEM input file. Finally, UTCHEM was used for all transport, degradation, advection, dispersion and remediation simulations.

4.4 Conceptual model

In order to run the predetermined simulations, a conceptual model was digitised in Processing MODFLOW converting it to a dynamic model. A detailed description of the pre-calibration model will be discussed in this section.

4.4.1 Boundary conditions

The surface water catchment U60F, rivers and coast were digitised and used to assign boundary conditions to the model. The rivers and oceans were digitised as a constant head where the water level remains the same. This boundary runs along the eastern margin. Figure 4-4 illustrates the boundaries of the model. The blue lineation represents the constant head boundary; the grey area represents the active modelling area. Everything that is not included in the diagram was considered to be the inactive area.

4.4.2 Topography and layer thickness

A total number of 2000 points were used in the U60F catchment to interpolate the topography using SRTM data. Figure 4-5 is a diagrammatic representation of the topography used in the model and Figure 4-6 illustrates the topography of a cross section, from point A to point B, in the study area.

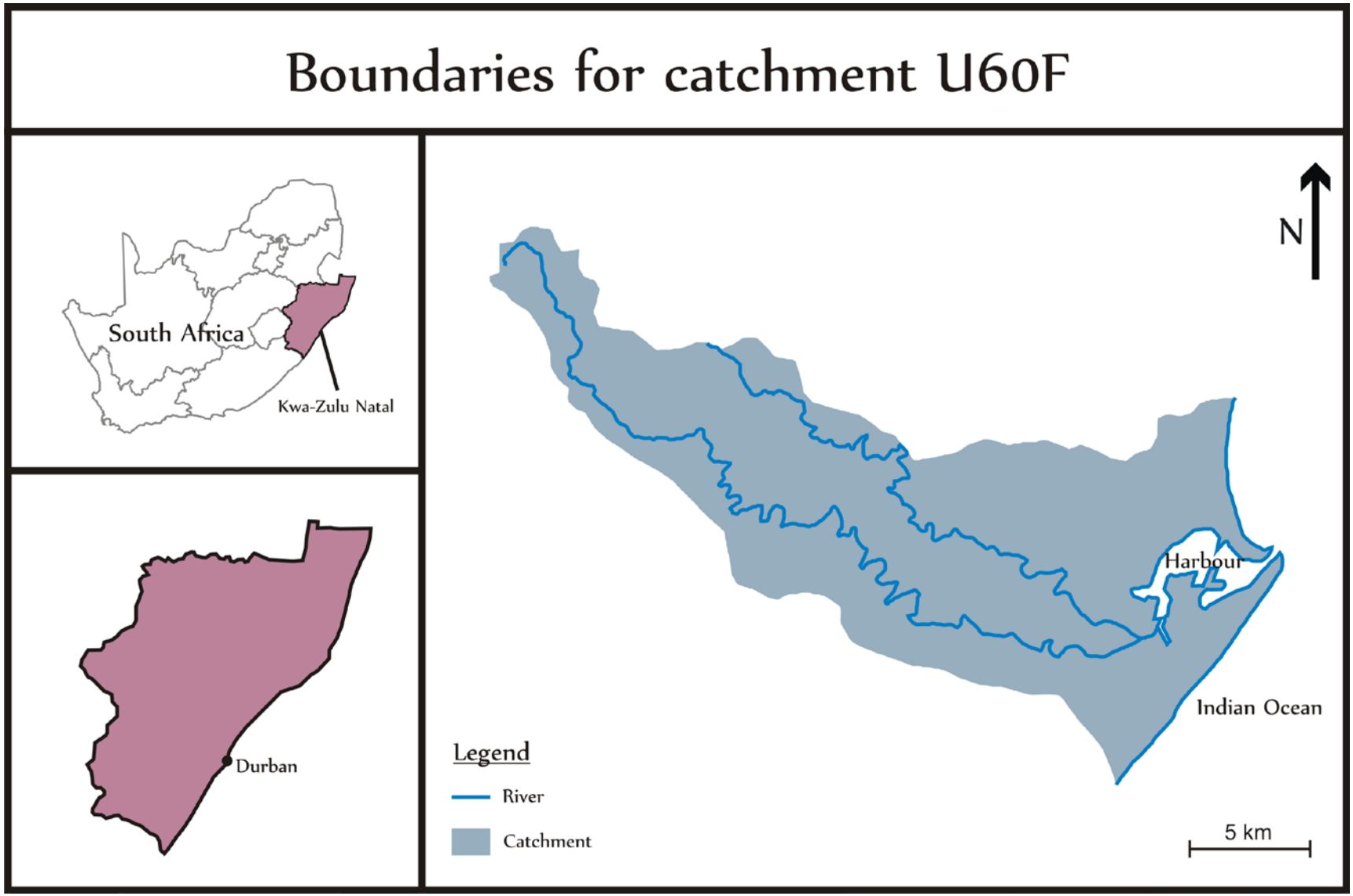

Figure 4-4: Image illustrating the boundary conditions of the model.

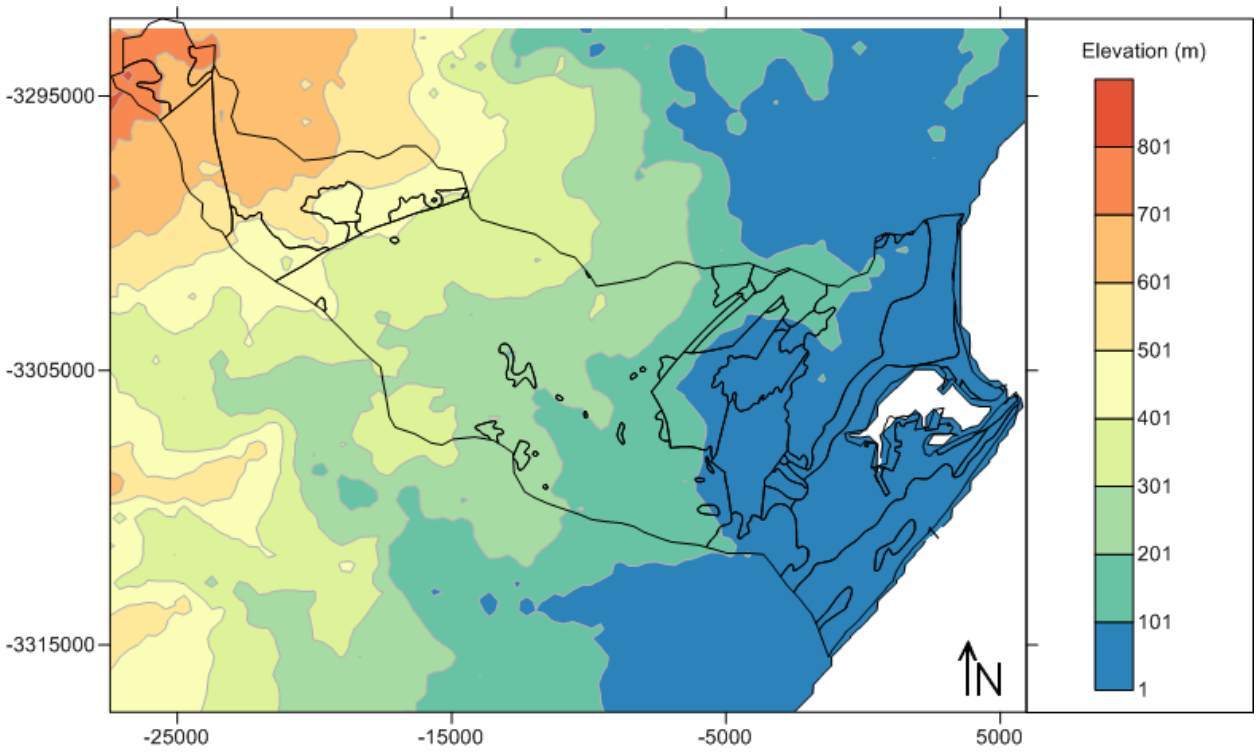

Figure 4-5: Contour map representing the topography used in the MODFLOW model. The black outline represents catchment U60F and the Geology within it.

4.4.3 Aquifer parameters and aquifer type

There were different horizontal hydraulic conductivity values in the model based on the geology of the area. The surface layer consists of different rock units with the following hydraulic conductivities calculated with values obtained from Spitz & Moreno (1996):

1. Dune and beach sand : 31 m/d
2. Decalcified sand : 30 m/d
3. Limestone : 0.05 m/d
4. Dolerite : 0.005 m/d
5. Dropstones with sandstone, mudstone, and shale : 0.1 m/d
6. Shale with think sandstone and siltstone lenses : 0.1 m/d
7. Sandstone, mudrock and conglomerate : 0.1 m/d
8. Granite : 0.02 m/d

The geology for the entire catchment is illustrated in Figure 4-7.

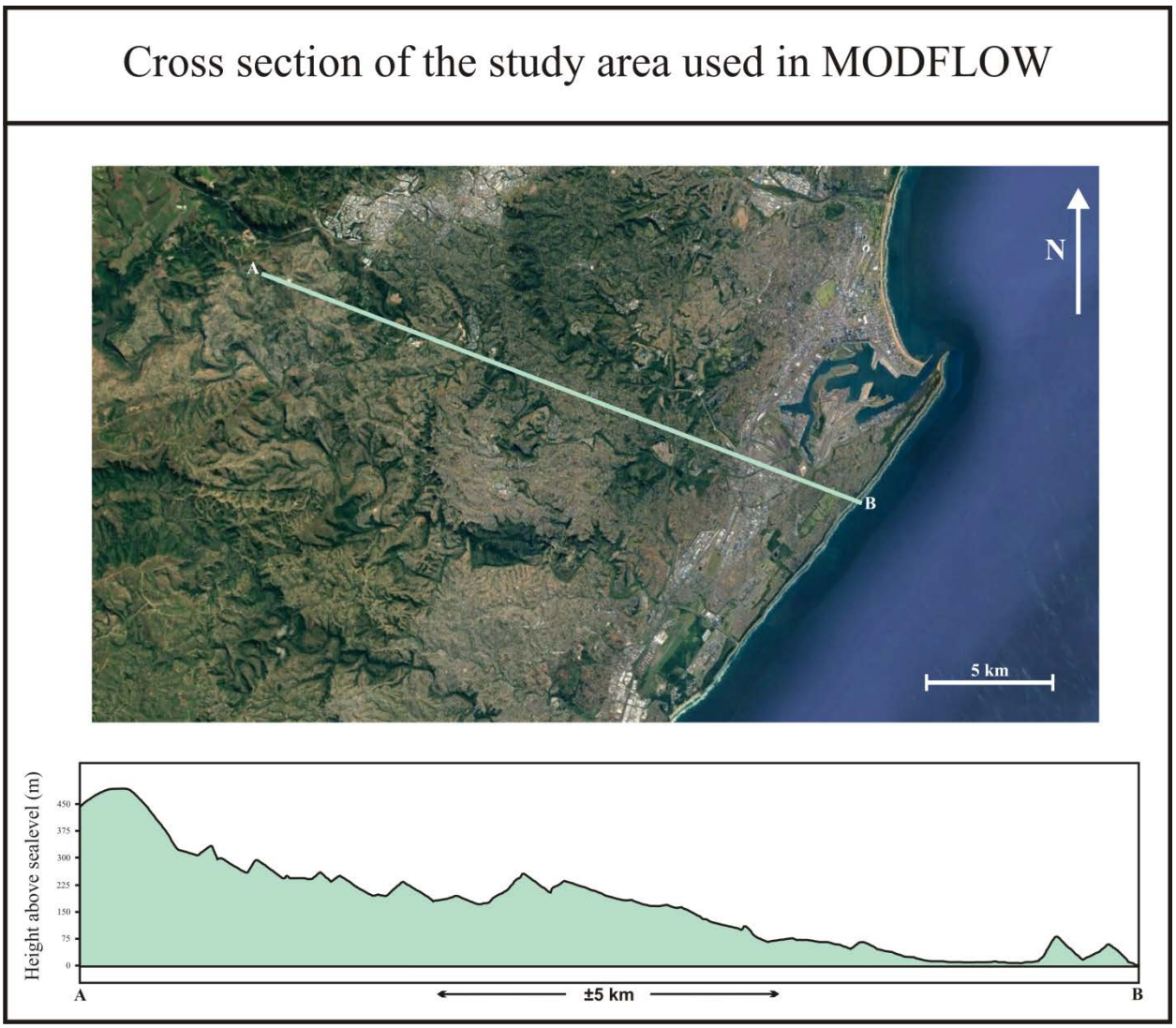

Figure 4-6: Diagrammatic representations of a cross section of the area along transect A-B.

4.4.4 Recharge

Recharge was calculated, using the total annual rainfall of 1000 mm/annum (Jury & Melice, 2000) and a recharge of 8 % (Campbell *et al*., 1992). The model became very sensitive to recharge and the value was therefore decreased from 0.00022 m/day to a values of 0.00015 m/day and 0.00012 m/day in unconsolidated rock material and hard rock surfaces respectively.

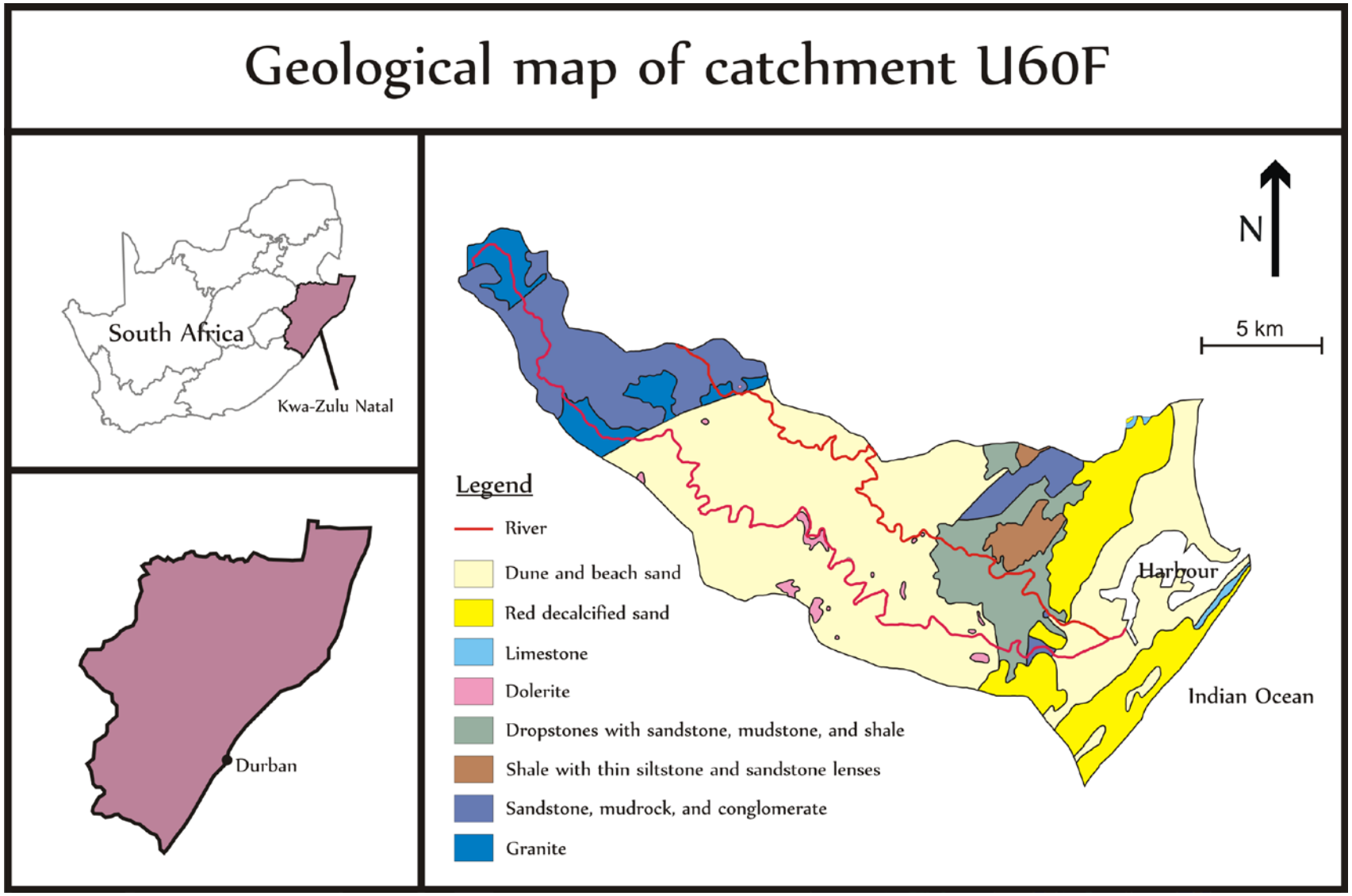

Figure 4-7: Map representing the surface geology of catchment U60F.

4.5 Numerical Model

4.5.1 Mesh size and layer type

The grid created consisted of 250 rows and 335 columns, and a single layer. Each cell was 100 m by 100 m in dimension making the entire surface area of the model 8.375×10^{8} km^2 (25 km × 33.5 km). The layer was defined as an unconfined/confined layer type.

4.5.2 Water levels and flow direction

The conceptualised water table was determined by interpolating the water levels within the 17 boreholes illustrated in Figure 4-3. This is done by using Bayesian interpolation. It is a method of interpolating water level data/values that combines both kriged groundwater contour maps and information from the digital elevation model (Peeters *et al*., 2010). Kriging is a geostatistical technique of interpolation (Khankham *et al*., 2015) that uses linear regression (Lv *et al*., 2013) while the digital elevation model considers the terrain. The problem associated with most interpolation methods is the occurrence of smoothing and isolated spikes where data is overemphasised. The Bayesian data framework method reduces these irregularities to improve the accuracy of the groundwater model (Peeters *et al*., 2010). The water along the shore line was kept at a constant hydraulic head of 0 m above sea level as it represents the sea level boundary. The resulting water levels were represented in a contour map represented in Figure 4-8. The arrows on the map indicate the flow direction while the size of the arrow is indicative of the magnitude of the flow rate. The greater the size of the arrow, the greater the flow rate will be.

4.5.3 Calibration

The model ran in steady state conditions while the hydraulic conductivity values were constantly altered to obtain an acceptable correlation between the initial water levels and the digital water levels. All hydraulic conductivity values were maintain throughout the model with the exception of the sandstone, mudstone, and conglomerate region indicated in baby blue on the north western area in the map in Figure 4-7. Values were significantly increased to 20 and 40 m/d to

the south and north of the northern river in the catchment. With minor alterations, a calibration value of 89.6 % was obtained and is illustrated in Figure 4-9. The calibration is calculated by comparing the simulated hydraulic heads to the actual hydraulic heads observed in the field.

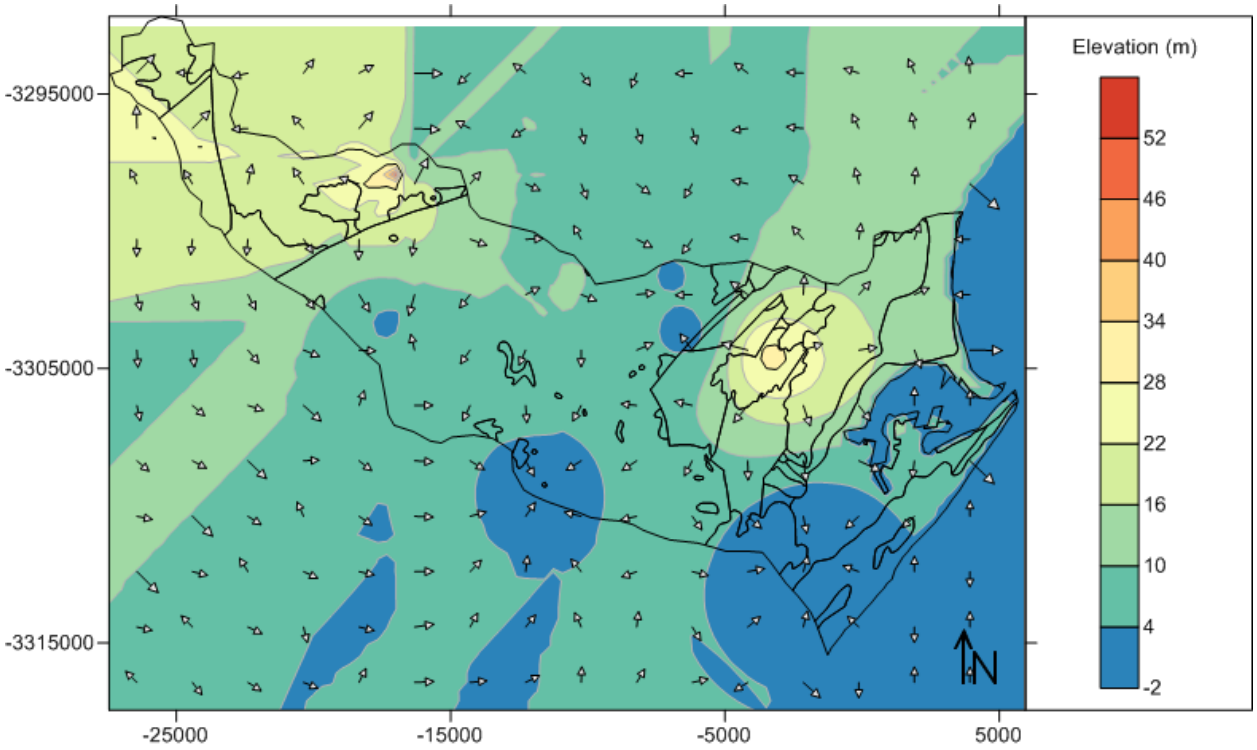

Figure 4-8: Contour map illustrating the hydraulic head, flow direction and relative flow rate used in the MODFLOW model.

4.6 UTCHEM file

The UTCHEM file was created using UTCHEMGUI 9.82. The INPUT file requires a more detailed description of the size, boundaries and properties of the problem area and properties of the components involved, injection and distribution rates, and a description of what needs to be written to the output files. It consists of a number of sections including:

- Title and reservoir description data,
- Output option data,
- General physical property data,
- Physical property data for the geochemical option,

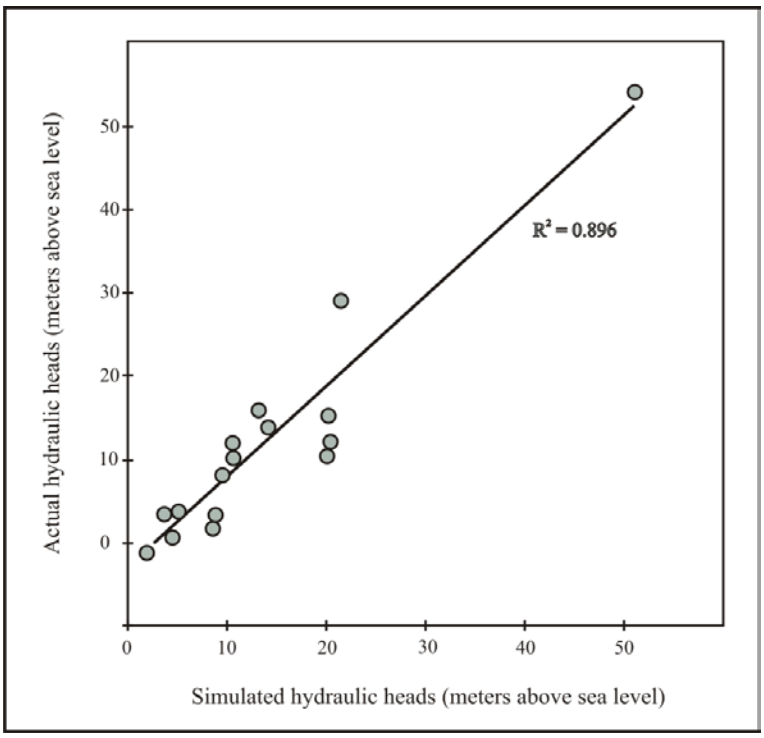

Figure 4-9: Scatter plot graph of the Initial hydraulic heads versus the simulated hydraulic heads.

- Data for biodegradation option if it is considered, and
- Recurrent injection or production data.

4.6.1 General numerical model

Even though the Processing MODFLOW model was generated to be transferred to UTCHEM, the size needed to be much smaller than that originally used for MODFLOW due to code constraints. Only a section of the original MODFLOW grid was used in the vicinity of the industrial area where the initial boreholes and petrol and diesel tanks are located. The number of grid blocks was reduced to 100 × 106 cells in the x and y directions respectively. Original topographical data was used so that the area modelled would represent a smaller version of reality. Lastly, an additional layer was added to determine the difference in vertical migration between LNAPLs and DNAPLs.

The permeability needed to be constant for each layer and instead of using the values calculated during the calibration process, values of 2500 and 700 millidarcies were adopted that represents a permeable dune surface and constraining second layer. The porosity was

estimated to be 0.172 fractions where land existed and 1 fraction where the ocean is found. Standard pressure (101 kPa) and temperature (25 ºC) was used for initial values because the aquifer is shallow and unconfined. Lobmeyer (1985), stated that groundwater temperatures in shallow aquifers reflect the annual mean temperature while Heath (1983), explains that the hydraulic pressure at the water table in unconfined aquifers is equal to atmospheric pressure. A longitudinal and transverse dispersion of 0.5 and 0.0001 respectively for the oleic phase adopted from UTCHEM example files for benzene.

UTCHEM requires chemical data for all compounds involved in each simulation. Organic compounds were simulated separately as the software did not allow for multiple organic species. Table 4-1 contains chemical properties of all compounds involved gathered from different literature for benzene, PCE, surfactant sodium dodecyl sulphate (SDS), polymer xanthan gum and ethanol. If the value is not given, it is not required by UTCHEM.

Table 4-1: Chemical properties of compounds used in the UTCHEM code.

	Type of compound	**Viscosity (cP)**	**Density (g/cm^3)**	**Diffusion coefficient (m^2/d)**	**Equilibrium concentration (volume fraction)**	**Critical micelle concentration (volume fraction)**
Benzene	LNAPL	[1]0.6468	[1]0.8765	[2]9.6×10^{-5}	[3]5.87×10^{-3}	
PCE	DNAPL	[4]0.54	[4]1.623	[5]8.8×10^{-5}	[6]1.227×10^{-4}	
SDS	Surfactant		[7]1.01	Assumed to be 0		[8]2.3328×10^{-3}
Xanthan gum	Polymer			Assumed to be 0		
Ethanol	Alcohol		[9]0.789	Assumed to be 0		

[1](Eby, 2004) [2](Currie *et al.,* 1994a) [3](American Petroleum Institute, 1985) [4](Hulling & Weaver, 1991) [5](Currie *et al.,*1994b) [6](Mccobb & Leblanc, 2002) [7](Hammouda, 2013) [8](Ouyang *et al.,* 2001) [9](Ortega, 1982)

4.6.2 Simulation scenarios

A total of 32 scenarios were created and simulated for benzene and PCE. They include a single general infiltration scenario and five different *in situ* chemical flushing, remediation examples.

The remediation examples were then varied using different concentrations of the remediation fluid and different injection rates. The aim of the simulation was to see where the non-aqueous phase and aqueous phase will migrate and how the remediation fluid will be able to mobilise the free phase to increase recovery. The recovery of the plume was not simulated, again due to model constrains. The six basic simulations include:

1. Infiltration of the benzene and PCE, and natural attenuation (dissolution, advection, and dispersion) over a three-month period.
2. Mobilisation of NAPL with the use of surfactant SDS and polymer xanthan gum for an additional three months.
3. Mobilisation of NAPL with the use of surfactant SDS.
4. Mobilisation of NAPL with the use of polymer xanthan gum for an additional three months.
5. Mobilisation of NAPL with the use of surfactant SDS and ethanol.
6. Mobilisation of NAPL with the use of ethanol.

The non-aqueous liquids were injected at 26 different sites indicated in Figure 4-10. Appendix C contains the X and Y co-ordinates for these boreholes. One volume fraction of benzene and PCE was infiltrated at a rate of 0.25 m^3/d over a period of three months. The positions were chosen based on the proximity of the petrol and diesel tanks. Remediation fluid was then injected at the same locations for an additional three months. The concentration of each remediation compound and the injection rate is indicated in Table 4-2. Each remediation scenario was repeated for benzene and PCE.

4.6.3 Assumptions and Limitations

Due to the constriction of UTCHEM and the extremely complex nature of the contaminant, there were a number of limitations when modelling the area. These include the following:

- Recharge was ignored;
- Pressure and temperature remained constant;
- Permeability was constant over both layers;
- There were two porosity values, one for the land, and another for the ocean;
- The initial model was completely saturated;
- Only the saturated zone was modelled;
- Adsorption of organic compounds was ignored;

- Geochemical modelling (biodegradation and oxidation) was ignored; and
- All values used for the concentration and injection rates were found in literature or assumed for input files available. The concentration of benzene and PCE injected were the same to better compare the results.

Table 4-2: Information regarding the concentration of each compound and the injection rate of the remediation fluid for all mobilisation simulations

Simulation no.	**Injection rate (m^3/d)**	**[Water] (*volume fraction)**	**[SDS] (*volume fraction)**	**[Xanthan gum] (*volume fraction)**	**[Ethanol] (*volume fraction)**
1	100	1	0.5	0.5	
2	100		0.5	0.5	
3	300		0.5	0.5	
4	100	1	1		
5	100		1		
6	300		1		
7	100	1		1	
8	100			1	
9	300			1	
10	100	1	0.3		0.5
11	100		0.5		0.5
12	300		0.5		0.5
13	100	1			1
14	100				1
15	300				1

*Volume fraction is a unit of concentration that refers to the volume of a compound divided by the volume of the entire solution within which the compound is dissolved (Reservoir Engineering Research Program, 2000).

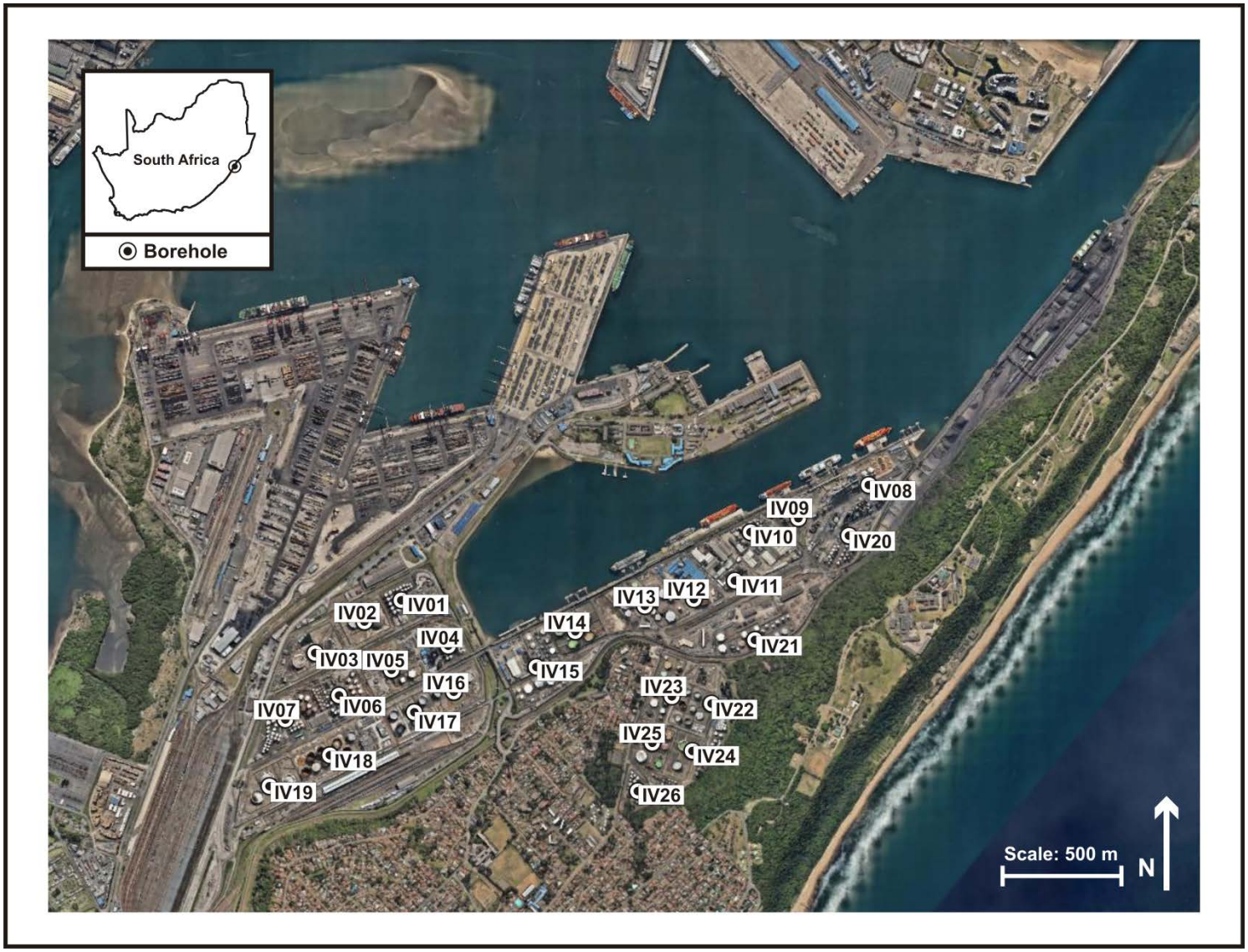

Figure 4-10: Google Earth image of the industrial area located in the Durban harbour.

These limitations will have an effect on the distribution of NAPLs. Pressure and temperature increases disrupt the free phase is such a way to increase mobility. Thermal remediation has been used as a technique to recover NAPLs in groundwater. A study done by O'Carroll and Sleep (2009) concludes that an increase in temperature results in downward migration of the DNAPL and that temperature does not affect LNAPLS (O'Carroll & Sleep, 2009).

The constant permeability used in the UTCHEM model creates a uniform environment and results in unobstructed flow which cannot occur in reality or in the more detailed, calibrated MODFLOW model. Lastly adsorption, biodegradation, and oxidation are all factors related to natural attenuation (Usher *et al*., 2008), if these are ignored, there will be a limited amount of degradation of the free phase into the water. That means that the aqueous phase will be under estimated in comparison to reality while the free phase will be overestimated (Usher *et al*., 2008 and Eby, 2004).

Recharge is the final limiting parameter that is considered in this study. UTCHEM does not have a primary option to introduce recharge into the system and therefore no research was found on the effect of recharge on the sensitivity of the model.

4.7 MODFLOW and MT3D

The code MT3D (an add on of MODFLOW) was used to simulate the migration of the benzene plume. All variables were kept the same as values used in the UTCHEM code to best duplicate the simulation however, the dispersivity needed to be increased due to cell size being larger in MODFLOW. The reason why this was done was to determine the direction of movement and fate of the surrounding environment. Cells of constant concentration were used in the cells where the 26 injection boreholes were located. The concentration remained constant at a value of 6×10^4 µg/l. Once this simulation was complete, the distribution of benzene after 20 years was used as the initial concentration before the contaminant was extracted at a rate of 300 m^3/d over one year. Extraction occurred at the same boreholes used to inject the NAPLs.

CHAPTER 5: RESULTS AND DISCUSSION - UTCHEM

5.1 Introduction

A total number of 128 maps were rendered using Surfer for the 32 simulations, four maps for each including a non-aqueous phase and aqueous phase for both the top and the bottom layers of the model. The maps depict the environment after the completion of the three-month period for the infiltration, migration and natural attenuation of the non-aqueous phase liquid, and after a three-month period for each remediation scenario.

The Surfer images were grouped together so they could be discussed and compared collectively. This chapter will begin with the discussion of the migration and degradation of the LNAPL, benzene, and the DNAPL, PCE. The distribution of each organic compound will be compared in order to better understand the differences in behaviour. Once this is completed, the change in migration of the non-aqueous phase, with the aid of the remediation fluid, will be discussed collectively for benzene and PCE. With respect to this section, only the top layers will be discussed as the remediation only made a significant difference in migration in the first layer. The reason for this can be because the density of surfactant SDS and ethanol are 1.01 (Hammouda, 2013) and 0.789 g/cm^3 (Ortega, 1982) respectively. The density of water is 0.988 g/cm^3 and therefore both the surfactant and alcohol would not sink to greater depths where it would impact the migration of the NAPL. These diagrams have been omitted from the results discussed but can be found in Appendices E-H. The different remediation scenarios will then be compared with the use of line graphs that represents the concentration at specific positions after the simulation has been completed. Lastly, the change in distribution of the aqueous phase will be discussed using the combination of surfactant SDS, polymer xanthan gum and ethanol as the remediation fluid.

The equilibrium concentrations of benzene and PCE are 5.87×10^{-3} (American Petroleum Institute, 1985) and 1.227×10^{-4} (Mccobb & Leblanc, 2002) volume fraction respectively and the compounds do not exceed this concentration in the aqueous phase. The free phase dissolves until equilibrium is reached. As the concentration of the aqueous phase decreases due to advection and dispersion, there will be a shift in equilibrium causing an increase in dissolution. In this manner, the maximum concentration at equilibrium will never be overcome (Kotz *et al.,* 2009). The NAPL concentration did not exceed the injected 1 volume fraction.

5.2 Simulation of the infiltration and migration of Non-Aqueous Phase Liquids

Figure 5-1 and Figure 5-2 contain Surfer maps depicting the extent of benzene (LNAPL) and PCE (DNAPL) after a concentration of 1 volume fraction has been infiltrated at a rate of 0.25 m^3/d. The non-aqueous free phase can be seen in Figure 5-1 while the dissolved plume is seen in Figure 5-2.

In both figures, the greatest mass of LNAPL (marked (a) and (b)) is found in the top layer with minor isolated plumes occurring at certain boreholes in the bottom layer. Benzene accumulates on the surface of the water table and forms a lens shaped structure. As the size increases, the added weight causes it to dip and can be found below the original height of the water table (Palmer, 1992).

Boreholes IV 18, 22, 23, 24, and 25 located further inland have larger plume sizes located directly in their vicinity. Alternatively, boreholes IV 1, 2, 4, 5, 7, 15, 16, and 19 seem to contain little to no contaminant. The reason for this is unclear although the contaminant seems to become trapped in certain areas and distribute and migrate in others to a point where there is none that can be observed. Figure 5-3 and Figure 5-4 are maps depicting the infiltration of benzene and PCE into the subsurface while the vector arrows indication the direction and magnitude of migration. Contamination plumes located below injection points IV 08 – 14 are smaller in size and are distributed towards the ocean within the harbour. These plumes closer to the coastal boundary are smaller than those located inland and the porosity could be the main cause. The porosity of the ocean is set to 1 fraction and the trapping of the contaminant will play a major part in the distribution. The NAPL will slowly seep into the ocean where it can then move freely and distribute over a larger surface area decreasing the NAPL significantly. On the other hand, it is unclear why the contaminated plume below injection boreholes IV 01 - 07 and IV 15, 16, 17, and 19 are so small or non-existent.

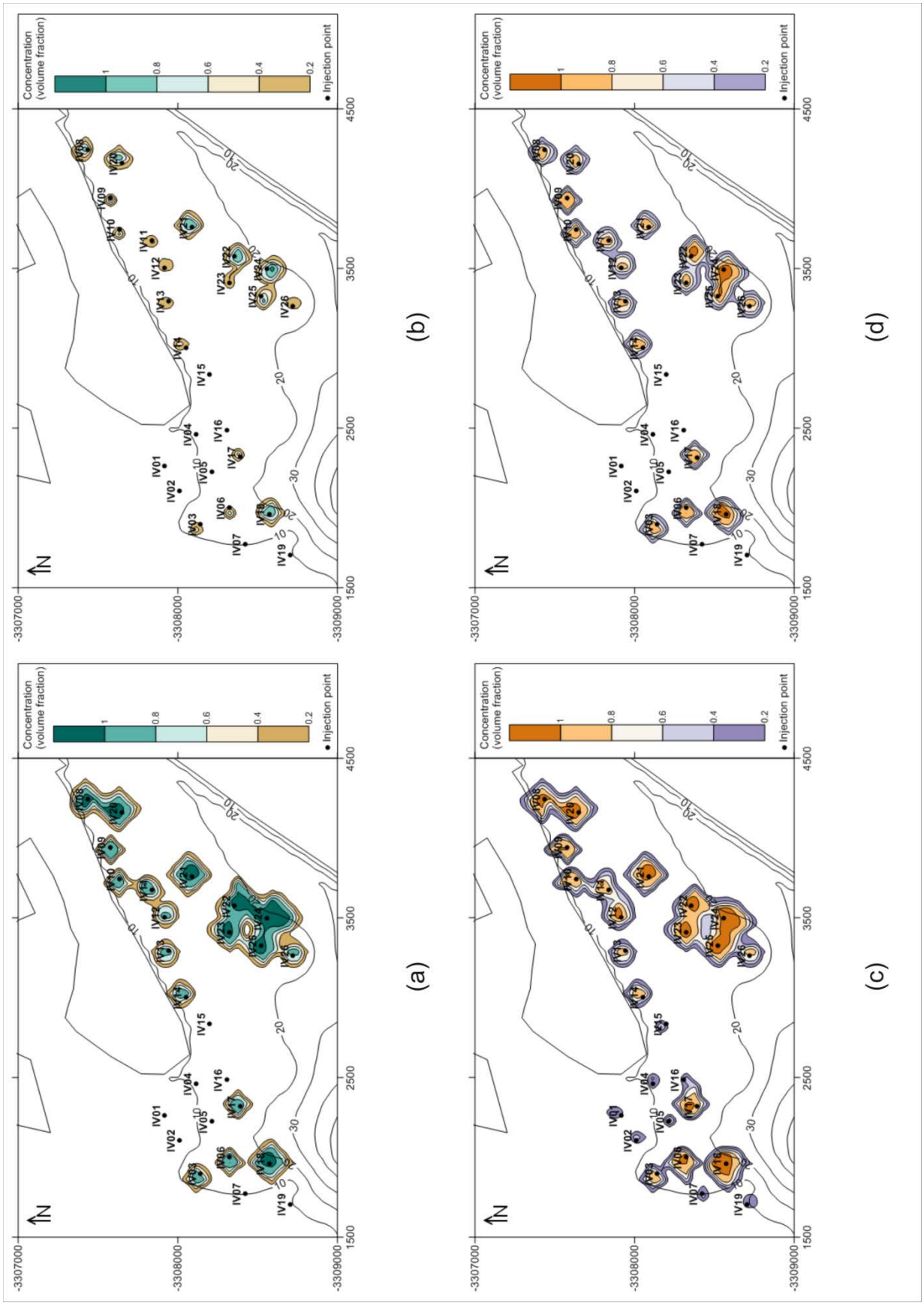

Figure 5-1: Maps illustrating the simulation results for the infiltration and migration of non-aqueous phase benzene and PCE. (a) Benzene in the top layer; (b) Benzene in the bottom layer; (c) PCE in the top layer; (d) PCE in the bottom layer.

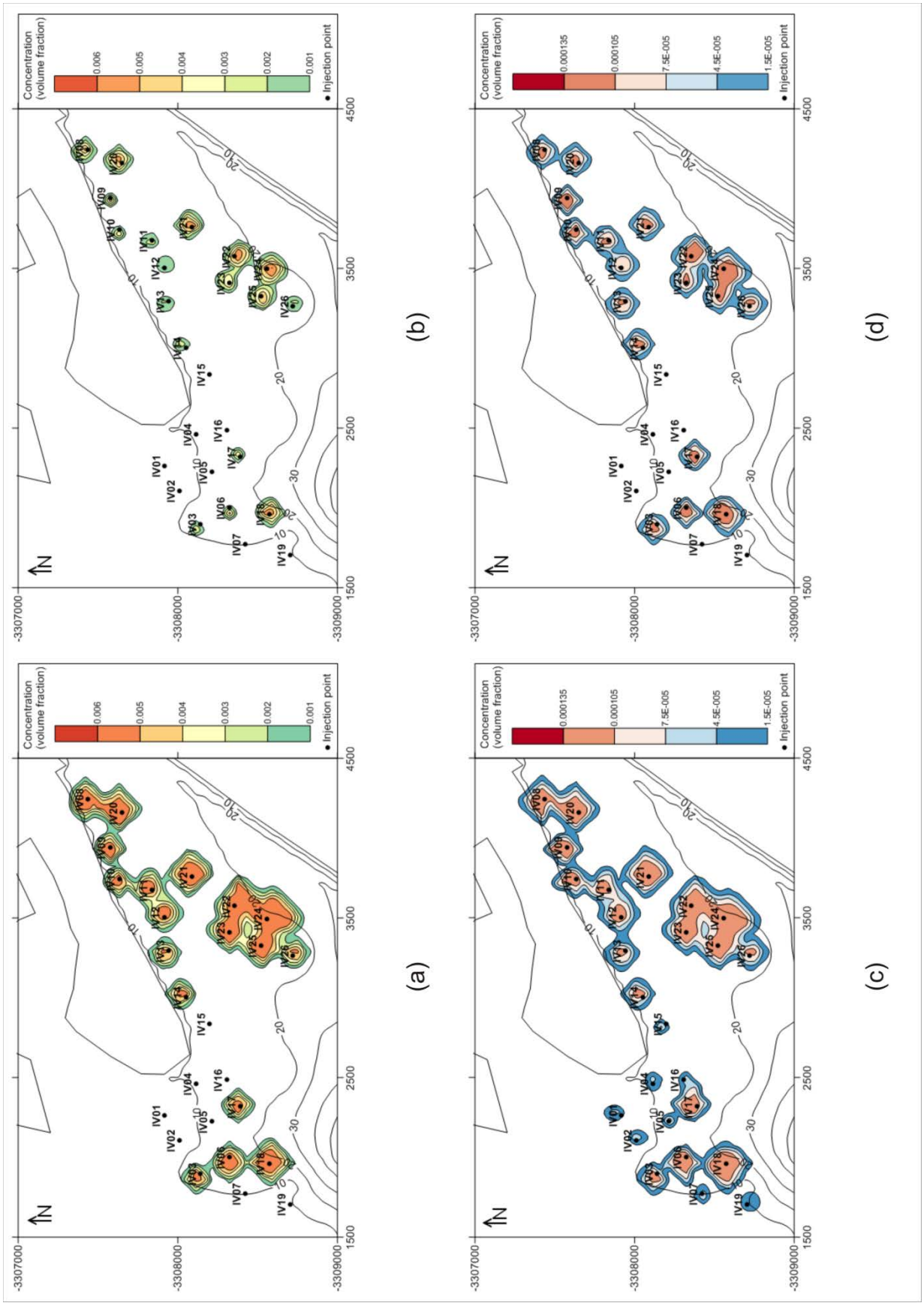

Figure 5-2: Maps illustrating the simulation results for the infiltration and migration of aqueous phase benzene and PCE. (a) Benzene in the top layer; (b) Benzene in the bottom layer; (c) PCE in the top layer; (d) PCE in the bottom layer.

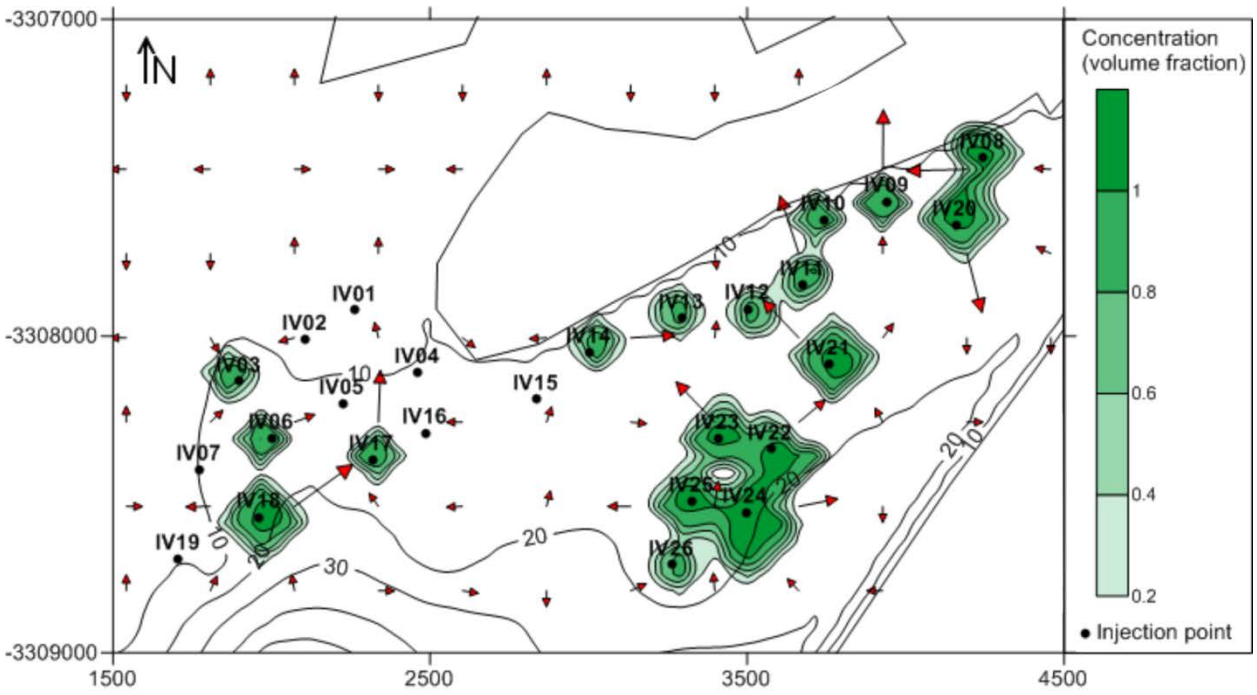

Figure 5-3: Map illustrating the simulation results for the infiltration and migration of non-aqueous phase benzene with vectors that represent the direction of migration.

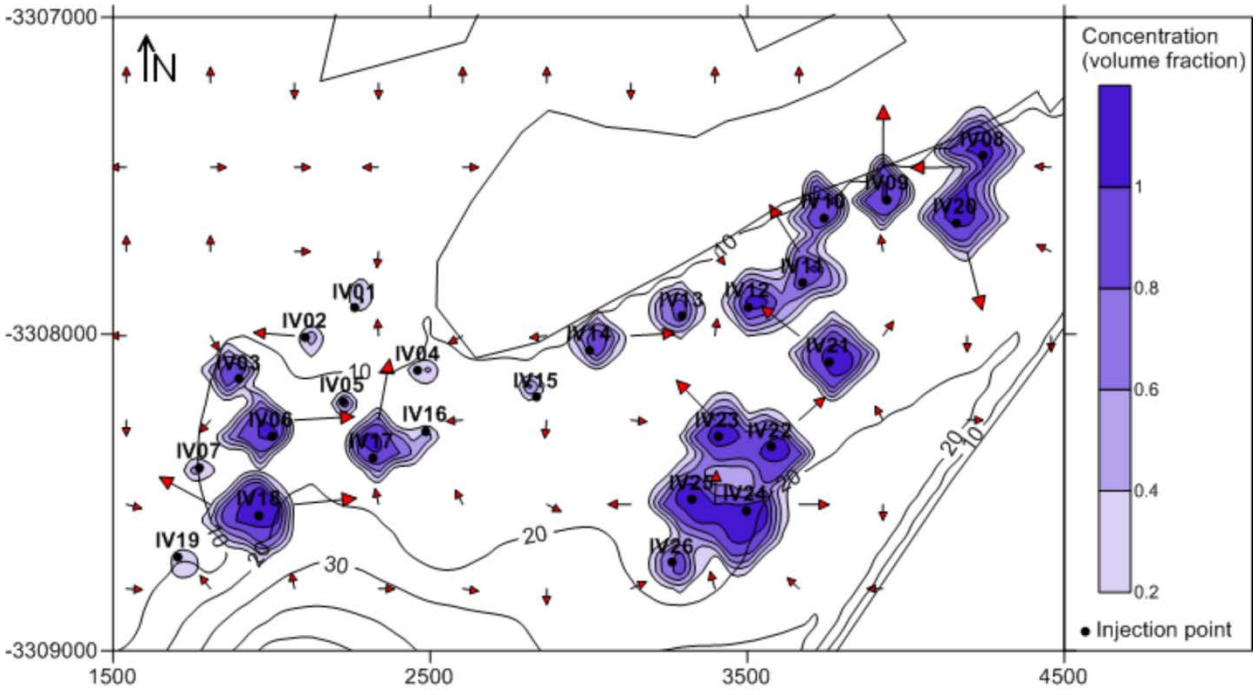

Figure 5-4: Map illustrating the simulation results for the infiltration and migration of non-aqueous phase PCE with vectors that represent the direction of migration.

5.3 Simulation of the remediation of Non-Aqueous Phase Liquids

5.3.1 Non-aqueous phase liquids benzene and tetrachloroethylene (PCE)

5.3.1.1 Remediation with the use of surfactant sodium dodecyl sulphate (SDS) and polymer xanthan gum

Figure 5-5 and Figure 5-6 contain maps that reflect the change in distribution after the area was treated with surfactant SDS and polymer xanthan gum. The map of the distribution of the NAPL prior to remediation is included in (a) in both figures to demonstrate the relative change and the change with respect to each scenario.

In all the maps generated, the use of SDS and xanthan gum managed to cause a change in distribution and concentration of benzene (Figure 5-5) and PCE (Figure 5-6). It is necessary to look at the change in size of the plume and the decrease in concentration that can be seen by the lighter areas within the plume. If the NAPL breaks apart in this manner, it has become mobile. Mobility is more evident directly below the positions where the remediation fluid was injected. Once mobility is achieved and the NAPL is removed, degradation and natural attenuation (advection, dispersion, oxidation, and biodegradation) would be more effective in improving the quality of the groundwater.

For benzene, the remediation scenario that causes the greatest distribution of the NAPL indicated by a larger plume surface area which occurs when the undiluted remediation fluid and higher infiltration rate (map (d) in Figure 5-5) is used. A volume fraction of 0.5 was used for SDS and xanthan gum at an infiltration rate of 300 m^3/d. At most injection boreholes, there was an improvement in mobility and a decrease in concentration with a few exceptions. Plumes located directly below boreholes IV06, 17, 18, and 20 react better to an infiltration rate of 100 m^3/d while the mobility of the plumes directly below IV08, 13, and 14 are enhanced by a diluted remediation fluid.

PCE reacts similarly to benzene with the use of all remediation fluids and is better mobilised when an undiluted, high injected rate is utilised. This is indicated in the map labelled (d) in Figure 5-6. There are exceptions where plume migration is greater surrounding boreholes IV13, 14, 17, and 18 where the diluted mix injected at 100 m^3/d is favourable.

In the case of surfactant SDS and polymer xanthan gum, the effectiveness is not restricted to a particular concentration or infiltration rate. Boreholes IV13, 14, 17, and 18 all required less intensive remediation methods. The effectiveness could be dependent on the hydraulic conditions of the area.

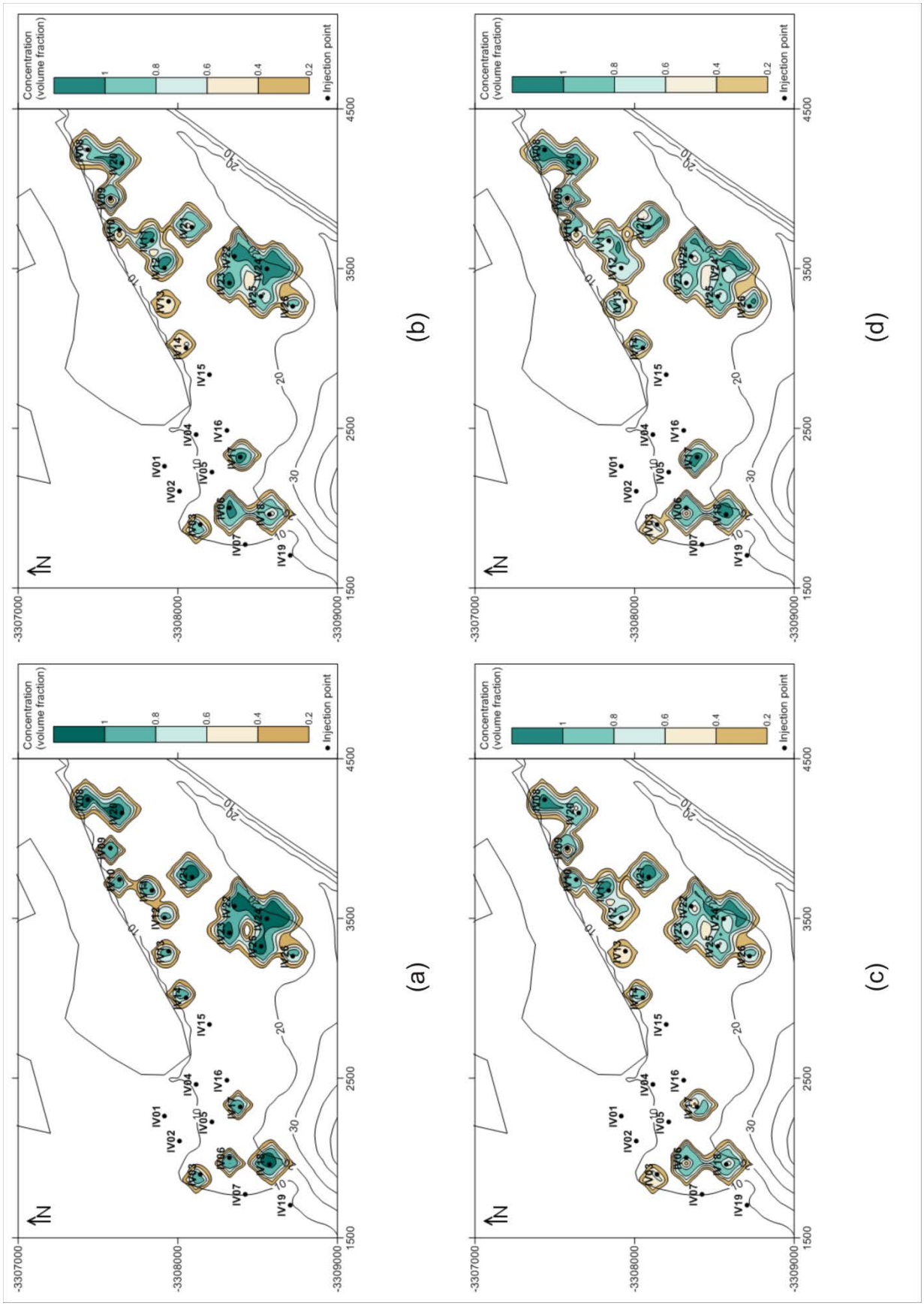

Figure 5-5: Maps illustrating the simulation results for the remediation of non-aqueous phase benzene with surfactant SDS and polymer xanthan gum. (a) Benzene without remediation; (b) Remediation using diluted SDS and xanthan gum; (c) Remediation using undiluted SDS and xanthan gum; (d) Remediation using undiluted SDS and xanthan gum and an increase in the rate of infiltration.

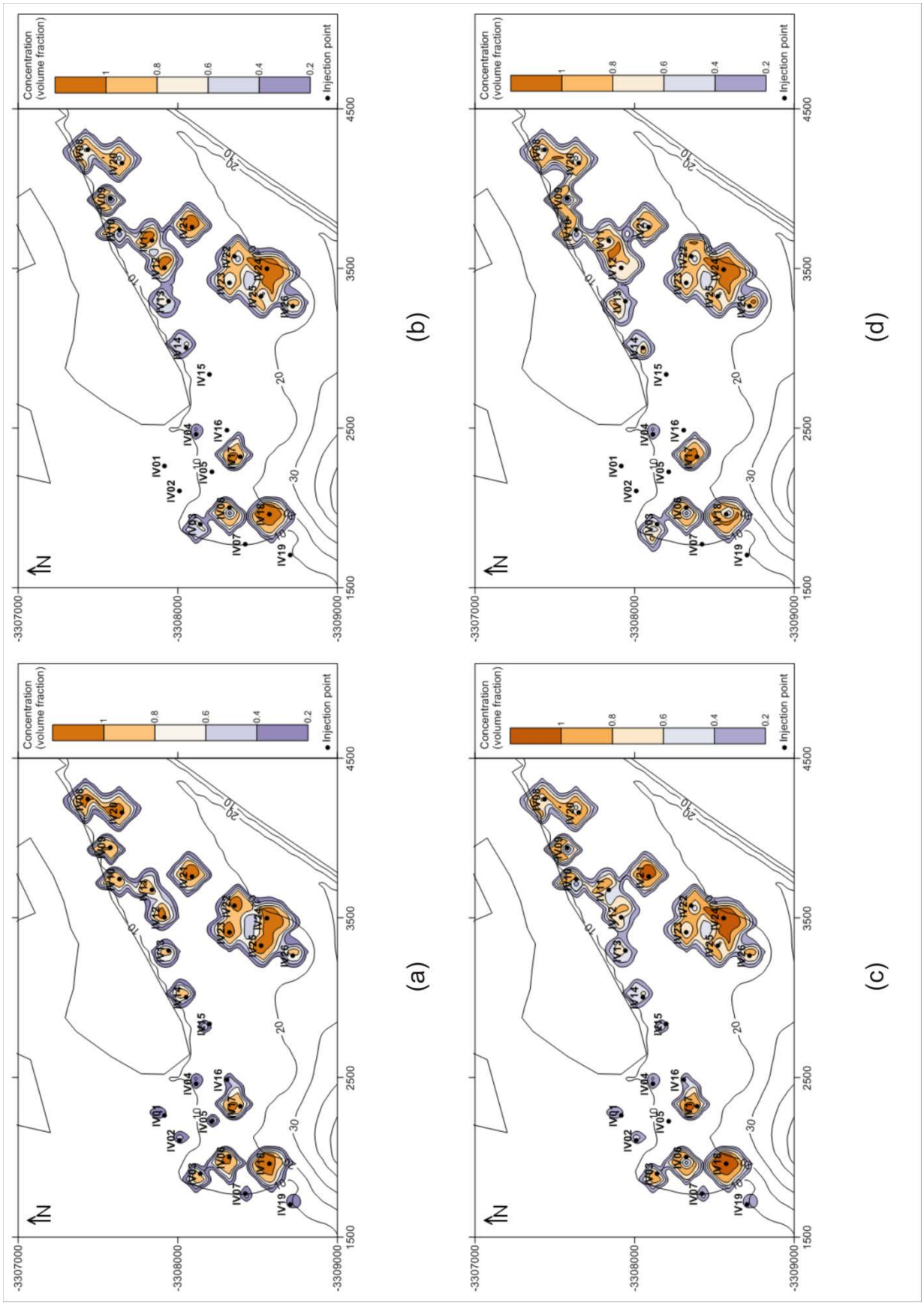

Figure 5-6: Maps illustrating the simulation results for the remediation of non-aqueous phase PCE with surfactant SDS and polymer xanthan gum. (a) PCE without remediation; (b) Remediation using diluted SDS and xanthan gum; (c) Remediation using undiluted SDS and xanthan gum; (d) Remediation using undiluted SDS and xanthan gum and an increase in the rate of infiltration.

5.3.1.2 Remediation with the use of surfactant sodium dodecyl sulphate (SDS)

In Figure 5-7 and Figure 5-8 maps are given representing the change in NAPL benzene and PCE respectively after remediation with surfactant SDS. The infiltration of the NAPL was indicated in (a) as before to demonstrate the variation.

The surfactant SDS was used in this scenario and seemed to improve mobility of the free phase and dissolved phase from the first remediation method (diluted surfactant injected at 100 m^3/d). There are distinct areas where the concentration of benzene and PCE has decreased and the plume size in all cases is slightly larger indicating an increase in mobility.

For the free phase, the method illustrated in Figure 5-7 (d) improved mobility and the concentration of benzene. This method includes the undiluted surfactant SDS injected at a rate of 300 m^3/d. There was a greater improvement around most boreholes with an exception seen at boreholes IV17, 20, and 22. At these boreholes a lower infiltration rate of 100 m^3/d is preferred. None of the plumes treated with a diluted surfactant are impacted more than those treated with an undiluted remediation fluid.

When comparing the change in extent of the PCE plume in Figure 5-8, there is no significant correlation with benzene. Even though an undiluted, high infiltration rate proved to be the better remediation option, the undiluted low injection rated was the least effective at all boreholes. The plume distribution and concentration at respective boreholes transformed differently. In this case, the contaminated area around boreholes IV4, 5, and 20 are greatly improved with the use of a diluted remediation fluid and a low injection rate.

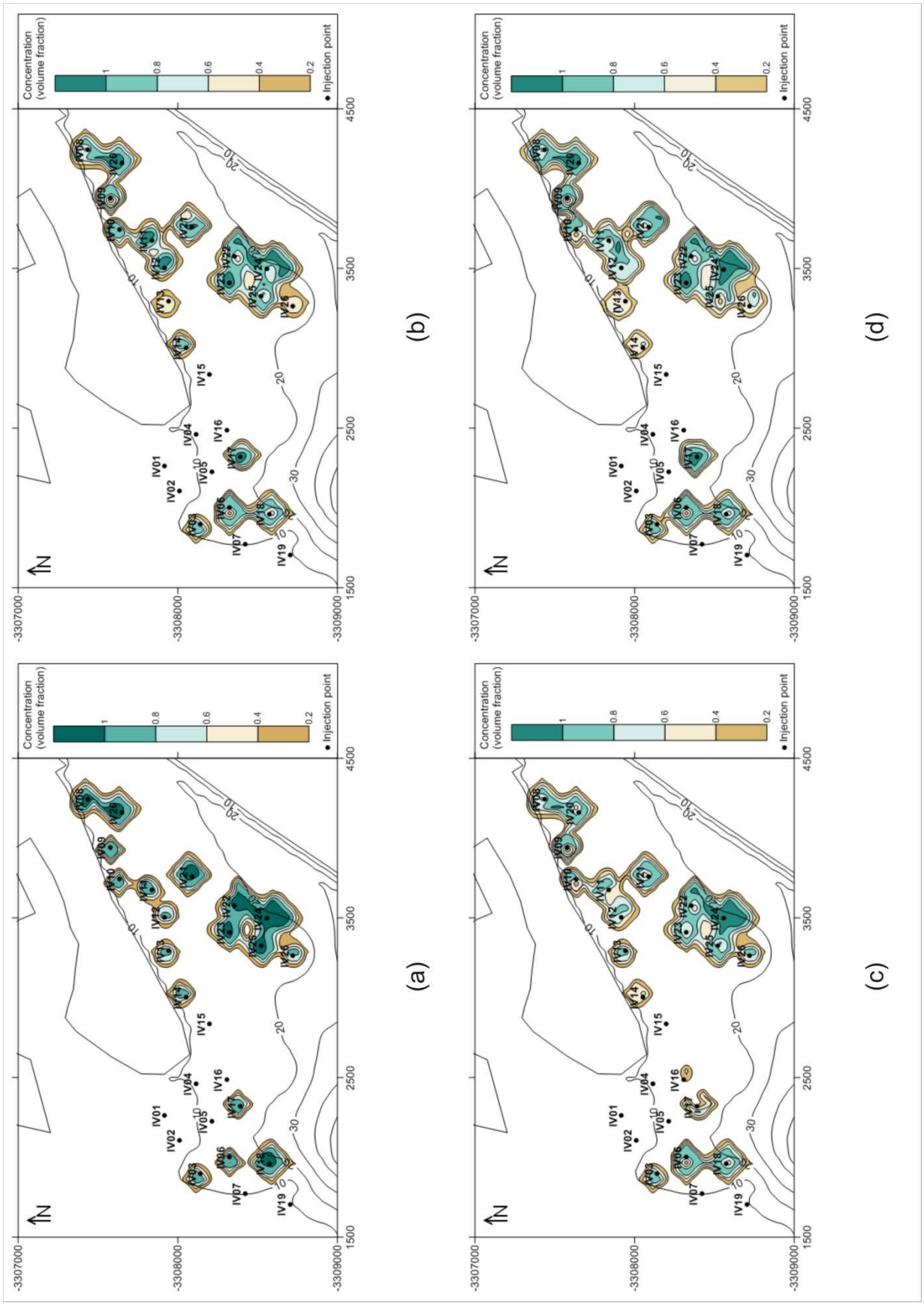

Figure 5-7: Maps illustrating the simulation results for the remediation of non-aqueous phase benzene with surfactant SDS. (a) Benzene without remediation; (b) Remediation using diluted SDS; (c) Remediation using undiluted SDS; (d) Remediation using undiluted SDS and an increase in the rate of infiltration.

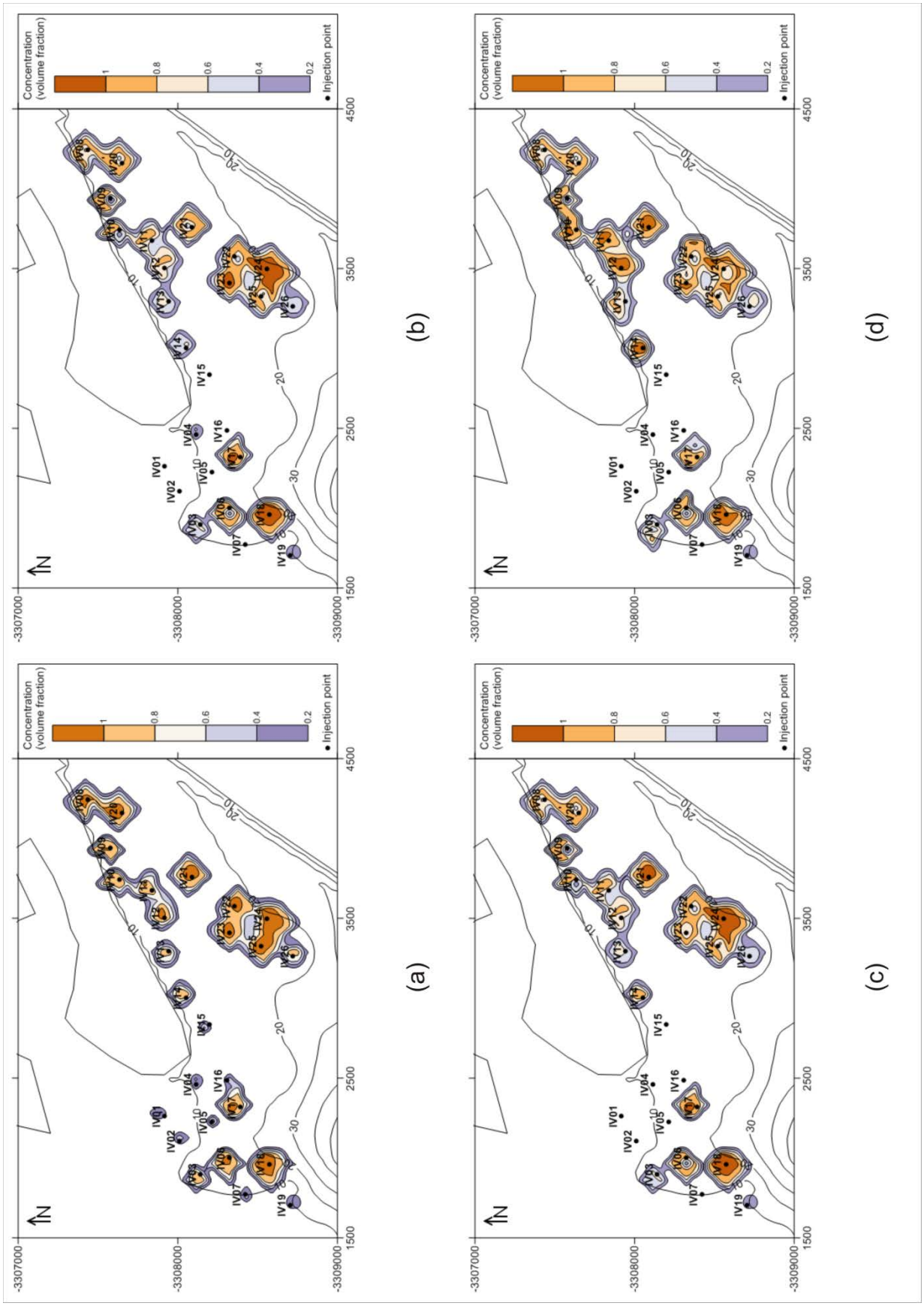

Figure 5-8: Maps illustrating the simulation results for the remediation of non-aqueous phase PCE with surfactant SDS. (a) PCE without remediation; (b) Remediation using diluted SDS; (c) Remediation using undiluted SDS; (d) Remediation using undiluted SDS and an increase in the rate of infiltration.

5.3.1.3 Remediation with the use of polymer xanthan gum

The use of a polymer in remediation is indicated in Figure 5-9 and Figure 5-10 for benzene and PCE respectively. Maps labelled (a) are those illustrating the distribution of benzene before remediation, (b) represents the area after treatment with diluted xanthan gum injected at a rate of 100 m^3/d, (c) illustrates a change in the extent of the NAPL with the addition of an undiluted polymer injected at 100 m^3/d, and (d) displays the contaminate plume after the undiluted polymer has been injected at 300 m^3/d.

Benzene has not been affected after the injection of a polymer. The relative size of the plume increased slightly, however, the concentration is unchanged and benzene does not break apart at all. The plume around borehole IV25 is the only borehole that is positively impacted only when the concentration of xanthan gum and the injection rate has been increased (maps (d) in Figure 5-9). There is no significant change around this borehole when comparing it to remediation with the use of a surfactant.

The use of xanthan gum as a remediation fluid to chemically flush PCE is possible however the NAPL was unchanged until it was undiluted and injected at a rate of 300 m^3/d indicated in Figure 5-10 map (d). According to the results, PCE will require a large volume of the polymer to become mobile.

Silva *et al.* (2012) used UTCHEM and laboratory experiments to demonstrate that a polymer increased the viscosity of an unknown non-aqueous phase liquid and improves the sweep efficiency by 90 %. This could be the reason for the increase in size of the benzene plume, however the lateral migration may be brought on by the added volume of the injected polymer. Jackson *et al*. (2003), mention that the purpose of polymers such as xanthan gum is used to increase the viscosity but does not increase mobility as the interfacial tension in the environment would remain the same. Results produced by Silva *et al*. (2012) demonstrated an improvement in sweep efficiency with a higher the use of concentrated xanthan gum however there was a reduction when the concentration was increased beyond 500 mg/l. The concentration of the polymer is the main factor that would need to be evaluated if the method is employed.

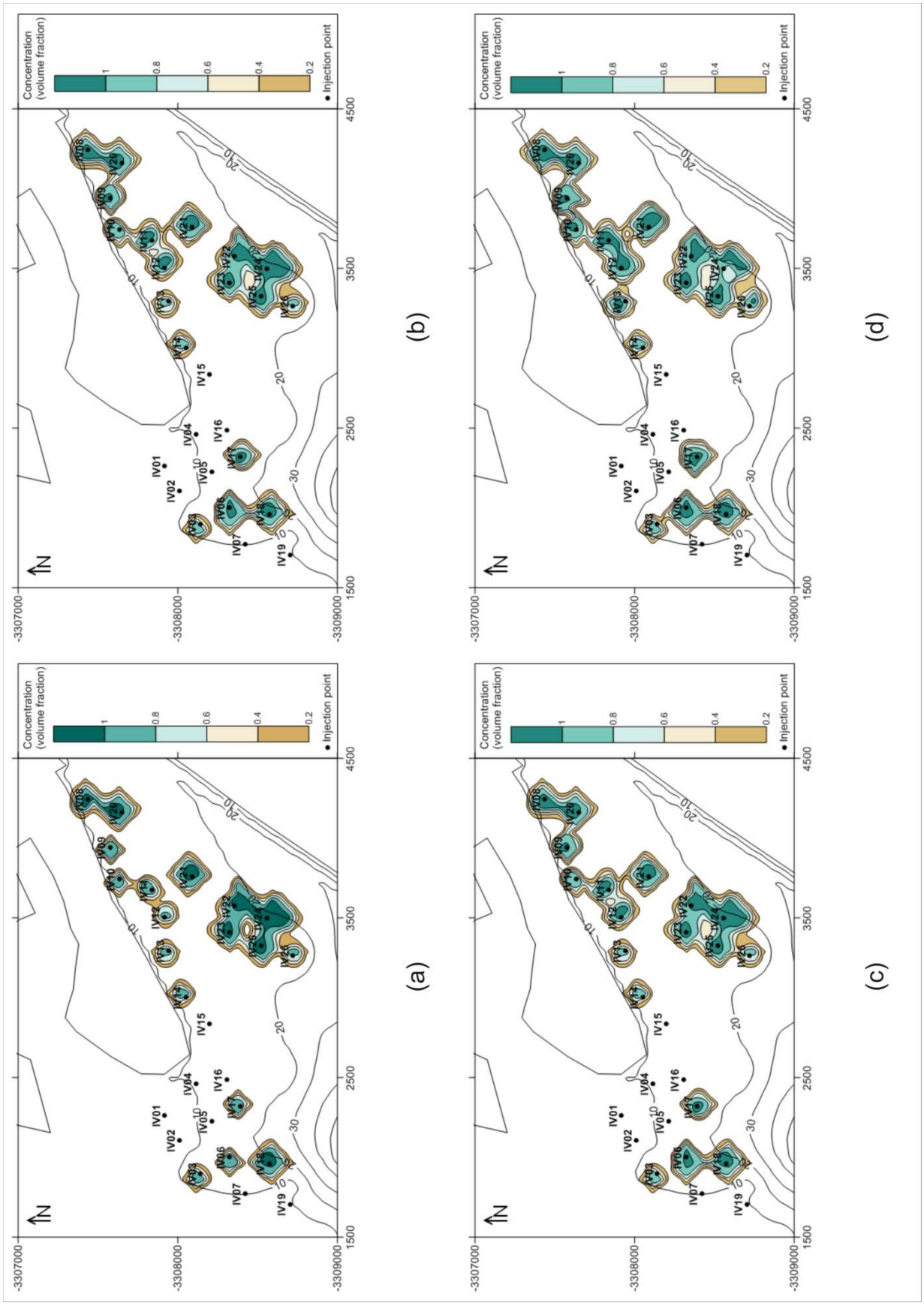

Figure 5-9: Maps illustrating the simulation results for the remediation of non-aqueous phase benzene with polymer xanthan gum. (a) Benzene without remediation; (b) Remediation using diluted xanthan gum; (c) Remediation using undiluted xanthan gum; (d) Remediation using undiluted xanthan gum and an increase in the rate of infiltration.

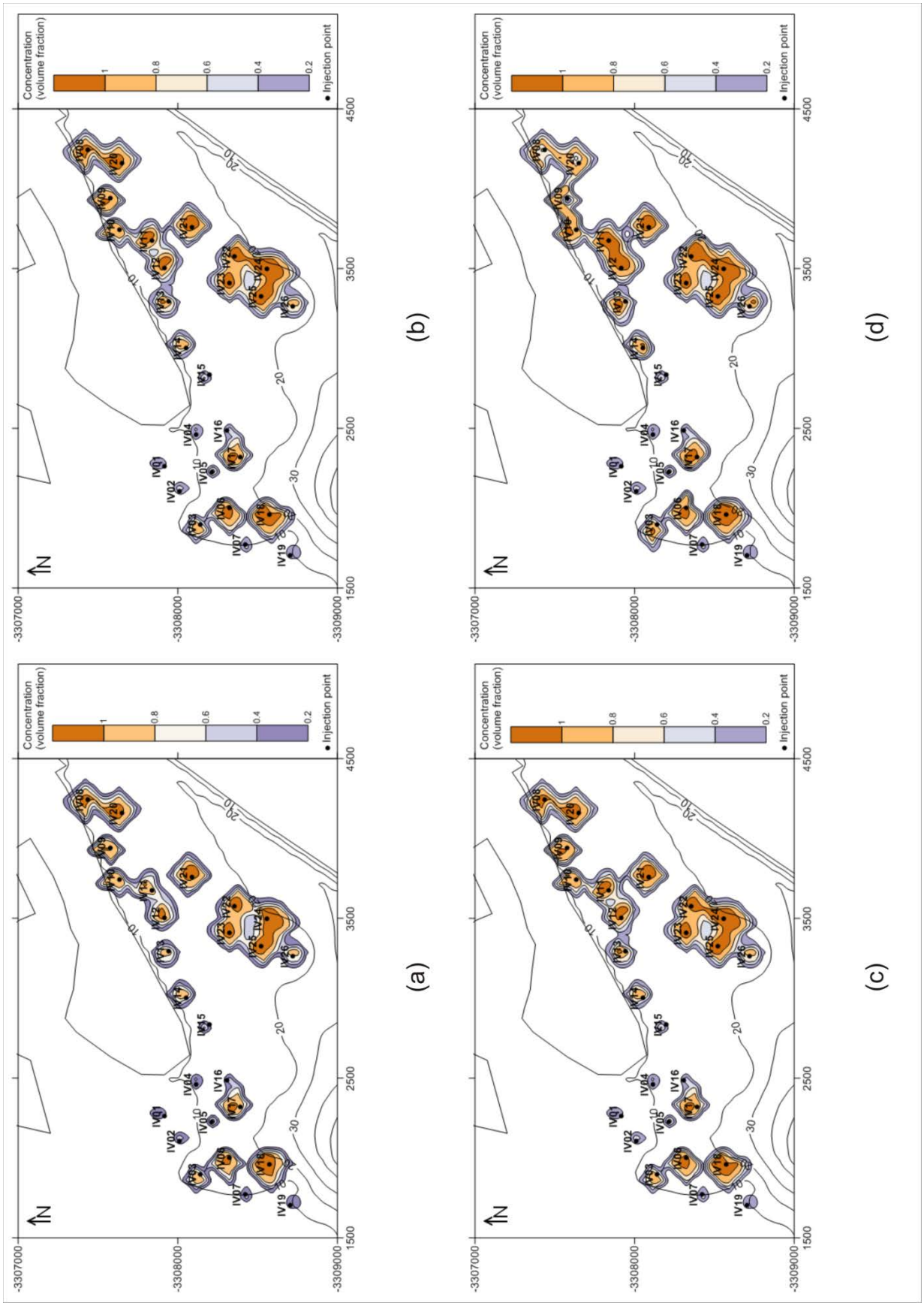

Figure 5-10: Maps illustrating the simulation results for the remediation of non-aqueous phase PCE with polymer xanthan gum. (a) PCE without remediation; (b) Remediation using diluted xanthan gum; (c) Remediation using undiluted xanthan gum; (d) Remediation using undiluted xanthan gum and an increase in the rate of infiltration.

5.3.1.4 Remediation with the use of surfactant sodium dodecyl sulphate (SDS) and ethanol

Figure 5-11 and Figure 5-12 contains maps illustrating the use of the combination of surfactant SDS and ethanol. The maps are arranged as before.

For these examples, all scenarios are effective in increasing the mobility, decreasing the concentration, and breaking up the mass of the free phase and dissolved plume. In the case of the benzene, the plumes located at all boreholes are improved with the injection of an undiluted remediation fluid at an increased rate of 300 m^3/d. The aqueous phase liquid corresponds to the non-aqueous phase however, the contaminated area around boreholes IV 20 and 22 are better distributed when the same concentration is injected at a rate of 100 m^3/d.

The change in extent of the contaminated plume increased as the remediation method intensified for PCE. The majority of affected areas greatly mobilised and decreased in concentration when SDS and alcohol were injected at a rate of 300 m^3/day. A reduced infiltration rate proved to be better suited for the contaminated regions beneath boreholes IV 06 and 14 indicated in Figure 5-12 (c). As seen, there is a major decrease in the size of the plume at borehole IV 14. In other areas, minor plumes became completely dispersed to a point where the concentration cannot be seen any longer indicated around boreholes IV 04, 05, 15, 16, and 19.

When comparing all remediation scenarios, the use of the surfactant SDS with the addition of an alcohol was the most effective method in mobilising benzene and PCE when considering the extent of the plume, and the change in concentration. Again, the distribution of PCE is visibly greater than that of benzene. Ouyang *et al.* (2001), states that surfactant SDS has the ability to promote solubilisation and mobilisation of a NAPL by forming a micro emulsion and dramatically decreasing the interfacial tension. Because there is a great difference between the interfacial tension of the NAPL and aqueous phase, NAPLs tend to become trap, reducing the interfacial tension with allow the NAPL to move freely (Bear, 1972). Surfactant SDS reduces the amount of NAPL saturated pore volumes that need to be extracted (Ouyang *et al.,* 2001)

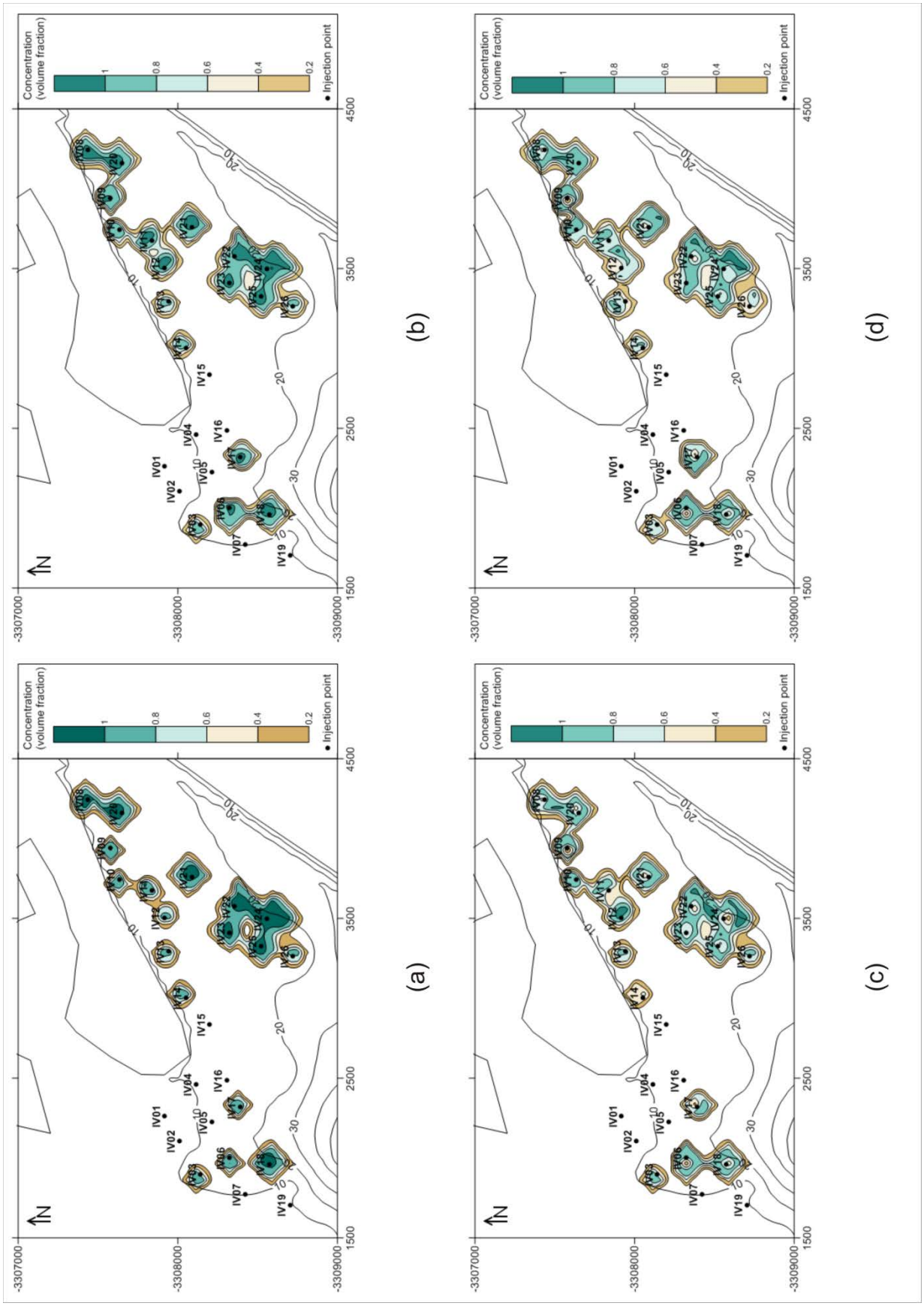

Figure 5-11: Maps illustrating the simulation results for the remediation of non-aqueous phase benzene with surfactant SDS and ethanol. (a) Benzene without remediation; (b) Remediation using diluted SDS and ethanol; (c) Remediation using undiluted SDS and ethanol; (d) Remediation using undiluted SDS and ethanol and an increase in the rate of infiltration.

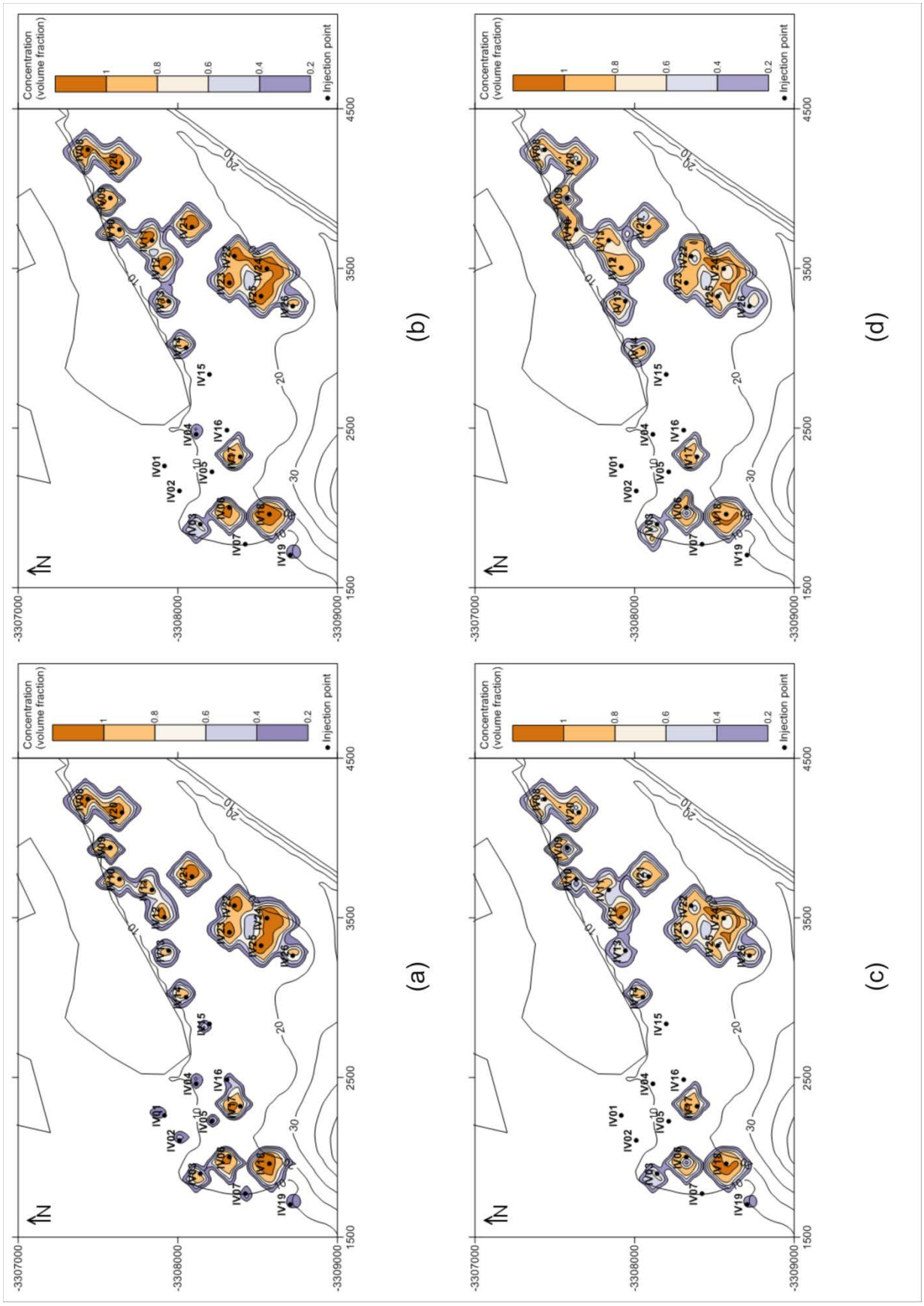

Figure 5-12: Maps illustrating the simulation results for the remediation of non-aqueous phase PCE with surfactant SDS and ethanol. (a) PCE without remediation; (b) Remediation using diluted SDS and ethanol; (c) Remediation using undiluted SDS and ethanol; (d) Remediation using undiluted SDS and ethanol and an increase in the rate of infiltration.

5.3.1.5 Remediation with the use of ethanol

The use of ethanol to flush the NAPL has been wildly used in the rehabilitation of non-aqueous phase liquids. This can be demonstrated in Figure 5-13 and Figure 5-14. Maps are labelled and arrange according to the method used previously.

The use of alcohol is the least effective method to improve mobility of benzene. In the aqueous and non-aqueous phases, the size and concentration of benzene is unchanged. In some areas the size of the plume decreases.

When considering ethanol as a remediation fluid indicated in Figure 5-14, the size of the contaminate plume remains constant when the undiluted and diluted ethanol was injected at a rate of 100 m^2/d. There was a slight spike in the change in distribution and concentration with an increase in the injected rate just as the reaction with use of polymer xanthan gum.

Agaogle *et al*. (2012) used UTCHEM to determine the equilibrium properties of pure NAPLs and to investigate the best recovery mechanism using ethanol at different concentrations. It was found that the recovery rate and concentration of ethanol are directly proportional and that the greatest ethanol concentration will work best to mobilise the NAPL. Falta (1998) said that ethanol enhances dissolution within the alcohol without allowing the difference in interfacial tension between the aqueous phase and NAPL to drop. This may be the reason why the model did not achieve positive results in terms of mobility. Organic compounds ethanol and methanol, with a low molecular weight will allow dissolution to take place, causing the NAPL to move freely while alcohols with a higher molecular weight such as propanol and butanol increases mobility by reducing the interfacial tension (Rao *et al*., 1997; Lunn and Kueper, 1997; Falta, 1998; Jawitz *et al*., 2000; Brooks *et al*., 2003).

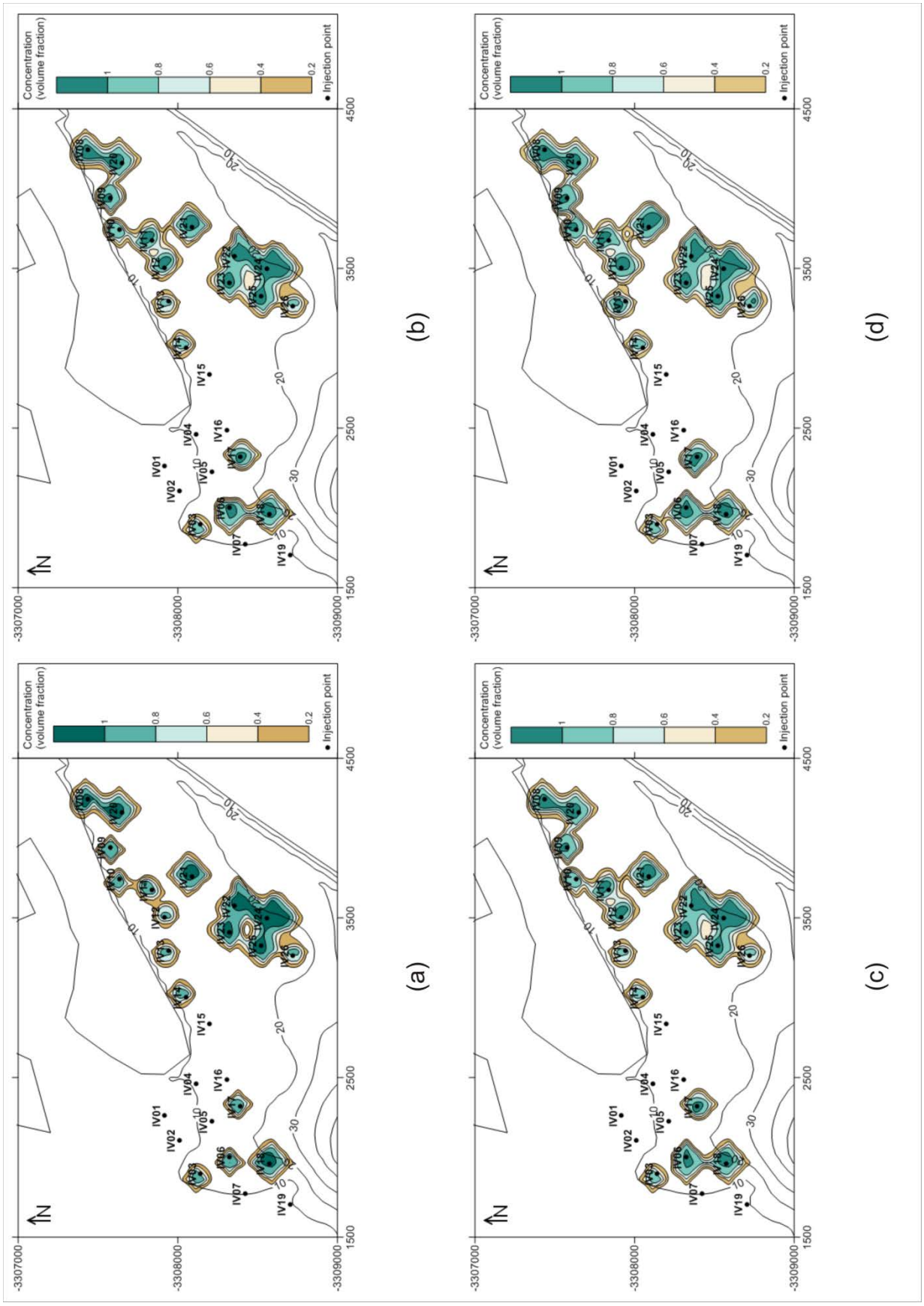

Figure 5-13: Maps illustrating the simulation results for the remediation of non-aqueous phase benzene with ethanol. (a) Benzene without remediation; (b) Remediation using diluted ethanol; (c) Remediation using undiluted ethanol; (d) Remediation using undiluted ethanol and an increase in the rate of infiltration.

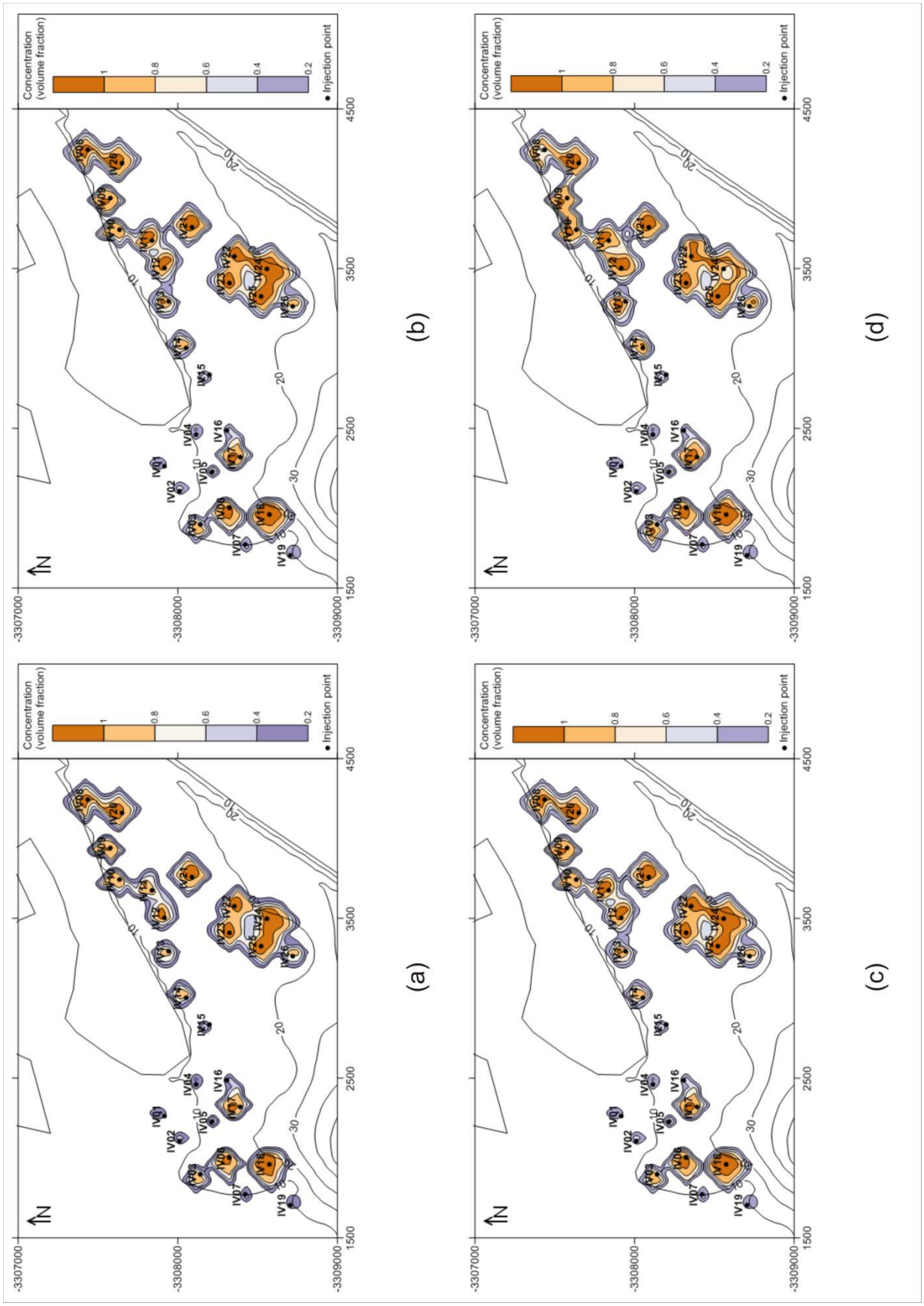

Figure 5-14: Maps illustrating the simulation results for the remediation of non-aqueous phase PCE with ethanol. (a) PCE without remediation; (b) Remediation using diluted ethanol; (c) Remediation using undiluted ethanol; (d) Remediation using undiluted ethanol and an increase in the rate of infiltration.

5.3.1.6 Comparison of the effectiveness of different remediation fluids

Figure 5-15 and Figure 5-16 contains graphs of the concentration of non-aqueous phase benzene and PCE, respectively, after the completion of each remediation simulation at three boreholes. These boreholes include the injection boreholes IV08, IV18, and IV 24 that can be seen in Figure 4-10 and all maps created for the simulation. On each graph from left to right, the concentrations can be seen after injection of SDS and xanthan gum, SDS, xanthan gum, SDS and ethanol. The diluted, undiluted, and undiluted with a higher injection rate is given using a key.

The change in concentration around the boreholes using SDS and xanthan gum is erratic. The behaviour in each borehole is different except boreholes IV08 and IV18 for LNAPLs where the concentration decreased when diluted and undiluted fluid is added but remains unchanged at a higher injection volume. This can be due to the redistribution of NAPL. Chemical flushing increases the viscosity of the NAPL making it easier to extract (Hulling & Weaver, 1991). There is a risk as the contaminant can be distributed to previously unaffected areas (Kueper *et al.*, 2003). Injection of ethanol and xhantan gum did not result in a significant change in mobility and therefore, the change cannot be a result of invasive injection. The use of SDS alone is equally irregular and only remains the same in boreholes IV08 and IV18 for LNAPLs and IV08 for DNAPLs. The concentrations of the NAPL decreased to zero volume fraction for all remediation scenarios indicating a significant change in mobility.

Xhantan gum has proven one of the least effective remediation fluids; however, data gathered from simulations were more reliable. Concentrations at all boreholes remained unchanged except at borehole IV24 for LNAPLs and IV08 for DNAPLs where the injection rate needed to be increased to ensure mobility. The same can be said for the use of ethanol alone where change in concentration is only seen at boreholes IV08 and IV24 for DNAPLs. As mentioned before, the use of both xanthan gum and ethanol cannot change the interfacial tension in the environment and is used to increase the viscosity and dissolution of the NAPL respectively.

The use of SDS and ethanol in the same mixture was the most effective and consistent of all the results. It ensured a positive decrease in concentration with each scenario. Concentrations decreased to a value of zero volume fraction at all boreholes once an undiluted solution was injected without increasing the injection rate. The only exception was borehole IV18 for DNAPLs where the decrease is far more gradual. A minimum concentration of 0.657 volume fraction is only achieved if an undiluted fluid is used at a high injection rate.

To summarise, the use of a surfactant is more likely to produced preferable recovery volumes. This creates an additional emulsion phase where the difference between the interfacial tensions is decreased and the NAPL is able to dissolve and become mobile.

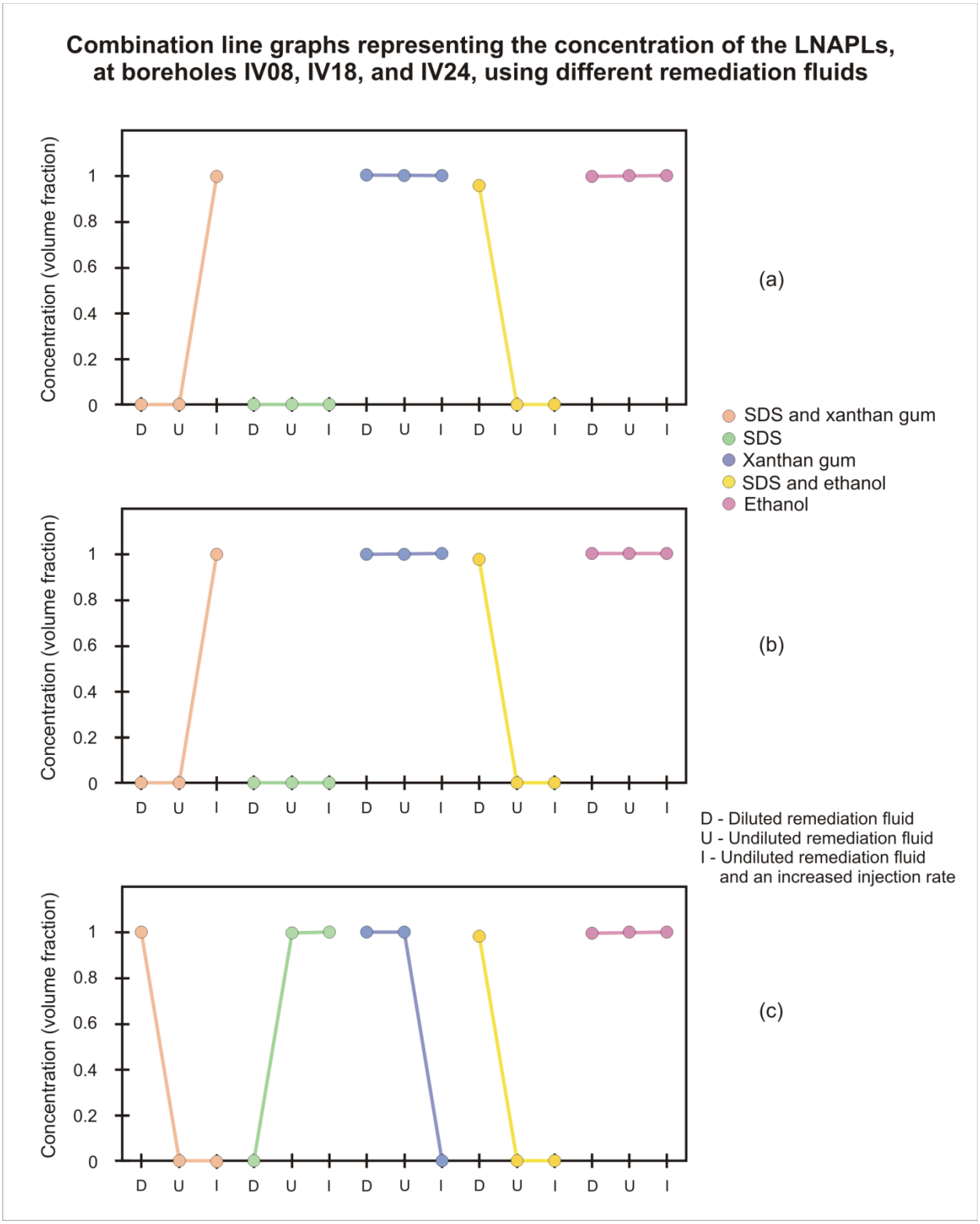

Figure 5-15: Graphs illustrating the concentrations of non-aqueous phase benzene at different boreholes after each remediation scenario. (a) borehole IV08; (b) borehole IV18; and (c) borehole IV24.

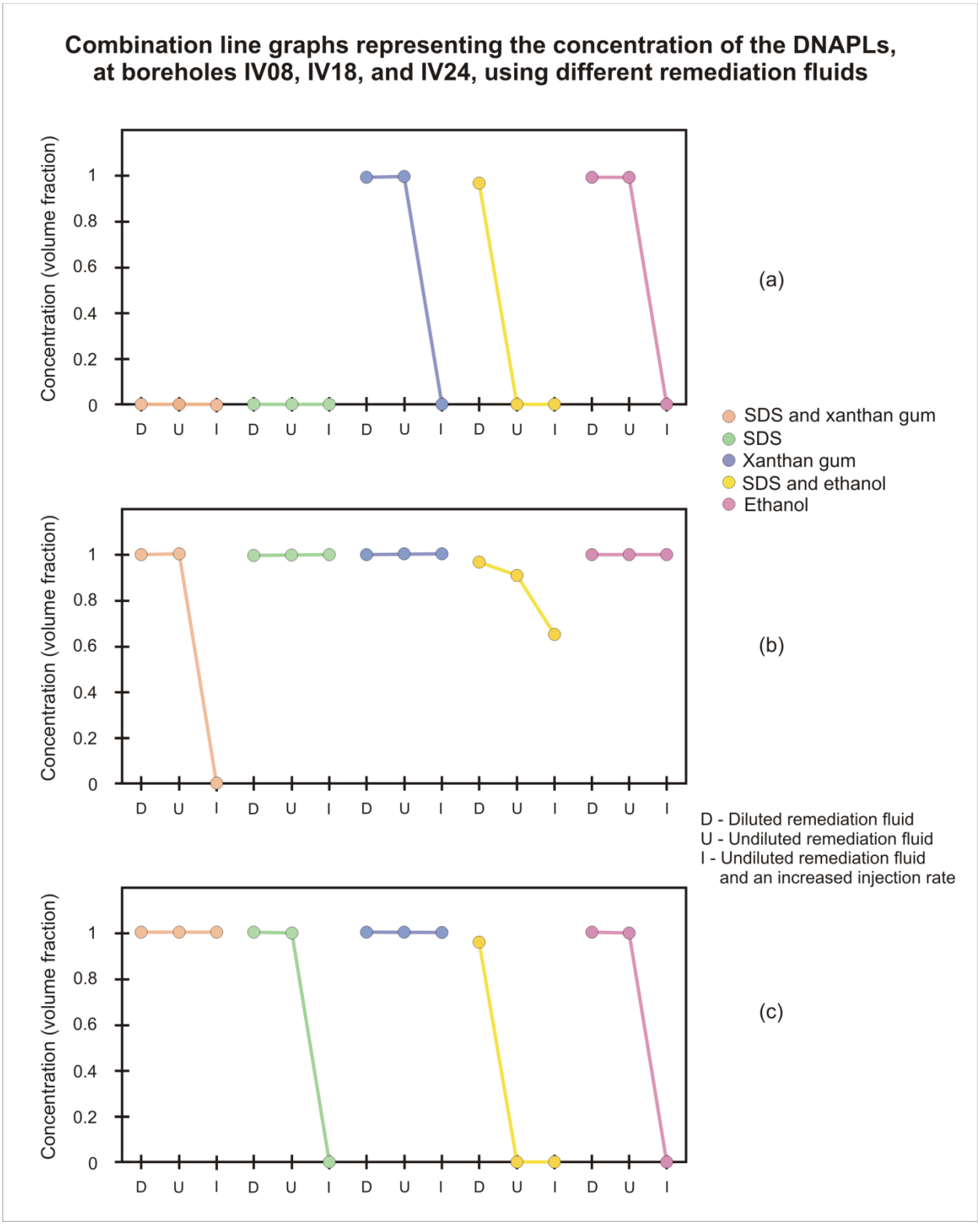

Figure 5-16: Graphs illustrating the concentrations of non-aqueous phase PCE at different boreholes after each remediation scenario. (a) borehole IV08; (b) borehole IV18; and (c) borehole IV24.

This dissolution is the mechanism that allows the concentration to decrease and improves natural attenuation in the aqueous phase. In most cases, an increase in concentration of the

remediation fluid and an increase in the injection rate improved NAPL migration and therefore recovery through *in situ* remediation. Agaogle *et al*. (2012) said that preferential flow paths are more likely to occur at higher velocities.

When xanthan gum and ethanol were used separately, there were relatively no major changes in the mobility of benzene. These two co-solvents are required in high volumes to mobilise and recover PCE. Overall PCE was more easily influenced by the remediation fluids. This may be due to the same conditions being used for a smaller volume of non-aqueous phase liquid in the top layer. Benzene will therefore require a larger volume of any remediation fluid used.

5.3.2 Aqueous phase liquids benzene and tetrachloroethylene (PCE)

5.3.2.1 Remediation with the use of surfactant sodium dodecyl sulphate (SDS) and polymer xanthan gum

Even though the mobility of the aqueous phase is not significant because it is already mobile, the addition of a remediation fluid does increase the mobility and improve the concentration of the NAPL. It is important to note for this method that a surfactant and co-solvent is used to mobilise the free phase to enhance recovery. This is the reason why there are only two examples given for the aqueous phase and because there is a direct visible correlation between changes in the non-aqueous phase and aqueous phase. Mobilisation with the use of SDS and xanthan gum, and xanthan gum alone will be discussed in this section. All diagrams that are not used in the discussion can be found in Appendices D to G.

Figure 5-17 and Figure 5-18 contain maps that reflect the change in distribution of the aqueous phase after the area was treated with surfactant SDS and polymer xanthan gum. Maps labelled (a) are those illustrating the distribution of benzene before remediation, (b) represents the area after treatment with diluted remediation fluid injected at a rate of 100 m^3/d, (c) illustrates a change in the extent of the NAPL with the addition of an undiluted remediation injected at 100 m^3/d, and (d) displays the contaminate plume after the undiluted surfactant and polymer has been injected at 300 m^3/d.

The used of a concentrated remediation fluid and a greater infiltration rate was more effective in increasing the distribution of the dissolved benzene just as the non-aqueous phase. There are a few exceptions. The plumes located at boreholes IV17, 20, and 24 showed an improvement in

mobility at a smaller infiltration rate, while the concentration of benzene at borehole IV14 and 15 are significantly lower with the use of a diluted SDS and xanthan gum.

The mobility of the PCE aqueous plume was improved from the first remediation scenario. Using an undiluted remediation fluid and injecting it at a higher rate increases mobility based on the change in distribution on the aqueous phase and the change in concentration, however, the affected area around boreholes IV08, 10, 11, 18, 20, and 21 is enhanced at a lower injection rate. Boreholes IV14 and 15 improved with the use of a diluted remediation mix. In most cases, the concentration and injection rate of the flushing fluid is borehole specific and may by dependant on the hydraulic characteristics of area around the borehole.

The increase in the distribution of the aqueous phase would improve oxidation and compounds can be transformed into less toxic substances.

5.3.2.2 Remediation with the use of polymer xanthan gum

The use of polymer xanthan gum is used to flush the non-aqueous phase and has been wildly used in the rehabilitation of non-aqueous phase liquids. This can be demonstrated in Figure 5-19 and Figure 5-20 where the effect of xanthan gum can be seen for benzene and PCE respectively. Maps are labelled and arranged according to the method used previously.

Benzene's non-aqueous phase was slightly affected by the use of xanthan gum as a flushing fluid. The size of the contaminated area increased slightly with all three methods, however, the concentration around borehole IV26 decreased when an undiluted polymer was injected into the system at 300 m^3/d. The same is true for the dissolved plume as indicated in Figure 5-19.

The same pattern is seen for the non-aqueous phase and aqueous phase of PCE. There is no change in the system when an undiluted and diluted polymer is added at a rate of 100 m^3/d. There is however a change when xanthan gum is injected at 300 m^3/d. As mentioned before, larger volumes of a polymer will be needed to improve the distribution of the aqueous phase for a DNAPL.

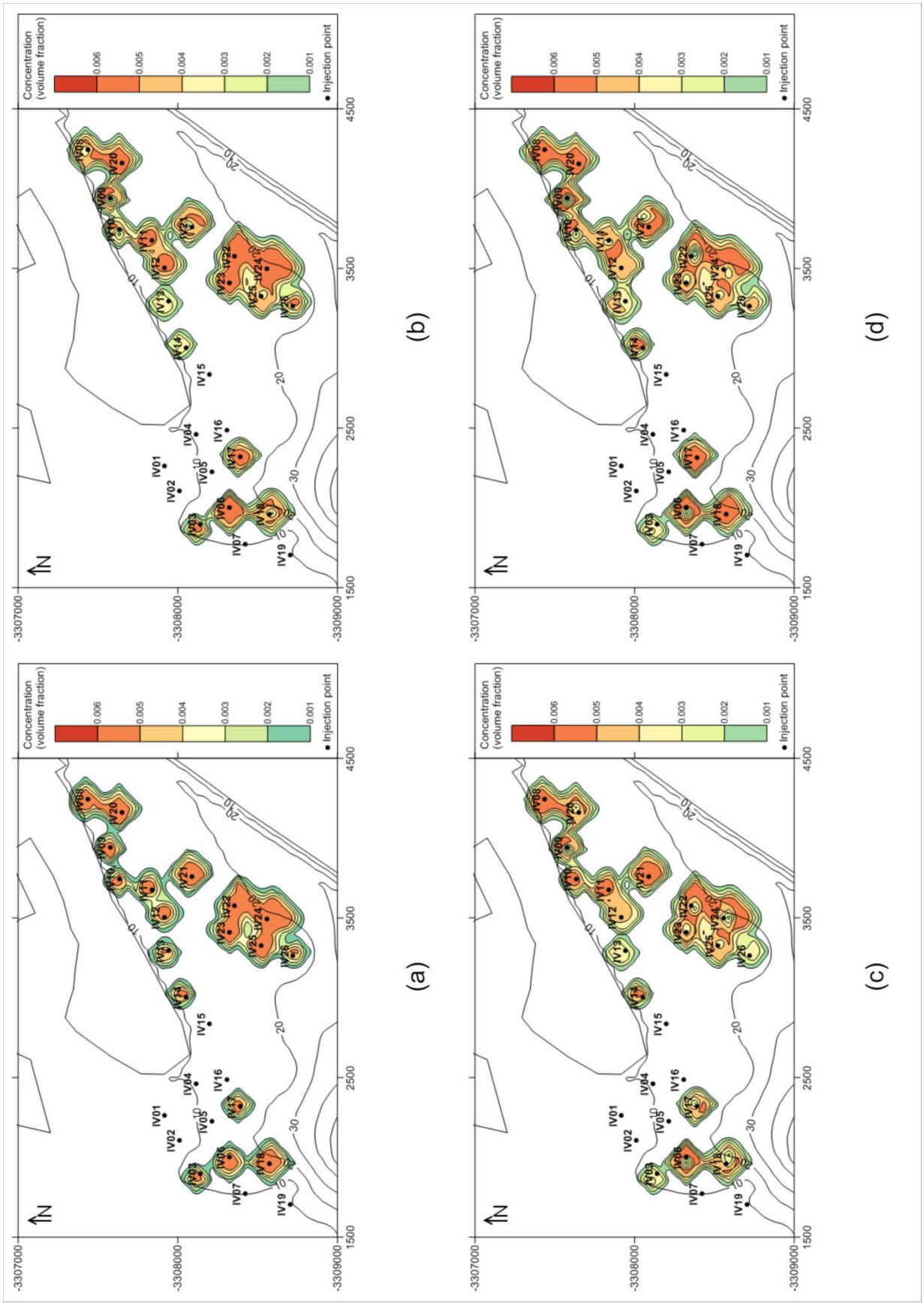

Figure 5-17: Maps illustrating the simulation results for the remediation of aqueous phase benzene with surfactant SDS and polymer xanthan gum. (a) PCE without remediation; (b) Remediation using diluted SDS and xanthan gum; (c) Remediation using undiluted SDS and xanthan gum; (d) Remediation using undiluted SDS and xanthan gum and an increase in the rate of infiltration.

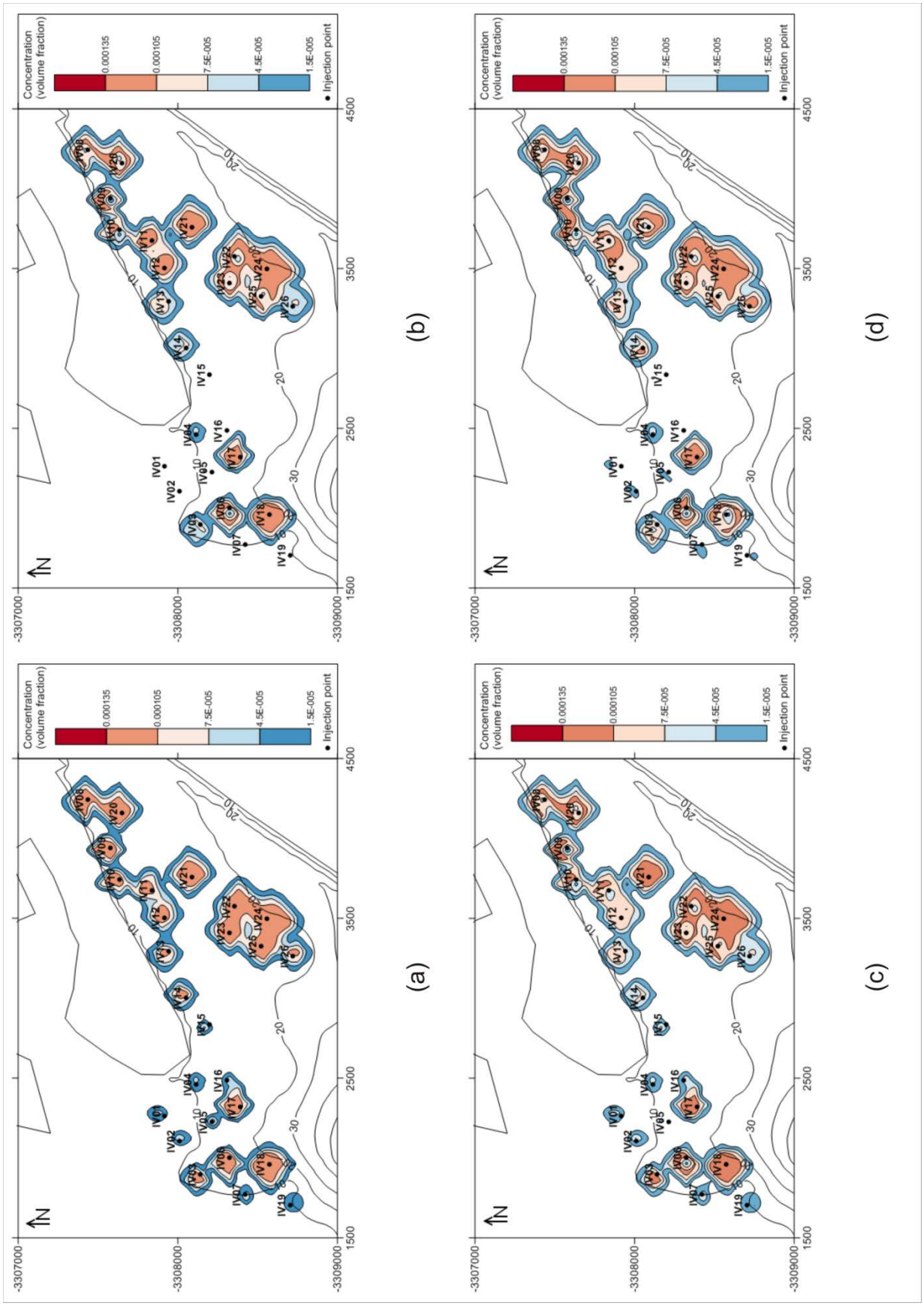

Figure 5-18: Maps illustrating the simulation results for the remediation of aqueous phase PCE with surfactant SDS and polymer xanthan gum. (a) PCE without remediation; (b) Remediation using diluted SDS and xanthan gum; (c) Remediation using undiluted SDS and xanthan gum; (d) Remediation using undiluted SDS and xanthan gum and an increase in the rate of infiltration.

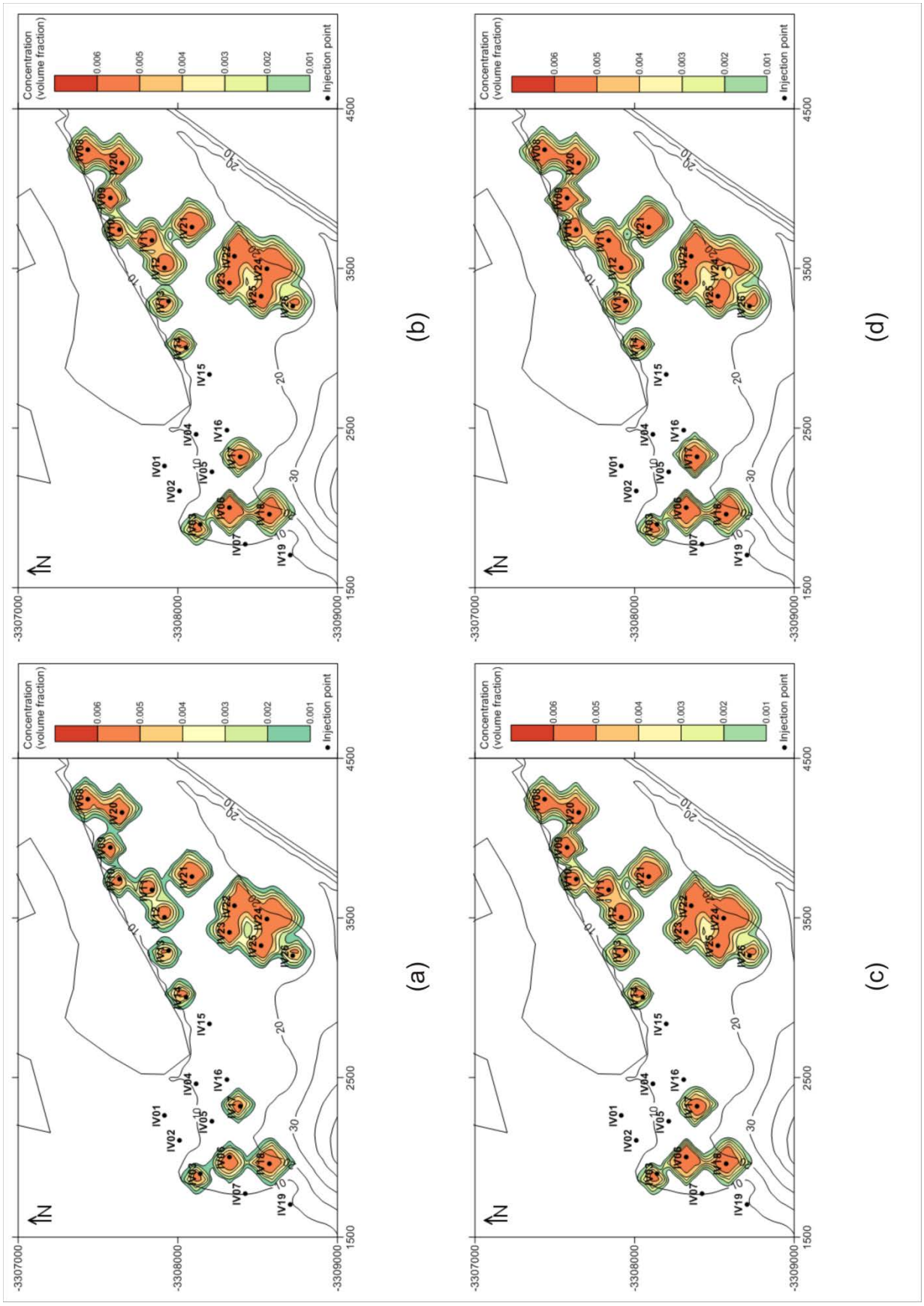

Figure 5-19: Maps illustrating the simulation results for the remediation of aqueous phase benzene with polymer xanthan gum. (a) benzene without remediation; (b) Remediation using diluted xanthan gum; (c) Remediation using undiluted xanthan gum; (d) Remediation using undiluted xanthan gum and an increase in the rate of infiltration.

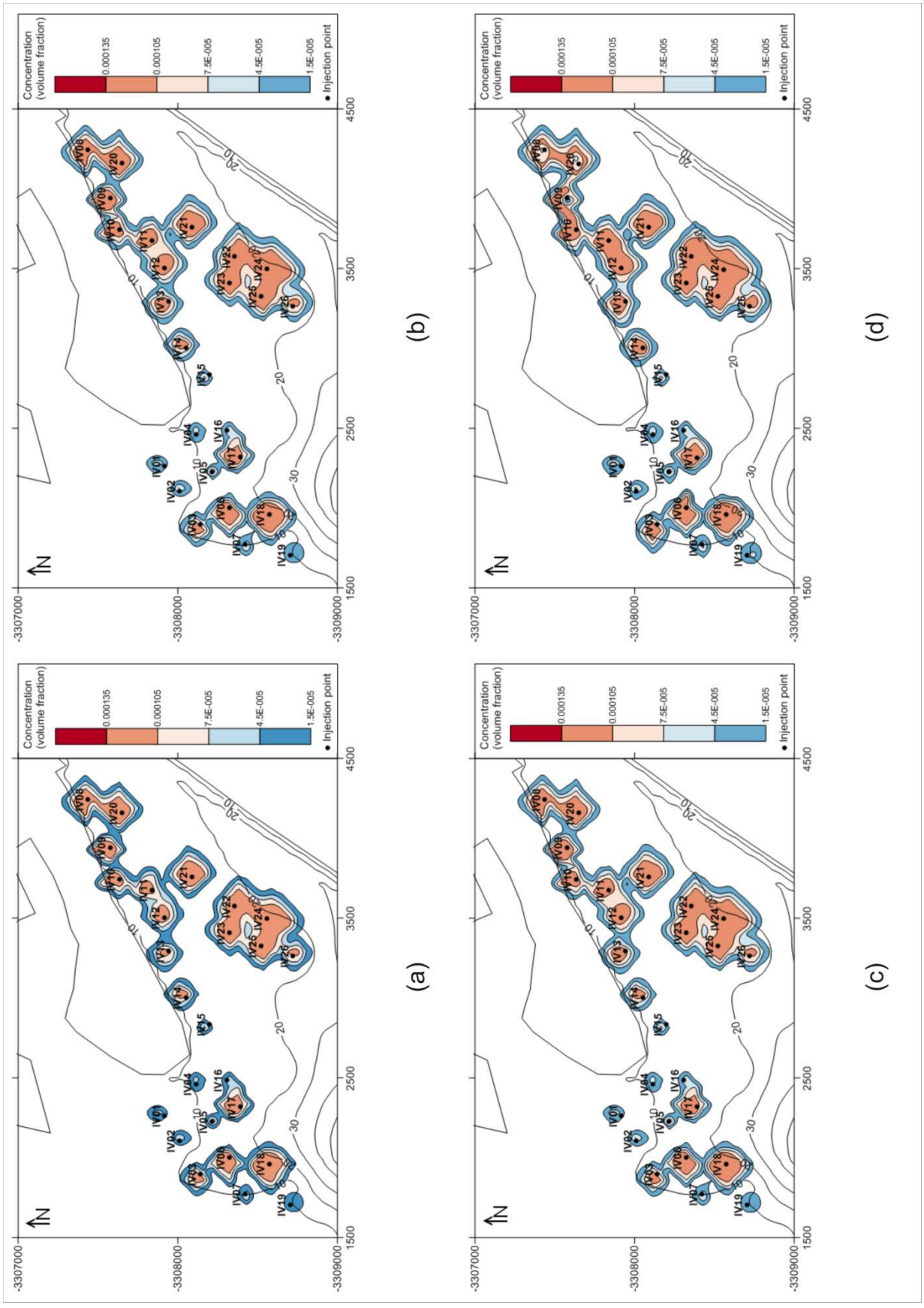

Figure 5-20: Maps illustrating the simulation results for the remediation of aqueous phase PCE with polymer xanthan gum. (a) PCE without remediation; (b) Remediation using diluted xanthan gum; (c) Remediation using undiluted xanthan gum; (d) Remediation using undiluted xanthan gum and an increase in the rate of infiltration.

CHAPTER 6: RESULTS AND DISCUSSION - MODFLOW

6.1 Introduction

Three maps were created in Surfer for two different model scenarios. The two maps depict the distribution of aqueous phase benzene after migration occurred over a duration of twenty years and the extraction of the resultant plume over a period of one year. A duration of twenty years was used to determine the flow direction and the shorter time period of one year was used as a comparison map in conjunction with that produced by UTCHEM. The plume did not illustrate a good flow direction over a shorter period and therefore a larger time period was used. The final map depicts the distribution of the aqueous phase after a flow duration of one year and is used for comparison with the aqueous UTCHEM results. The change over time is illustrated with line graphs that represent the concentration versus time. This will be discussed separately along with a comparison between the UTCHEM and MODFLOW simulations.

6.1.1 The distribution of aqueous benzene

Figure 6-1 is a contour map depicting the benzene plume simulated by MODFLOW. The concentration remained constant at the injection positions at 6×10^4 µg/l which is approximate equal to the value used in UTCHEM as the equilibrium concentration (58.7 mg/l) (Currie *et al.,* 1994a). The model simulation period was ten years and resulted in a plume distribution indicated in Figure 6-1.

The concentration of benzene in the top layer reaches values up to 5.5×10^4 µg/l (equivalent to 40 mg/l) and is found in the vicinity of borehole IV 01, 02, 04, 04, 16 and 17 depicted in Figure 6-1. The general direction of migration is toward the ocean at majority of boreholes with the exception of borehole IV 26 where the plume is elongated in a southerly direction towards the dune area. All other plumes are directed towards the north east, moving towards the harbour itself. Plumes located in the vicinity of boreholes IV 21 25 appear to be smaller in comparison to the rest. The plume size is related to the hydraulic gradient. When there is a steep gradient, as in this case along beach dunes, the rate of distribution is significantly increased (Palmer, 1992) and the plume size appears smaller due to the decrease in concentration. The plume is spread over a larger surface area and therefore does not seem to be as high as those found in areas

where a gradual change in hydraulic head exists. In the vicinity of borehole IV 01, 02, 04, 05, 16, and 17, the plume accumulates on the flattened surface, gradually draining into the ocean.

In the breakthrough curve in Figure 6-2, the concentration over the duration of the simulation increases steadily at most existing boreholes with the exception of borehole SAP 46 that increases exponentially. Borehole SAP 46 is located in between boreholes IV 16 and 17 where the largest plume concentration is found. The position of the boreholes used to create the breakthrough curve can be identified in Figure 4-1 and are boreholes collected from the consulting company.

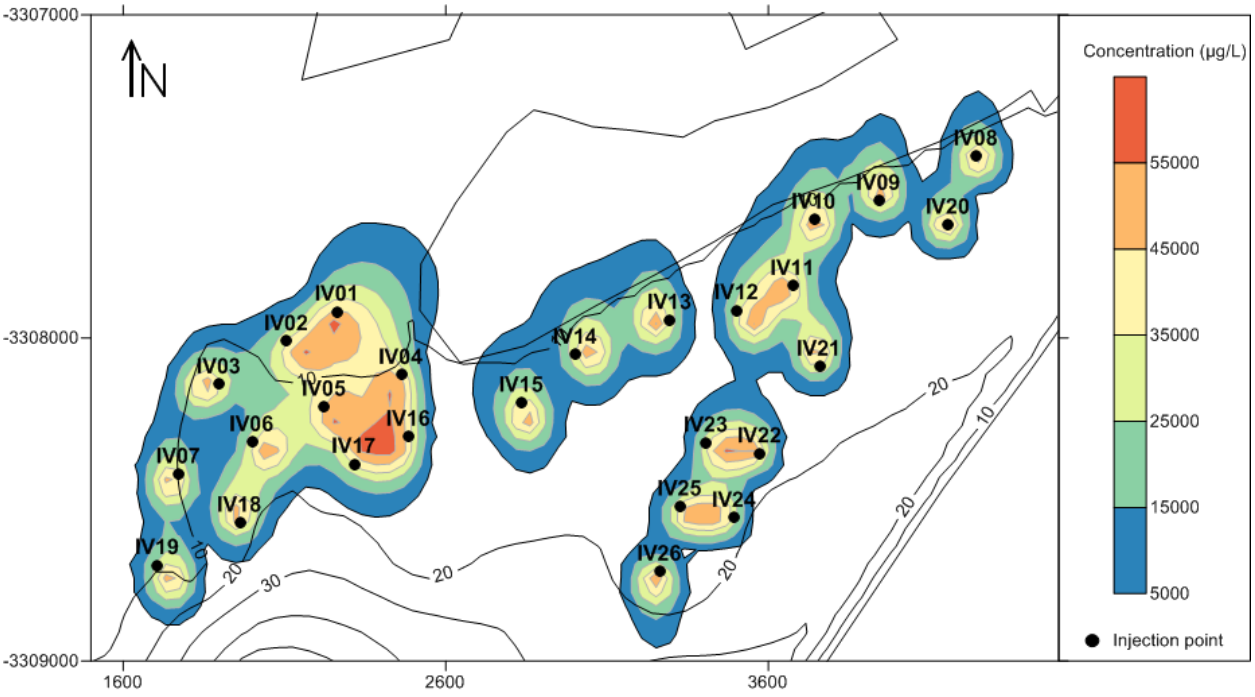

Figure 6-1: Map illustrating the distribution of aqueous phase benzene using MODFLOW after a simulation duration of twenty years in the subsurface.

6.1.2 The distribution of aqueous benzene after it has been extracted

Once the distribution of benzene was achieved after a twenty-year simulation, the concentrations were used in the following simulation as the initial concentration to be extracted as a remediation option. Extraction was conducted at a rate of 300 m^3/d, for a period of one year. The results can be seen in Figure 6-3. There is a reduction in the concentration of the benzene plume. Sufficient amounts of benzene have been recovered through extraction to reduce the concentration from a maximum of 5.5×10^4 µg/l (55 mg/l) to a maximum value of 4.5×10^4 µg/l (45 mg/l), which can be identified in an isolated area adjacent to injection point IV 01.

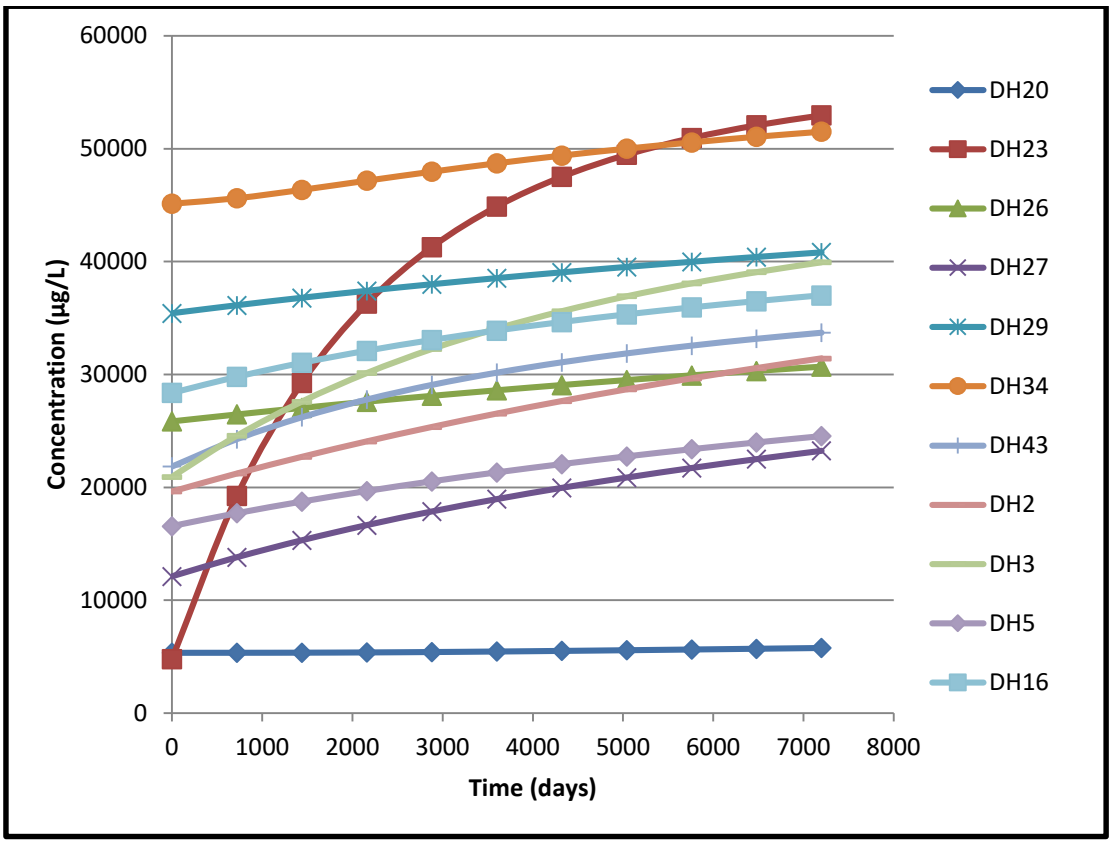

Figure 6-2: Line graph representing the change in concentration of aqueous benzene over the duration of 20 years measured at different boreholes located within the contaminated region.

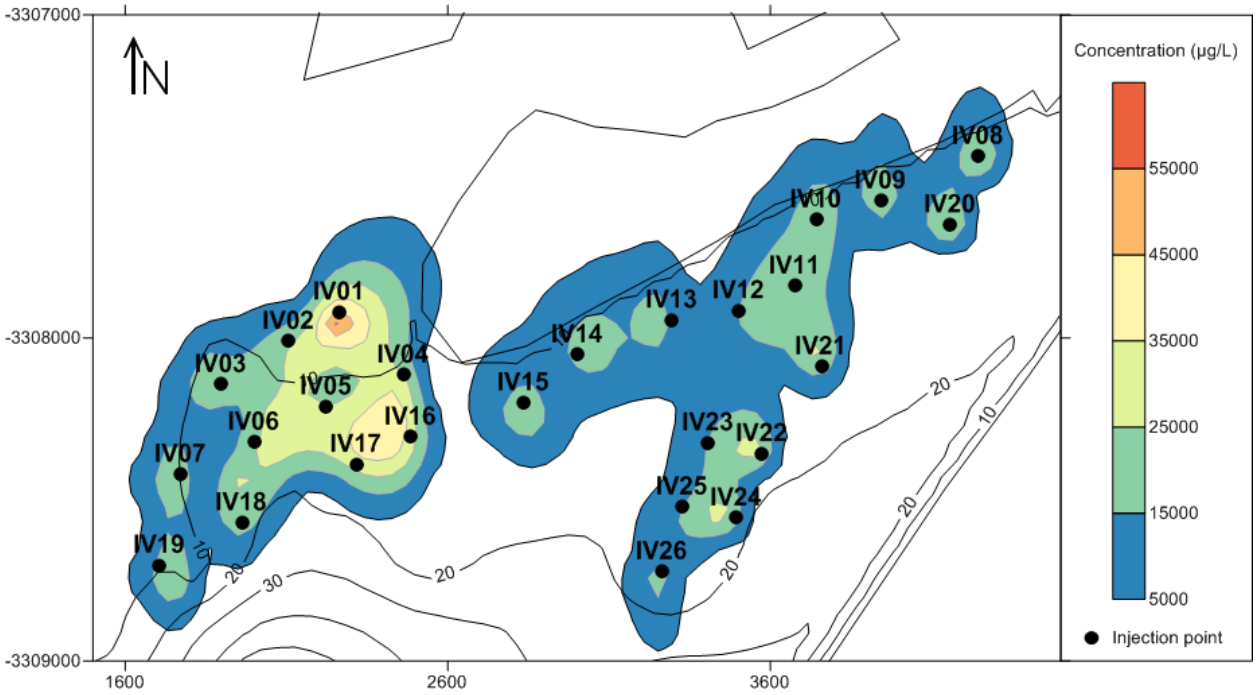

Figure 6-3: Map illustrating the distribution of aqueous phase benzene in the subsurface after an extraction period of one year.

This is once again illustrated in the line graph in Figure 6-4 where the concentration is decreased at some boreholes within the plume boundary. The position of the boreholes used to create the breakthrough curve can be identified in Figure 4-1 and are existing boreholes collected from the consulting company.

Even though there has been a reduction in concentration of the plume, the size and extent of the affected area seem to increase after extraction when comparing Figure 6-1 and Figure 6-3. The concentration in some boreholes, however, tends to increase slightly by about approximately 3 g/L. This is illustrated in the breakthrough curves in Figure 6-5. Gebrekristos *et al.* (2008), state that pumping of the groundwater can lead to instability and redistribution on the NAPL. This can cause migration on the aqueous to previously uncontaminated areas, however, the concentration can be reduced to less harmful values below that which may cause a health risk.

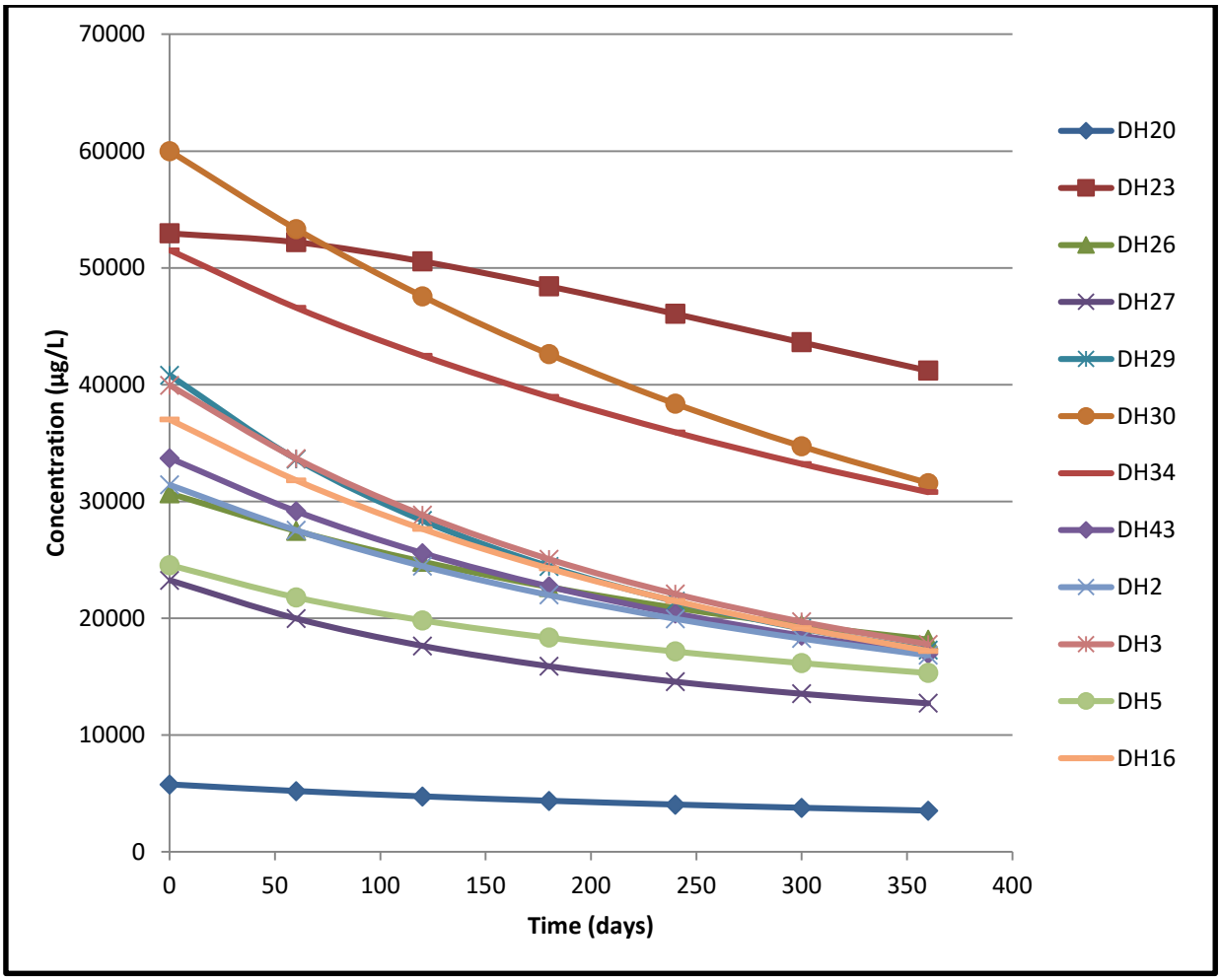

Figure 6-4: Line graph representing the decrease in concentration of aqueous benzene over the extraction period of one year measured at different boreholes located within the contaminated region.

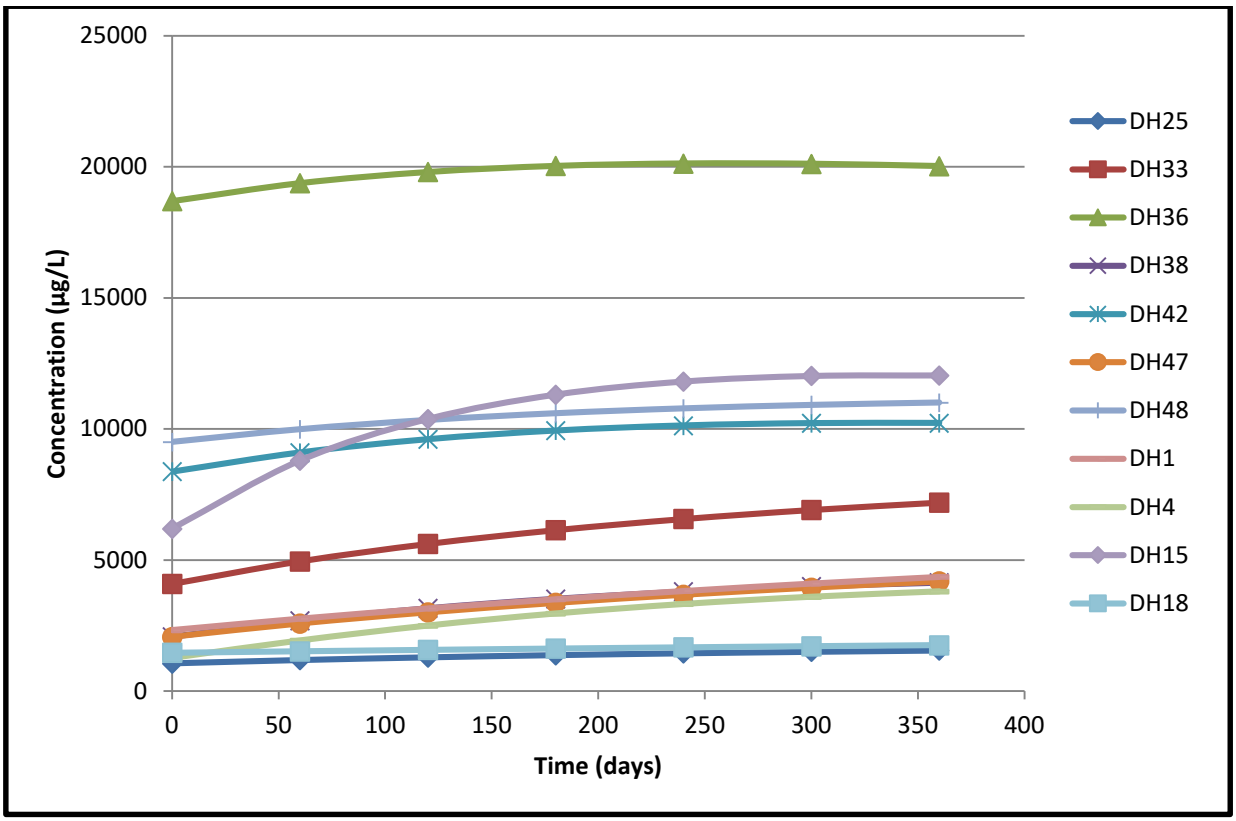

Figure 6-5: Line graph representing the increase in concentration of aqueous benzene over the extraction period of one year measured at different boreholes located within the contaminated region.

6.1.3 The difference between UTCHEM and MODFLOW

Figure 6-6 and Figure 6-7 contain maps illustrating the results obtain for the top layer for MODFLOW and UTCHEM respectively. The two diagrams are visually very different. The injection time for the UTCHEM model was three months however the MODFLOW model was four times greater in size and therefore it is compared after a period four times greater than that of the UTCHEM model (one year). The degree of contamination in both figures is similar in comparison; however, the migration is very different. In Figure 6-6 the MODFLOW model illustrates the movement of hydrocarbons towards the harbour and towards lower lying areas which cannot be similarly created in the UTCHEM model. Plumes within the UTCHEM model appear to be less mobile as they are not elongated in shape and seem to be migrating towards the adjacent dune and coastline and not towards the harbour. Due to software restrictions, UTCHEM could unfortunately not demonstrate the movement of hydrocarbons in the subsurface accurately. Work done by Bernardez *et al.* (2009) and Sedaghat *et al.* (2013) both demonstrate that UTCHEM could only predict migration of the free phase in sand columns and micro-models with some effort after codes had been manipulated.

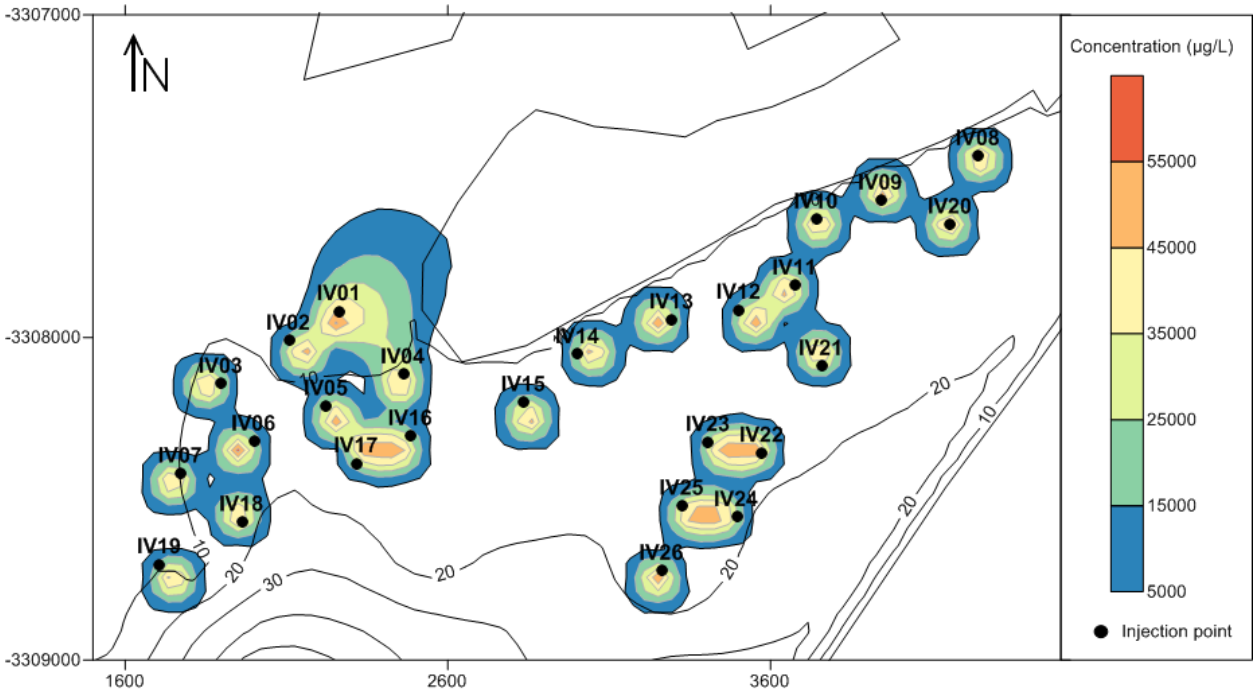

Figure 6-6: Map illustrating the distribution of aqueous phase benzene after a simulation duration of one year in the top 11 m of the subsurface (MODFLOW).

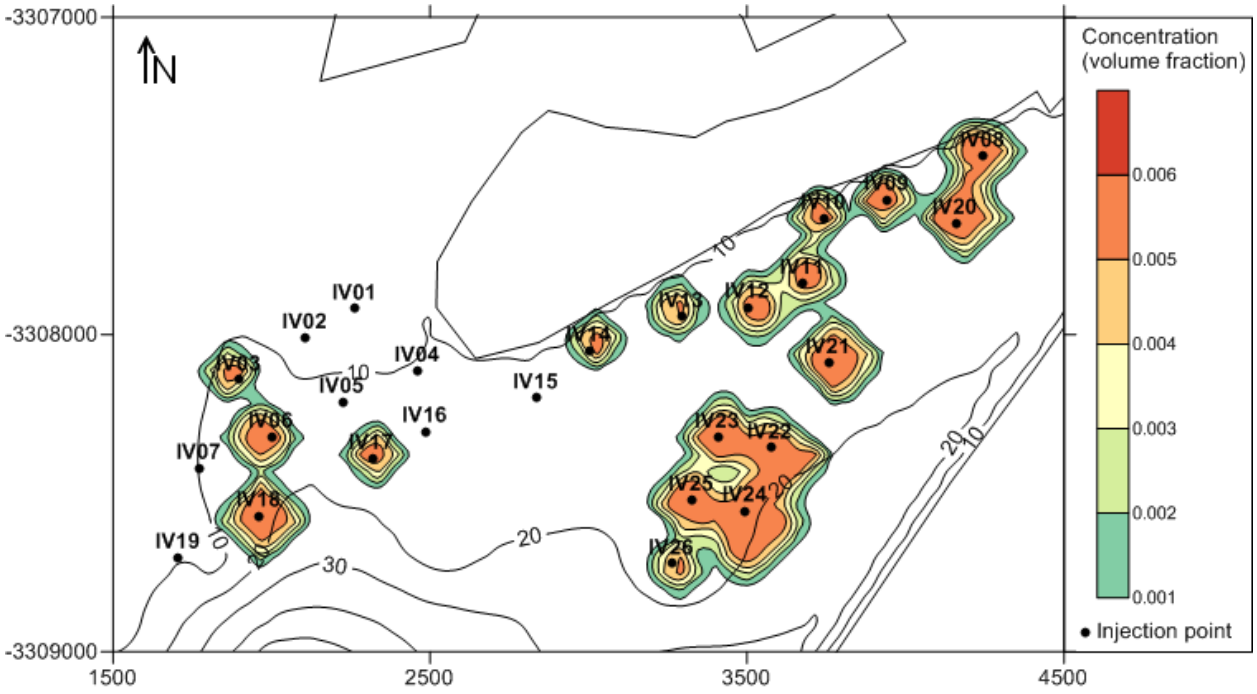

Figure 6-7: Map illustrating the distribution of aqueous phase benzene after a simulation duration of three months in the top 11 m of the subsurface (UTCHEM).

Even though UTCHEM and MODFLOW can both model the dissolved phase, data required by each are quite different. Where MODFLOW requires hydraulic conductivity values, UTCHEM needs permeability values which are far less detailed than that used in MODFLOW. Permeability values had to be generalised for each layer, without which the UTCHEM model would not run. In the UTCHEM code, recharge is not considered in the form of precipitation but is defined in the MODFLOW model where it has a major influence of the hydraulic heads. Additionally, the flow regime in MODFLOW is governed by the presence of constant head boundaries that represents areas where the hydraulic head is kept constant in the case of a river, for example. This would be a controlling factor to determine the groundwater flow direction that UTCHEM does not consider. MODFLOW also requires initial head values instead of initial saturation values required by UTCHEM. These are a few of the physical property differences in the models that results in inconsistencies when compared.

A major difference between plume shapes could be due to the source in each model. In the case of MODFLOW the dissolved benzene is injected at a slow rate at each borehole and is therefore a point source but the same cannot be said for the UTCHEM model. The source of the dissolved benzene in the UTCHEM model is derived from the entire NAPL plume covering a lager surface area. The non-aqueous phase will decay and dissolve over the surface available.

As for the analytical code, Gebrekristos *et al.* (2008) states that there is no right answer when deciding on a model because each model has their own weakness and assumptions and therefore are very different. It would be inappropriate to compare models and use one to validate another. Verification can only be determined from field observations, however, this has become increasing difficult with the development of more sophisticated models (Gebrikristos *et al*., 2008)

CHAPTER 7: DISCUSSION - PROPOSED METHODOLOGY

To summarise, UTCHEM demonstrated that it does not have the ability to predict the movement of hydrocarbons; however, the change in behaviour with the use of different remediation cocktails does coincide to results found in literature. The software was not able to determine the migration of the non-aqueous phase as there are many limitations for an environment that is so complex. It was however possible to demonstrate some differences between the LNAPL, benzene, and DNAPL, PCE. The LNAPL tends to accumulate closer to the surface and migrates laterally and therefore can cover a larger area in comparison to its dense counterpart. DNAPLs will migrate downward by the forces of gravity until a less permeable boundary is reached. Thereafter, there can be further migration in the subsurface depending on the permeability on the confining boundary.

Gebrekristos *et al*. (2008) state, that there are important uncertainties related to multiphase models that are not unique to this kind of problem. The issue lies in the fact that any model is a simplified version of reality based on various assumptions and results should be interpreted with these considerations. Due to its inherent nature, multiphase models are very limited in what they may achieve. It is not the intention of modelling to provide quantitative results but rather give a qualitative impression of what could be. For the remediation scenarios, modelling cannot predict exactly what may happen in reality, however, a relative decision can be made when comparing results to determine what would work best to increase the mobility of the free phase.

The use of surfactant, alcohol, and polymers showed good variations at different concentrations and injection rates. Migration of the plume increased with increases in both concentration and injection rate. The use of surfactant, SDS, resulted in the greatest distribution after the duration of the simulation in comparison to ethanol and xanthan gum. This would cause the NAPL to easily migrate and disintegrate therefore reducing the density and improving the viscosity making the solution much easier to recover, it will, however, be much more difficult to control. Ethanol and xanthan gum would need to be used at high concentrations and injection rates to make a significant difference. The effectiveness of remediation was concentrated in the top layer due to the fact that the remediation mixtures are more often than not, less dense than water. This would make it much harder to recover DNAPLs. Considering all injection cocktails, the use of SDS and ethanol would be the best option to increase mobility of the free phase. It demonstrated the ability to decrease the concentration of the NAPL at each borehole consistently. There was only improvement once an undiluted mixture, and an undiluted mixture at an increased injection rate was added.

A MODFLOW model illustrated that a benzene plume would move towards the ocean and towards lower lying areas in the direction of a decrease in hydraulic head. This distribution mechanism was confirmed by Palmer (1992). The majority of the contaminant was distributed near the surface with minor plumes in certain areas at depths. Extraction of the aqueous contaminant at a rate of 300 m^3/d improved the quality of the water in the top layer. The maximum concentration of benzene reduced from 40 mg/l to a maximum value of 12 mg/l. The bottom layer was undisturbed. When comparing aqueous phase benzene in each model, there was a difference in flow direction in each, however, the calibrated model was used in MODFLOW that was more detailed that the uncalibrated model used in UTCHEM.

Modelling of the multiphase environment has proven how complicated hydrocarbons can be as a contaminant. It is extremely difficult to determine where the NAPL will migrate and the time it may take for it to be distributed to a place of high concern such as a usable aquifer or surface water resource. The aqueous phase, on the other hand, is more predictable and easier to conceptualise. Gebrekristos *et al.* (2008) and Steyl *et al*. (2012), states that failure to adequately determine the behaviour of a NAPL will result in misguided site characterisation and remedial efforts. For this reason, a proposed procedure to assess NAPL contaminated areas have been set out that may facilitate future studies. Please note, the site in this investigation could not be accessed and all field procedures are based on literature. The processed followed is illustrated in Figure 6-8.

An initial on site investigation is important to retrieve existing information that would not be accessible in literature. This includes the types of chemicals found on site, a detailed description of operations conducted on site to determine where hydrocarbon products are stored, and doing a walk over the site to identify any visible spillage area. In the manual for site assessment at DNAPL contaminated sites (Gebrekristos *et al.,* 2008), it addressed the value gained by interviewing employees to estimate volumes of products that have not been recorded such as amounts that were purchased and how often were they delivered. Historical site engineering drawings and aerial photographs may facilitate in identifying underground and surface storage tanks and pipelines, respectively that can be characterised as a source or potential source. The advantage of this step is to identify the contaminant and its properties as well as the potential sources of contamination. If this is known, it would limit the surface area that would require assessment. This information is not always readily available, especially at relatively older storage facilities (Gebrekristos *et al.,* 2008).

Once the site assessment is completed, a desktop study needs to be conducted to compile historical data and literature. This process is done by collecting old reports that are relevant to the area that will provide information related to the geology of the area, historical borehole logs and data, geophysical investigations done on site, historical water levels and pump test

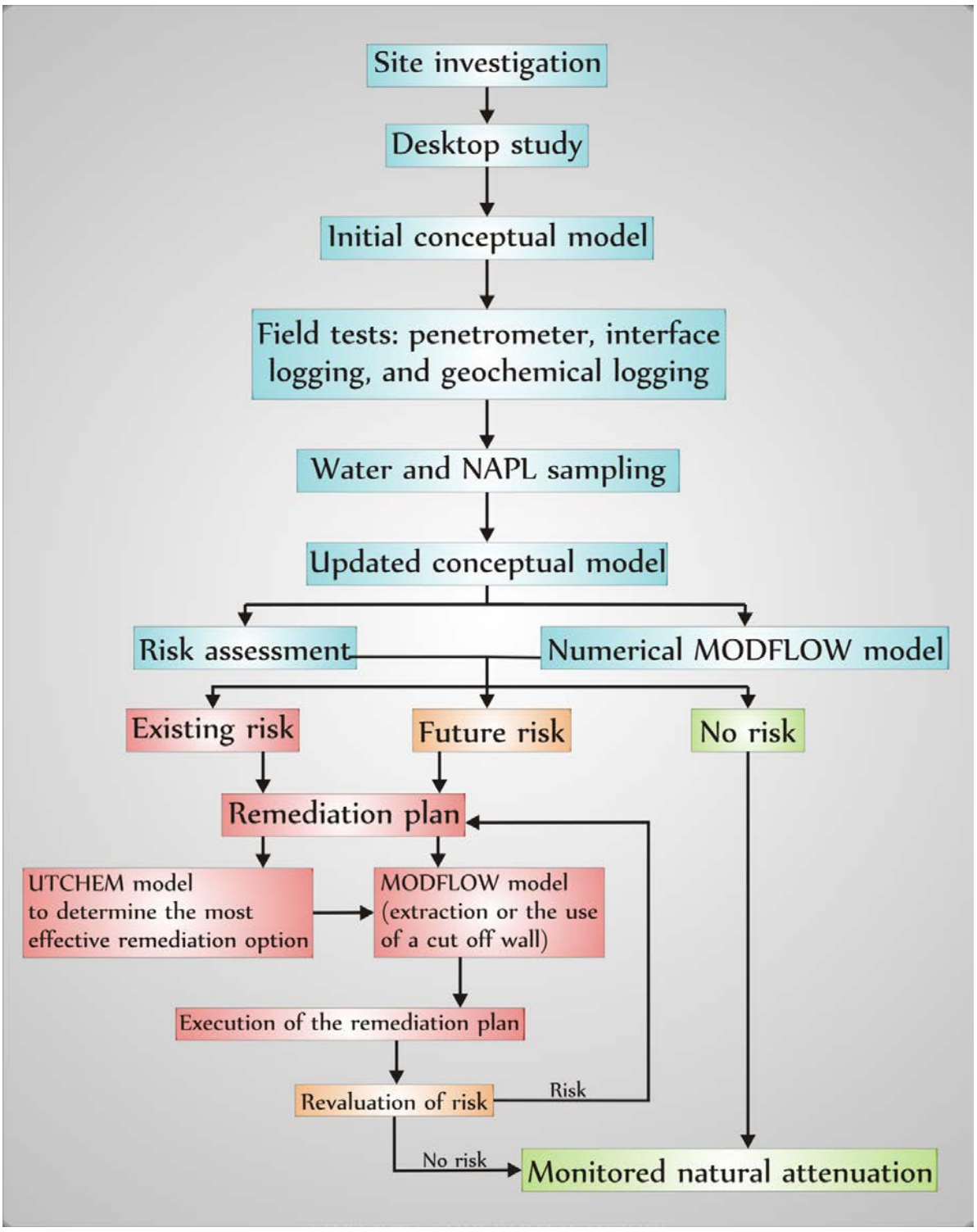

Figure 6-8: Flow diagram representing the procedure of the proposed methodology for a site assessment and remediation evaluation.

analysis, the thickness of the NAPL layer within boreholes and chemical and physical characteristics of the NAPL. A disadvantage is that this would be a time consuming process, however, if parameters are known it will limit the time and costs needed to establish new information.

An initial conceptual model is then created using all existing data. This process is essential to plan for further site analysis and to identify any gaps that exist. The following information is required from historical data as a check list.

- Geology and geological structure – to understand the material that governs the flow in the subsurface
- Fractures and subsurface features – to identify any groundwater pathways
- Hydraulic gradients – to be able to determine the direction of flow
- Hydraulic flow parameters – to use in the numerical model
- Chemical characteristics of the water and NAPL – to understand the contaminated
- Recharge – to use in the numerical model
- Source terms – to use in the numerical model and to facilitate the delineation of the NAPL

Boreholes are usually present at these sites, so many of the parameters needed should be available from the borehole installation documents.

During field assessments, it is most important to fill the gaps in information if they exist or if current information is out-dated. When this has been achieved, the NAPL needs to be delineated and characterised. The surface distribution of the NAPL should be determined using the penetrometer. As mentioned before, this is a cone shaped device that is forced into the underlying soil that measures the resistance. It can assist to calculate the porosity and identify changes in porosity if pores are filled with the free phase (Hulling & Weaver, 1991). This method is proposed instead of the soil gas survey because it does not give an over estimation of the surface distribution (Gebrekristos *et al.,* 2008). The penetrometer can also be used to determine the presence of the NAPL at greater depths without excavation. This method is advantageous because it is cheap, easy to carry out, and yields additional porosity data. The disadvantages of this method are there needs to be sufficient space for the procedure to be done if the area is highly industrialised and it is quite difficult to determine where the free phase could occur. These problems can be corrected by removing cement slabs and creating a grid sampling procedure to make sure that the entire area is covered. Additionally, because the penetrometer can only give an indication of the NAPL in unconsolidated material, there is no way to determine the extent of the plume beyond the soil/rock boundary.

The thickness of the free phase can be determined using the interface borehole logging method at all existing boreholes in the vicinity. This is done by allowing an interface meter into a borehole that can detect the interface between the NAPL and air, the water and the NAPL, and air and water. In the borehole, the NAPL apprears to be thicker in comparison to the thickness in a geological formation, this can be corrected if the properties of the formation and the

borehole material are known. The advantages of this method are that it is quick, cost effective, and can be done on site. A disadvantage is that the thickness is only known adjacent to boreholes and is assumed by interpolation over the entire area. Once the location of the free phase is known, water and NAPL samples need to be taken from the boreholes to characterise the NAPL and determine the concentration of the free phase and dissolved phase in the water. This should be done using a bailer and not by extraction as extraction will redistribute the free phase (Gebrekristos *et al.,* 2008).

The last proposed method is geochemical borehole logging. It involves the insertion of a probe to determine the chemical nature of layers of fluid in a borehole. The probe is connected to a multimeter that can determine chemical parameters such as electrical conductivity, pH, temperature, redox potential and dissolved oxygen. This method can be used to predict the extent of natural attenuation that could take place, and to identify fractures in boreholes where water with a high salinity passes through. The advantages of this method are that it is non-invasive, cost effective, quick to implement and can be conducted on site. However, it cannot be used to determine flow magnitude and direction (Gebrekristos *et al.,* 2008).

All information gathered and tested needs to aid in developing an accurate and concise updated conceptual model. Conceptual models have been routinely used to characterise chemical migration and remediation efforts (Gebrekristos *et al.,* 2008; Steyl *et al*., 2012). The conceptual model should focus on contaminant fate and transport, and the processes that govern migration. This includes geological and manmade pathways, the type of contaminant and process that affect its concentration such as dilution, advection, dispersion, biodegradation, and salinity (Gebrekristos *et al.* 2008; Steyl *et al*., 2012).

Once the conceptual model is complete, an assumption can be made regarding where the plume may migrate to, a numerical MODFLOW model should be created to evaluate the discharge points or boundaries. This is done to determine where the plume may migrate to and whether surrounding water bodies may become vulnerable in the future. Additionally, the toxic and carcinogenic risk needs to be identified if the harmful organic compound is in contact with humans and animals.

Because benzene and other hydrocarbons are toxic in very small concentrations, a toxic risk assessment will be conducted to see if a health threat exists and how the threat may change based on the relative scenarios modelled (Wu et al., 2011). To determine the risk involved, the dose of the hydrocarbon is first calculated as follows (Dennis, 2013):

$$\boldsymbol{Dose = C \times IR \times ED}$$

Where:

Dose = The total dose

C = Maximum concentration

IR = Average intake rate

ED = Exposure duration

There after average daily dose would first be determined. This is done using the following equations (Dennis, 2013):

$$ADD = Dose/(BW \times ED)$$

Where:

ADD = The average daily dose

BW = The average body weight over exposed duration

ED = Exposure duration (Average life expectancy)

Once the average dose has been calculated, the risk may be calculated as follows (Dennis, 2013):

$$Risk = ADD/RfD$$

Where:

RfD = The reference dose

This would give an indication of the risk involved for a person to become ill that could eventually result in death. The carcinogenic risk would determine whether a person could develop cancer. This is calculated by first calculating the lifetime daily dose by using the total dose (Dennis, 2013):

$$LADD = Total\ dose/(BW \times lifetime)$$

The carcinogenic risk could then be calculated as follows (Dennis, 2013):

$$Risk = 1 - e^{-LADD \cdot CPF} \approx LADD \times CPF$$

Where:

CPF = Cancer Potency factor

The reference dose is the approximate concentration per day that is likely to not have a health effect during a lifetime. Appendix I contain the health effects certain polycyclic organic hydrocarbons have on animals and humans, the reference intake dose and the cancer potency factor. A risk assessment was not done in this study because dissolved benzene and PCE were far too high and unrealistic. This is because an equilibrium concentration was used that does not consider salinity, temperature, pressure and absorption variability. In a natural environment, concentrations will be much lower as they are a function of the amount of NAPL in the product in question, the salinity of the groundwater, and the temperature and pressure (Eby, 2004).

The contamination plume is then classified into one of three risk categories: existing risk if there is seepage of the contaminant into a usable water resource in high concentrations, future risk if there will be seepage of the contaminant into water resources in the future and no risk if a current and future threat does not exist. If there is a risk and the contaminant is compromising the integrity of a water resource, a remediation plan is required for clean-up. It will then be necessary to make use of UTCHEM to determine which remediation option will best suit the environment and MODFLOW to establish a plan for extraction. If the risk does not require immediate attention and if the plume is relatively isolated, MODFLOW can be used to estimate whether a cut off wall can be used to contain the plume. An example of this would be an underground storage tank at a petrol station. With this said, it should be emphasised that MODFLOW is mass conservative and anything in the system is a reflection of ideal conditions. After a decision is made, remediation can commence with periodic monitoring until the risk is alleviated. This is done by redoing the “remediation plan” as illustrated in the loop in Figure 6-8. Models created should be updated and an alternative plan of action should be used to alleviate the risk. As soon as there is no further threat to the environment, NAPL concentration can be managed through natural attenuation. This will only be possible once the source has been removed. The pathway and receptor will need to be monitored until site closure or project closure occurs.

CHAPTER 8: CONCLUSION AND RECOMMENDATIONS

To summarise the proposed methodology, it begins with a site assessment where information regarding the site and site activities are obtained though a site walk over, interviews, historic aerial photography, followed by the collection of historical data from site reports and available literature. All information gained in this process is used to construct an initial conceptual model where the following information should be known:

- Geology and geological structure
- Fractures present and subsurface features, if any
- Hydraulic gradients
- Hydraulic flow parameters
- Chemical characteristics of the water and NAPL
- Recharge
- Source terms

The conceptual model will help to evaluate the site procedure for site assessment methods as well as highlight any necessary information needed before the next step. Once this is conducted the following methods are utilised in the field and in laboratories:

- Penetrometer – to predict the extent of the NAPL in the unconsolidated material on the surface of the affected area
- Interface meter – to determine the thickness of the free phase
- NAPL and water samples – to characterise the NAPL and determine the concentration of the dissolved phase
- Geochemical logging – to determine the natural attenuation potential and in addition identify fracture zones.

After the field and laboratory analysis is completed, the conceptual model is updated and a risk assessment and numerical MODFLOW model is created to determine if there is a potential of elevated dissolved concentrations reaching a water resource. If there is no risk, the natural attenuation will be monitored. If there may be a potential risk, concentrations are determined and the MODFLOW model is updated at regular intervals. If there is an immediate risk, a remediation plan is needed and a simplified UTCHEM model can be created to determine which method would be best for the site. The idea is to increase mobility of the free phase so that it can be extracted from the groundwater system. The dissolved phase can then be monitored to ensure concentrations decrease through natural attenuation.

The proposed method consists of an assessment section and a section for remediation only if it is necessary. It is different from the method proposed by Gebrekristos *et al.* (2008) which only contains an assessment. The methodology proposed in this document streamlines the one proposed by Grebrekistos *et al*. (2008) because it requires far less field and lab assessments. The advantage of this is that it would be faster and cheaper to execute. Limited resources and man power is needed in comparisons. Quantification of a risk based approach has been included to this approach to standardise risk at all sites. The disadvantages for both methodologies are that it still remains difficult to determine the thickness of the NAPL and modelling only remains a tool for understanding and not a quantitative method to determine contaminant migration.

It is recommended in future research to use field measurements to calibrate the chemistry for the MODFLOW and UTCHEM model in order to determine the actual risk. The concentration of the aqueous phase can be controlled by altering the equilibrium concentration. Additionally, the effectiveness of the various surfactant options should be analysed by conducting small batch tests in a laboratory. This will bring confirmation to the UTCHEM results obtained in this study and those found in literature. There is a large amount of research conducted in this regard but there is no data base or paper done on different remediation cocktails. Articles collected by Bernardez *et al.* (2009), Ouyang *et al*. (2001) and Silva *et al*. (2012) have demonstrated that the use of a single remediation mix, used at different concentrations and injection rates, optimises field procedures during remediation. Another option would be to create in lab micro-models to predict where the NAPL will propagate in different structural environments and recreate this within the UTCHEM software. Sedaghat *et al*. (2013) conducted such a study to determine the migration of NAPLs within fractions at various orientations. The same could be done for other types of impermeable limitations that disturb migration. It could be interesting to determine the time taken for a NAPL to reach the base of a physical micro-model that contains minor clay lenses and one that has no obstructions while validating this process in UTCHEM. Lastly, it would be beneficial to simulate oxidation and biodegradation in the UTCHEM software to be able to predict natural attenuation more accurately.

REFERENCES

Agaoglu, B., Scheytt, T. & Copty, N.K. 2012. Laboratory-scale experiments and numerical modelling of cosolvent flushing of multi-component NAPLs in saturated porous media. *Journal of Contaminated Hydrology.* 140-141: 80-94.

American Petroleum Institute. 1985. Laboratory study of solubilities of petroleum hydrocarbons in groundwater. API Publication No. 4395.

Anon. 2016. The bottleneck: New investment alone will not fix Africa's ports. Governments need to deal with pilfering officials, too. *The Economist*, 19 March. https://www.economist.com/news/middle-east-and-africa/21695054-new-investment-alone-will-not-fix-africas-ports-governments-need-deal Date of access: 22 Feb. 2018

Bear, J. 1972. Dynamics of fluids in porous media. New York: American Elsevier.

Bernardez, L.A., Therrien, R., Lefebvre, R. & Martel, R. 2009. Simulating the injection of micellar solutions to recover diesel in a sand column. *Journal of Contaminated Hydrology*. 103(3-4):99-108.

Botha, G.A. & Singh, R. 2012. Geological, geohydrological and development potential zonation influences; Environmental Framework for Umkhanyakude District, Kwazulu-Natal. Council for Geoscience, Pietermaritzburg.

Brooks, M.C., Annable, M.D., Rao, P.S.C., Hatfield, K., Jawitz, J.W., Wise, W.R., Wood, A.L. & Enfield, C.G. 2003. Controlled release, blind test of DNAPL remediation by ethanol flushing. *Journal of Contaminant Hydrology*. 69(4):281-297.

Campbell, E.E., Parker-Nance, T., & Bate, G.C. 1992. A compilation of information on the magnitude, nature and importance of coastal aquifers in South Africa. WRC Report No. 370/1/92. Water Research Commission, Pretoria.

Cobbing, J.E. 2014. Groundwater for rural supplies in South Africa. Port Elizabeth: Nelson Mandela Metropolitan University. (Project proposal).

Currie, R.C., Chiao, F. & Mckone, T.E. 1994a. Intermedia transfer factors for contaminants found at hazardous waste sites: Benzene. University of California, Department of Environmental Toxicology, California.

Currie, R.C., Chiao, F. & Mckone, T.E. 1994b. Intermedia transfer factors for contaminants found at hazardous waste sites: Tetrachloroethylene (PCE). University of California, Department of Environmental Toxicology, California.

Dennis, I. 2013. Introduction to geohydrology: Groundwater assessments-Block Module notes. Centre for Water Sciences and Management, North West University, Potchefstroom.

Dingle, R.V., Siesser, W.G. & Newton, A.R. 1983. Mesozoic and Tertiary geology of southern Africa. A. A. Balkema, Rotterdam.

Eby, G.N. 2004. Principles of environmental geochemistry. Balmont, United States of America: Brooks/Cole, Cengage.

Falkenmark, M. 1989. The massive water scarcity now threatening Africa – Why isn't it being addressed? *Journal of the Human Environment*. 18(2):112-118.

Falta, R.W. 1998. Using phase diagrams to predict the performance of cosolvent floods for NAPL remediation*. Journal for Groundwater Monitoring and Remediation.* 18(3):94-102

Gebrekristos, R.A., Pretorius, J.A., & Usher, B.H. 2008. Manual for site assessment at DNAP contaminated sites in South Africa. WRC Report no.: 1501/2/08, Water Research Commission, Pretoria.

Hammouda, B. 2013. Temperature effect on the nanostructure of SDS micelles in water. *Journal of Research of the National Institute of Standards and Technology*. 118:151-167.

Harvey, J.W. & Odum, W.E. 1990. The influence of tidal marshes on upland groundwater discharge to eustuaries. *Journal of Biochemistry.* 10(3):217-236.

Heath, R.C. 1983. Basic ground-water hydrology. U. S. Geological Survey Water-Supply Paper 2220.

Hulling, S.G. & Weaver, J.W. 1991. Dense nonaqueous phase liquids. Ground Water Issue, EPA504/4-91-002, United States Environmental Protection Agency, Ada, Oklahoma.

ITRC (Interstate Technology & Regulatory Council). 2011. Integrated DNAPL Site Strateg. IDSS-1. Integrated DNAPL Site Strategy Team. Interstate Technology & Regulatory Council, Washington, D.C.

Jackson, R.E., Dwarakanath, V., Meinardus, H.W. & Young, C.M. 2003. Mobility control: how injected surfactants and biostimulants may be forced into low-permeability units. *Remediation Journal*. 13(3):59-66.

Jawitz, J.W., Sillan, R.K., Annable, M.D., Rao, P.S.C., Warner, K. 2000. In-situ alcohol flushing of a DNAPL source zone at a dry cleaner site. *Journal of Environmental Science and Technology.* 34(12):3722-3729.

Johnson, M.R., Anhaeusser, C.R. & Thomas, R.J. 2006. The Geology of South Africa. Johannesburg: Geological Society of South Africa. Council for Geoscience, Pretoria.

Jury, M.R. & Melice, J.L. 2000. Analysis of Durban rainfall and Nile river flow 1871 – 1999. *Theoretical and Applied Climatology*. 67(3):161-169.

Kelbe, B, Germishuyse, T. 2010. Groundwater / surface water relationships with specific reference to Maputuland. WRC Report no. 1168/1/10. Water Research Commission, Pretoria.

Kelbe, B., Germishuyse, T., Snyman, N. & Fourie, I. 2001. Geohydrological studies of the primary costal aquifer in Zululand. Water Research Commission, Pretoria.

Khankam, S., Luadsong, A. & Aschariyaphotha, N. 2015. MLPG method based on kringing interpolation for solving convection-diffusion equations with integral condition. *Journal of King Saud University – Science*. 27(4):292-301

King, L.C. 1972. The coastal plain of S. East of Africa: its form, deposits and development. *Zeitsch, fũr Gedorphologie*. 16:239-251.

Kotz, J.C., Treichel, P.M., Townsend, J.R. 2009. Chemistry and Chemical Reactivity. Thomson Higher Education. Belmont, USA.

Kueper, B.H., Wealthhall, G.P., Smith, J.W.N., Leharne, S.S., & Lerner, D.H. 2003. An illustrated handbook of DNAPL transport and fate in the subsurface. Environment Agency R&D, Bristol, United Kingdom.

Liang, H. & Falta, R.W. 2007. Modeling field-scale cosolvent flooding for DNAPL source zone remediation. *Journal of Contaminated Hydrology*. 96(1-4):1-16.

Lobmeyer, D.H. 1985. Freshwater heads and ground-water temperatures in aquifers of the Northern Great Plains in parts of Montana, North Dakota, South Dakota, and Wyoming. U.U. Geological Survey Professional Paper 1402-D, Washington.

Lumby, A.B. 1992. The development of The Port of Durban during the “long capitalist boom”. The Australian Association for Maritime History. 14(2):105-113.

Lunn, S.R.D. & Kueper, BH. 1997. Removal of pooled dense, non-aqueous phase liquid from saturated porous media using upward gradient alcohol floods. *Water Resource Research*. 33(10):2207-2219.

Lv, J.H., Miao, Y., Zhu, H.P. & Li, Y.P. 2013. A kriging interpolation-based boundary face method for 3D potential problems. *Engineering Analysis with Boundary Elements*. 37(5):812-817

Mccobb, T.D. & Leblanc, D.R. 2002. Detection of fresh ground water and a contaminant plume beneath Red Brook Harbor, Cape Cod, Massachusetts, 2000. Water-Resources Investigation Report 02-4166, Northborough, Massachusetts.

Mercer, J.W. & Cohen, R.M. 1990. A review of immiscible fluids in the subsurface: Properties, models, characterization, and remediation. *Journal of Contaminated Hydrology*. 6(2):107-163.

Milliman, J.D., Broadus, M. & Gable, F. 1989. Environmental and economic implications of rising sea level and subsiding deltas: The Nile and Bengal examples. *A Journal of the Human Environment*. 18(6):340-345.

Mkhwanazi, M.N. 2010. Establishment of the relationship between the sediments mineral composition and ground water quality of the primary aquifers in the Maputuland coastal plain. MSc dissertation. University of Zululand, Richards Bay.

Mucina, L., Scott-Shaw, C.R., Rutherford, M.C., Kemp, K.G.T., Matthews, W.S., Powrie, L.W., Hoare, D.B., 2006. Indian Ocean coastal belt. (*In* Mucina, L., Rutherford, M.C. *ed*. The Vegetation of South Africa, Lesotho and Swaziland. Pretoria: Strelitzia, vol. 19. p. 569–583).

Neff, J.M. 1988. Composition and fate of petroleum and spill-treating agents in the marine environment. (*In* Geraci,J. & St. Aubin, D. *ed*. Sea Mammals and Oil: Confronting the Risks. New York: Academic Press. p. 1-33).

Newell, C.J., Acree, S.D., Ross, R.R. & Hulling, S.G. Undated. Light nonaqueous phase liquids. Superfund Technology Support Centre for Ground Water, Ada, Oklahoma.

Norman, N. & Whitfield, G. 2006. Geological Journeys. Struik, Cape Town, South Africa.

Ortega, J. 1982. Densities and refractive indices of pure alcohols as a function of temperature. *Journal of Chemical and Engineering Data*. 27(3):312-317

Ouyang, Y., Cho, J.S. & Mansell, R.S. 2001. Simulated formation and flow of microemulsions during surfactant flushing of contaminated soils. *Water Research*. 36(1):33-40.

O'Carroll, D.M. & Sleep, B.E. 2009. Role of NAPL thermal properties in the effectiveness of hot water flodding. *Transport in Porous Media*. 79:393-405.

Palmer, C.M. 1992. Principles of contaminant hydrogeology. Lewis, Michigan, United State of America.

Peeters, L., Fasbeender, D., Batelaan, O. & Dassargues, A. 2010. Bayesian data fusion for water table interpolation: Incorporating a hydrogeological conceptual model in kriging. *Water Resource Research*. 46:1-11.

Reservoir Engineering Research Program. 2000. Technical documentation for UTCHEM, A three-dimensional chemical flood simulator: volume 2. Centre of Petroleum and Geosystems Engineering. The University of Texas, Austin.

Rao, P.S.C., Annable, M.D., Sillan, R.K., Dai, D., Hatfield, K., Graham, W.D., Wood, A.L. & Enfield, C.G. 1997. Field-scale evaluation of in-situ cosolvent flushing for enhanced aquifer remediation. *Water Resource Research*. 33(12):2673-2686.

Sedaghat, M.H., Ghazanfari, M.H., Masihi, M. & Rashtchian, D. 2013. Experimental and numerical investigation of polymer flooding in fractured heavy oil five-spot systems. *Journal of Petroleum Science and Engineering.* 108:370–382.

Silva, J.A.K, Smith, M.M., Munakata-Marr, J. & McCray, J.E. 2012. The effect of system variables on in situ sweep-efficiency improvements via viscosity modification. *Journal of Contaminated Hydrology.* 136-137:117-130.

Soga, K., Page, J.W.E. & Illangasekare, T.H. 2004. A review of NAPL source zone remediation efficiency and the mass flux approach. *Journal of Hazordous Material*. 110(1-3):13-27.

South Africa. Department of Water and Sanitation. Undated. Provincial rainfall: Kwa-Zulu Natal. www.dwa.gov.za/hydrology/Provincial%20Rain/Default.aspx Date accessed: 8 Dec.2016.

Spitz, K. & Moreno, J. 1996. Practical guide to groundwater and solute transport modeling. John Wiley & Sons, New York.

Steyl, G., Gomo, M. Vermaak, K., Bothwel, J. Van Tonder, G.J., Surridge, K., Lorentz, S. Ngaleka, J., Sikosana, S., Dlamini, M., Zondi, N. & Revil-Bourdard, S. 2012. Field investigations to study the fate and transport of light non-aqueous phase liquids (LNAPLs) in groundwater. WRC Report no: 1766/1/12, Water Research Commission, Pretoria.

Thornhill, M. & van Vuuren, D. 2009. Status Quo Report: Environmental Management Framework for the Richards Bay Port Expansion Area and Industrial Development Zone. Report No. TX2009/C007-14, Pietermaritzburg, South Africa.

Usher, B.H., Pretorius, J.A. & Gebrekristos, R.A. 2008. Guidelines for the acceptance of monitored natural attenuation processes in South Africa. Institute for Groundwater Studies, University of the Free State, Bloemfontein, South Africa.

Walmsley, R.D. , Walmsley, J.J. & Silberbauer, M. 1999. Freshwater systems and resources. National State of the Environment Report. http://www.ngo.grida.no/soesa/nsoer/issues/water/intro.htm Date accessed: 22 Feb. 2018.

Worthington, P.F. 1978. Groundwater Conditions In the Zululand Coastal Plain around Richards Bay. Council for Scientific and Industrial Research, Pretoria.

Wu, B., Zhang, Y., Zhang, X. & Cheng. 2011. Health risk assessment of polycyclic aromatic hydrocarbons in the source water and drinking water of China: Quantitative analysis based on published monitoring. *Science of the Total Environment*. 410-411:112-118.

Xu, S., Liu, W. & Tao, S. 2006. Emission of polycyclic aromatic hydrocarbons in China. *Environmental Sciences and Technology*. 40:702-708.

Younger, P.L. 2007. Groundwater in the environment, An introduction. Blackwell, Oxford.

Zhang, Y., Tao, S. Cao, J & Coveney, R. M. 2007. Emmision of polycyclic hydrocarbons in China by country. *Environmental Sciences and Technology*. 41:683-687.

APPENDICES

Appendix A: Description of software packages capable of modelling multiphase systems

Software	Description & capabilities	Limiting factors
UTCHEM	A 3D multicomponent (water, organic contaminants, surfactant, alcohols, polymer, chloride, calcium, other electrolytes, microbiological species, electron acceptors, etc.), multiphase (air, water, oil, and microemulsion), compositional flow model that considers complex phase behaviour, chemical and physical transformations in a heterogeneous porous medium. Includes other chemical processes and a variety of geochemical reactions between the aqueous and solid phases. UTCHEM groundwater applications : • NAPL spill and migration in both saturated and unsaturated zones • Remediation using surfactant/cosolvent/polymer • Bioremediation • Geochemical reactions	UTCHEM has a more complicated input system in comparison to common models. The input of data becomes a tedious process.
MARS	(Multiphase Areal Remediation Simulator) models flow of water and light non-aqueous phase liquid (LNAPL), and aqueous phase transport of up to five species in ground water with multiple pumping and/or injection wells. MARS allows accurate representation of highly irregular material and physical boundaries in a heterogeneous media. Included with MARS is the finite-element model, BIOF&T 3-D, that allows: Convection, dispersion, diffusion, adsorption, desorption, and biodegradation.	Does not physically model the migration of NAPL but illustrates the transportation over time graphically. Expensive software package. Does not model the change with different remediation methods.
STOMP	(Subsurface transport over multiple phases) is a computer model used to simulate multifluid subsurface flow and transport. The simulator's modelling capabilities include: multiple-phase systems, nonwetting fluid entrapment, nonaqueous phase liquids, first-order chemical reactions, radioactive decay, solute transport, nonequilibrium dissolution, and surfactant-enhanced dissolution and mobilization of organics.	It is not certain wether the software as a 2D or 3D interface and there is no trial package to be able to test the capabilities. Does not model the change with different remediation methods. Expensive software package.

Appendix A (continues): Description of software packages capable of modelling multiphase systems

Footprint	A simple, user-friendly model used to estimate the distribution of benzene, toluene, ethylbenzene, and xylene (BTEX) plumes in groundwater, produced from a petrochemical spill that contains ethanol. It is able to access the migration of solutes by advection and dispersion as well as biodegradation of NAPLs.	The type of interface is unknown. Does not model the change with different remediation methods.
HSSM	The Hydrocarbon Spill Screening Model (HSSM) simulates flow of the light nonaqueous-phase liquid (LNAPL) and transport of a chemical constituent of the LNAPL from the surface to the water table; migration thereafter, as well as chemical degradation and transport constituents within the aquifer.	Only available with a one/two dimensional interface. Does not model the change with different remediation methods.
NAPL simulator	NAPL Simulator simulates the contamination of soils and aquifers as a result of NAPL sills. The simulator considers three interrelated zones: a vadose zone, a capillary zone, and an aquifer zone. Three mobile phases are accommodated: water, NAPL, and gas. NAPL dissolution and volatilization are taken into consideration. This model is available as two-dimensional and three-dimensional version.	Does not model the change with different remediation methods.

Appendix B: A list of existing boreholes used to calibrate the MODFLOW flow model with their coordinates and respective water levels

Borehole name	X coordinate (m)	Y coordinate (m)	Water level (m above sea level)
DH01	3971.08	-3307733.99	2.000
DH02	3702.78	-3307611.96	2.855
DH03	3541.77	-3307888.03	2.590
DH04	3353.92	-3307795.98	2.940
DH05	3194.00	-3307987.36	2.370
DH06	3085.55	-3307920.05	3.015
DH07	3659.67	-3307707.28	2.265
DH08	3522.90	-3307700.37	2.620
DH09	3038.94	-3308121.34	1.845
DH10	2978.22	-3307979.99	1.965
DH11	2360.41	-3308036.15	2.465
DH12	2100.35	-3308229.09	1.750
DH13	3449.04	-3308180.32	1.790
DH14	3319.24	-3308447.10	1.760
DH15	3300.05	-3308658.04	1.960
DH16	3917.55	-3307520.03	2.810
DH17	4172.81	-3073774.02	2.480
DH18	4269.72	-3307570.93	2.465
DH19	4105.23	-3307796.01	2.160
DH20	2512.05	-3308065.90	2.440
DH21	1663.43	-3308474.00	1.870
DH22	2253.81	-3307858.00	1.950
DH23	2414.74	-3308257.98	2.575
DH24	3820.24	-3307913.85	2.300
DH25	3895.73	-3308023.06	1.940

Appendix B (continues): A list of existing boreholes used to calibrate the MODFLOW flow model with their coordinates and respective water levels

Borehole name	X coordinate (m)	Y coordinate (m)	Water level (m above sea level)
DH26	3756.32	-3308104.05	1.740
DH27	3546.07	-3308029.15	2.130
DH28	3787.78	-3307897.32	2.240
DH29	3434.32	-3308319.99	2.465
DH30	3541.62	-3308349.95	2.415
DH31	3461.03	-3308473.97	4.170
DH32	3380.75	-3307857.95	2.660
DH33	3368.24	-3308030.76	2.345
DH34	2146.45	-3308072.03	2.255
DH35	2135.08	-3307913.18	2.085
DH36	1985.51	-3308166.00	2.150
DH37	1931.83	-3308012.02	2.085
DH38	1836.53	-3308811.98	2.780
DH39	1702.14	-3308606.69	2.340
DH40	2361.11	-3307888.05	2.720
DH41	2133.01	-3308283.28	1.840
DH42	4110.69	-3307514.04	2.345
DH43	2870.85	-3308196.01	1.450
DH44	2819.21	-3308050.90	2.110
DH45	4238.80	-3307348.33	2.565
DH46	2307.37	-3308533.97	2.485
DH47	2575.72	-3308411.99	2.970
DH48	1851.33	-3308288.02	1.880
DH49	1818.36	-3308507.17	2.760

Appendix C: A list of positions used to infiltrate NAPLs in the UTCHEM model and their coordinates

Borehole name	X coordinate (m)	Y coordinate (m)	Water level (m above sea level)	Source
SGC1	-6516.52	-3303636.95	1.90	Consultant
SGC3	-16054.70	-3300579.51	16.00	Consultant
SGC4	-14784.00	-3299562.48	14.00	Consultant
SGC5	-7000.97	-3301567.78	3.41	Consultant
SGC6	-16623.10	-3297994.44	15.40	Consultant
SGC7	-16461.70	-3297902.20	10.6	Consultant
SGC9	-16945.20	-3297884.08	54.00	Consultant
SGC10	-16624.20	-3297255.08	12.3	Consultant
SGC11	-16937.30	-3303038.26	3.89	Consultant
SGC12	-17339.90	-3303297.16	3.50	Consultant
SGC13	-3304.46	-3304564.78	29.04	Consultant
SGC18	-11278.70	-3301635.03	8.22	Consultant
SCG19	-11006.70	-3301747.39	12.00	Consultant
SCG20	-11001.00	-3301877.30	10.30	Consultant
71	-11641.60	-3300277.17	8.00	University of Kwa-Zulu Natal
SGC21	-11711.30	-3309031.65	0.87	Consultant
NBH	-1931.27	-3311246.00	-0.90	National Groundwater Archive

Appendix D: A list of positions used to infiltrate NAPLs in the UTCHEM model and their coordinates

Infiltration position no.	X coordinate (m)	Y coordinate (m)
IVS 01	2264.129	-3307919
IVS 02	2107.149	-3308010
IVS 03	1897.908	-3308143
IVS 04	2462.100	-3308115
IVS 05	2223.501	-3308213
IVS 06	1999.586	-3308322
IVS 07	1772.683	-3308421
IVS 08	4244.653	-3307437
IVS 09	3942.643	-3307575
IVS 10	3742.670	-3307634
IVS 11	3676.531	-3307839
IVS 12	3502.929	-3307915
IVS 13	3295.053	-3307945
IVS 14	3002.833	-3308052
IVS 15	2835.208	-3308200
IVS 16	2485.625	-3308306
IVS 17	2317.060	-3308391
IVS 18	1961.679	-3308572
IVS 19	1706.669	-3308703
IVS 20	4157.830	-3307649
IVS 21	3758.261	-3308089
IVS 22	3574.169	-3308357
IVS 23	3407.660	-3308324
IVS 24	3495.386	-3308557
IVS 25	3326.466	-3308522
IVS 27	3263.818	-3308723

Appendix E: Maps illustrating the simulation results for the infiltration and migration of non-aqueous benzene

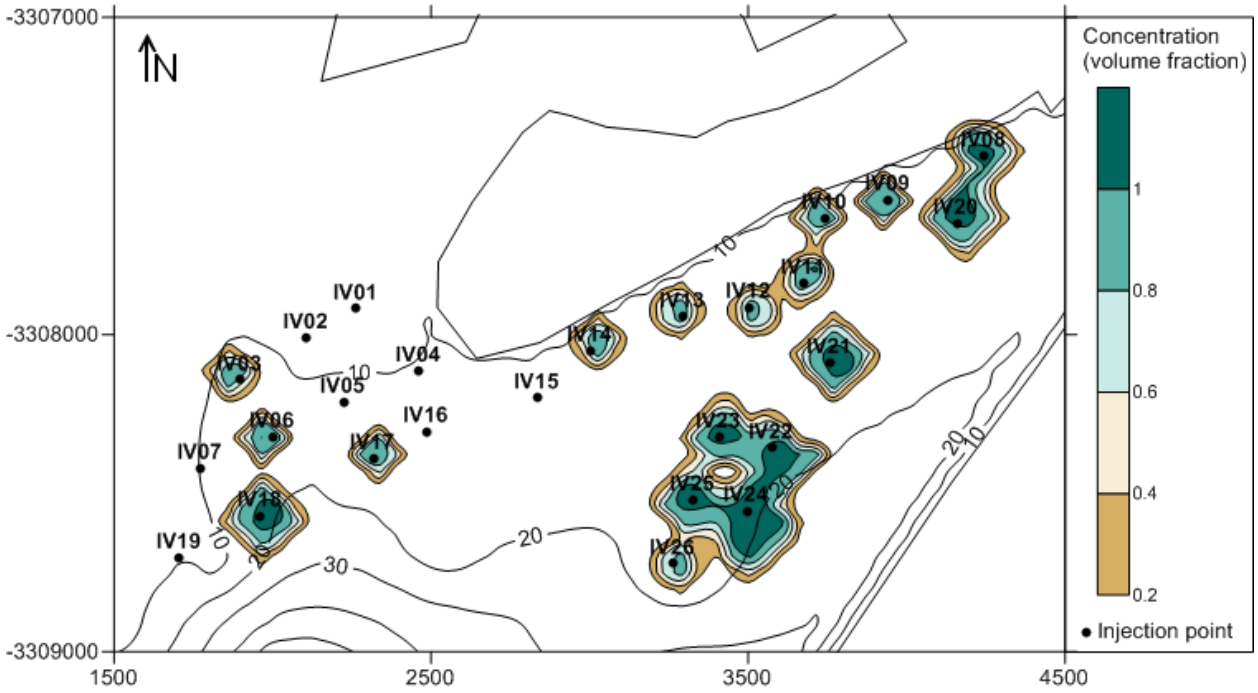

E1: Map illustrating the simulation results for the infiltration and migration of non-aqueous phase benzene in the top layer.

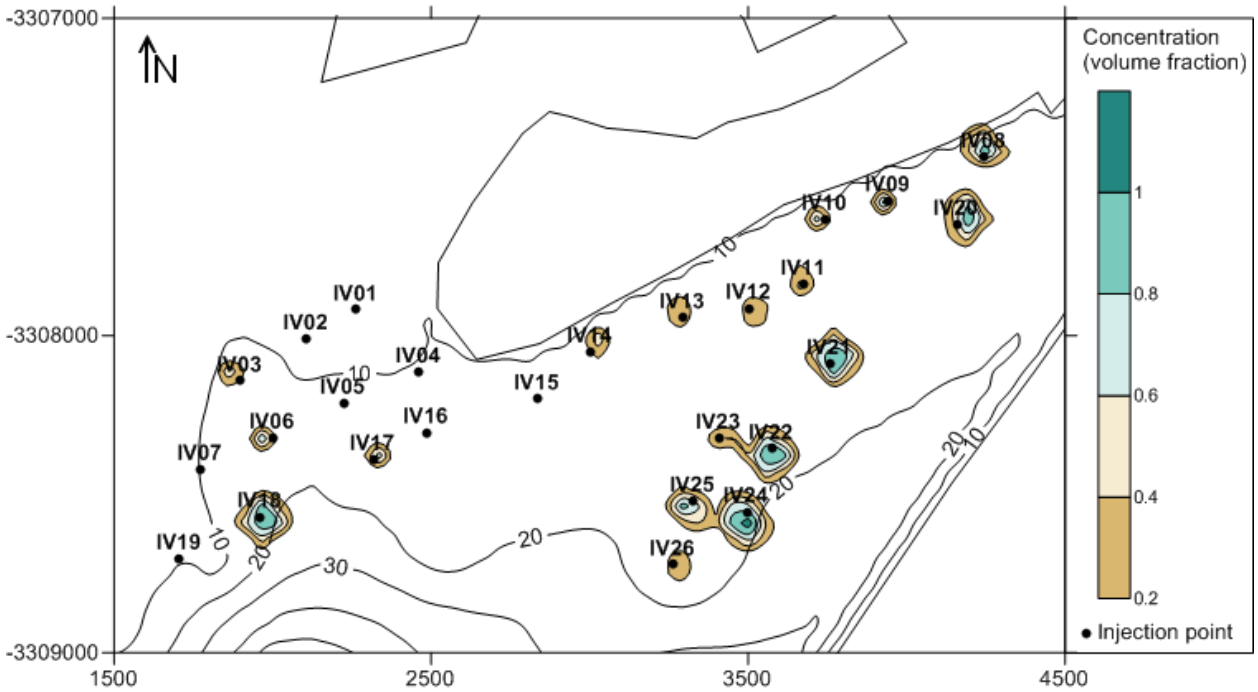

E2: Map illustrating the simulation results for the infiltration and migration of non-aqueous phase benzene in the bottom layer.

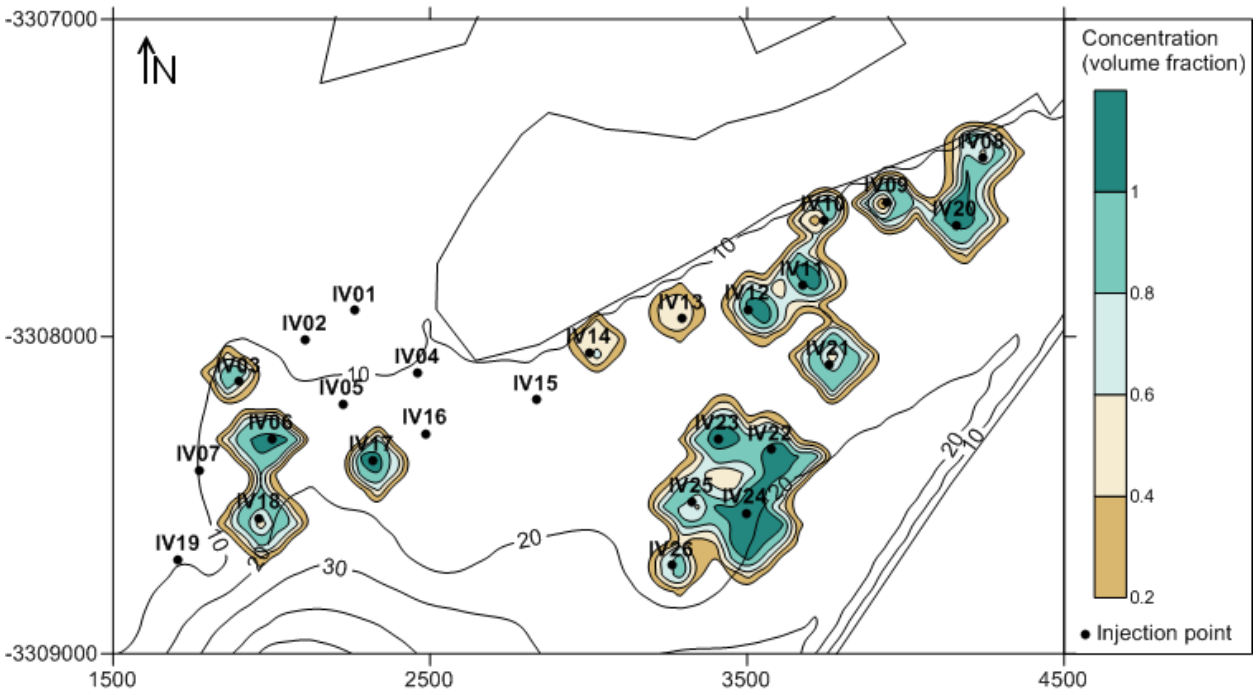

E3: Map illustrating the simulation results for the remediation of non-aqueous phase benzene with diluted surfactant SDS and polymer xanthan gum at a low infiltration rate in the top layer.

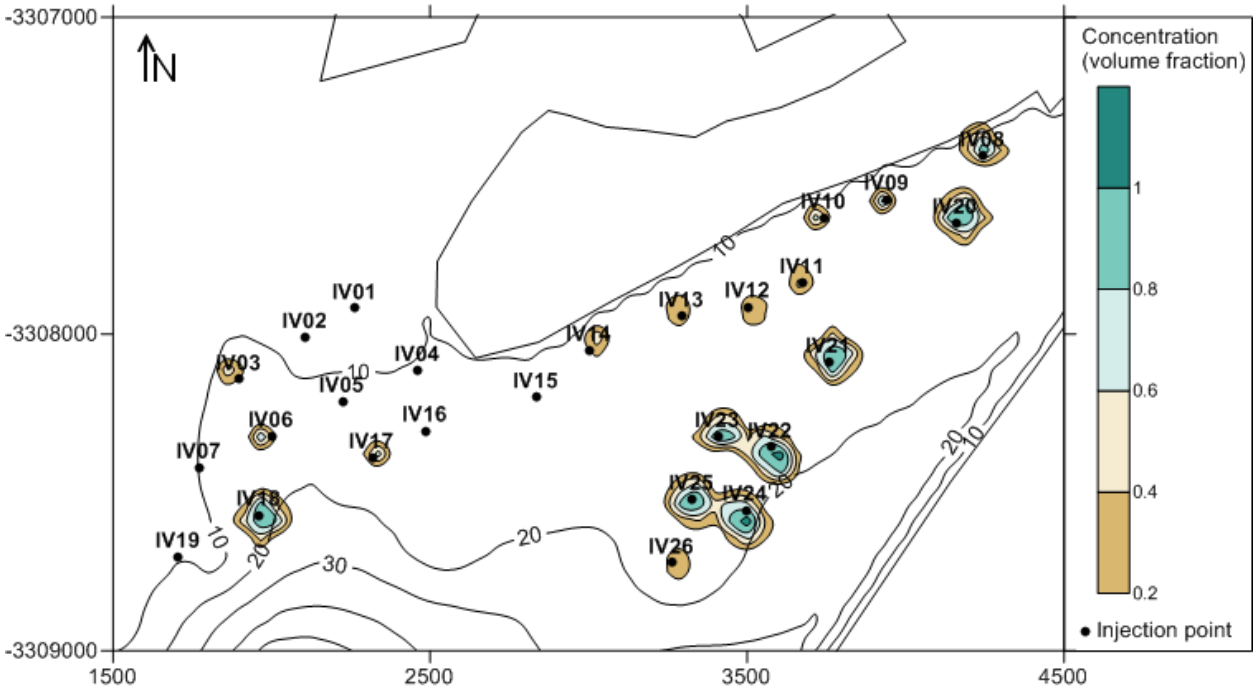

E4: Map illustrating the simulation results for the remediation of non-aqueous phase benzene with diluted surfactant SDS and polymer xanthan gum at a low infiltration rate in the bottom layer.

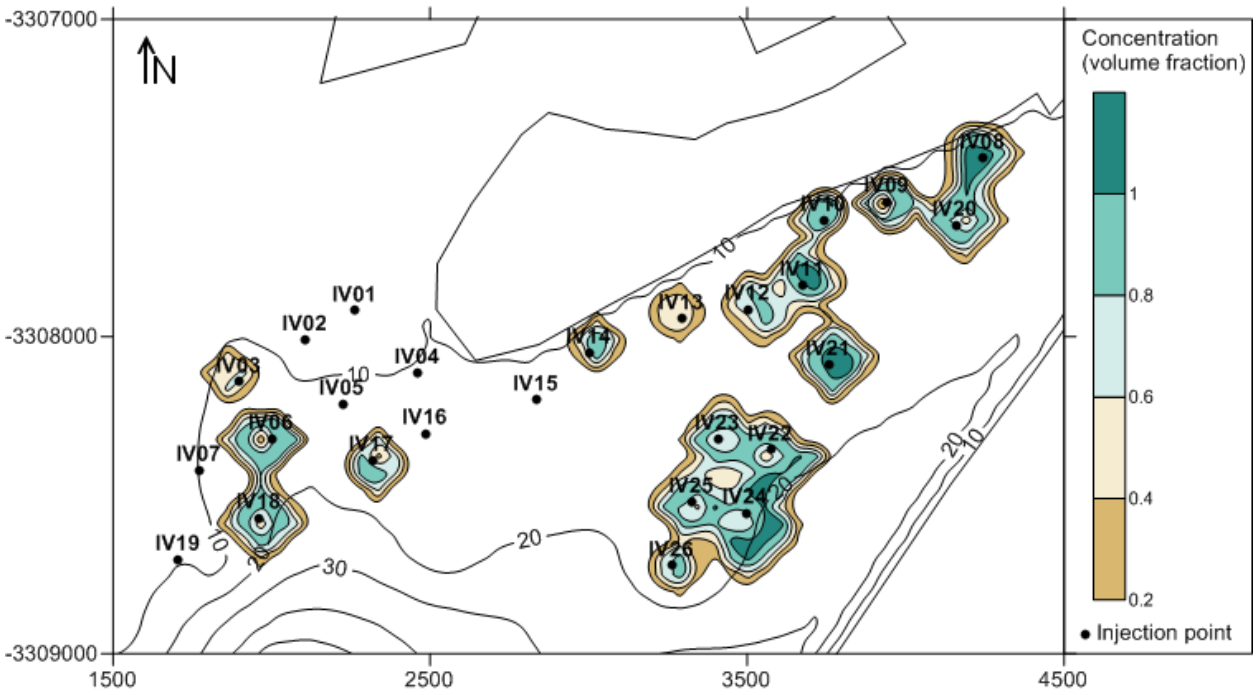

E5: Map illustrating the simulation results for the remediation of non-aqueous phase benzene with undiluted surfactant SDS and polymer xanthan gum at a low infiltration rate in the top layer.

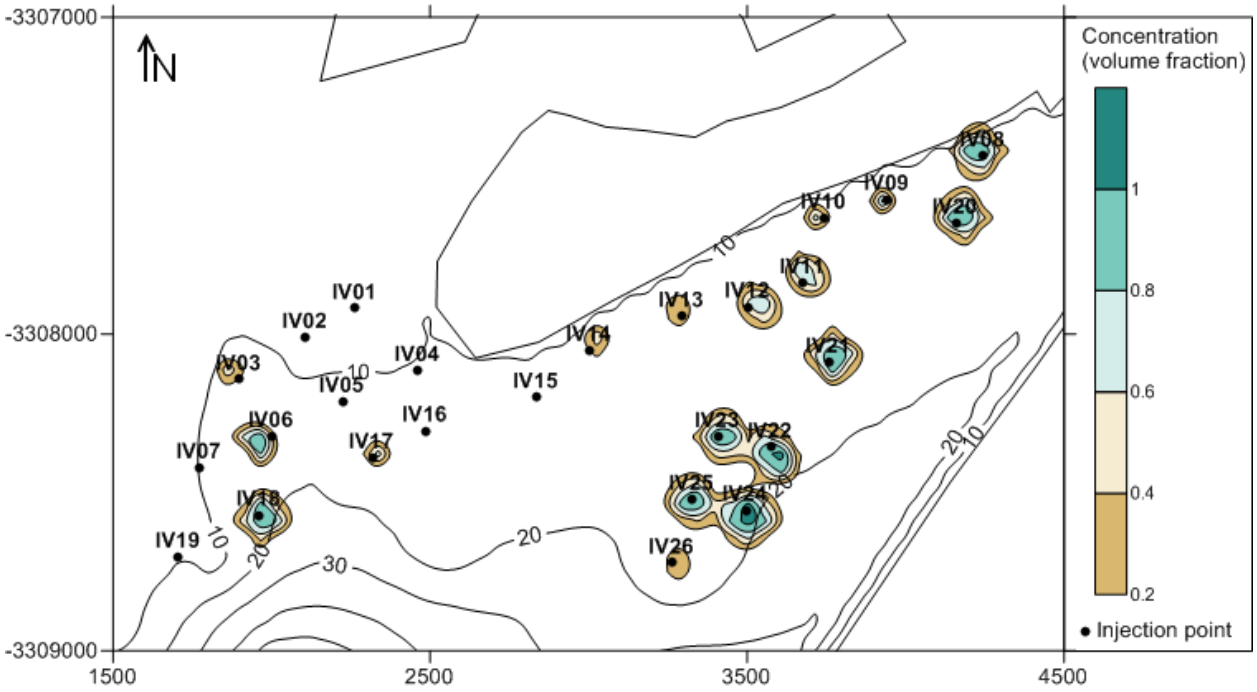

E6: Map illustrating the simulation results for the remediation of non-aqueous phase benzene with undiluted surfactant SDS and polymer xanthan gum at a low infiltration rate in the bottom layer.

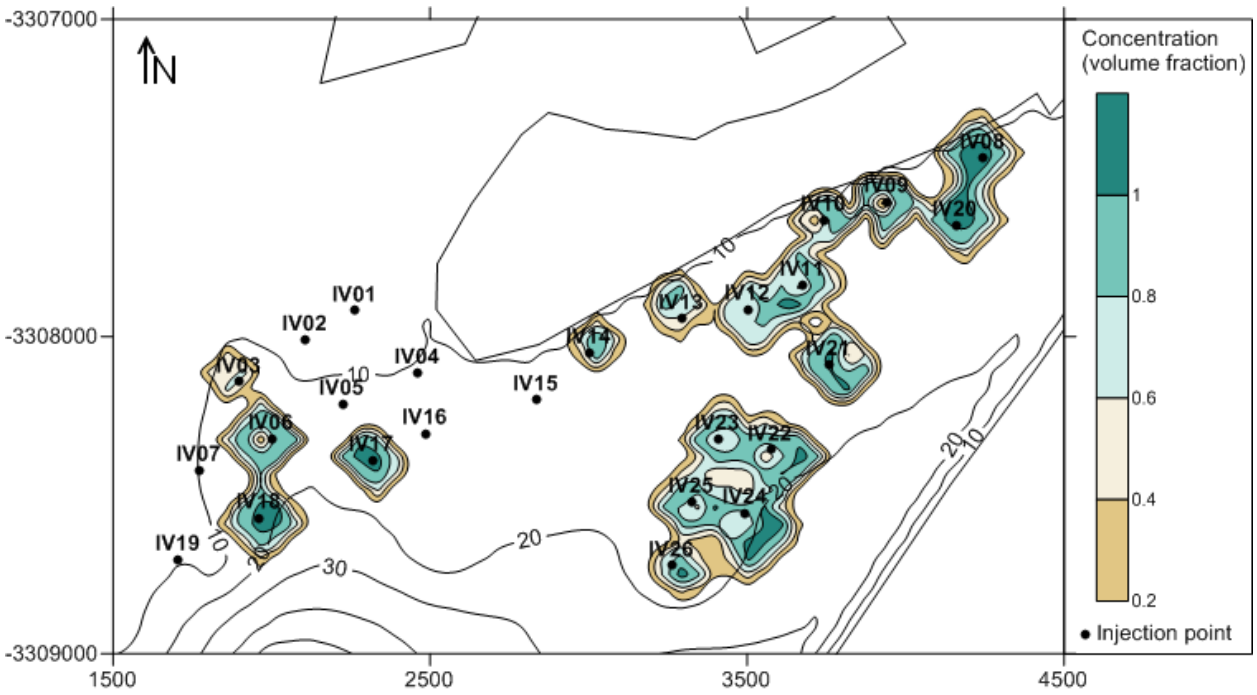

E7: Map illustrating the simulation results for the remediation of non-aqueous phase benzene with undiluted surfactant SDS and polymer xanthan gum at a high infiltration rate in the top layer.

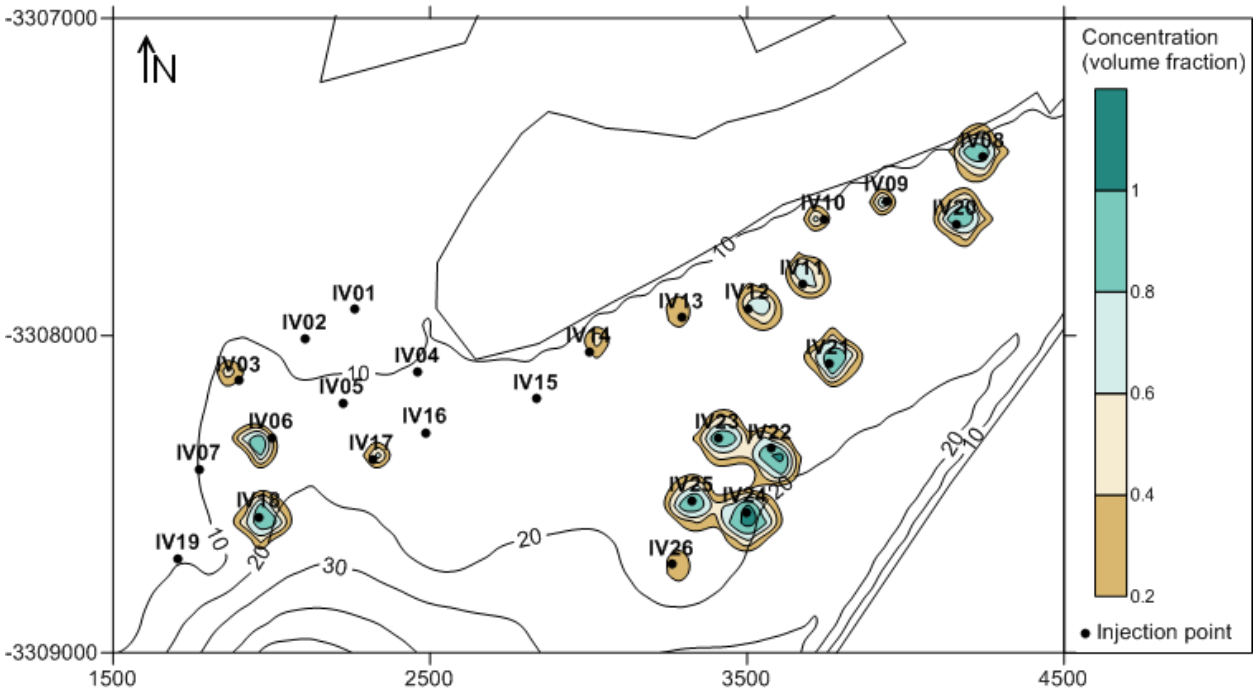

E8: Map illustrating the simulation results for the remediation of non-aqueous phase benzene with undiluted surfactant SDS and polymer xanthan gum at a high infiltration rate in the bottom layer.

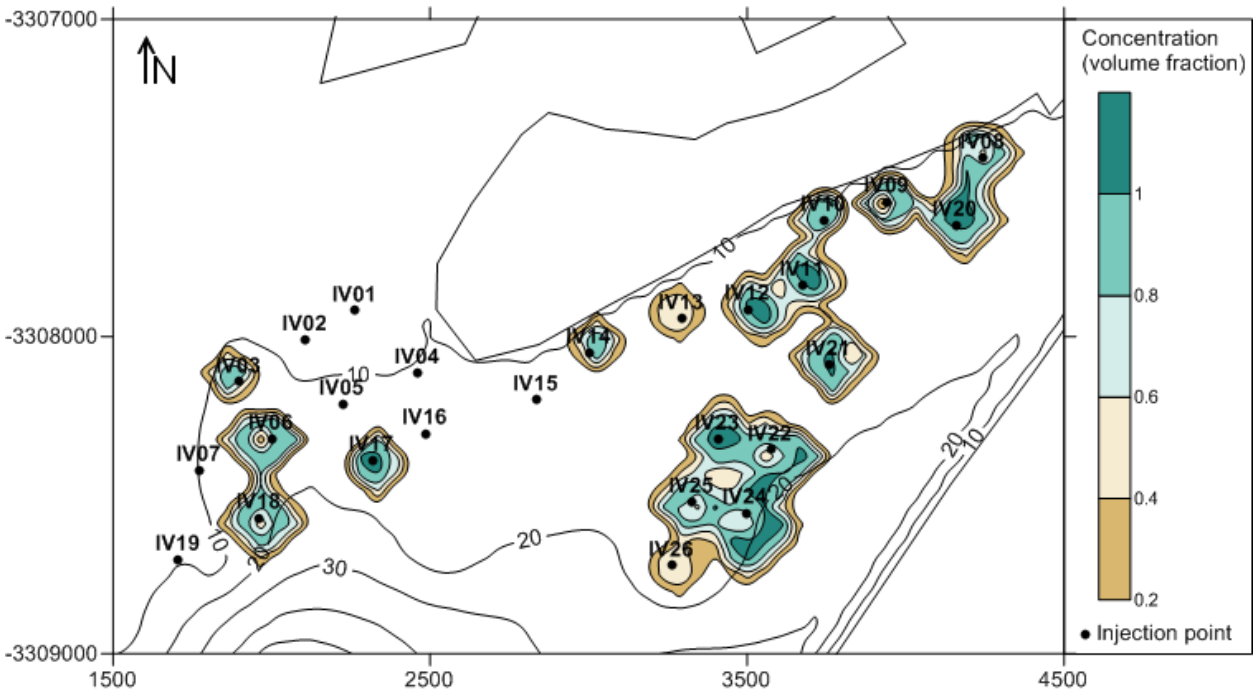

E9: Map illustrating the simulation results for the remediation of non-aqueous phase benzene with diluted surfactant SDS at a low infiltration rate in the top layer.

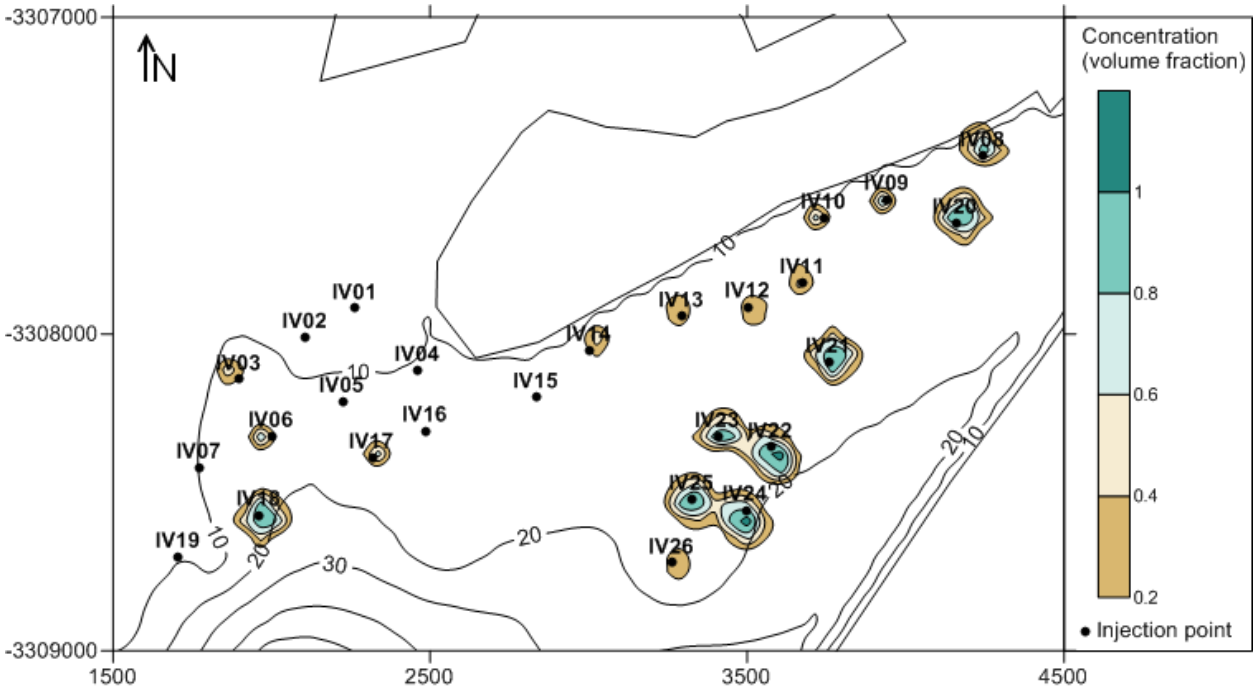

E10: Map illustrating the simulation results for the remediation of non-aqueous phase benzene with diluted surfactant SDS at a low infiltration rate in the bottom layer.

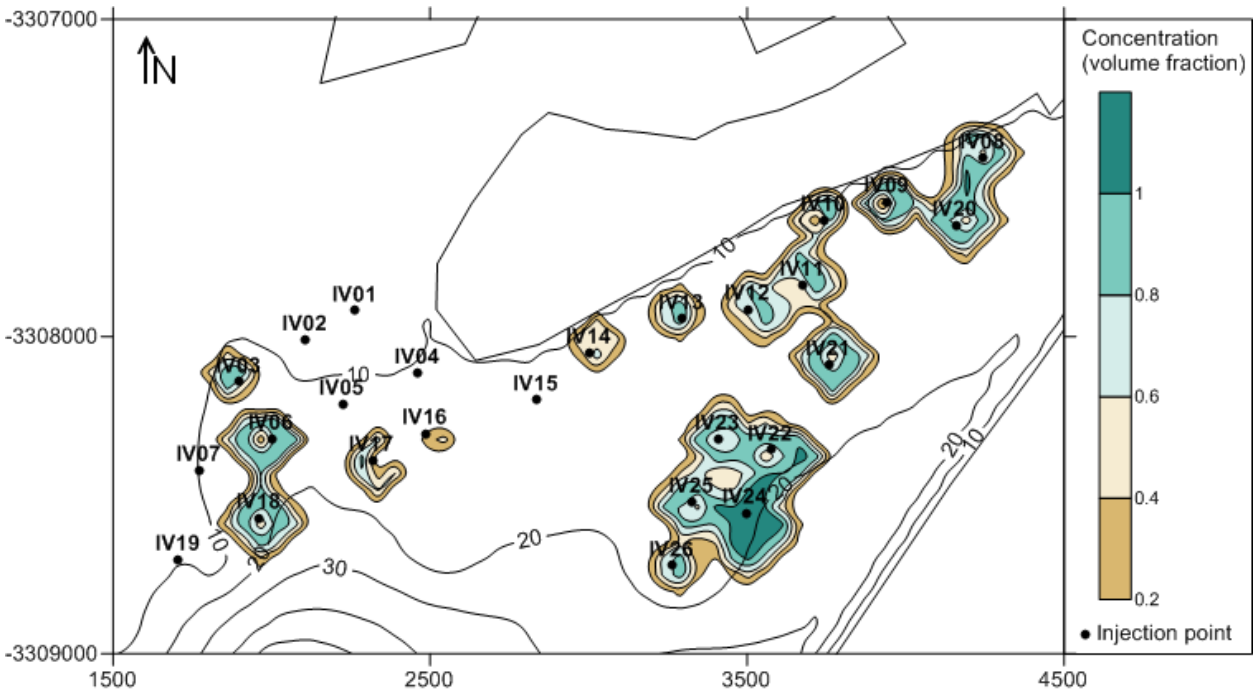

E11: Map illustrating the simulation results for the remediation of non-aqueous phase benzene with undiluted surfactant SDS at a low infiltration rate in the top layer.

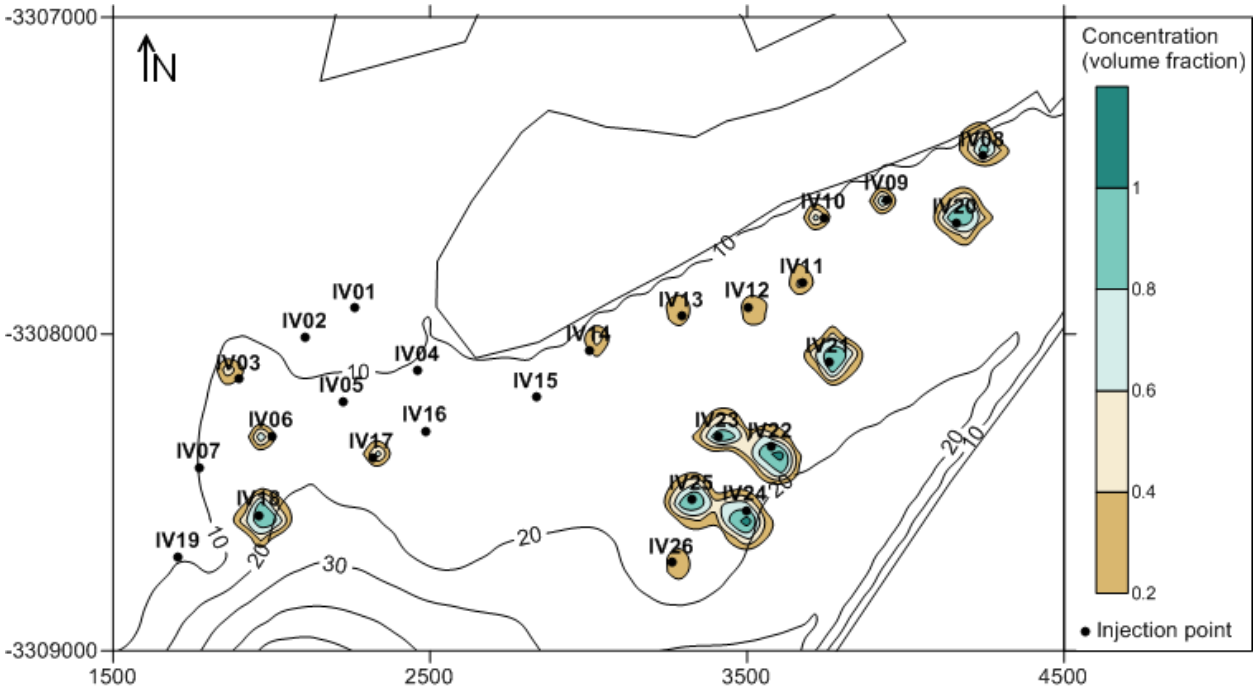

E12: Map illustrating the simulation results for the remediation of non-aqueous phase benzene with undiluted surfactant SDS at a low infiltration rate in the bottom layer.

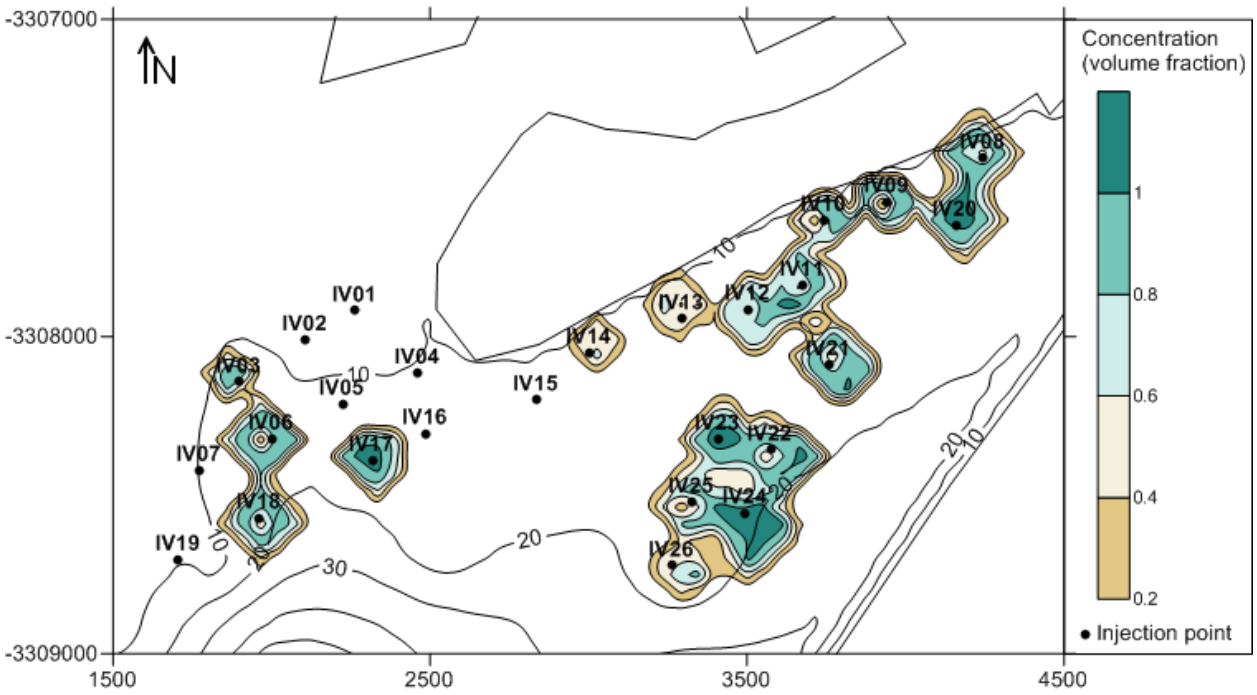

E13: Map illustrating the simulation results for the remediation of non-aqueous phase benzene with undiluted surfactant SDS at a high infiltration rate in the top layer.

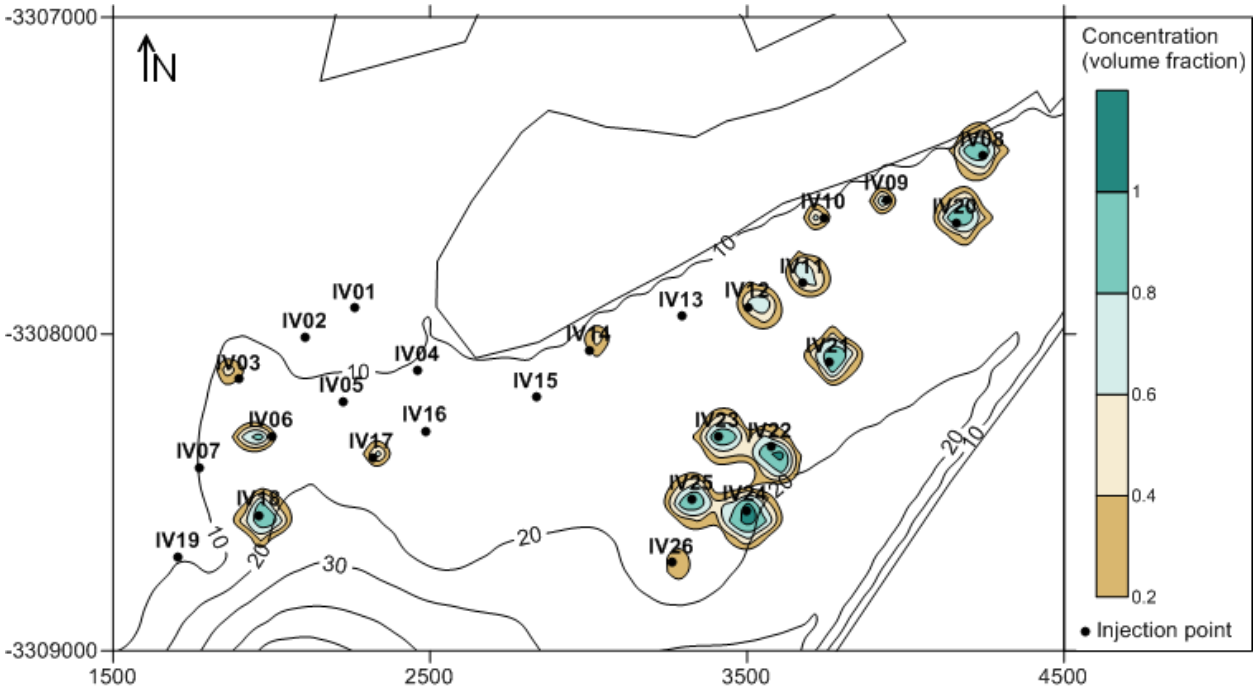

E14: Map illustrating the simulation results for the remediation of non-aqueous phase benzene with undiluted surfactant SDS at a high infiltration rate in the bottom layer.

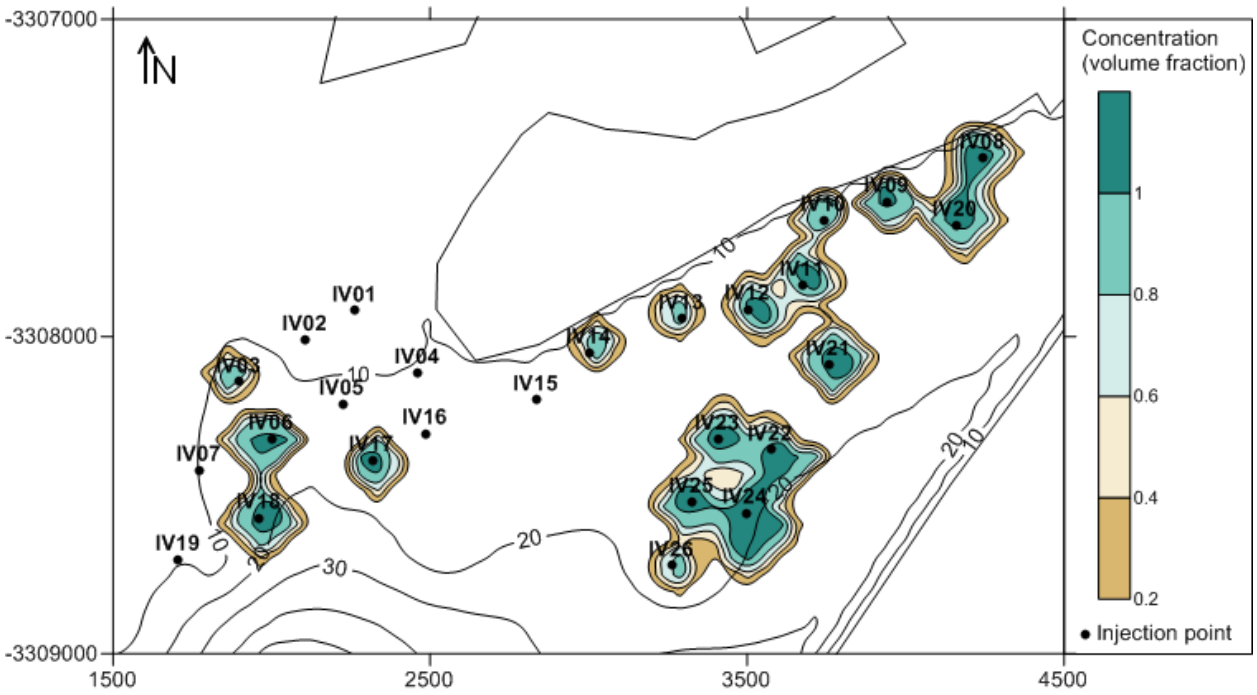

E15: Map illustrating the simulation results for the remediation of non-aqueous phase benzene with diluted polymer xanthan gum at a low infiltration rate in the top layer.

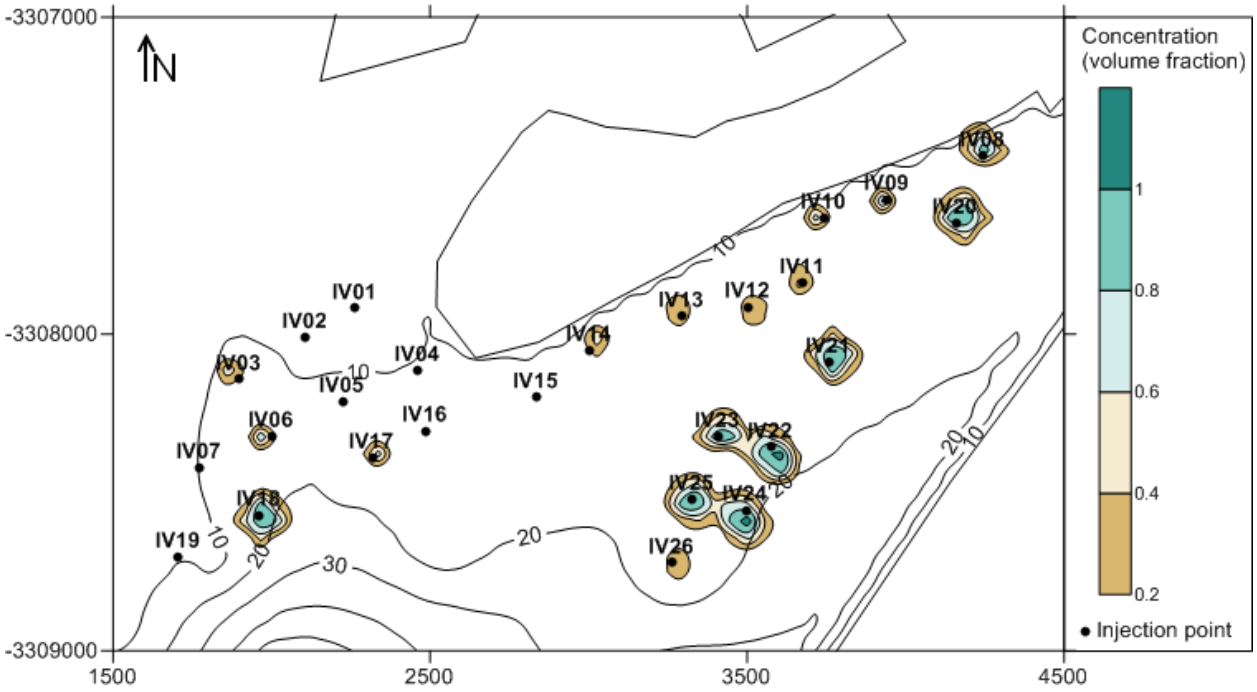

E16: Map illustrating the simulation results for the remediation of non-aqueous phase benzene with diluted polymer xanthan gum at a low infiltration rate in the bottom layer.

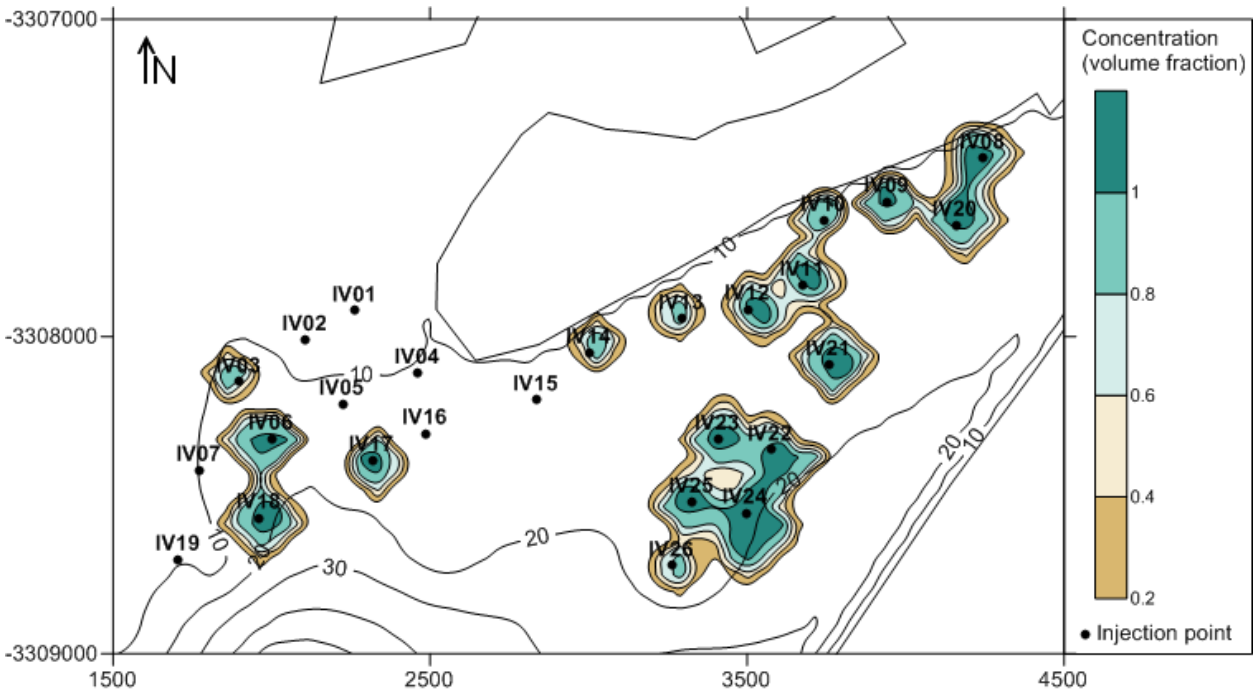

E17: Map illustrating the simulation results for the remediation of non-aqueous phase benzene with undiluted polymer xanthan gum at a low infiltration rate in the top layer.

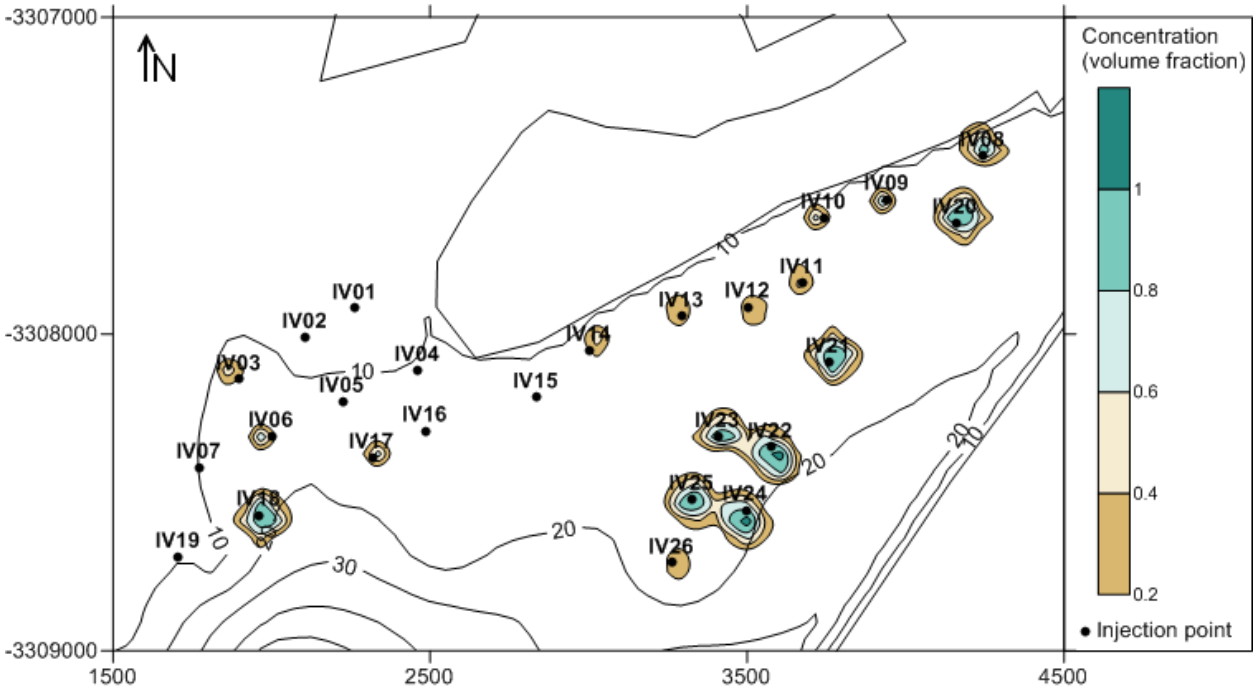

E18: Map illustrating the simulation results for the remediation of non-aqueous phase benzene with undiluted polymer xanthan gum at a low infiltration rate in the bottom layer.

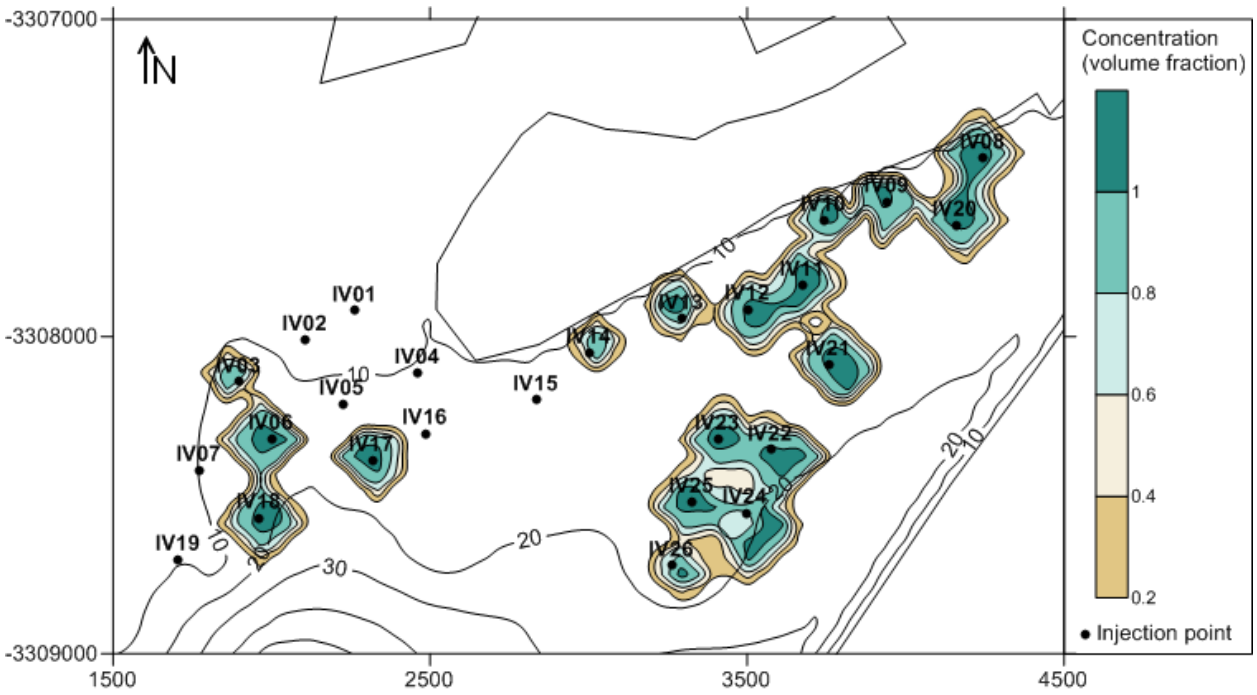

E19: Map illustrating the simulation results for the remediation of non-aqueous phase benzene with undiluted polymer xanthan gum at a high infiltration rate in the top layer.

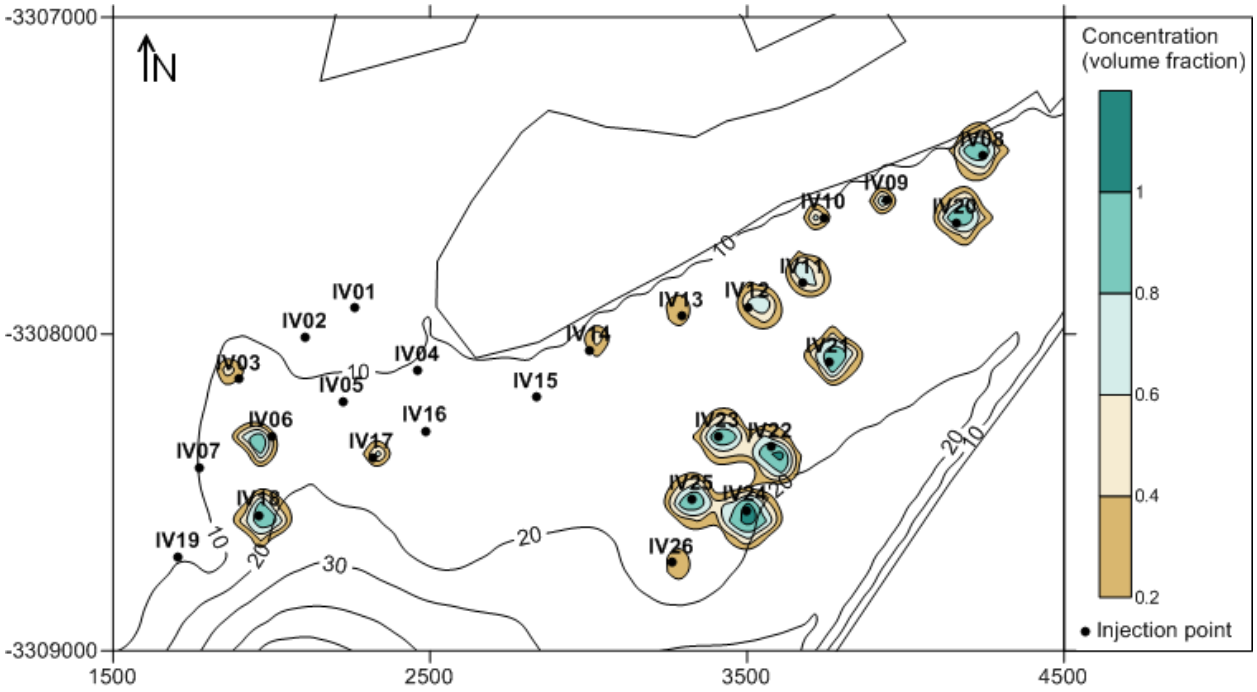

E20: Map illustrating the simulation results for the remediation of non-aqueous phase benzene with undiluted polymer xanthan gum at a high infiltration rate in the bottom layer.

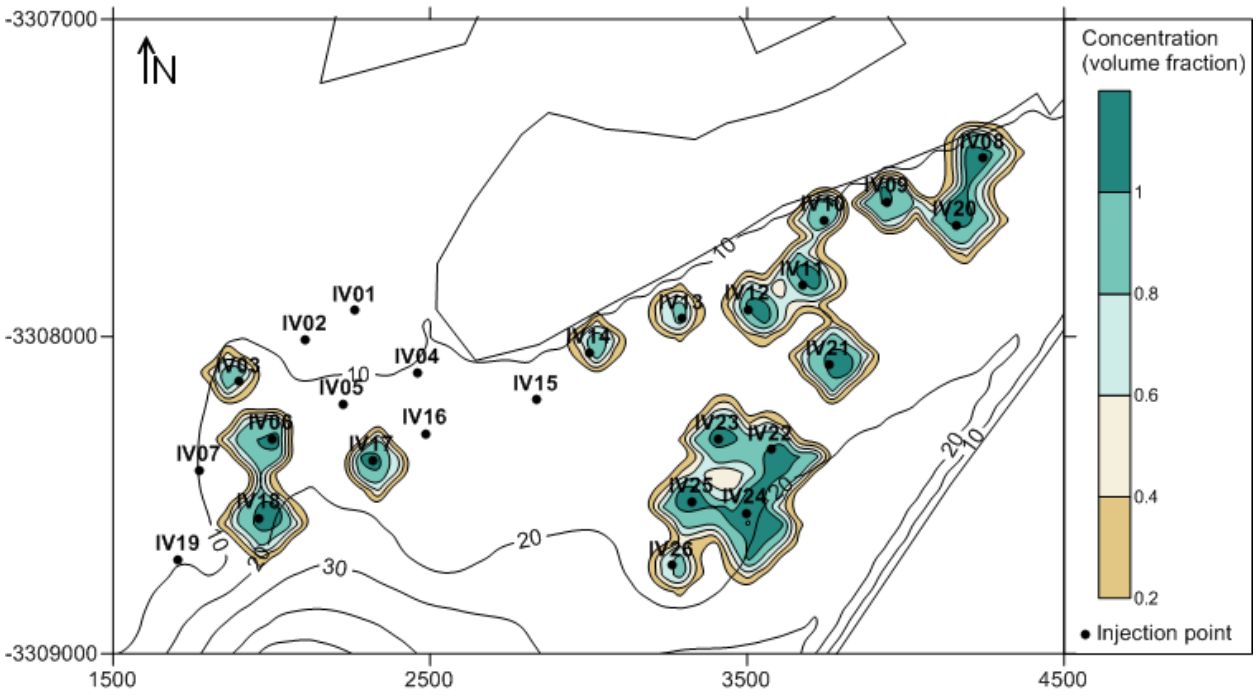

E21: Map illustrating the simulation results for the remediation of non-aqueous phase benzene with diluted surfactant SDS and ethanol at a low infiltration rate in the top layer.

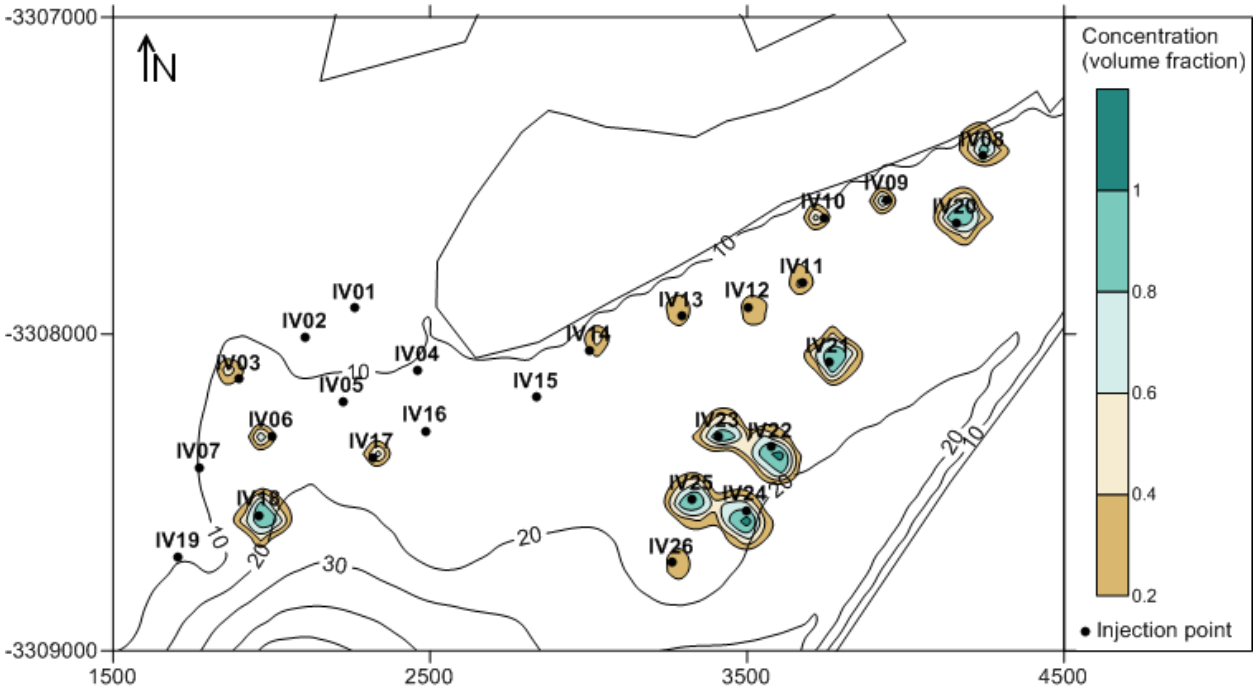

E22: Map illustrating the simulation results for the remediation of non-aqueous phase benzene with diluted surfactant SDS and ethanol at a low infiltration rate in the bottom layer.

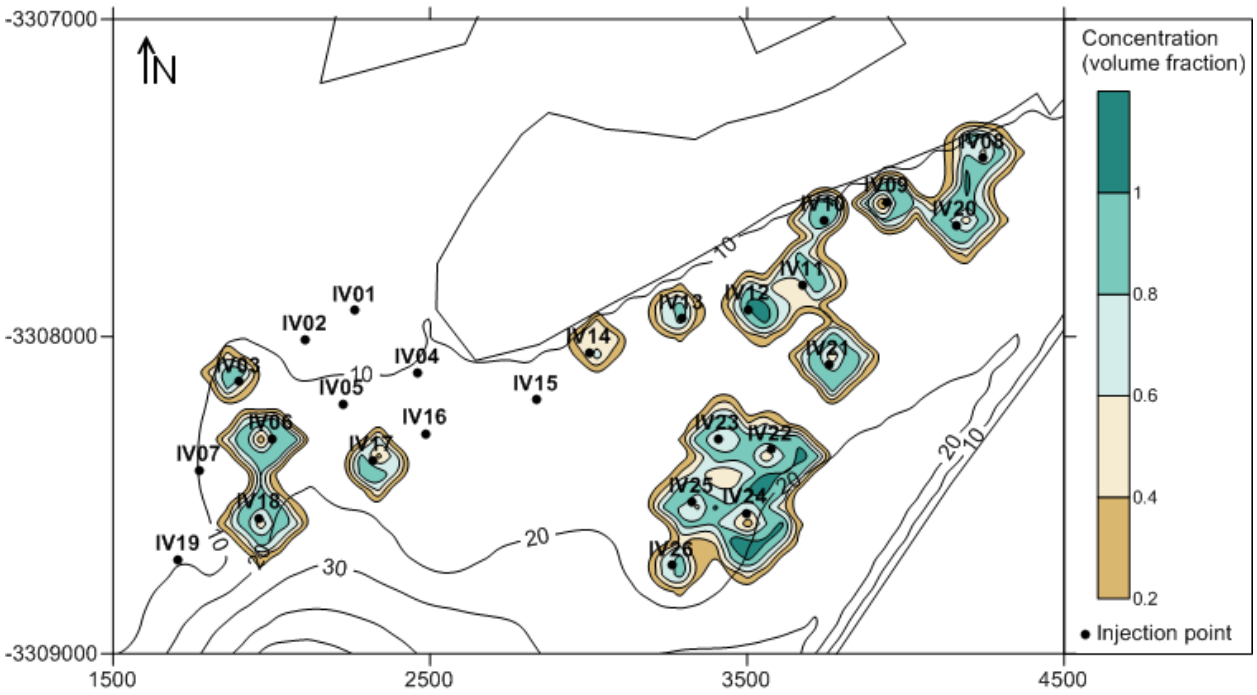

E23: Map illustrating the simulation results for the remediation of non-aqueous phase benzene with undiluted surfactant SDS and ethanol at a low infiltration rate in the top layer.

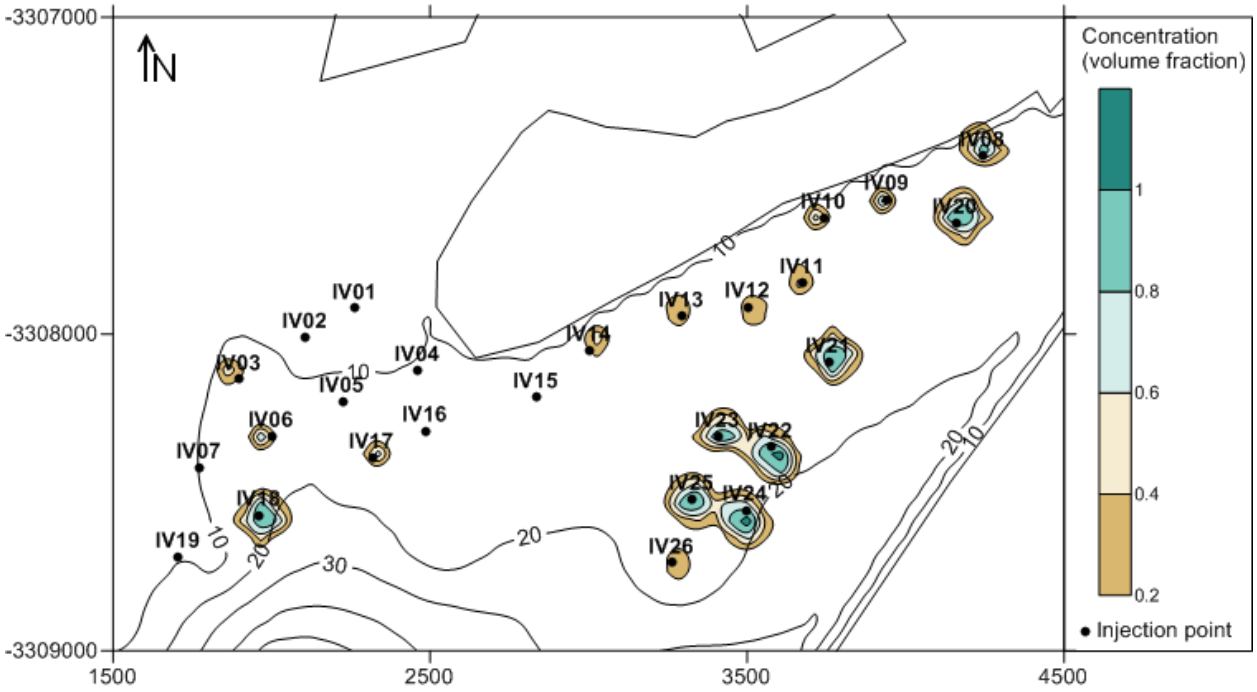

E24: Map illustrating the simulation results for the remediation of non-aqueous phase benzene with undiluted surfactant SDS and ethanol at a low infiltration rate in the bottom layer.

E25: Map illustrating the simulation results for the remediation of non-aqueous phase benzene with undiluted surfactant SDS and ethanol at a high infiltration rate in the top layer.

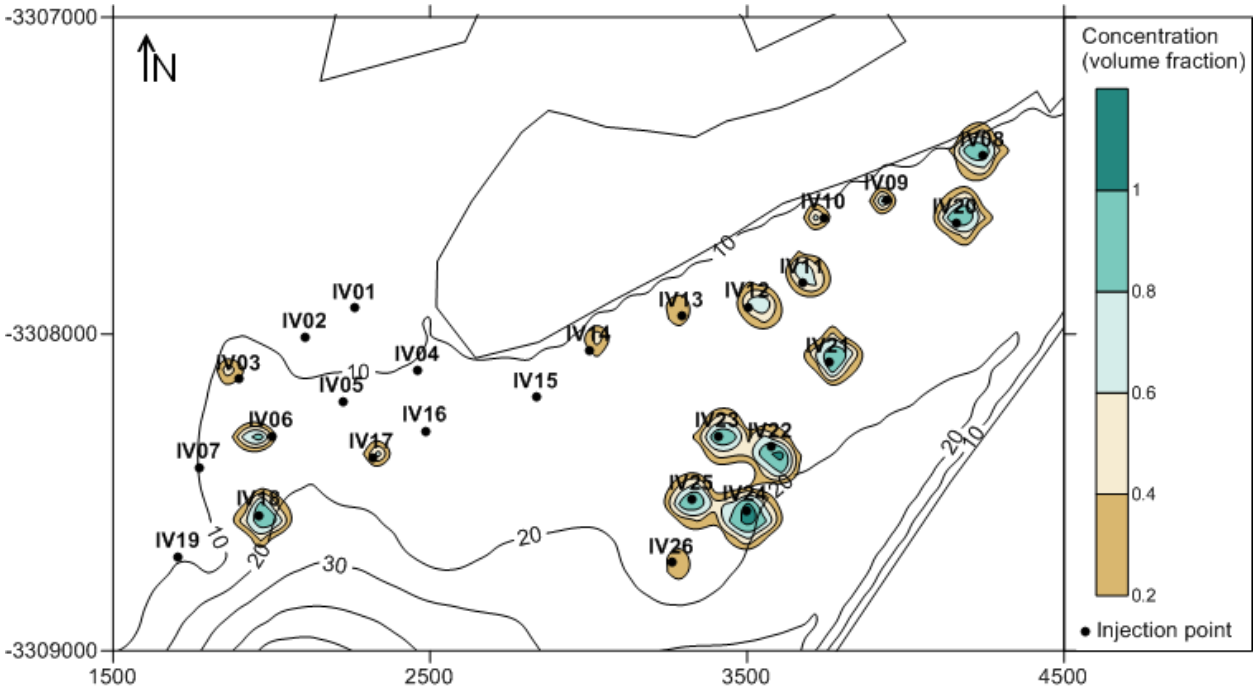

E26: Map illustrating the simulation results for the remediation of non-aqueous phase benzene with undiluted surfactant SDS and ethanol at a high infiltration rate in the bottom layer.

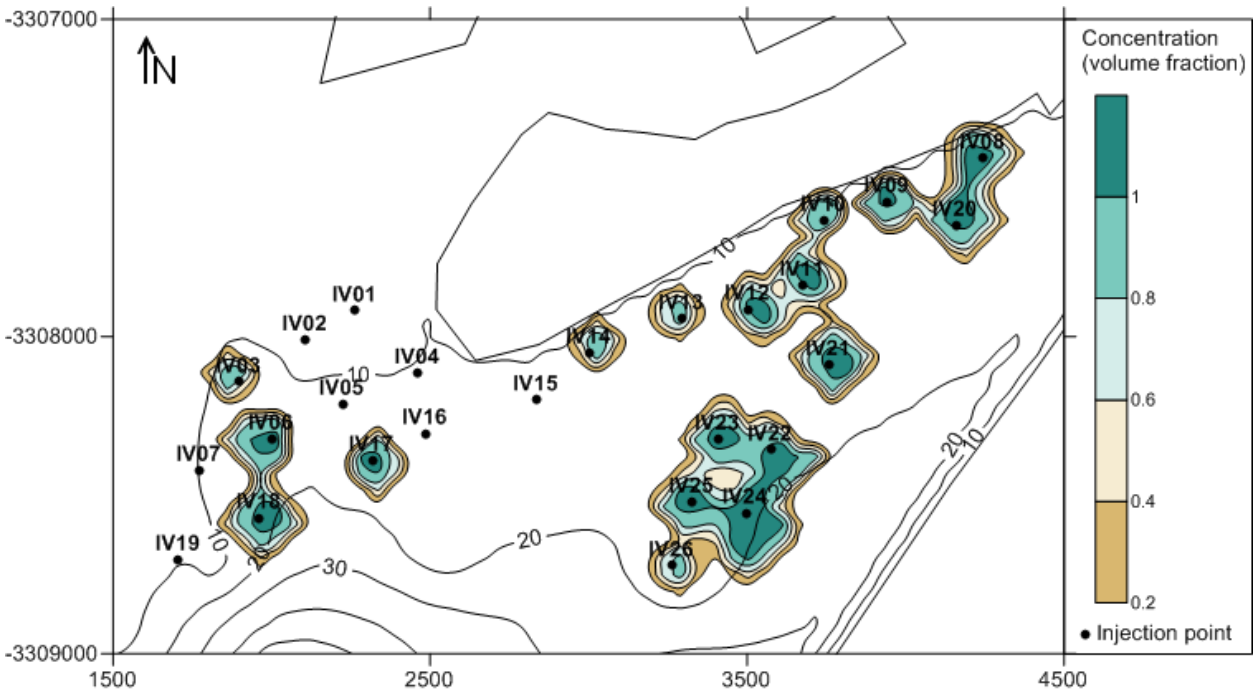

E27: Map illustrating the simulation results for the remediation of non-aqueous phase benzene with diluted ethanol at a low infiltration rate in the top layer.

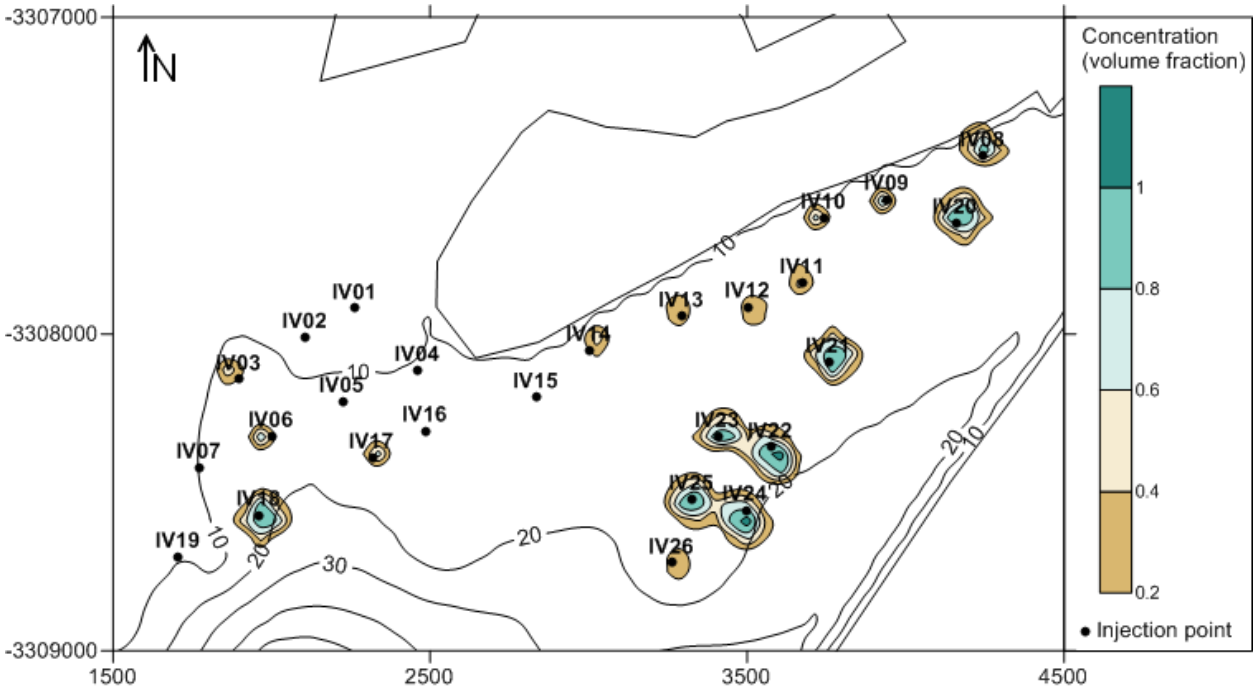

E28: Map illustrating the simulation results for the remediation of non-aqueous phase benzene with diluted ethanol at a low infiltration rate in the bottom layer.

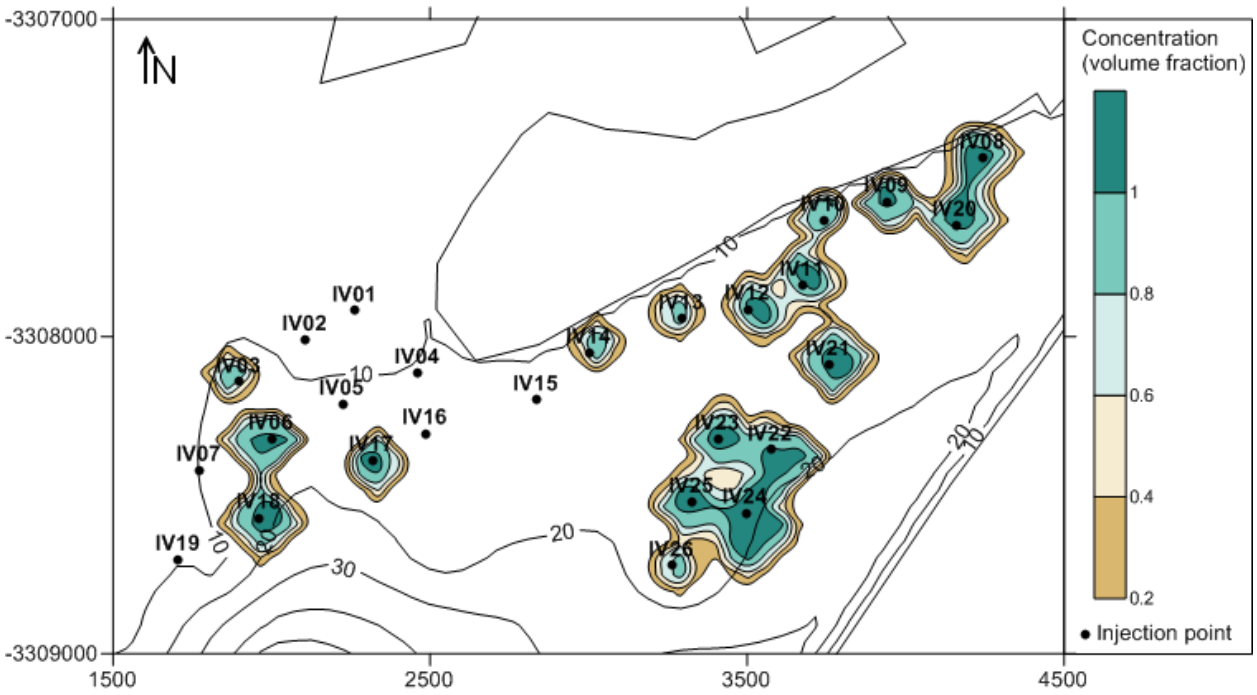

E29: Map illustrating the simulation results for the remediation of non-aqueous phase benzene with undiluted ethanol at a low infiltration rate in the top layer.

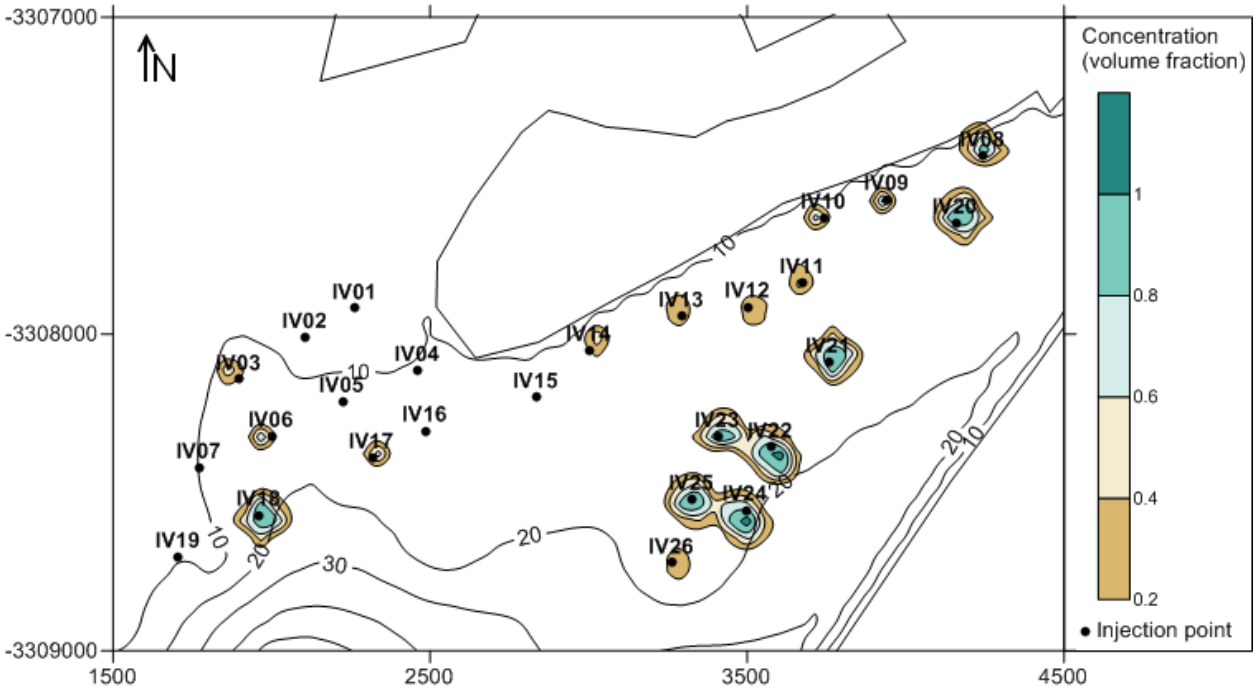

E30: Map illustrating the simulation results for the remediation of non-aqueous phase benzene with undiluted ethanol at a low infiltration rate in the bottom layer.

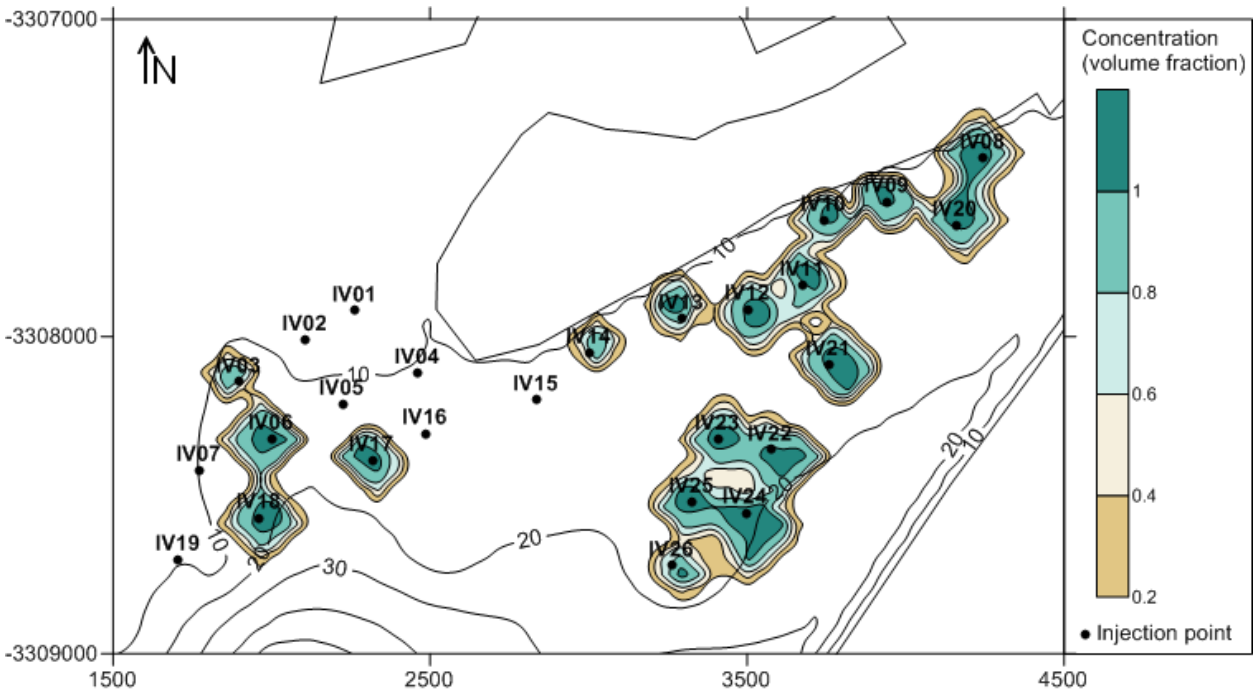

E31: Map illustrating the simulation results for the remediation of non-aqueous phase benzene with undiluted ethanol at a high infiltration rate in the top layer.

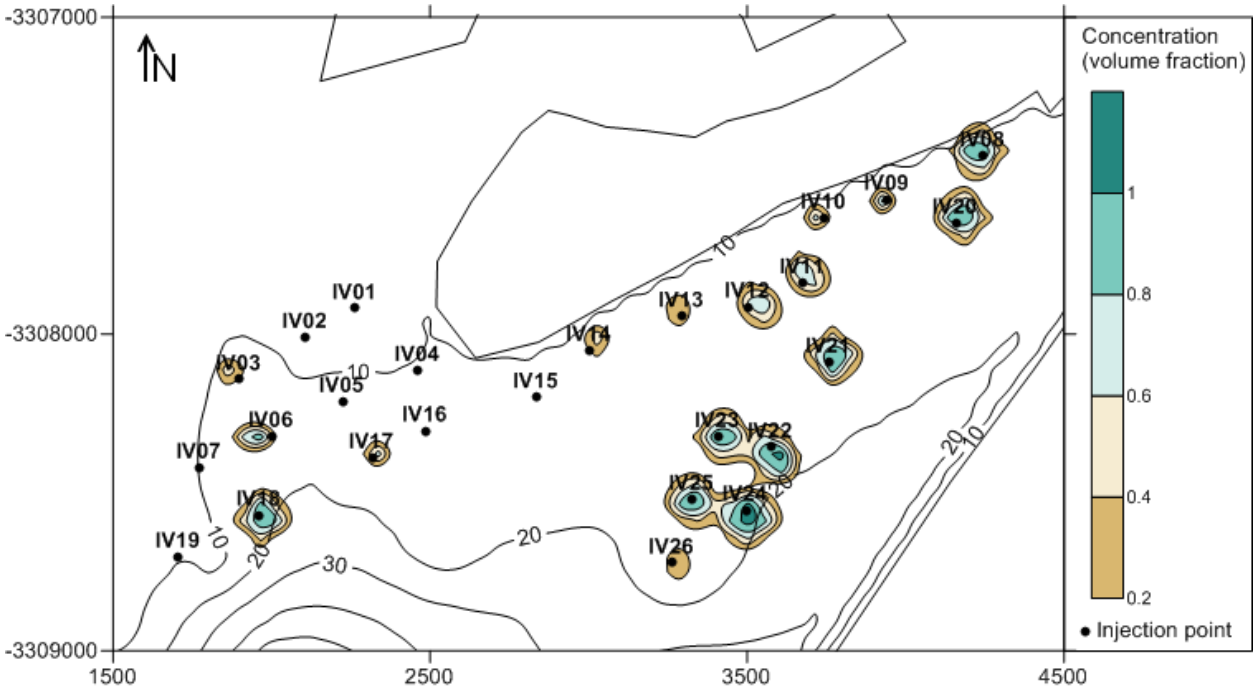

E32: Map illustrating the simulation results for the remediation of non-aqueous phase benzene with undiluted ethanol at a high infiltration rate in the bottom layer.

Appendix F: Maps illustrating the simulation results for the infiltration and migration of aqueous benzene

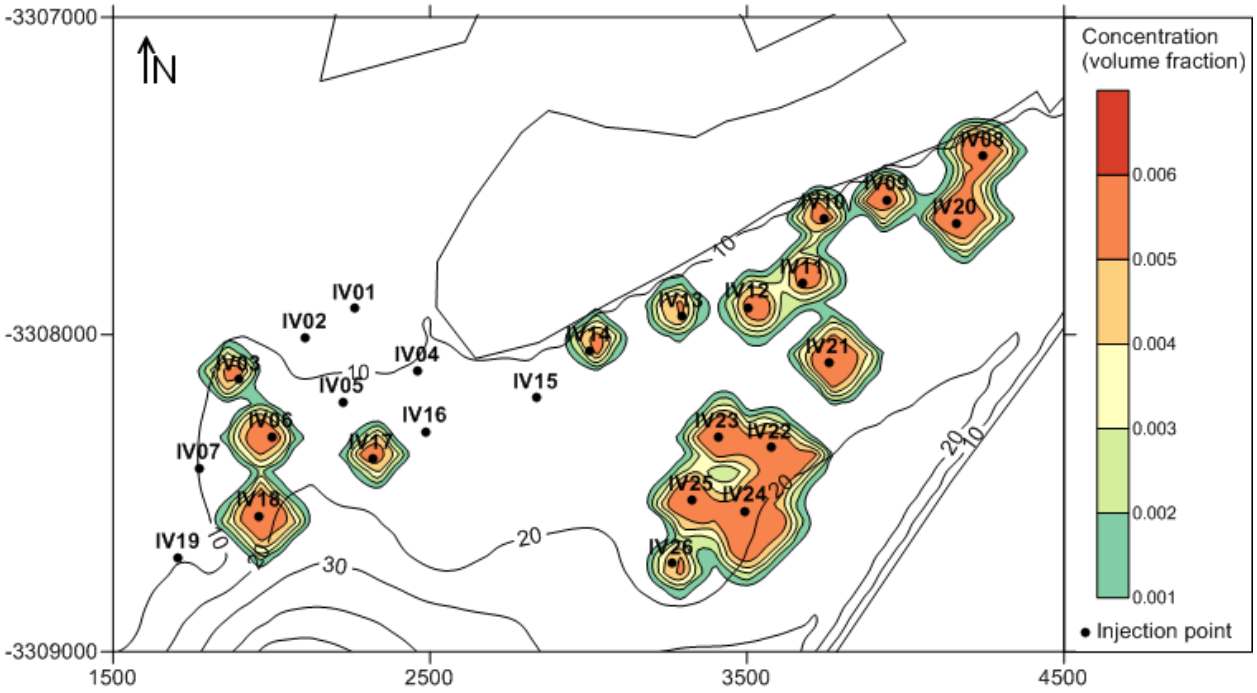

F1: Map illustrating the simulation results for the infiltration and migration of aqueous phase benzene in the top layer.

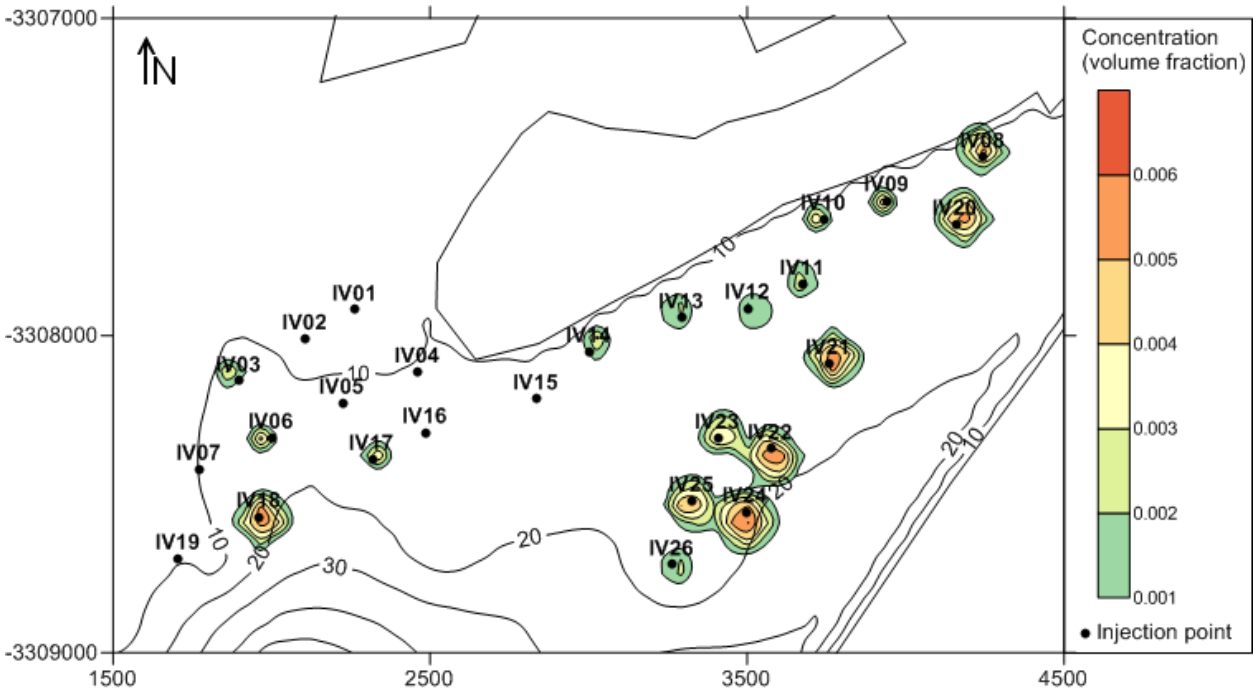

F2: Map illustrating the simulation results for the infiltration and migration of aqueous phase benzene in the bottom layer.

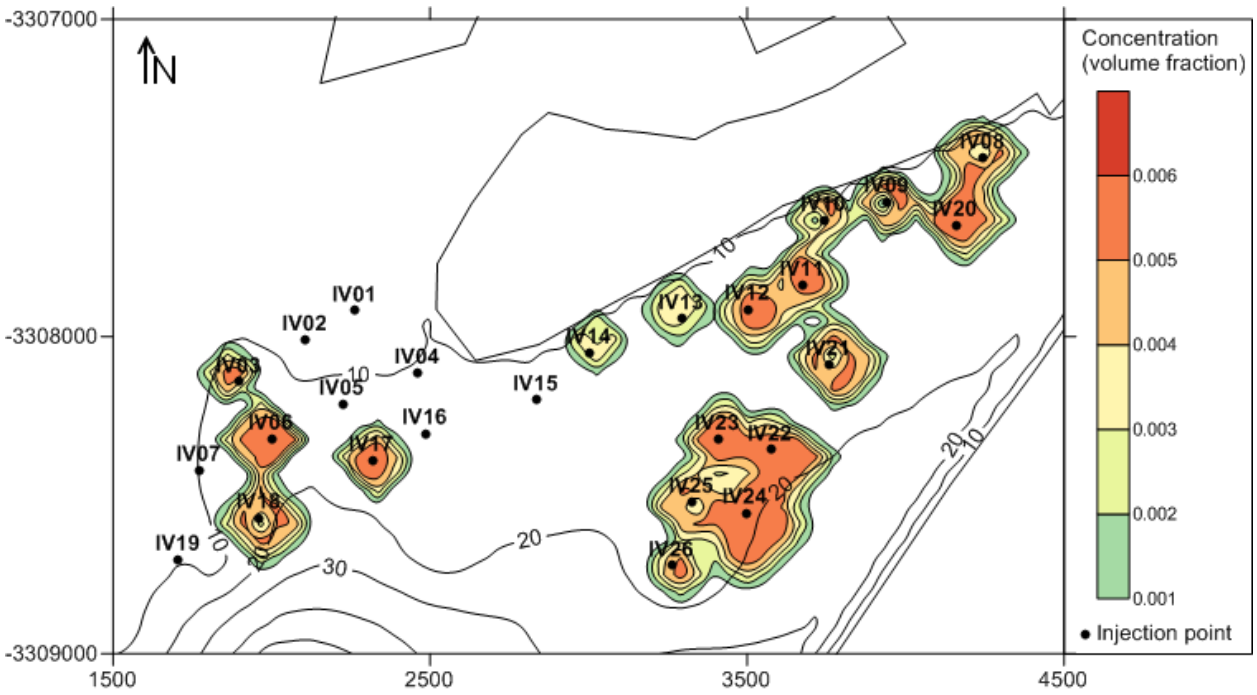

F3: Map illustrating the simulation results for the remediation of aqueous phase benzene with diluted surfactant SDS and polymer xanthan gum at a low infiltration rate in the top layer.

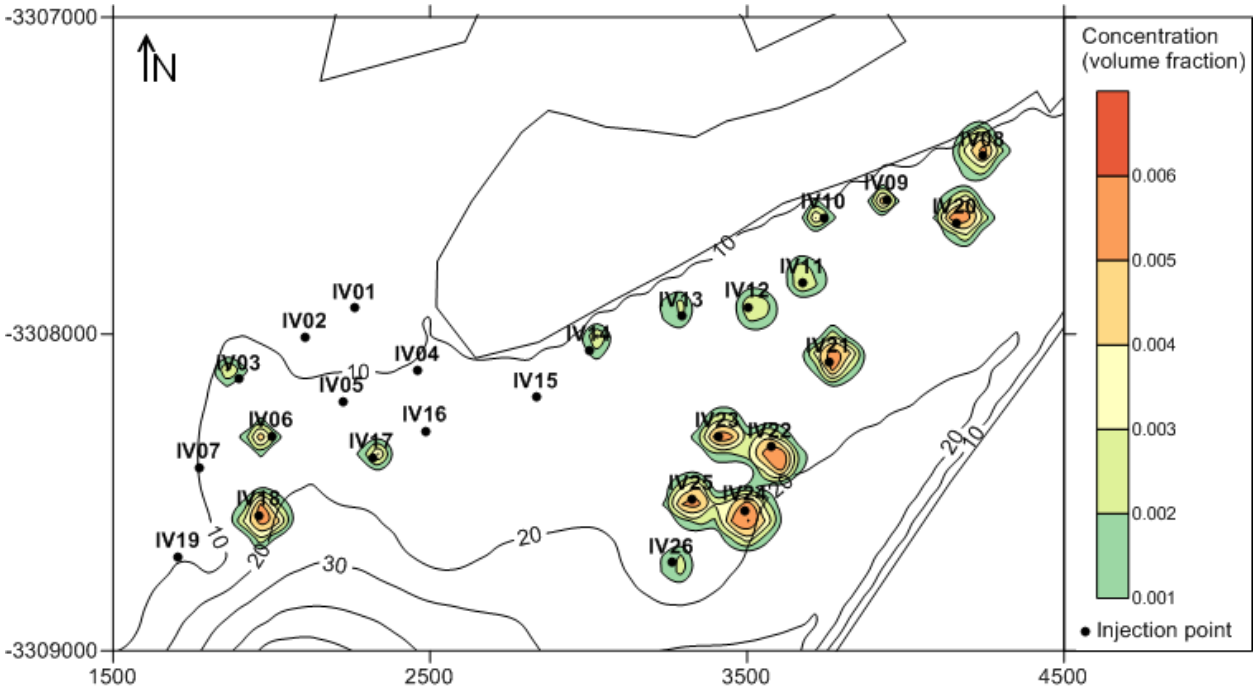

F4: Map illustrating the simulation results for the remediation of aqueous phase benzene with diluted surfactant SDS and polymer xanthan gum at a low infiltration rate in the bottom layer.

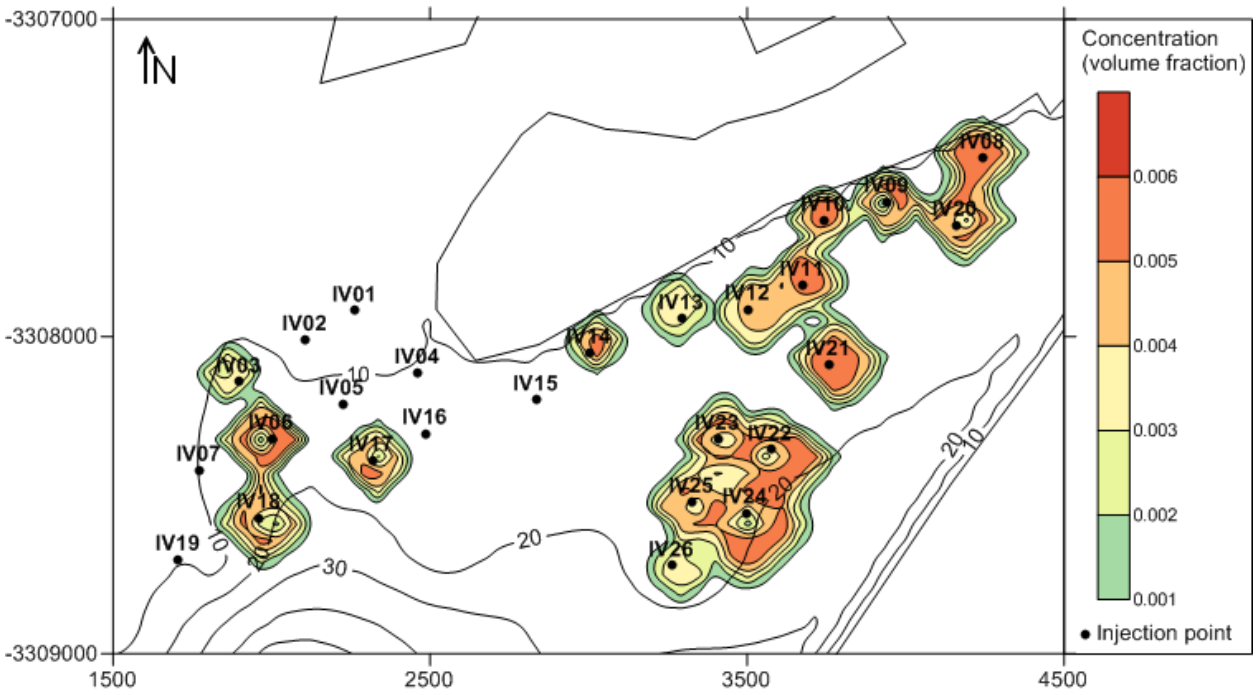

F5: Map illustrating the simulation results for the remediation of aqueous phase benzene with undiluted surfactant SDS and polymer xanthan gum at a low infiltration rate in the top layer.

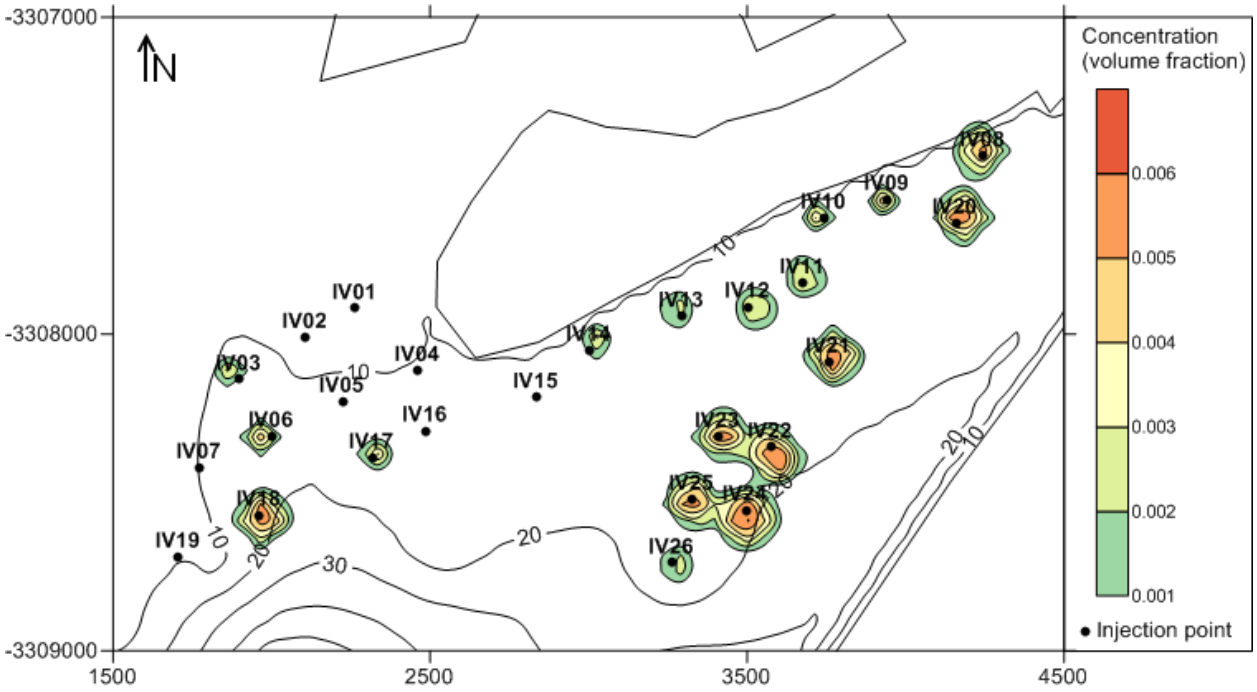

F6: Map illustrating the simulation results for the remediation of aqueous phase benzene with undiluted surfactant SDS and polymer xanthan gum at a low infiltration rate in the bottom layer.

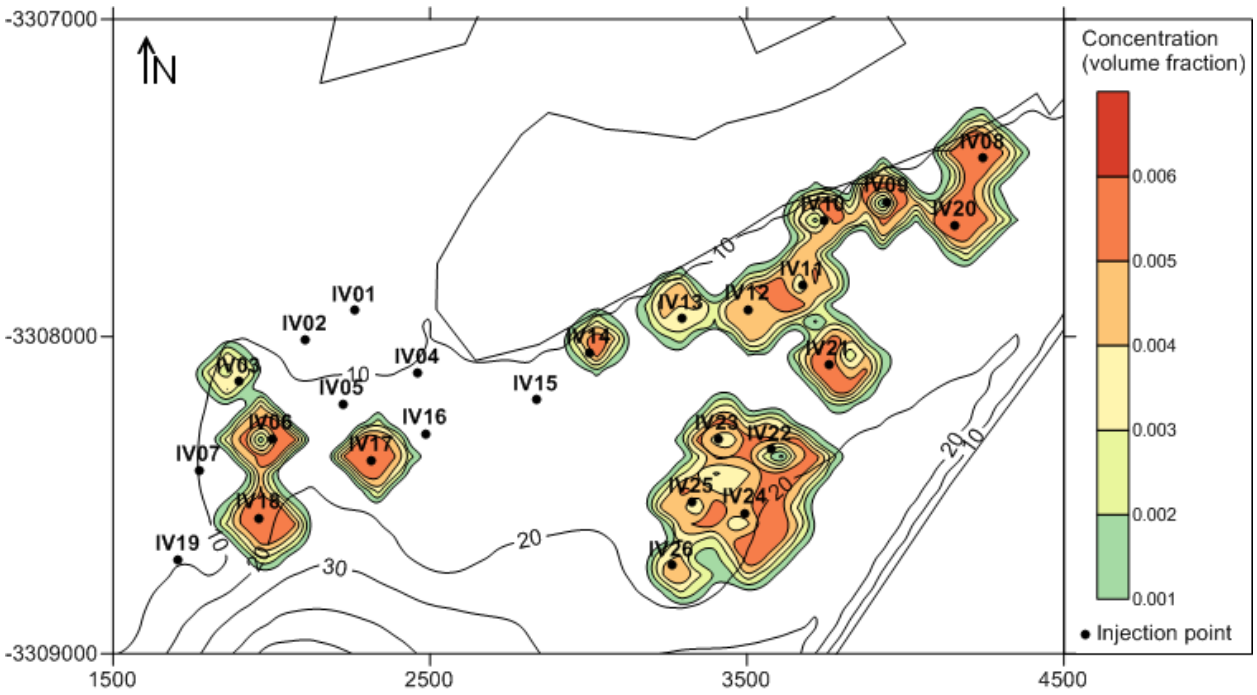

F7: Map illustrating the simulation results for the remediation of aqueous phase benzene with undiluted surfactant SDS and polymer xanthan gum at a high infiltration rate in the top layer.

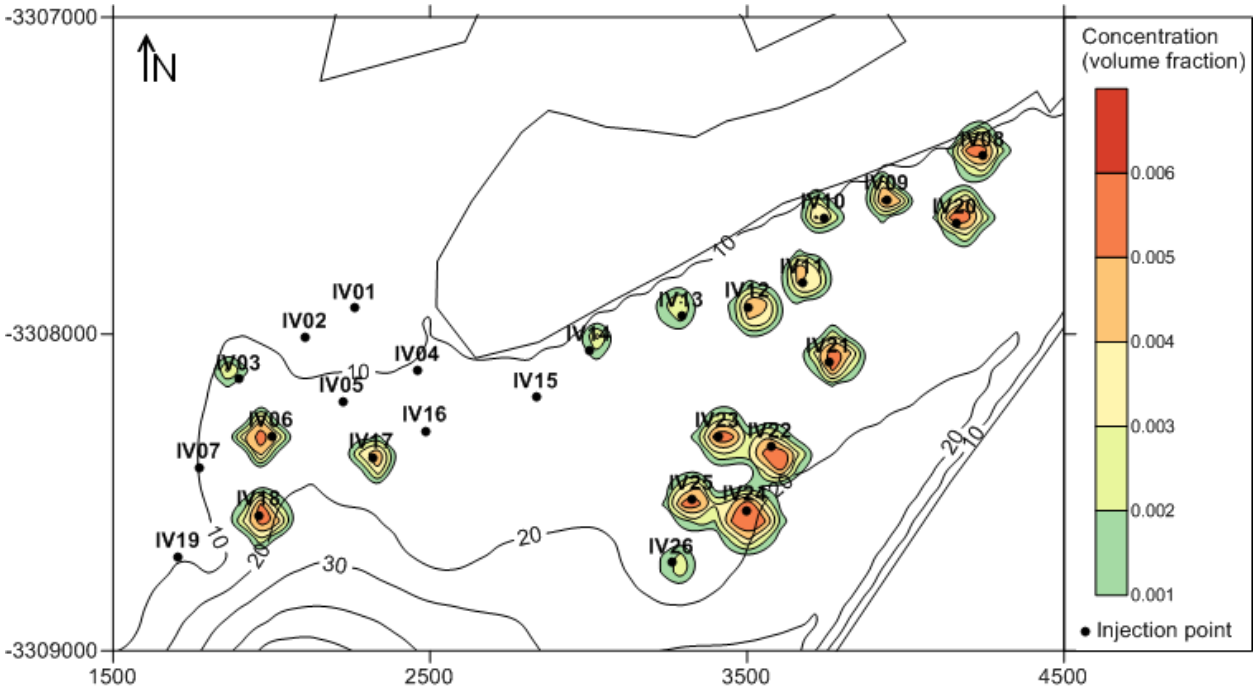

F8: Map illustrating the simulation results for the remediation of aqueous phase benzene with undiluted surfactant SDS and polymer xanthan gum at a high infiltration rate in the bottom layer.

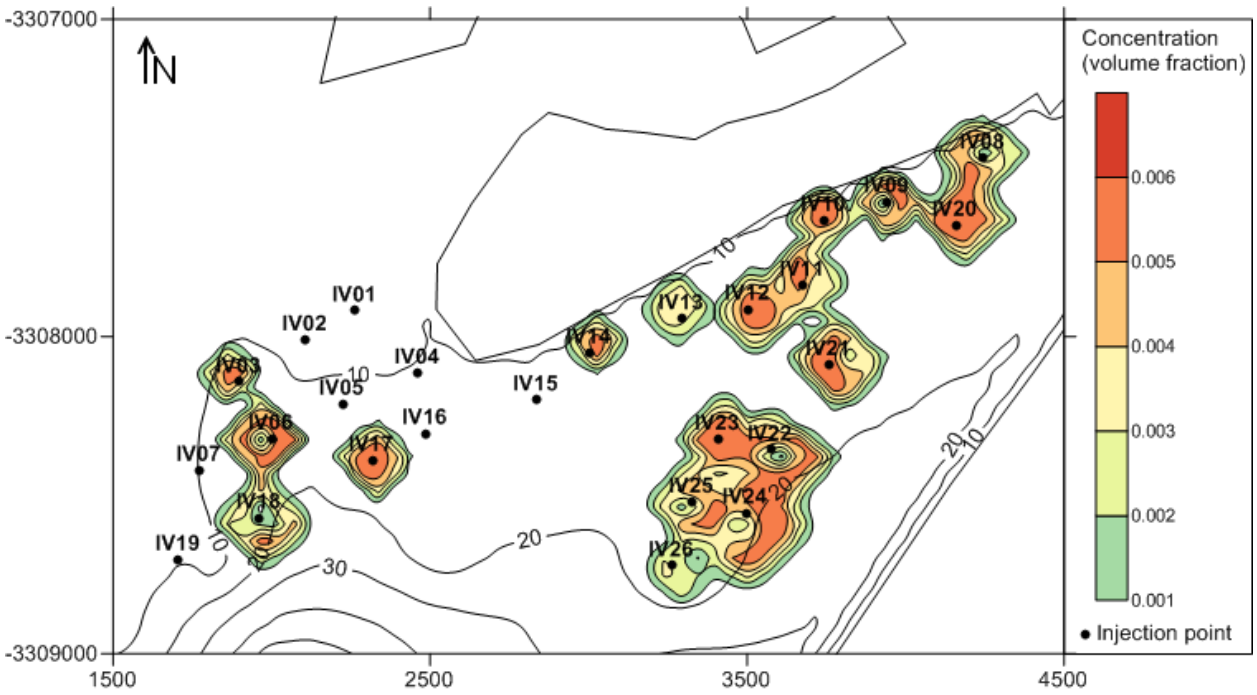

F9: Map illustrating the simulation results for the remediation of aqueous phase benzene with diluted surfactant SDS at a low infiltration rate in the top layer.

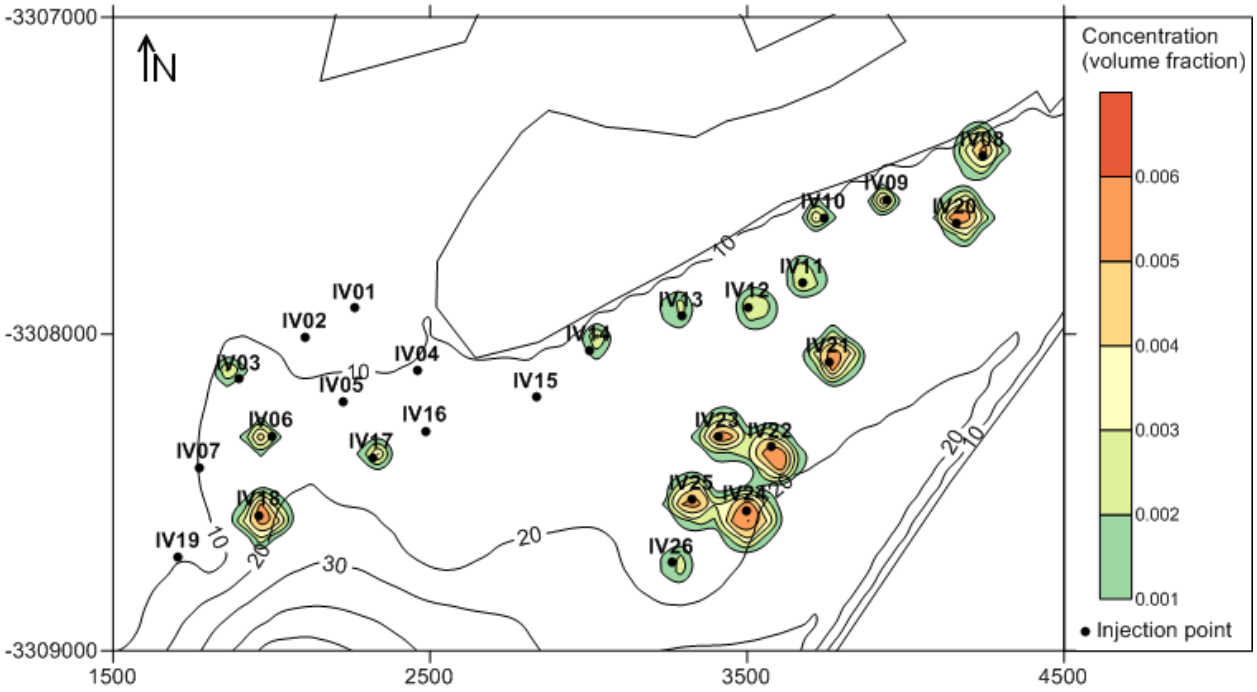

F10: Map illustrating the simulation results for the remediation of aqueous phase benzene with diluted surfactant SDS at a low infiltration rate in the bottom layer.

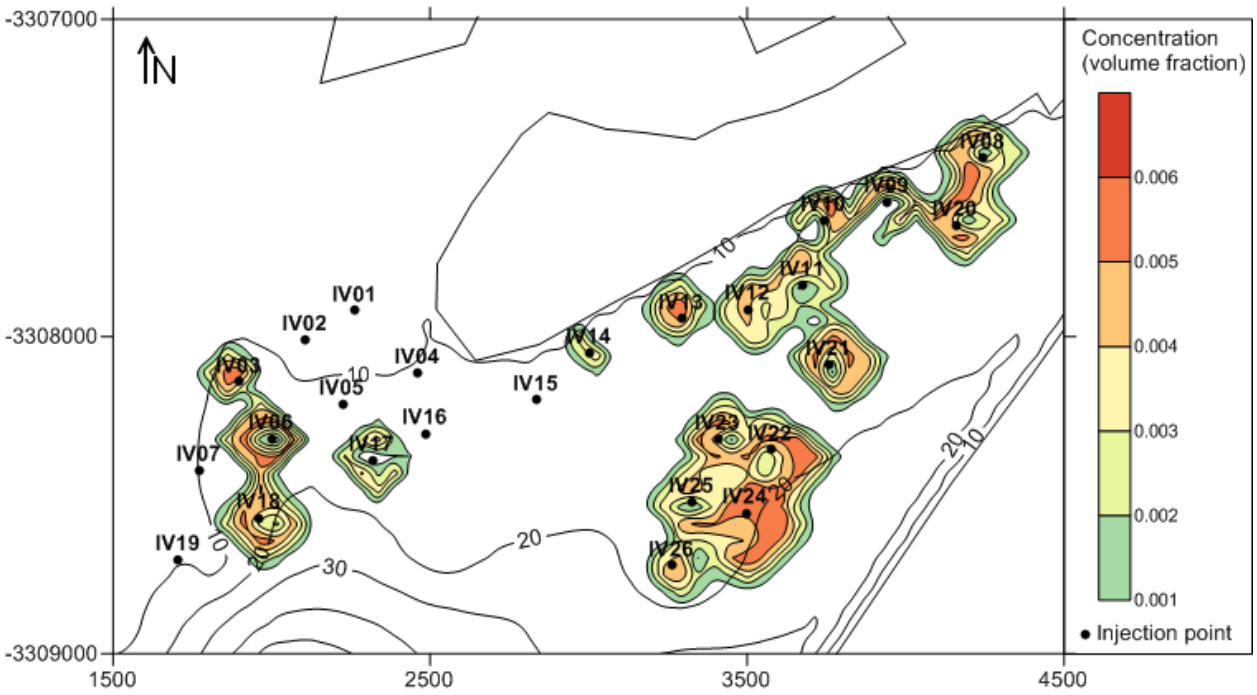

F11: Map illustrating the simulation results for the remediation of aqueous phase benzene with undiluted surfactant SDS at a low infiltration rate in the top layer.

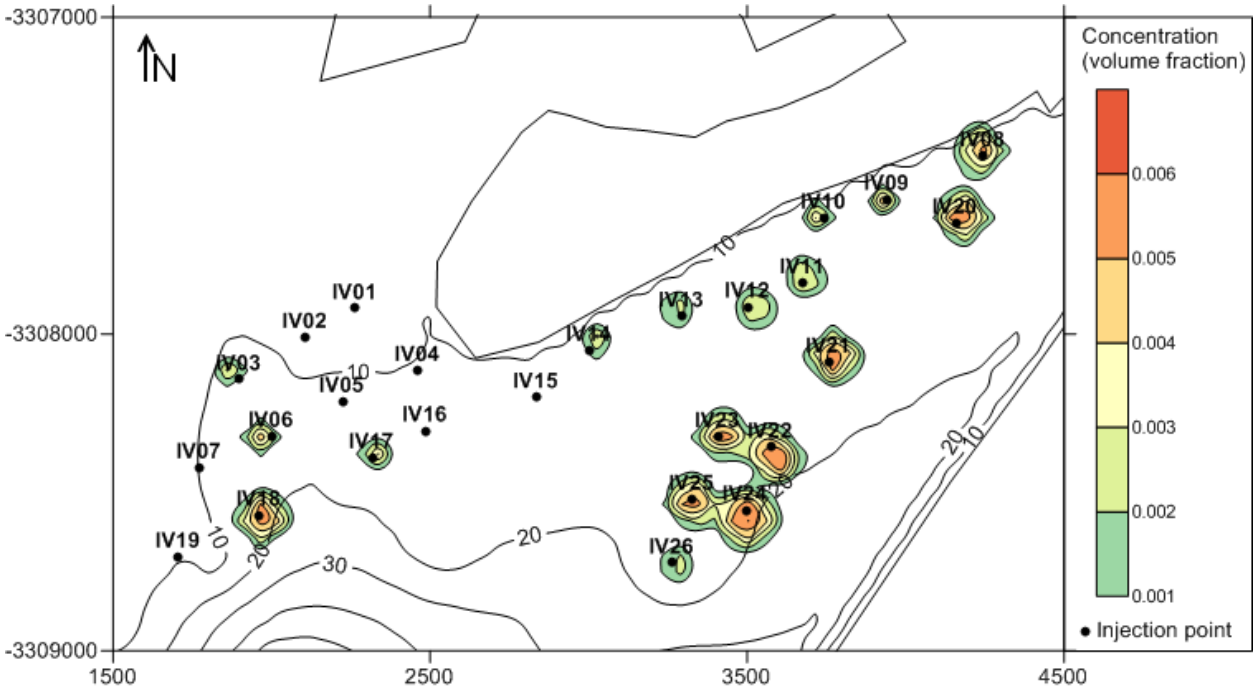

F12: Map illustrating the simulation results for the remediation of aqueous phase benzene with undiluted surfactant SDS at a low infiltration rate in the bottom layer.

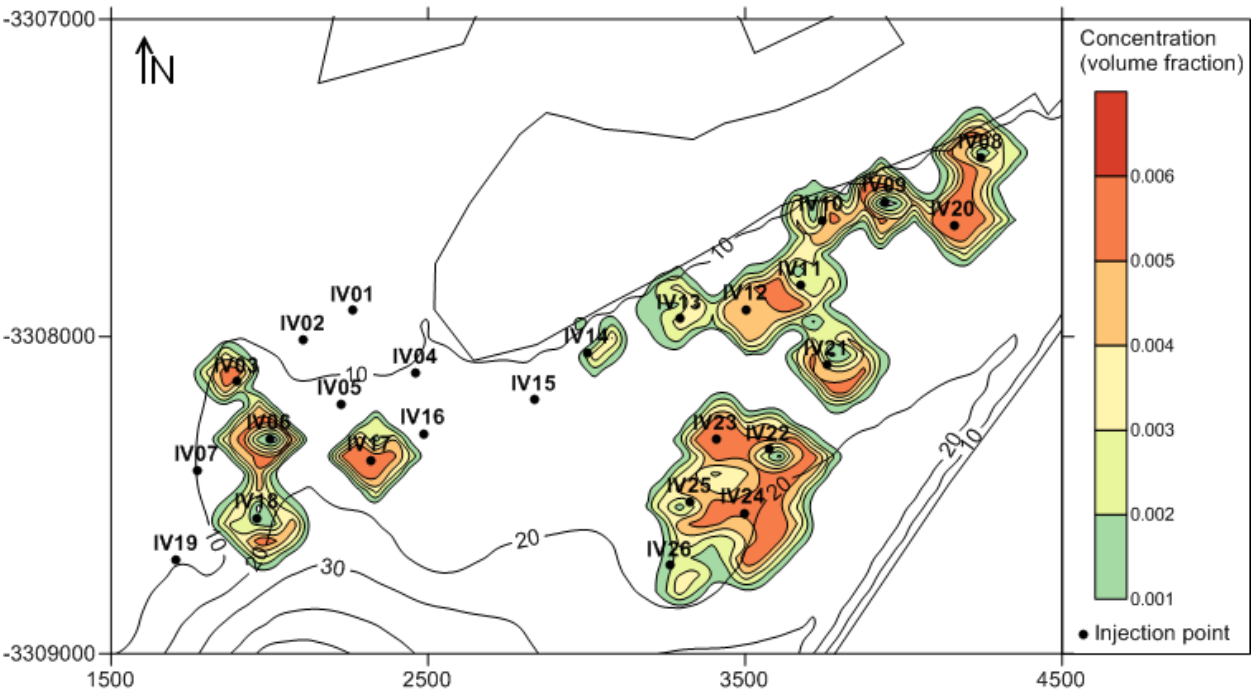

F13: Map illustrating the simulation results for the remediation of aqueous phase benzene with undiluted surfactant SDS at a high infiltration rate in the top layer.

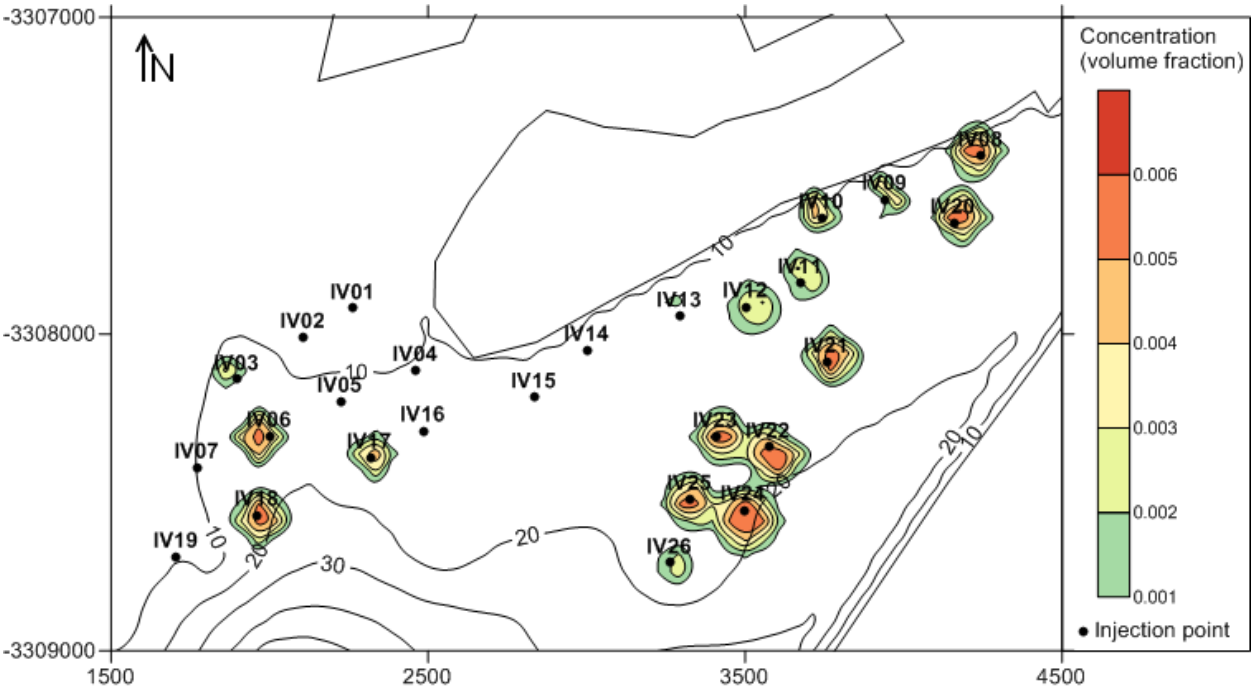

F14: Map illustrating the simulation results for the remediation of aqueous phase benzene with undiluted surfactant SDS at a high infiltration rate in the bottom layer.

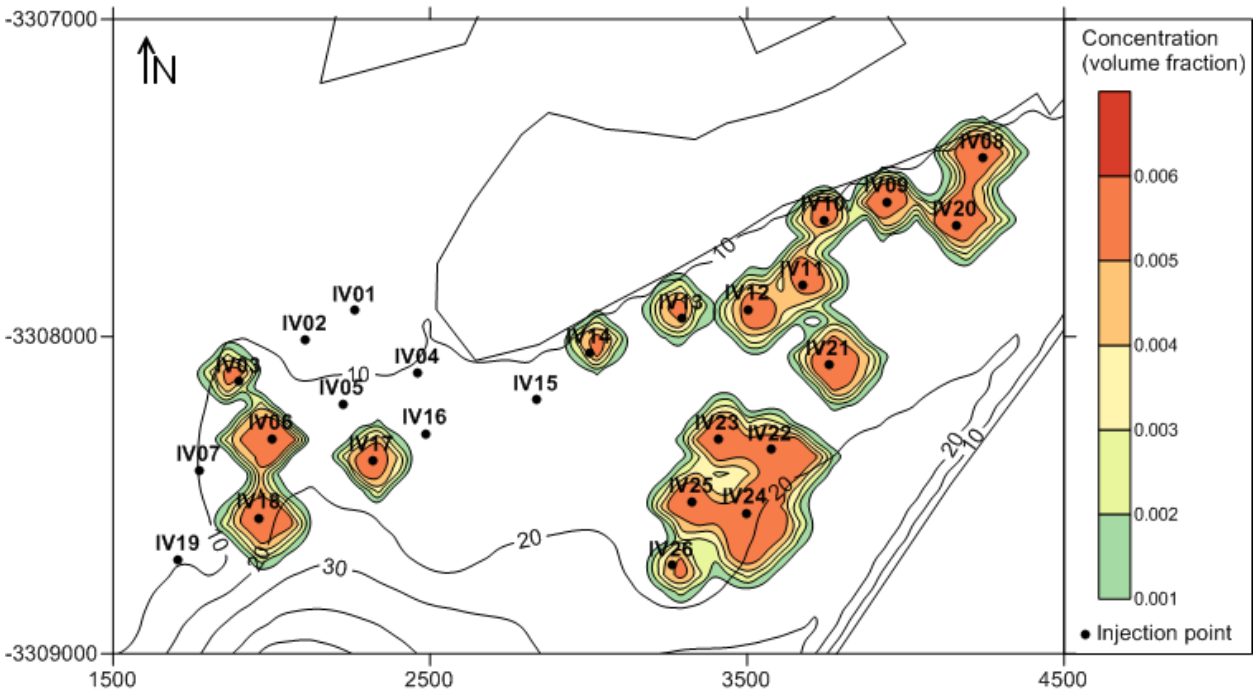

F15: Map illustrating the simulation results for the remediation of aqueous phase benzene with diluted polymer xanthan gum at a low infiltration rate in the top layer.

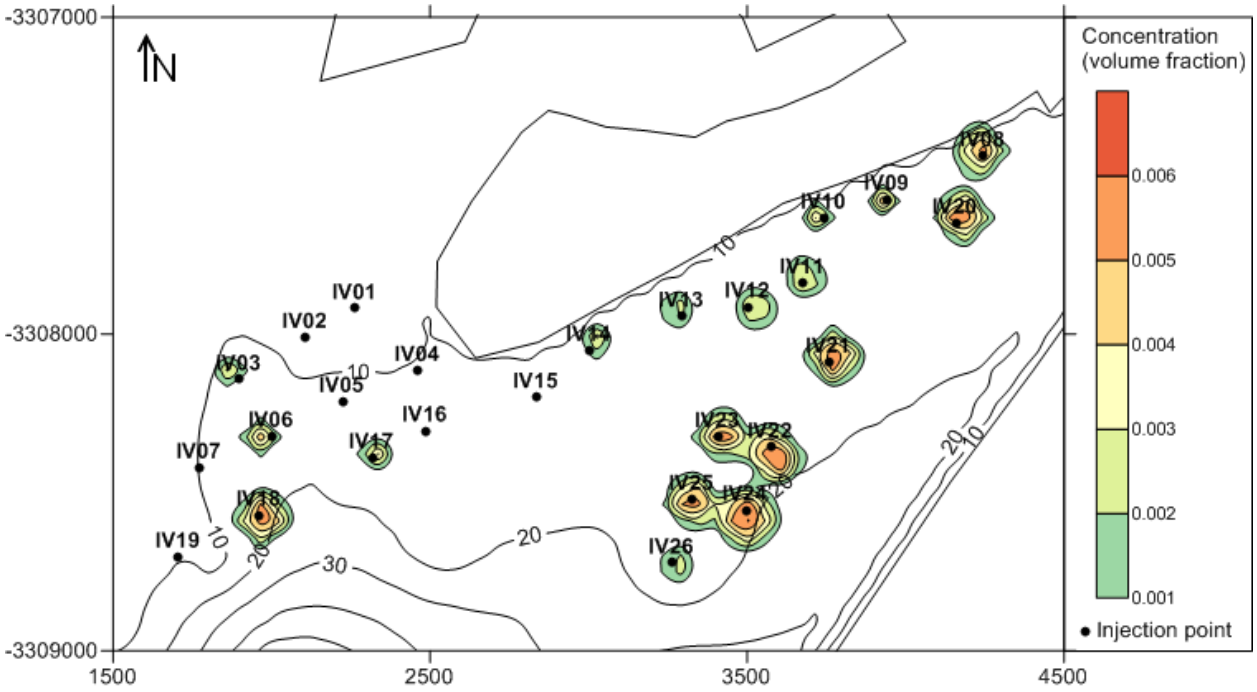

F16: Map illustrating the simulation results for the remediation of aqueous phase benzene with diluted polymer xanthan gum at a low infiltration rate in the bottom layer.

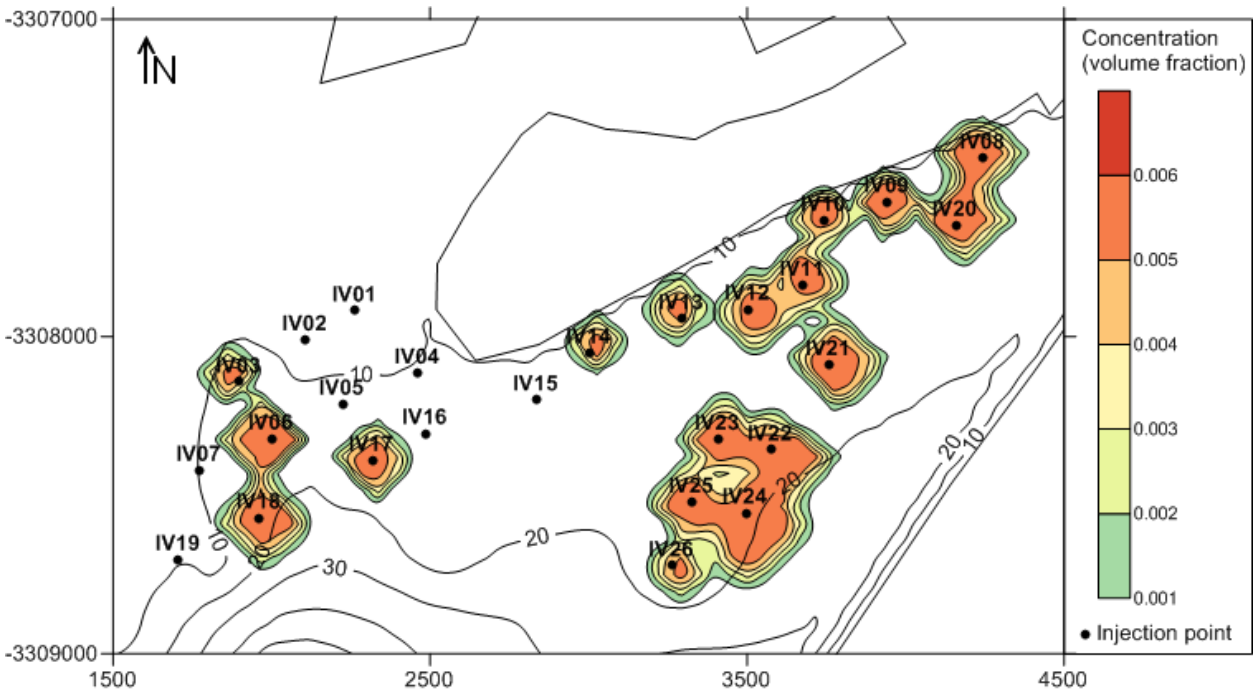

F17: Map illustrating the simulation results for the remediation of aqueous phase benzene with undiluted polymer xanthan gum at a low infiltration rate in the top layer.

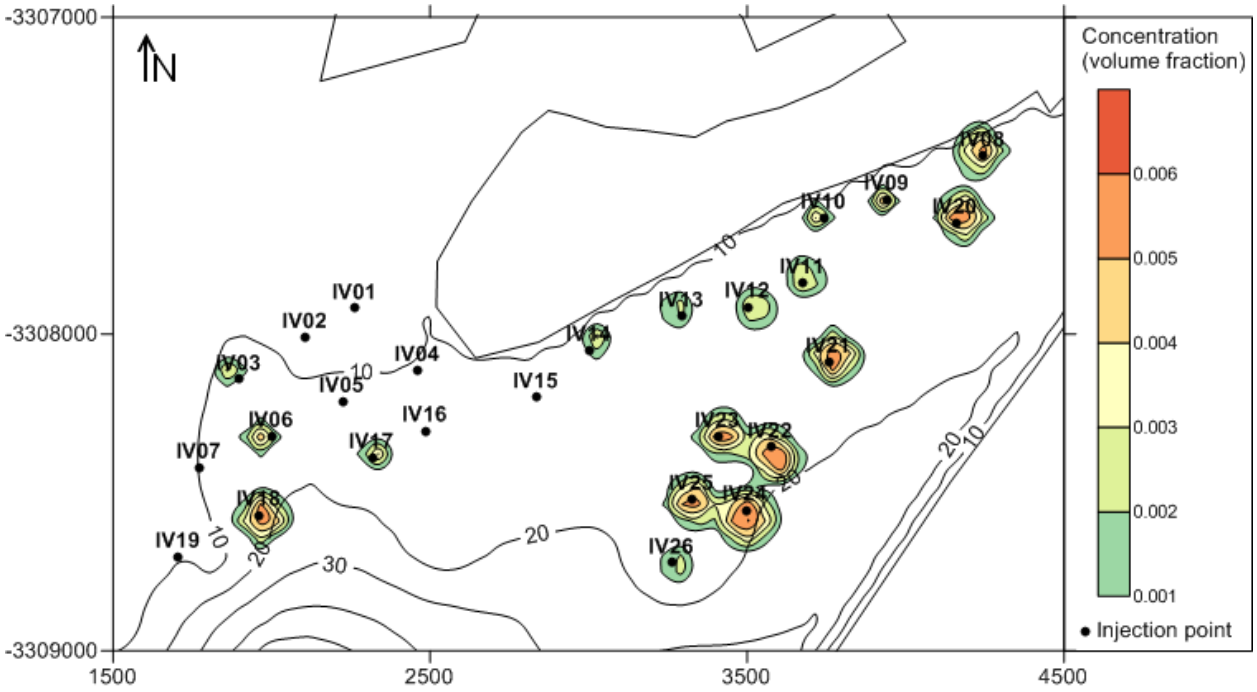

F18: Map illustrating the simulation results for the remediation of aqueous phase benzene with undiluted polymer xanthan gum at a low infiltration rate in the bottom layer.

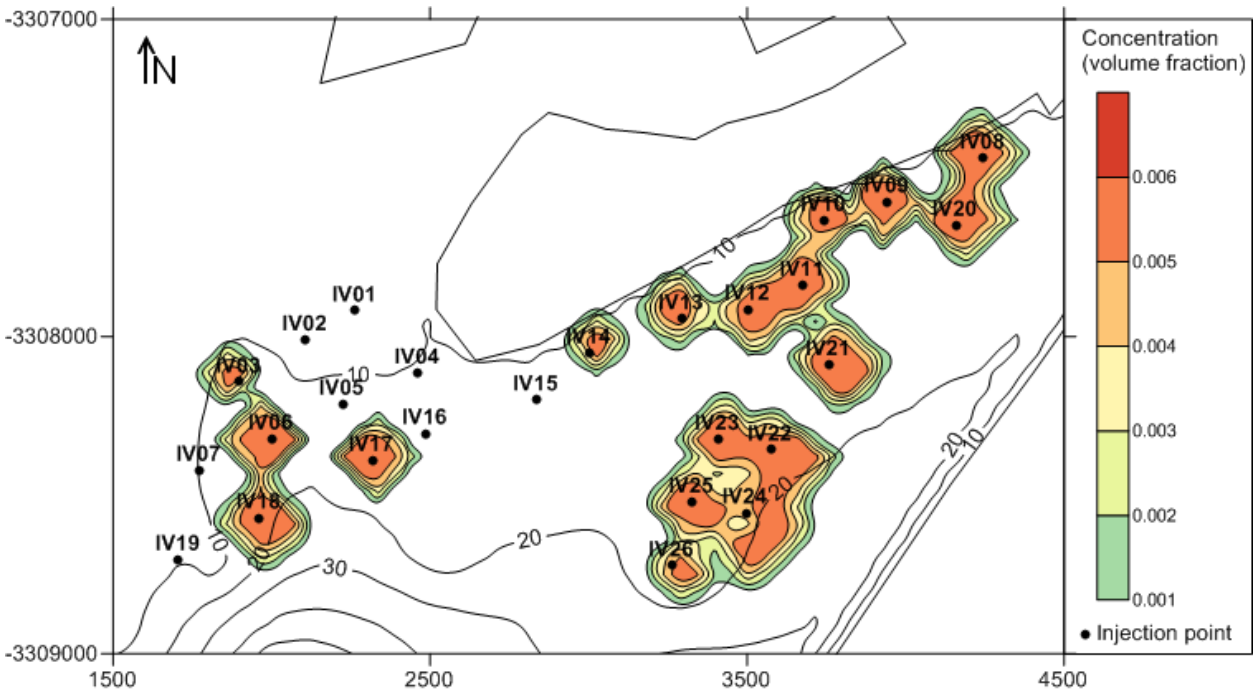

F19: Map illustrating the simulation results for the remediation of aqueous phase benzene with undiluted polymer xanthan gum at a high infiltration rate in the top layer.

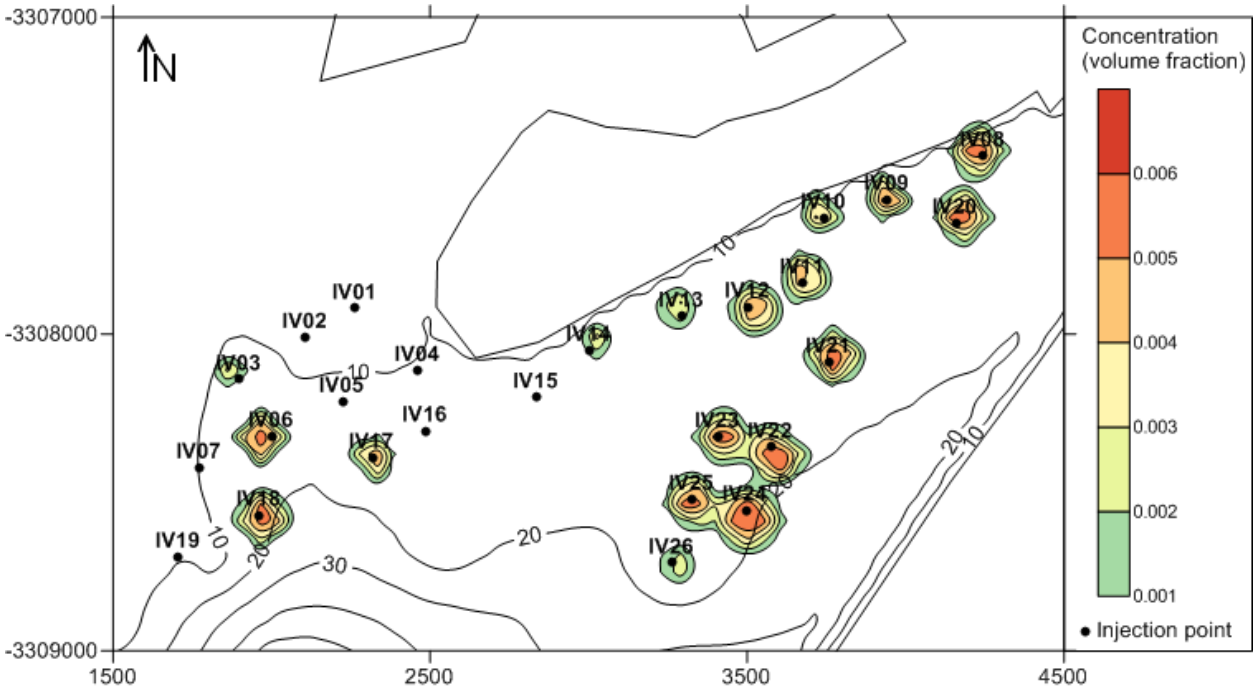

F20: Map illustrating the simulation results for the remediation of aqueous phase benzene with undiluted polymer xanthan gum at a high infiltration rate in the bottom layer.

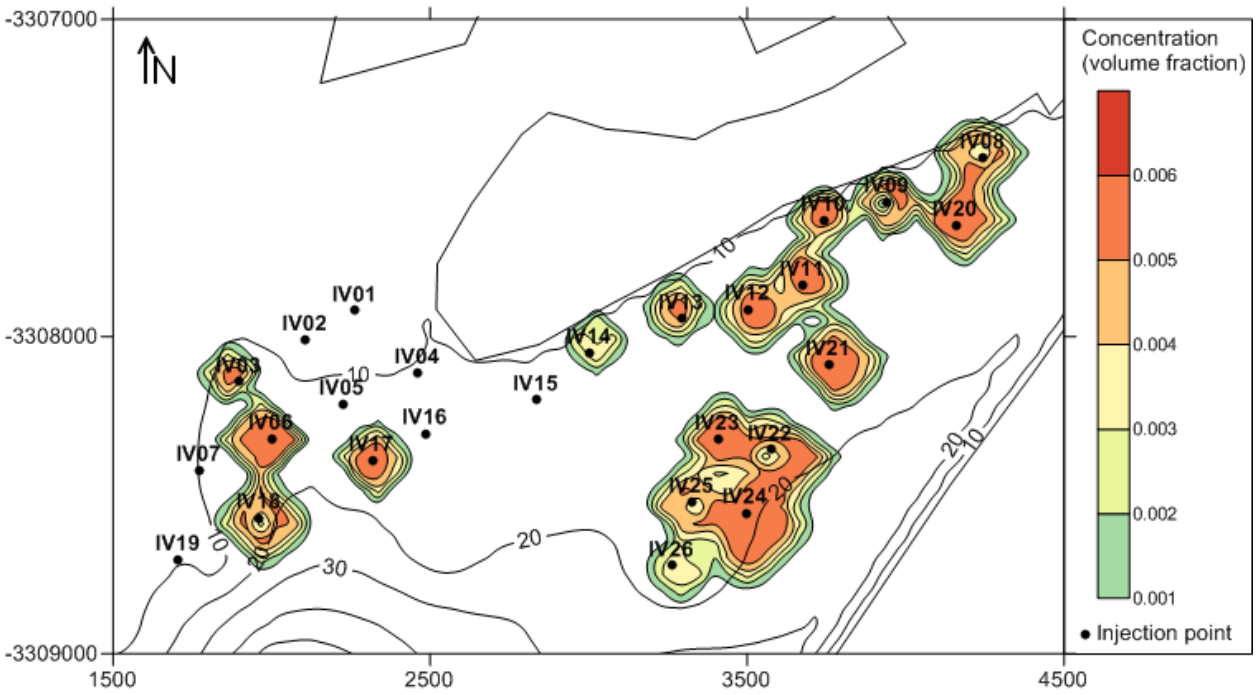

F21: Map illustrating the simulation results for the remediation of aqueous phase benzene with diluted surfactant SDS and ethanol at a low infiltration rate in the top layer.

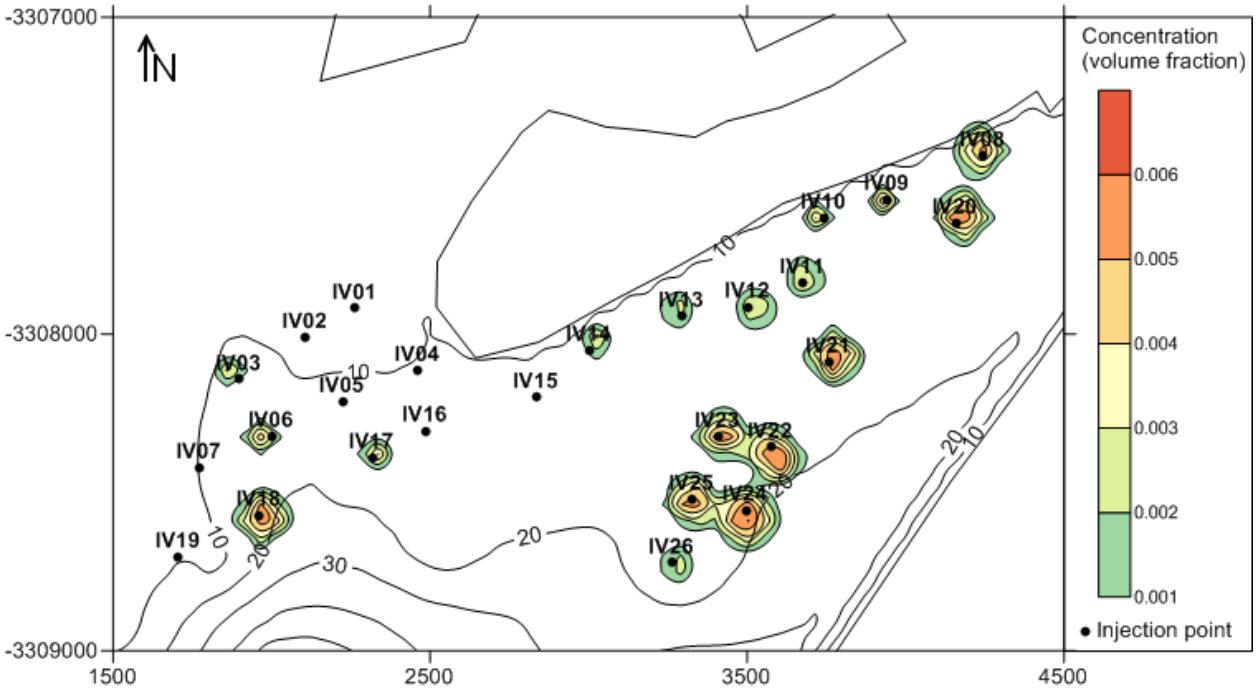

F22: Map illustrating the simulation results for the remediation of aqueous phase benzene with diluted surfactant SDS and ethanol at a low infiltration rate in the bottom layer.

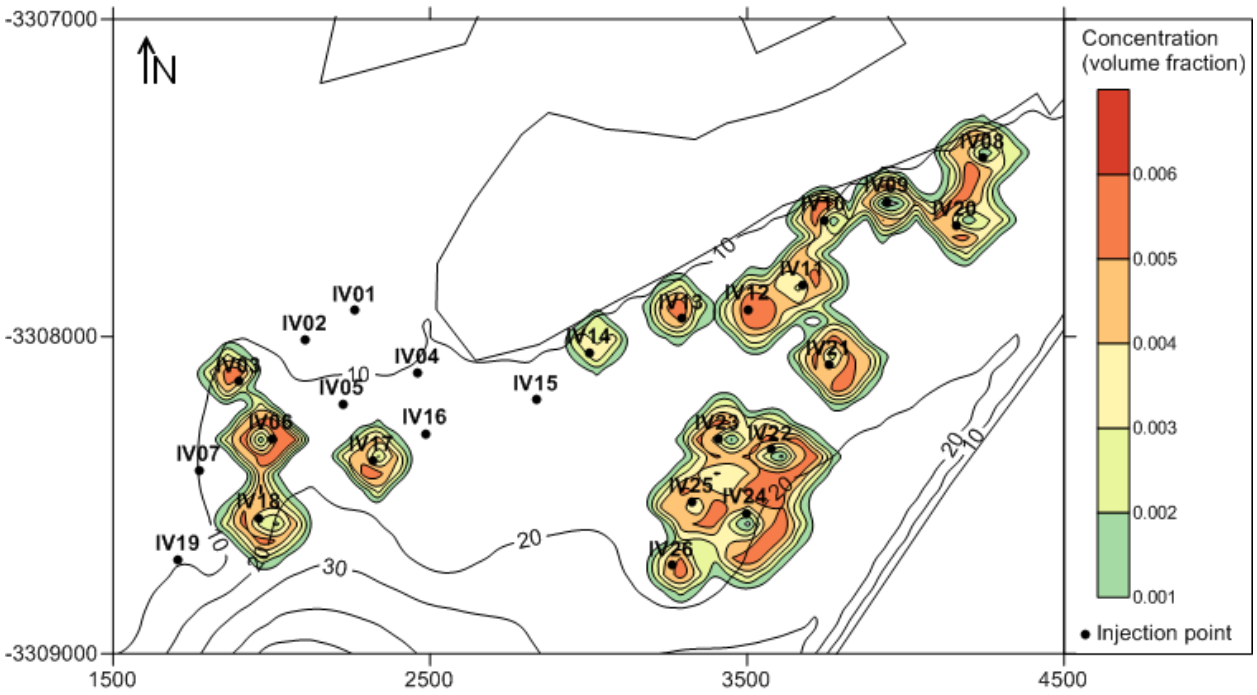

F23: Map illustrating the simulation results for the remediation of aqueous phase benzene with undiluted surfactant SDS and ethanol at a low infiltration rate in the top layer.

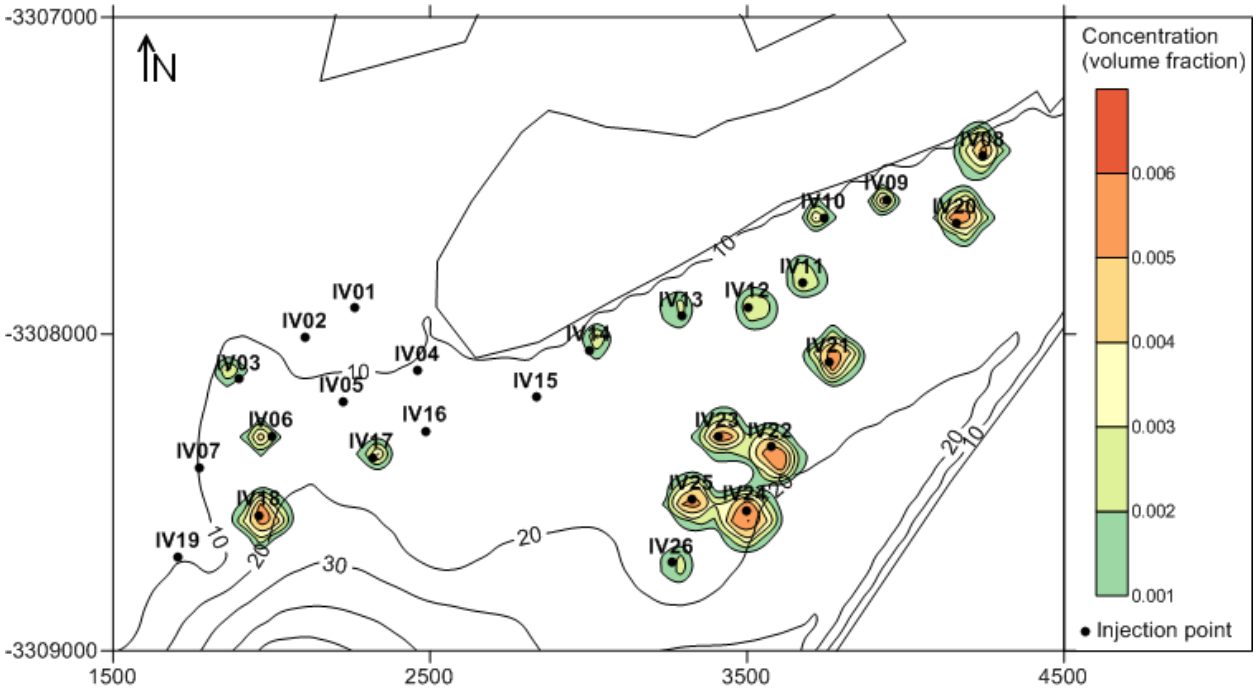

F24: Map illustrating the simulation results for the remediation of aqueous phase benzene with undiluted surfactant SDS and ethanol at a low infiltration rate in the bottom layer.

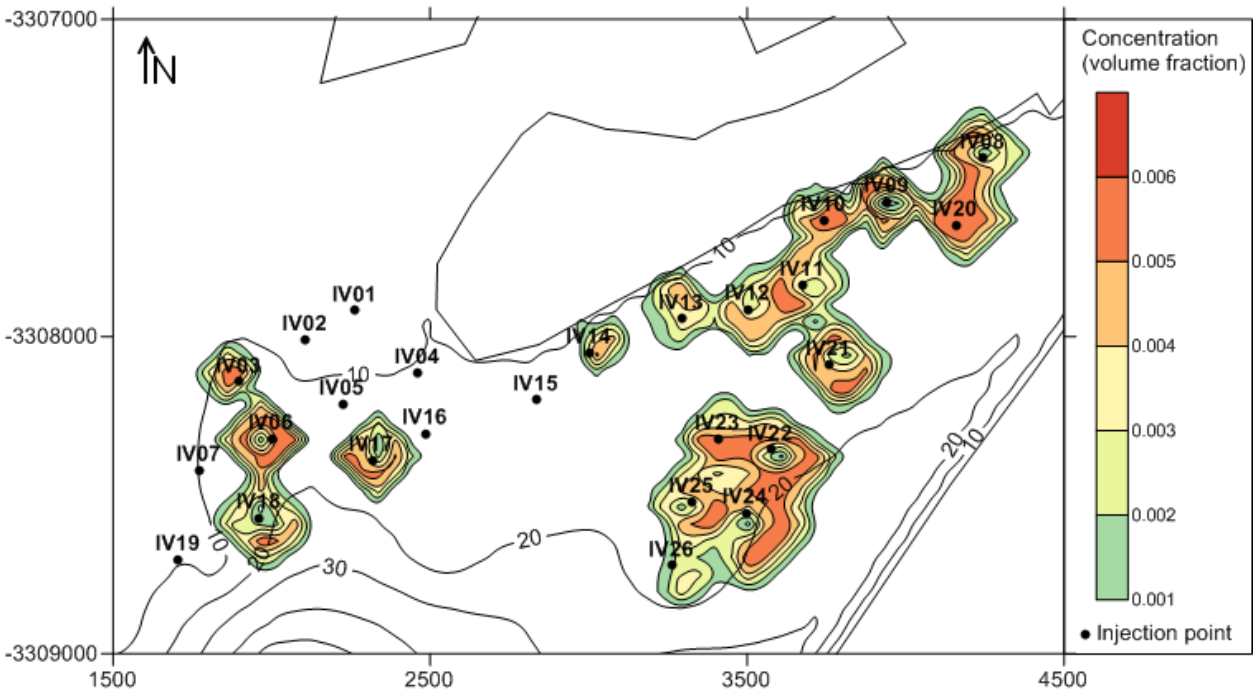

F25: Map illustrating the simulation results for the remediation of aqueous phase benzene with undiluted surfactant SDS and ethanol at a high infiltration rate in the top layer.

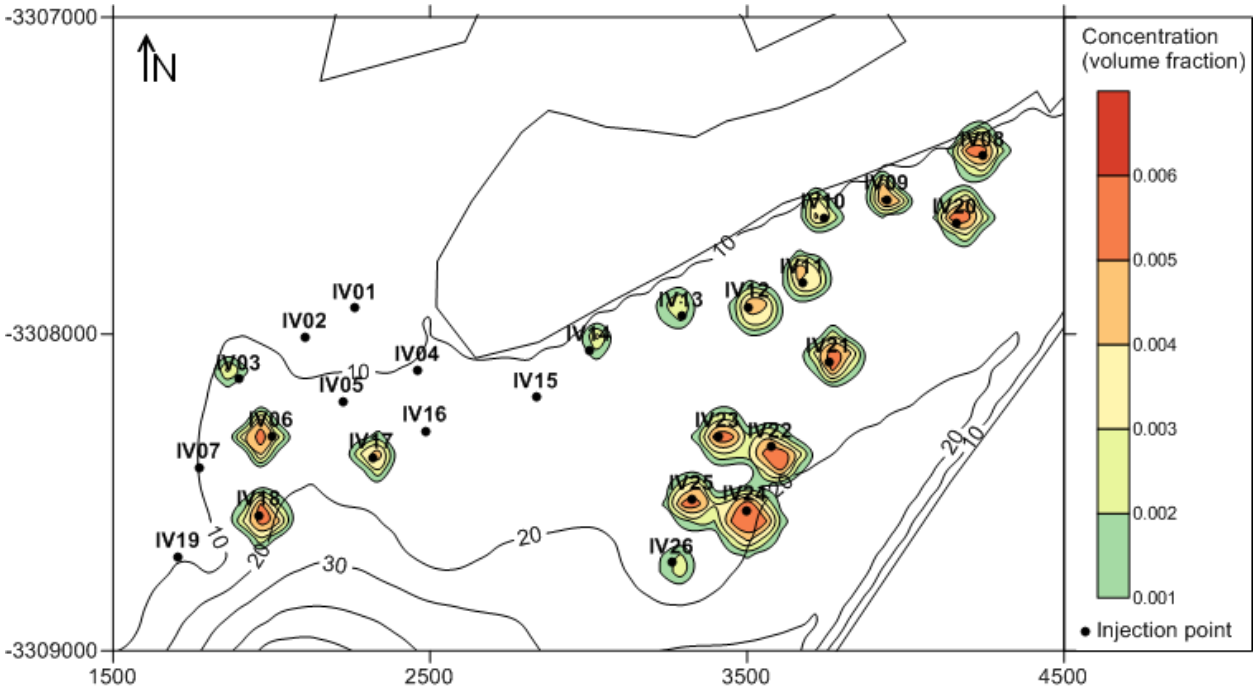

F26: Map illustrating the simulation results for the remediation of aqueous phase benzene with undiluted surfactant SDS and ethanol at a high infiltration rate in the bottom layer.

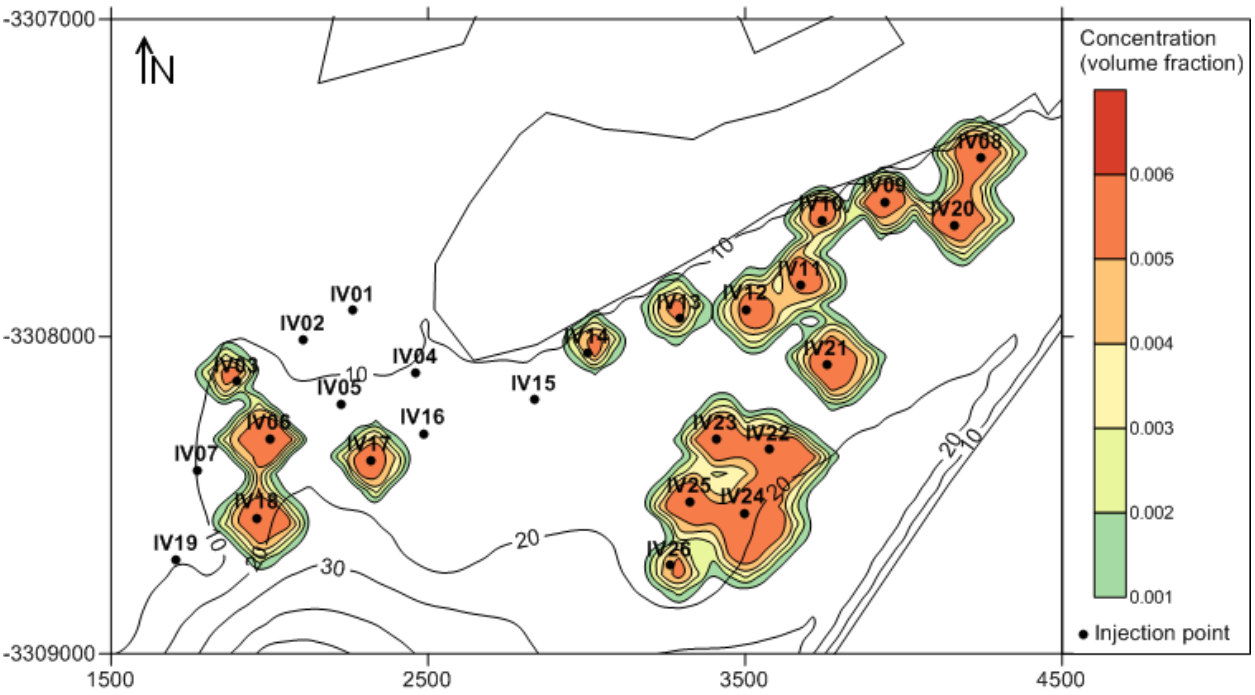

F27: Map illustrating the simulation results for the remediation of aqueous phase benzene with diluted ethanol at a low infiltration rate in the top layer.

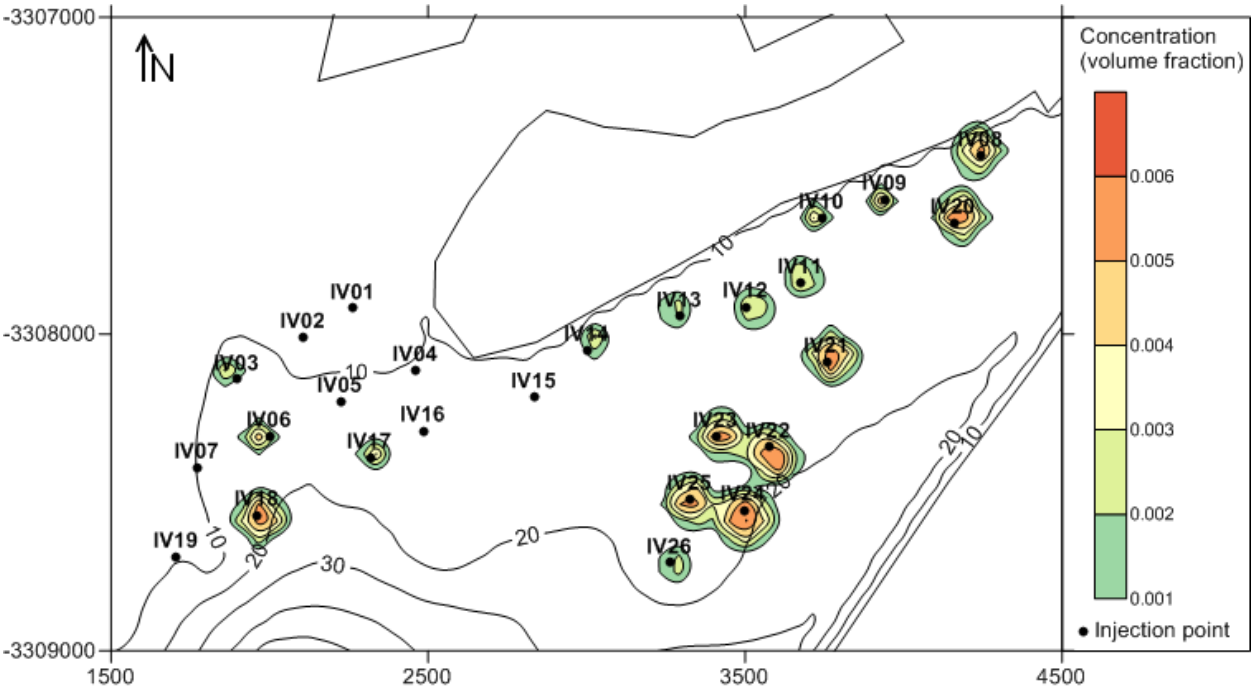

F28: Map illustrating the simulation results for the remediation of aqueous phase benzene with diluted ethanol at a low infiltration rate in the bottom layer.

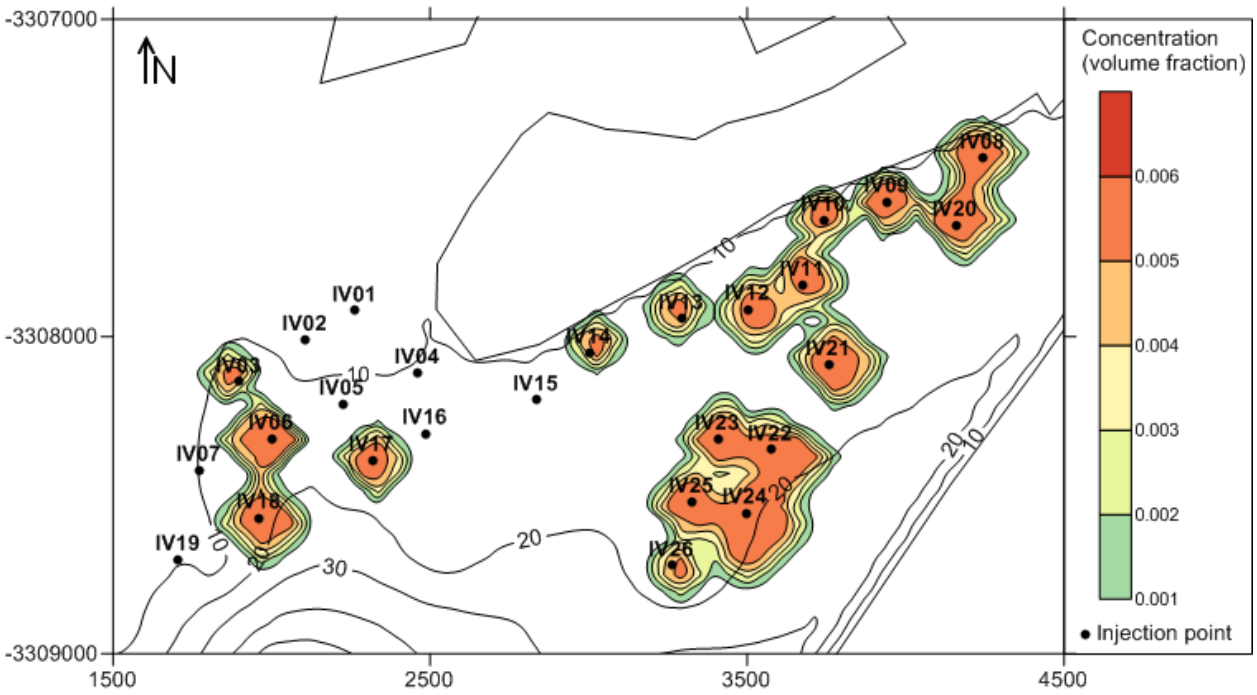

F29: Map illustrating the simulation results for the remediation of aqueous phase benzene with undiluted ethanol at a low infiltration rate in the top layer.

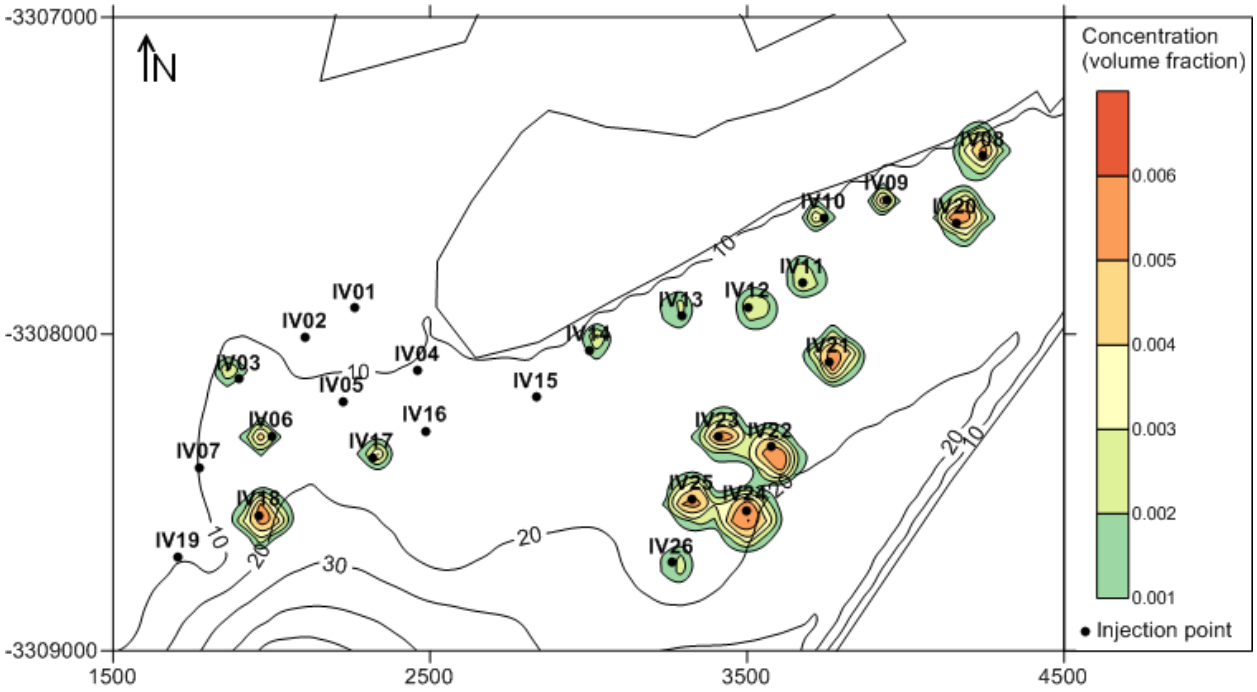

F30: Map illustrating the simulation results for the remediation of aqueous phase benzene with undiluted ethanol at a low infiltration rate in the bottom layer.

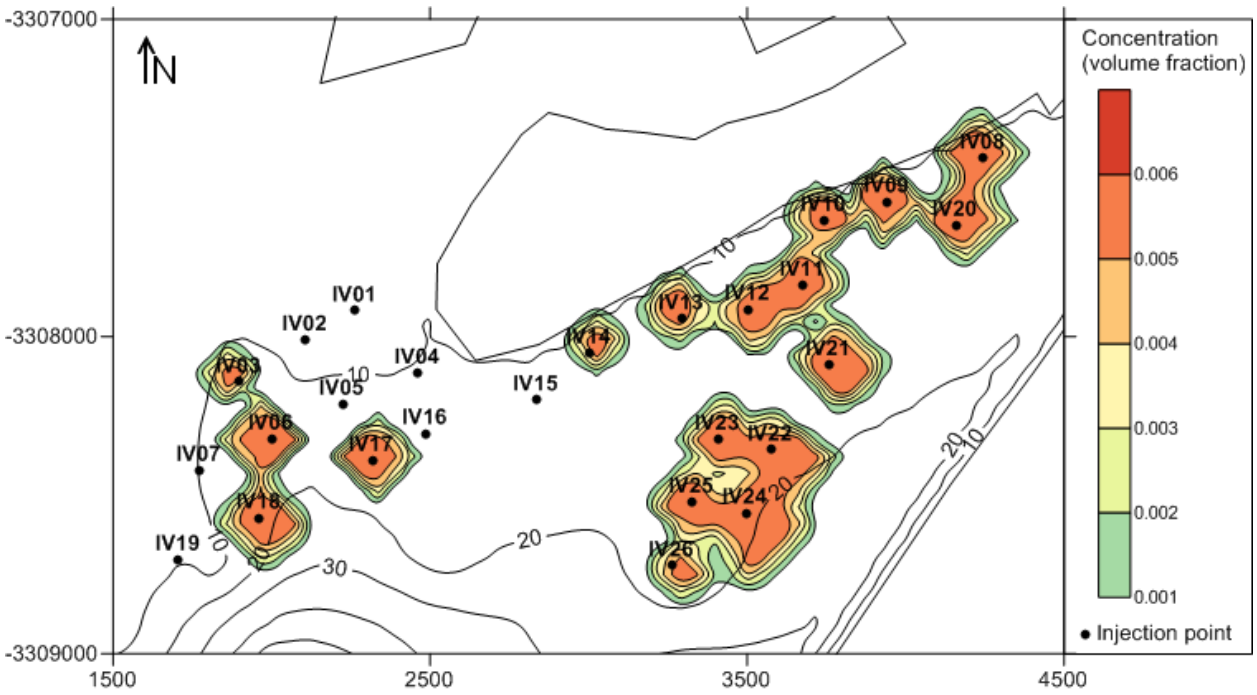

F31: Map illustrating the simulation results for the remediation of aqueous phase benzene with undiluted ethanol at a high infiltration rate in the top layer.

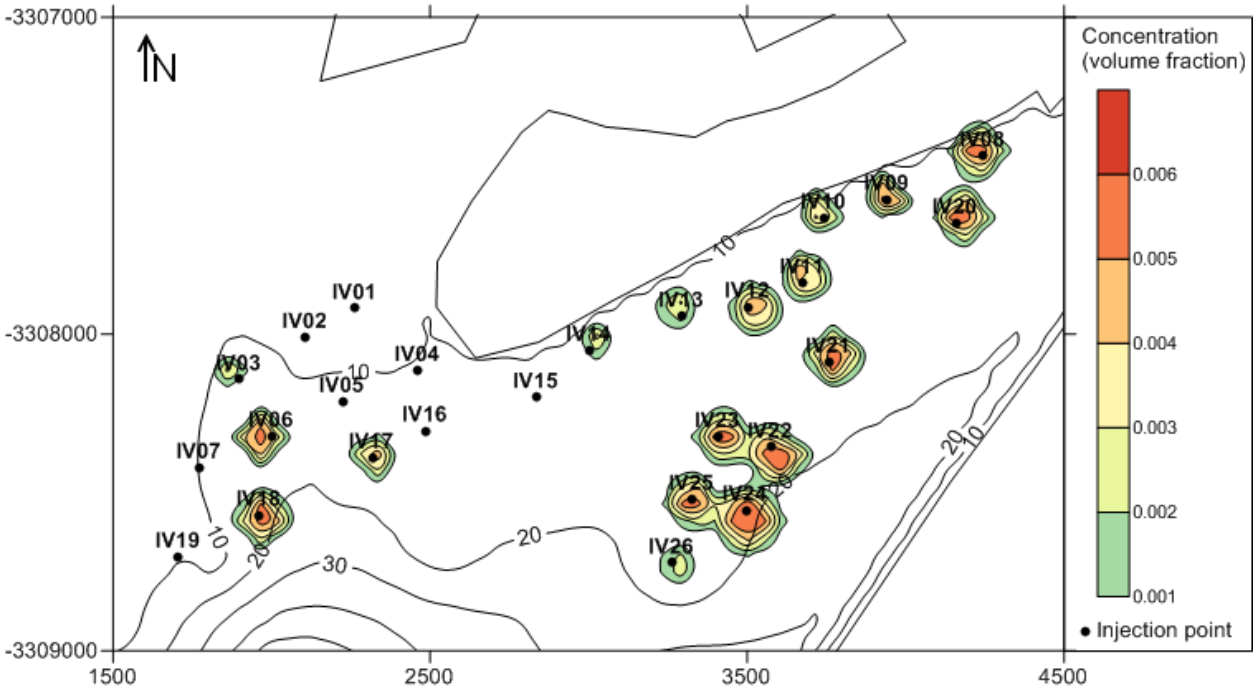

F32: Map illustrating the simulation results for the remediation of aqueous phase benzene with undiluted ethanol at a high infiltration rate in the bottom layer.

Appendix G: Maps illustrating the simulation results for the infiltration and migration of non-aqueous PCE

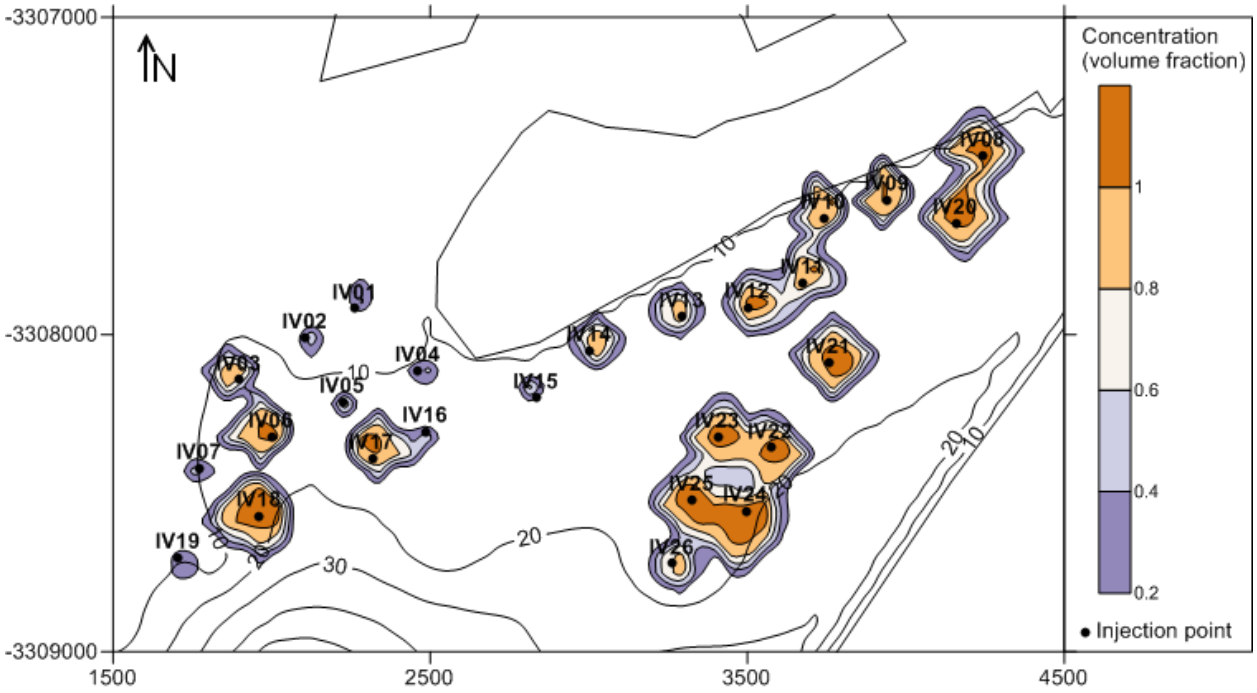

G1: Map illustrating the simulation results for the infiltration and migration of non-aqueous phase PCE in the top layer.

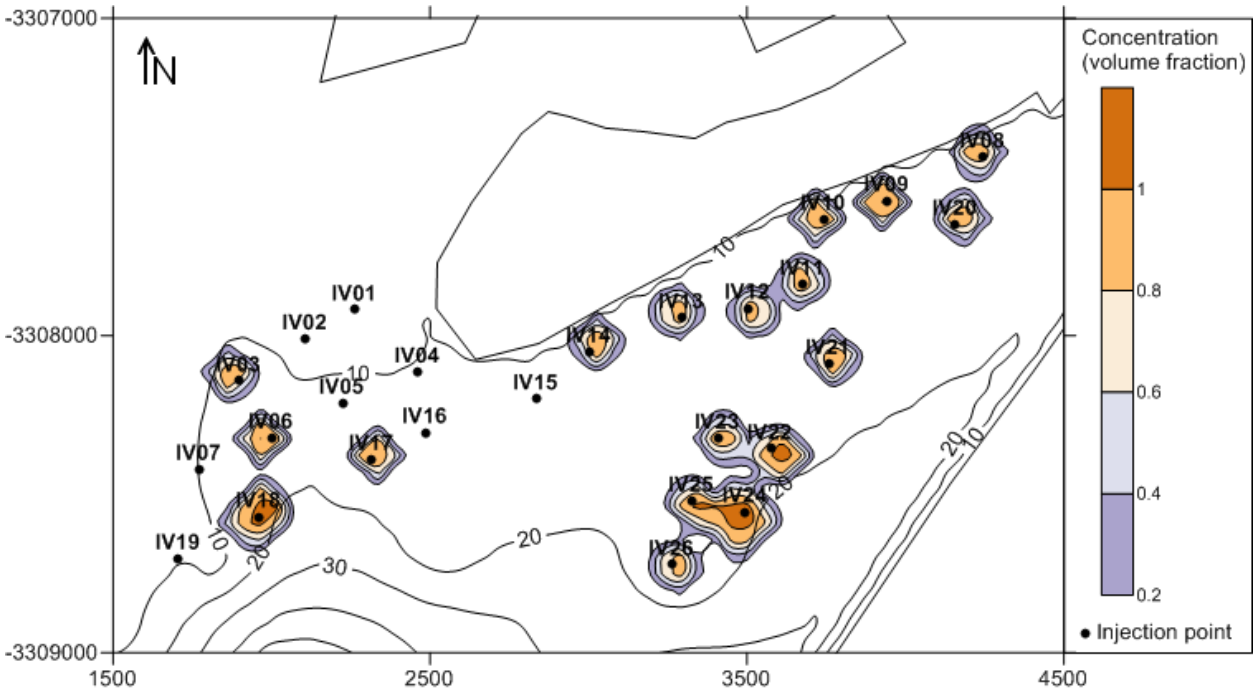

G2: Map illustrating the simulation results for the infiltration and migration of non-aqueous phase PCE in the bottom layer.

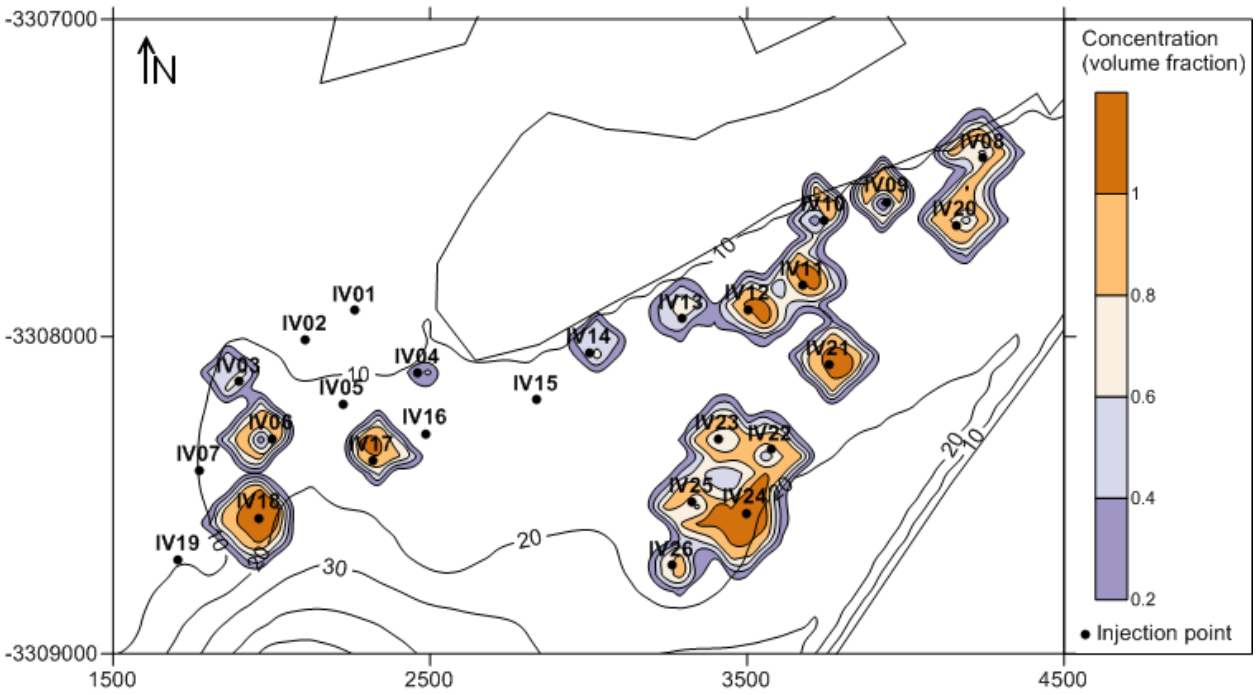

G3: Map illustrating the simulation results for the remediation of non-aqueous phase PCE with diluted surfactant SDS and polymer xanthan gum at a low infiltration rate in the top layer.

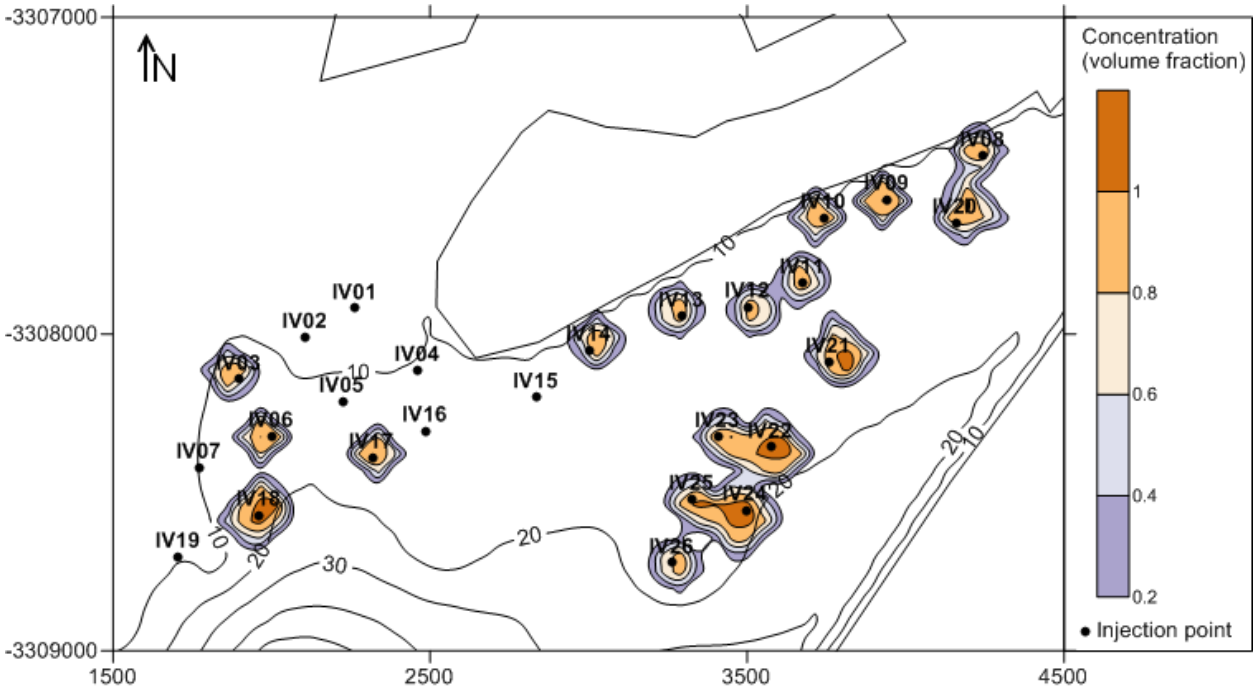

G4: Map illustrating the simulation results for the remediation of non-aqueous phase PCE with diluted surfactant SDS and polymer xanthan gum at a low infiltration rate in the bottom layer.

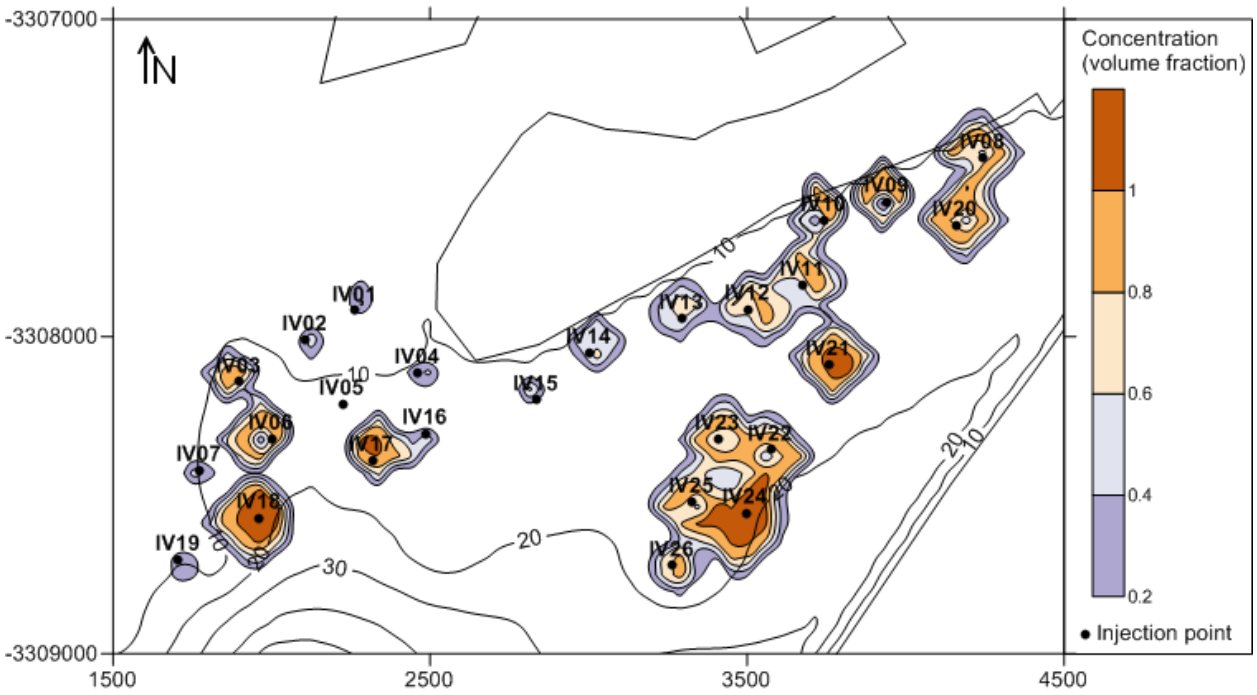

G5: Map illustrating the simulation results for the remediation of non-aqueous phase PCE with undiluted surfactant SDS and polymer xanthan gum at a low infiltration rate in the top layer.

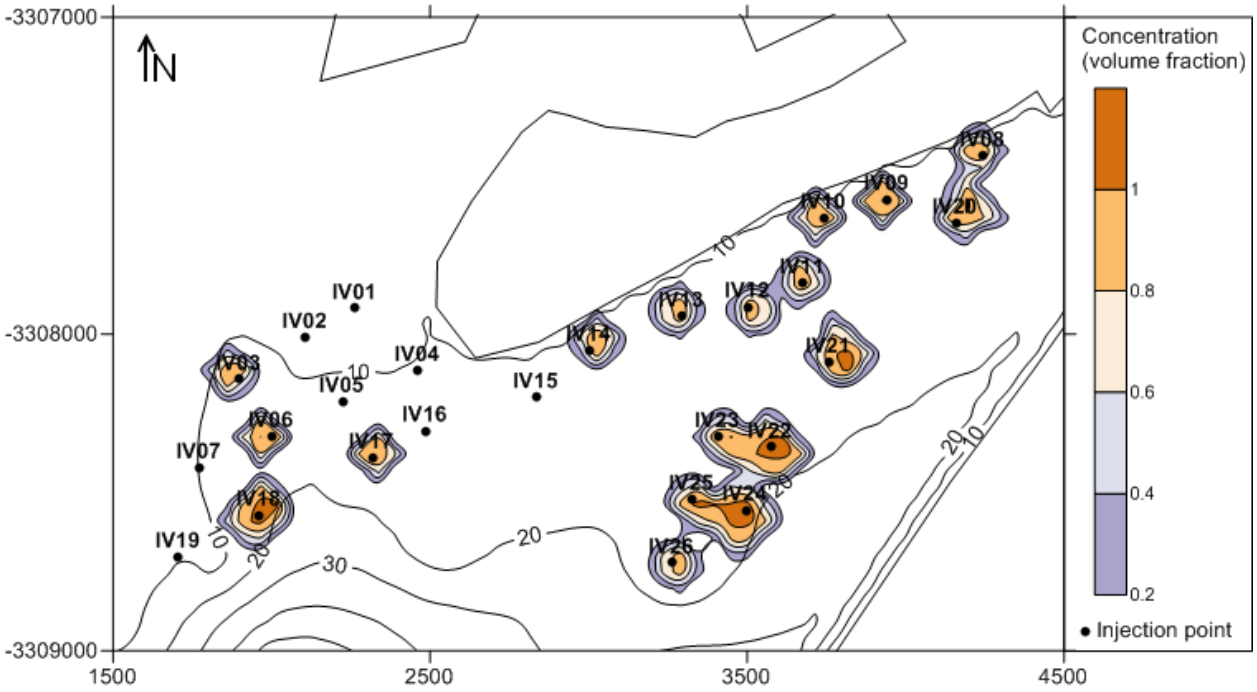

G6: Map illustrating the simulation results for the remediation of non-aqueous phase PCE with undiluted surfactant SDS and polymer xanthan gum at a low infiltration rate in the bottom layer.

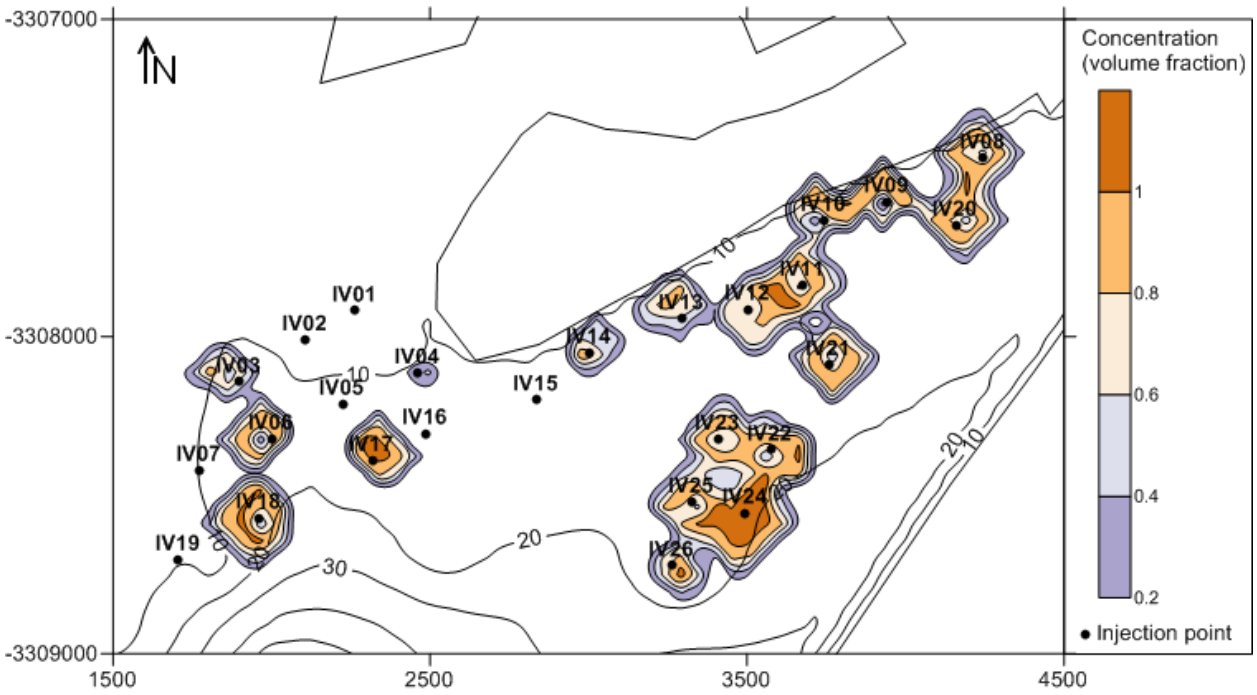

F7: Map illustrating the simulation results for the remediation of non-aqueous phase PCE with undiluted surfactant SDS and polymer xanthan gum at a high infiltration rate in the top layer.

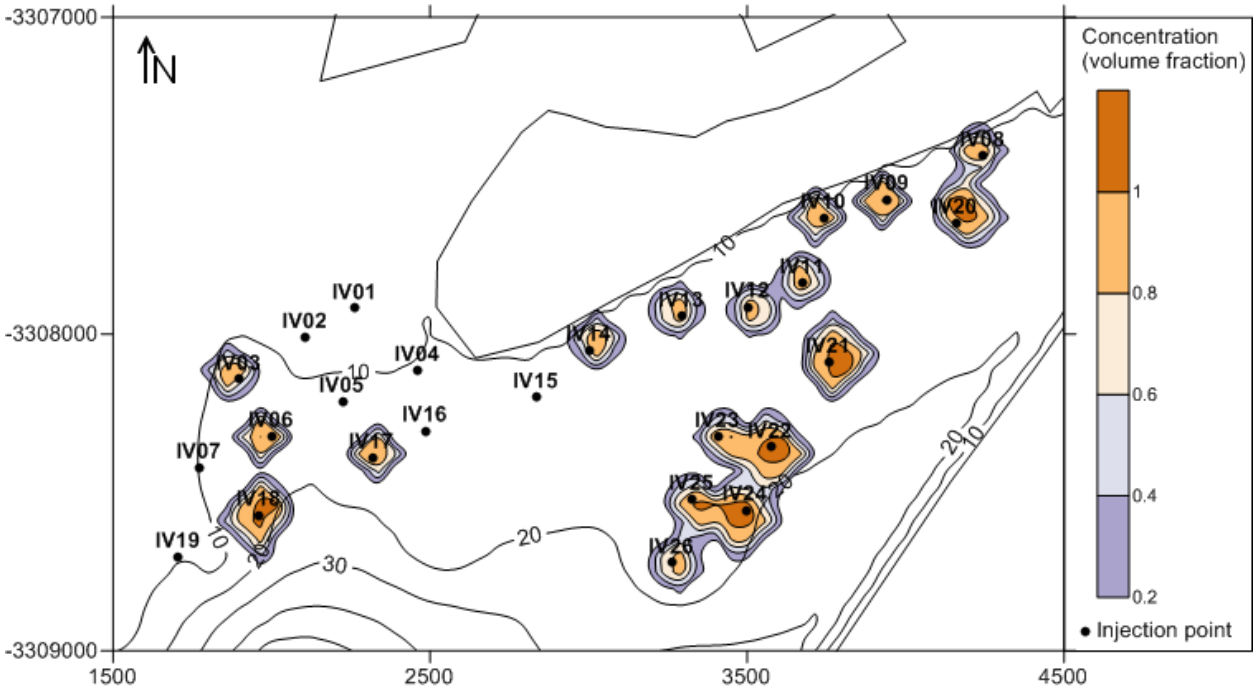

F8: Map illustrating the simulation results for the remediation of non-aqueous phase PCE with undiluted surfactant SDS and polymer xanthan gum at a high infiltration rate in the bottom layer.

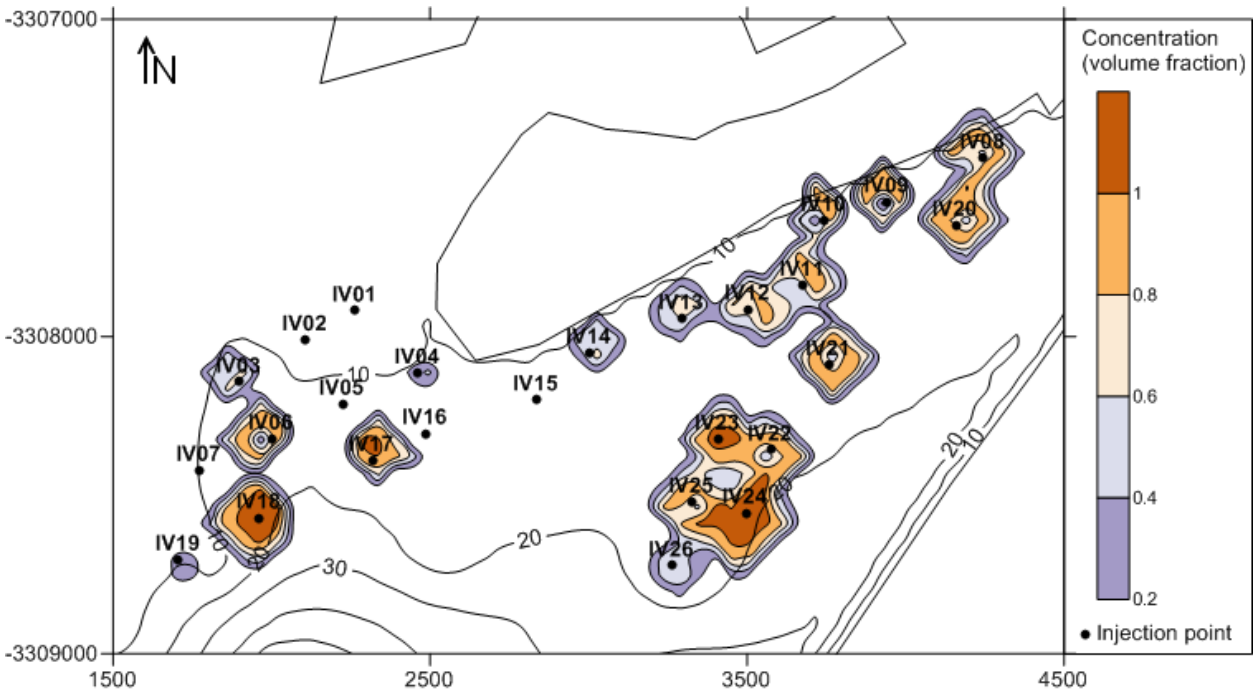

G9: Map illustrating the simulation results for the remediation of non-aqueous phase PCE with diluted surfactant SDS at a low infiltration rate in the top layer.

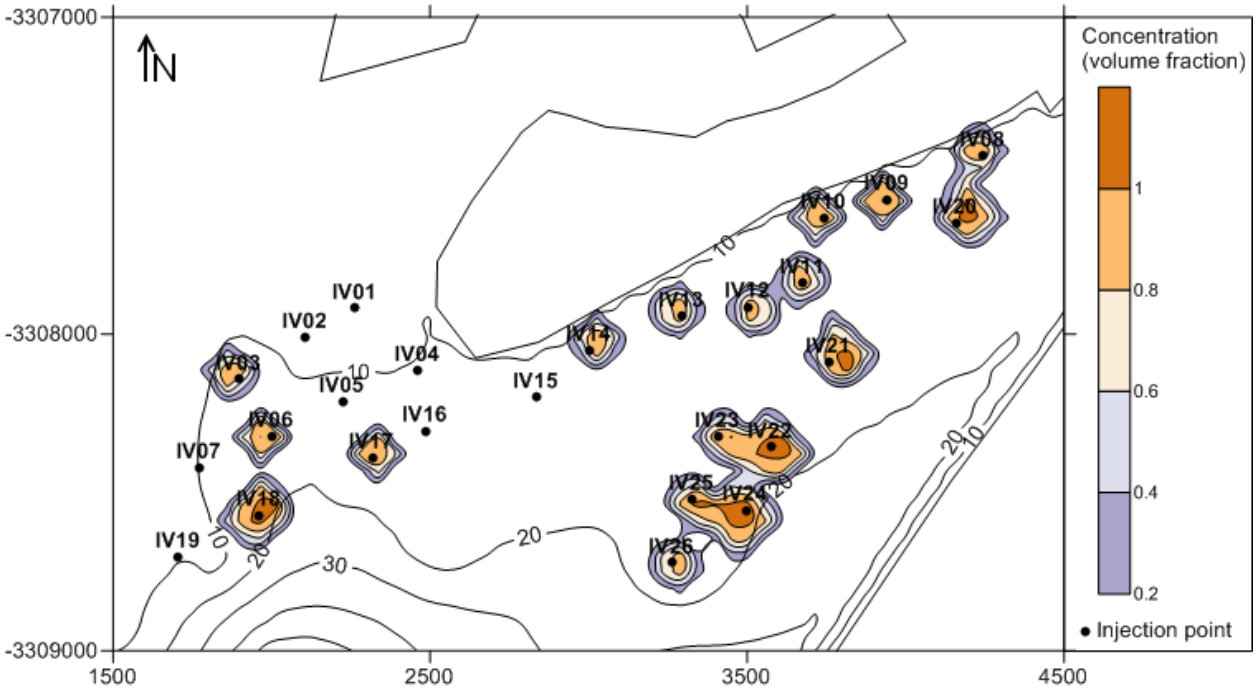

G10: Map illustrating the simulation results for the remediation of non-aqueous phase PCE with diluted surfactant SDS at a low infiltration rate in the bottom layer.

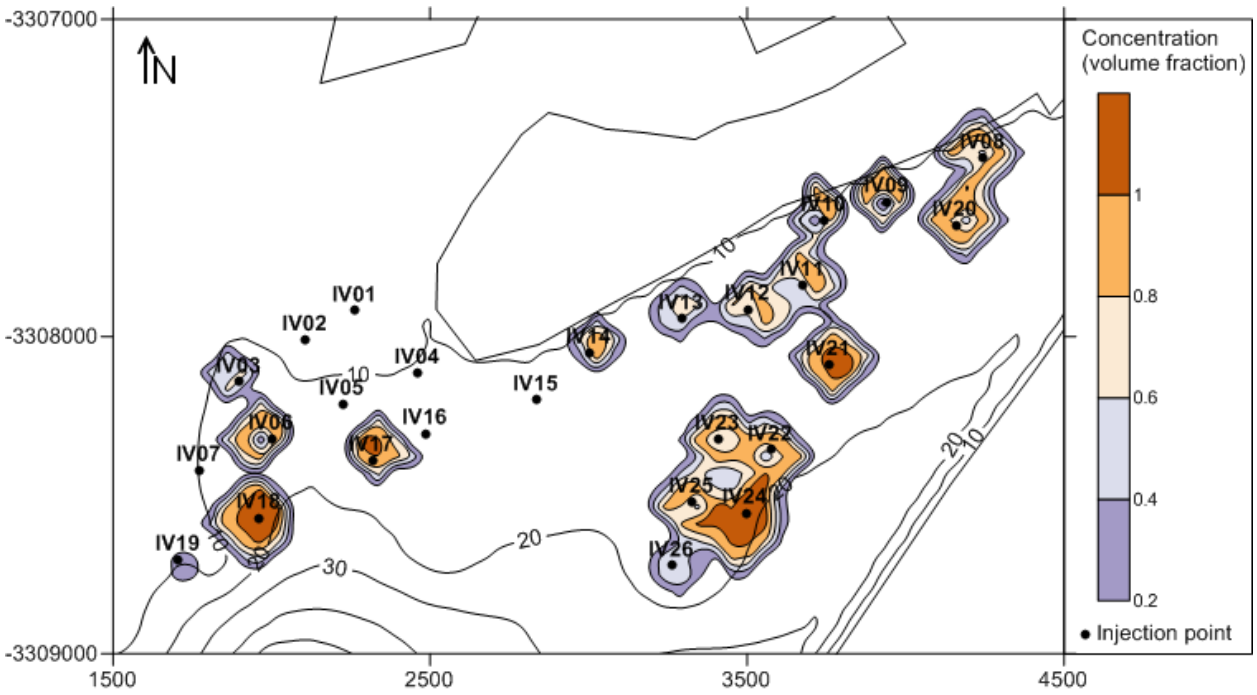

G11: Map illustrating the simulation results for the remediation of non-aqueous phase PCE with undiluted surfactant SDS at a low infiltration rate in the top layer.

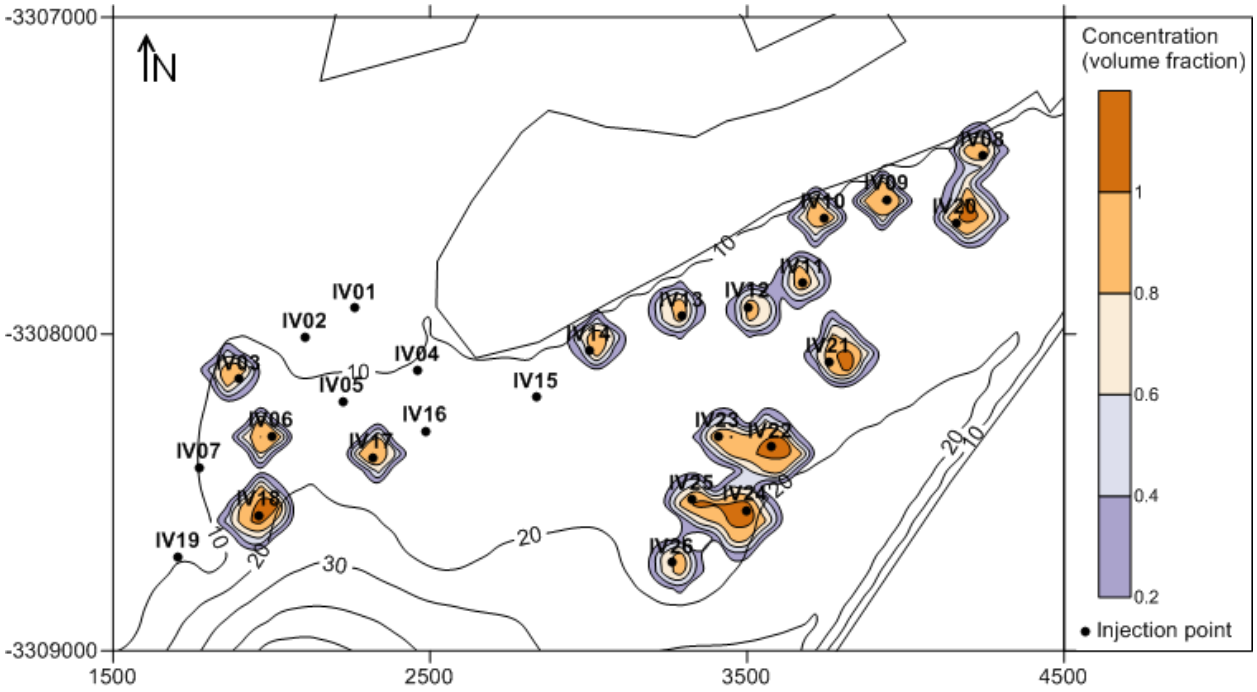

G12: Map illustrating the simulation results for the remediation of non-aqueous phase PCE with undiluted surfactant SDS at a low infiltration rate in the bottom layer.

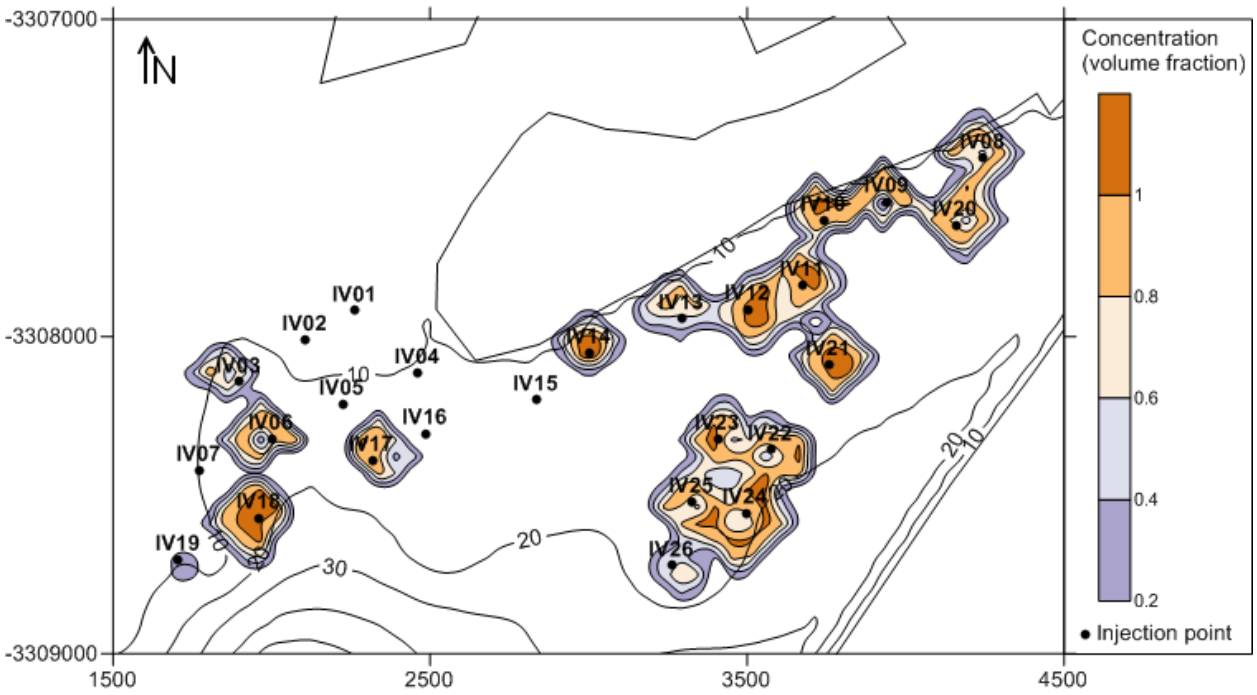

G13: Map illustrating the simulation results for the remediation of non-aqueous phase PCE with undiluted surfactant SDS at a high infiltration rate in the top layer.

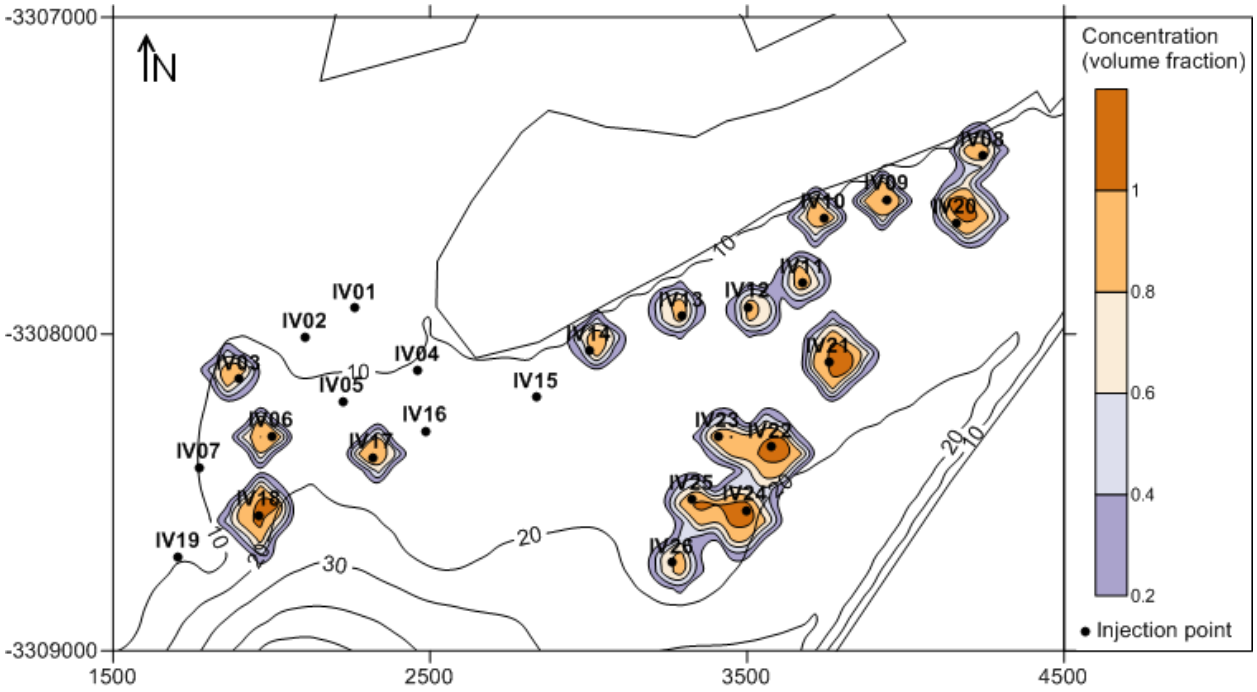

G14: Map illustrating the simulation results for the remediation of non-aqueous phase PCE with undiluted surfactant SDS at a high infiltration rate in the bottom layer.

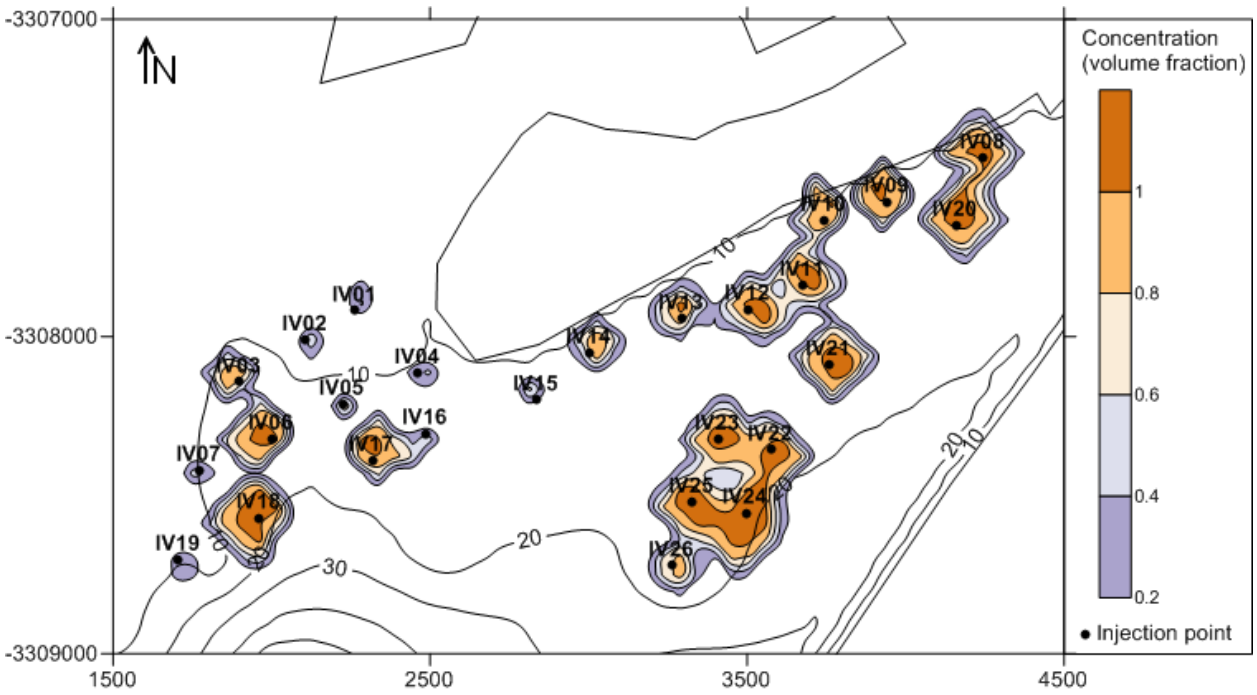

G15: Map illustrating the simulation results for the remediation of non-aqueous phase PCE with diluted polymer xanthan gum at a low infiltration rate in the top layer.

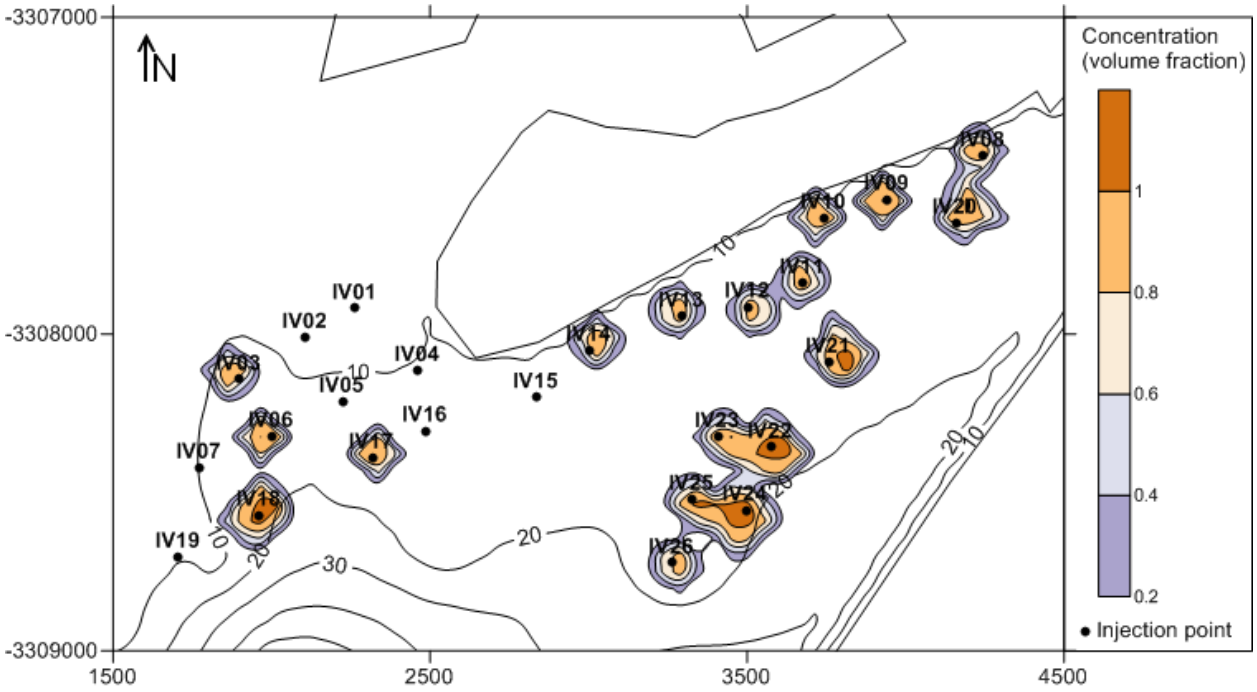

G16: Map illustrating the simulation results for the remediation of non-aqueous phase PCE with diluted polymer xanthan gum at a low infiltration rate in the bottom layer.

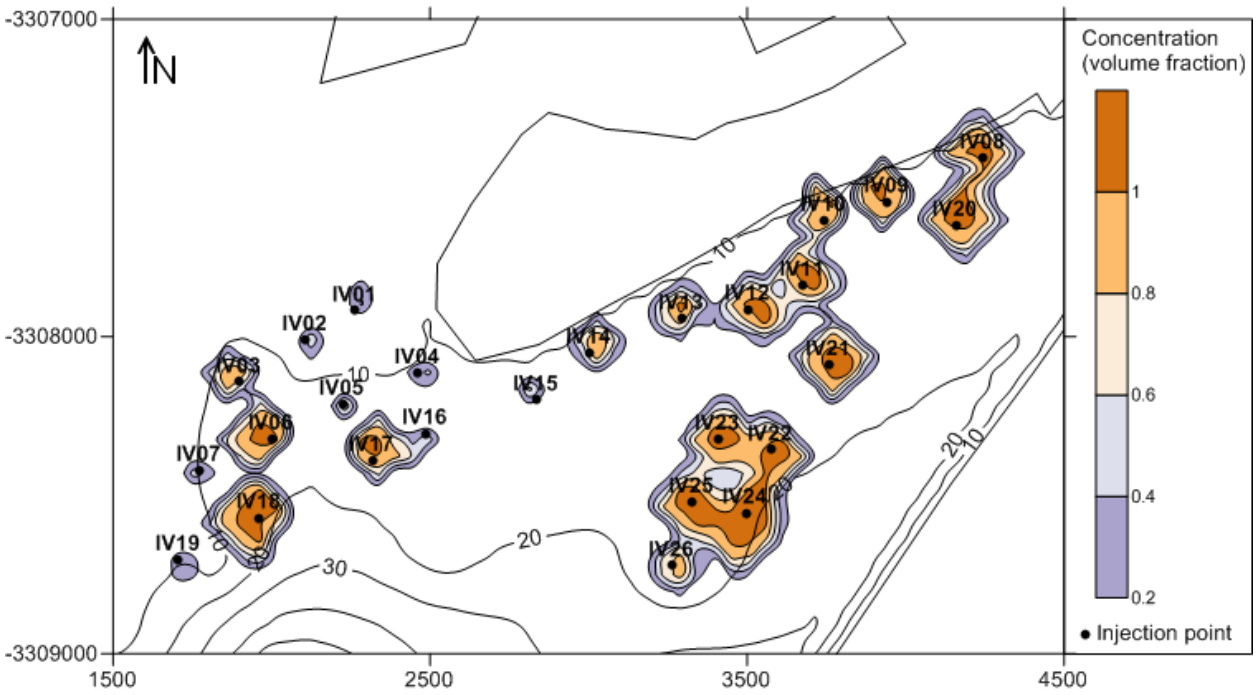

G17: Map illustrating the simulation results for the remediation of non-aqueous phase PCE with undiluted polymer xanthan gum at a low infiltration rate in the top layer.

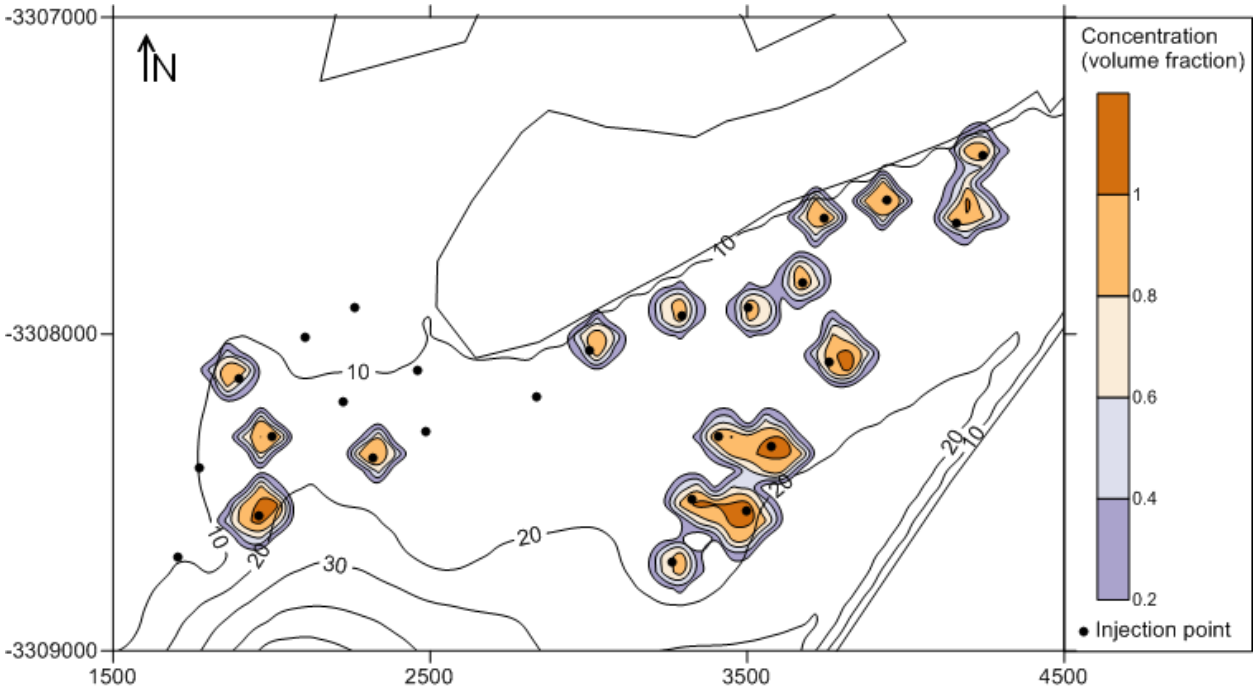

G18: Map illustrating the simulation results for the remediation of non-aqueous phase PCE with undiluted polymer xanthan gum at a low infiltration rate in the bottom layer.

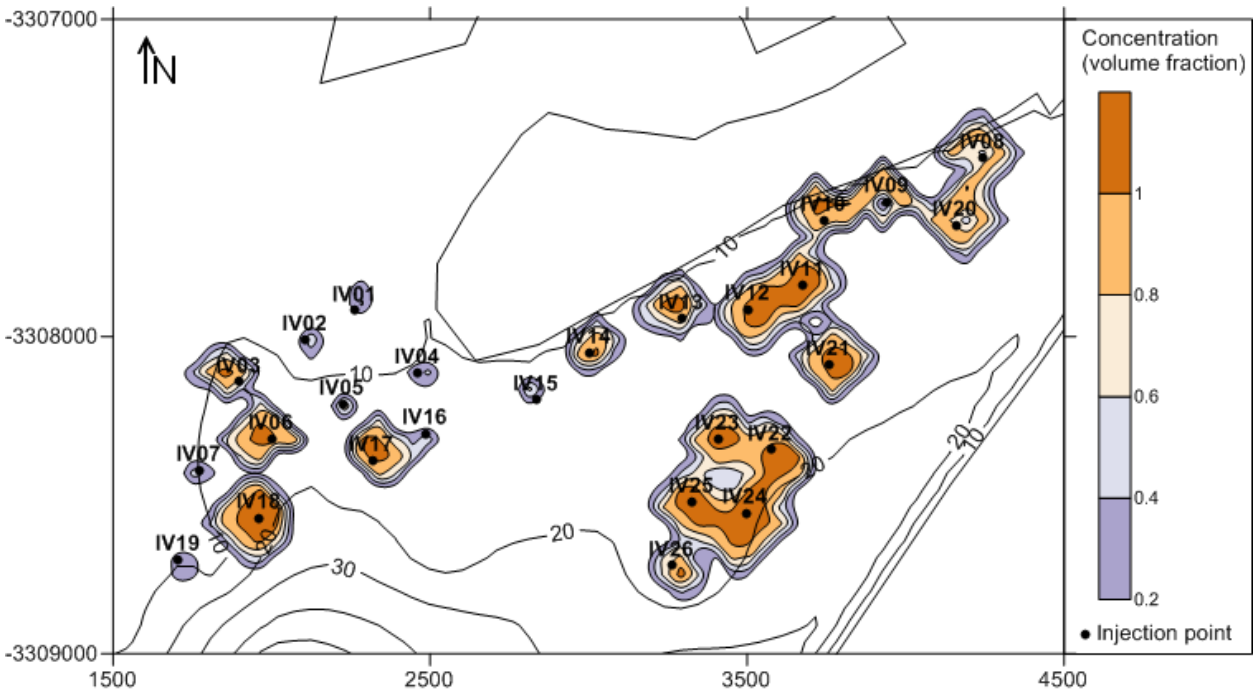

G19: Map illustrating the simulation results for the remediation of non-aqueous phase PCE with undiluted polymer xanthan gum at a high infiltration rate in the top layer.

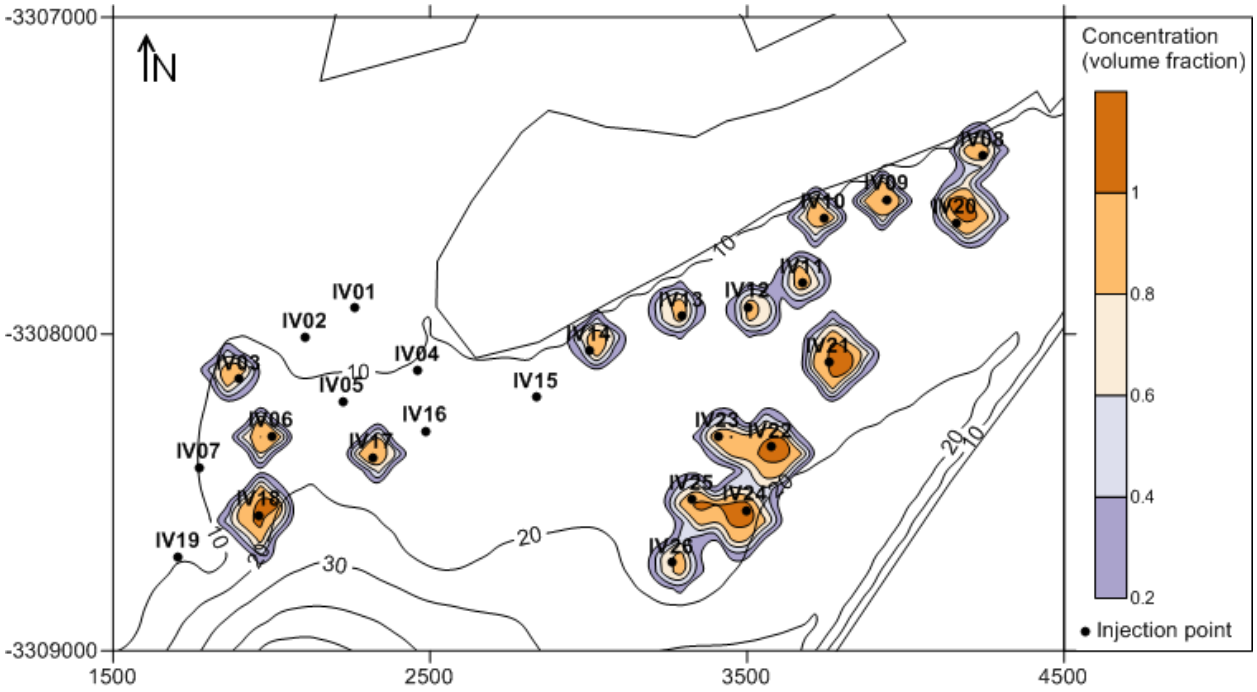

F20: Map illustrating the simulation results for the remediation of non-aqueous phase PCE with undiluted polymer xanthan gum at a high infiltration rate in the bottom layer.

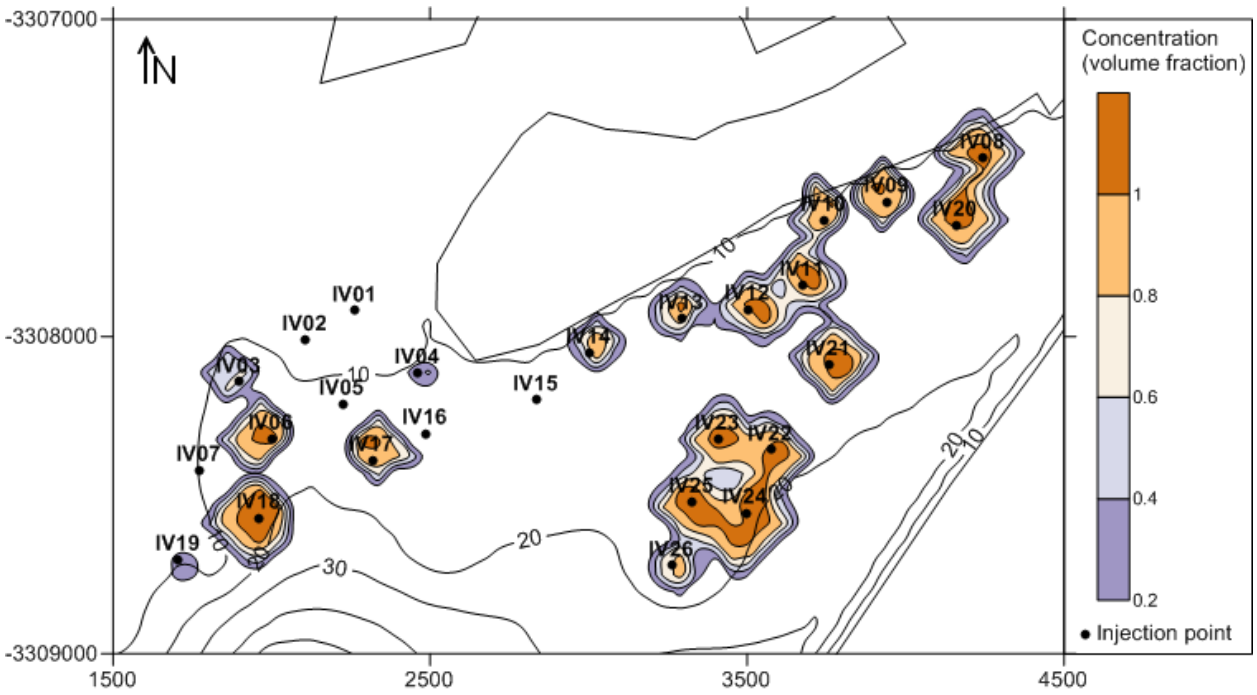

G21: Map illustrating the simulation results for the remediation of non-aqueous phase PCE with diluted surfactant SDS and ethanol at a low infiltration rate in the top layer.

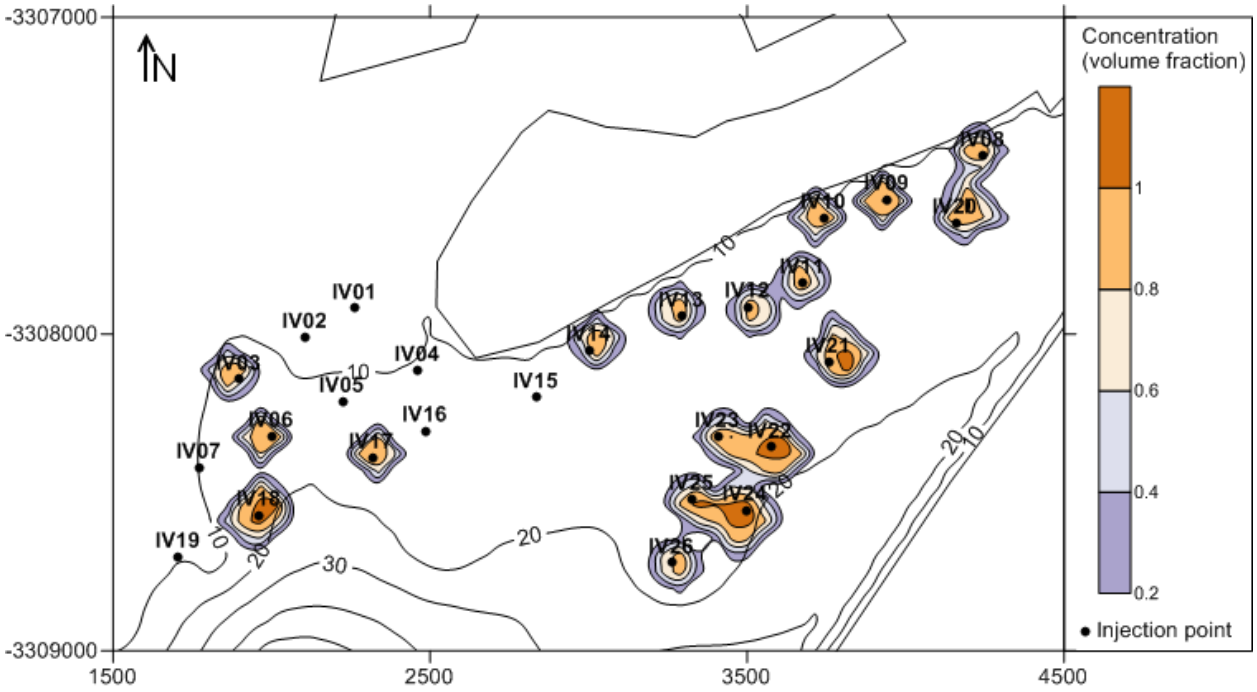

G22: Map illustrating the simulation results for the remediation of non-aqueous phase PCE with diluted surfactant SDS and ethanol at a low infiltration rate in the bottom layer.

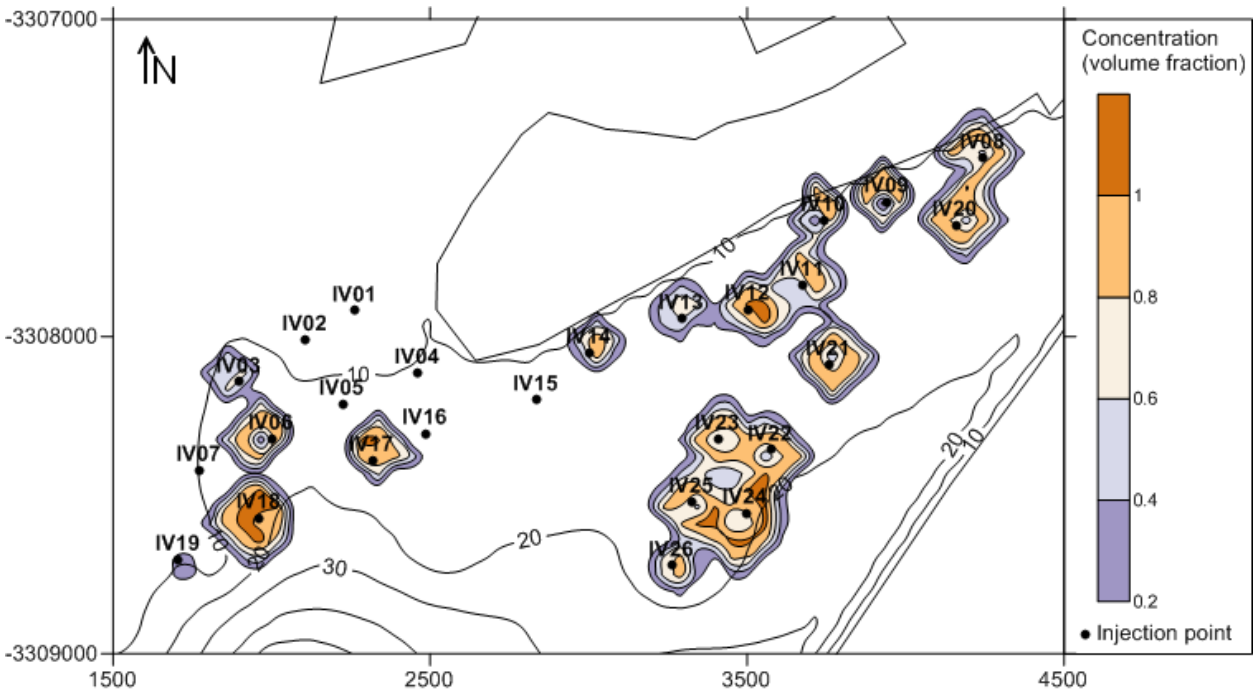

G23: Map illustrating the simulation results for the remediation of non-aqueous phase PCE with undiluted surfactant SDS and ethanol at a low infiltration rate in the top layer.

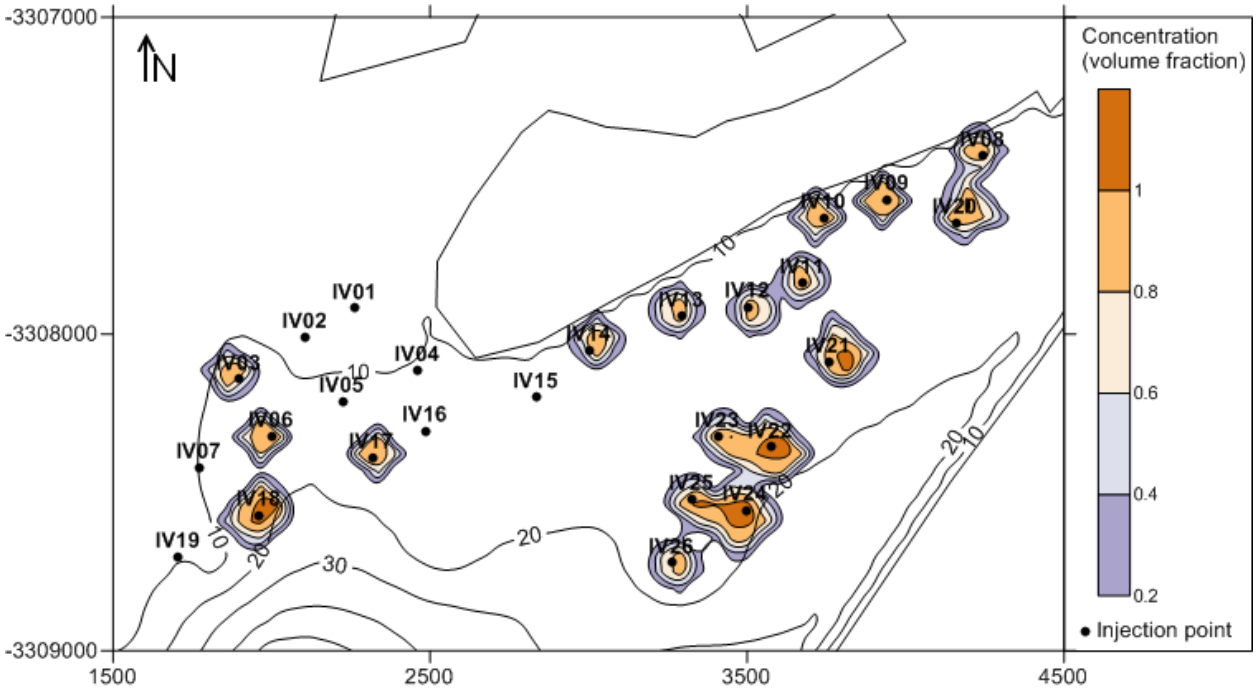

G24: Map illustrating the simulation results for the remediation of non-aqueous phase PCE with undiluted surfactant SDS and ethanol at a low infiltration rate in the bottom layer.

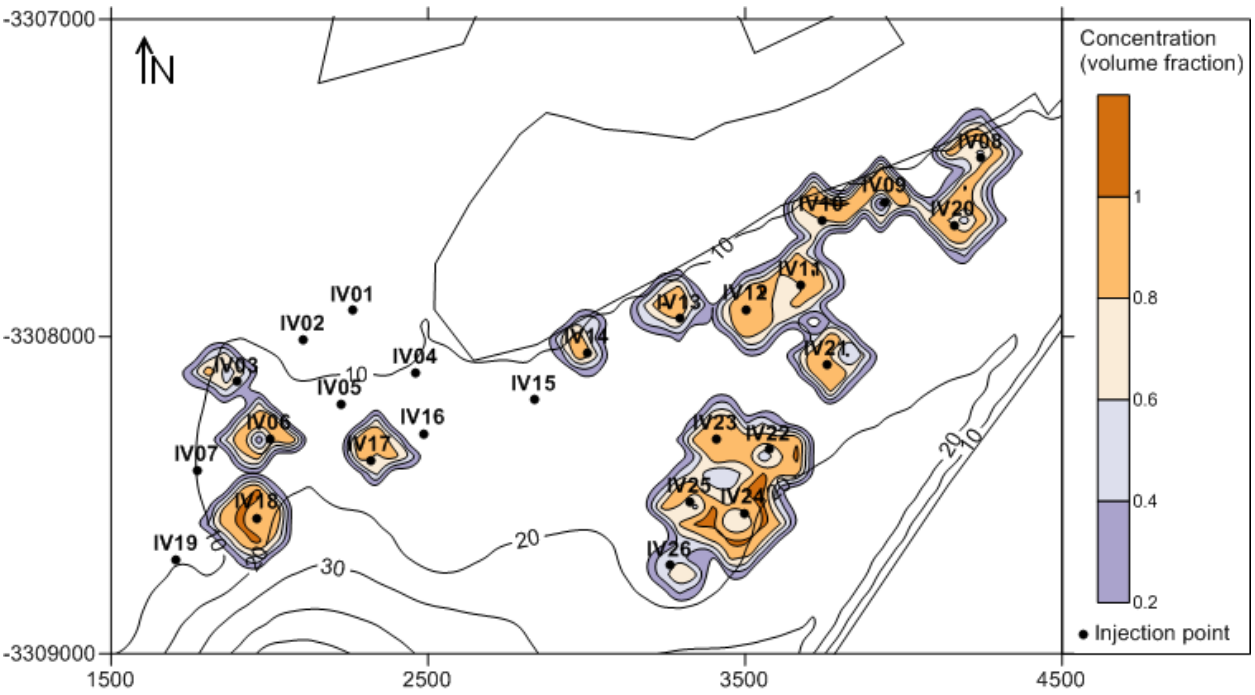

G25: Map illustrating the simulation results for the remediation of non-aqueous phase PCE with undiluted surfactant SDS and ethanol at a high infiltration rate in the top layer.

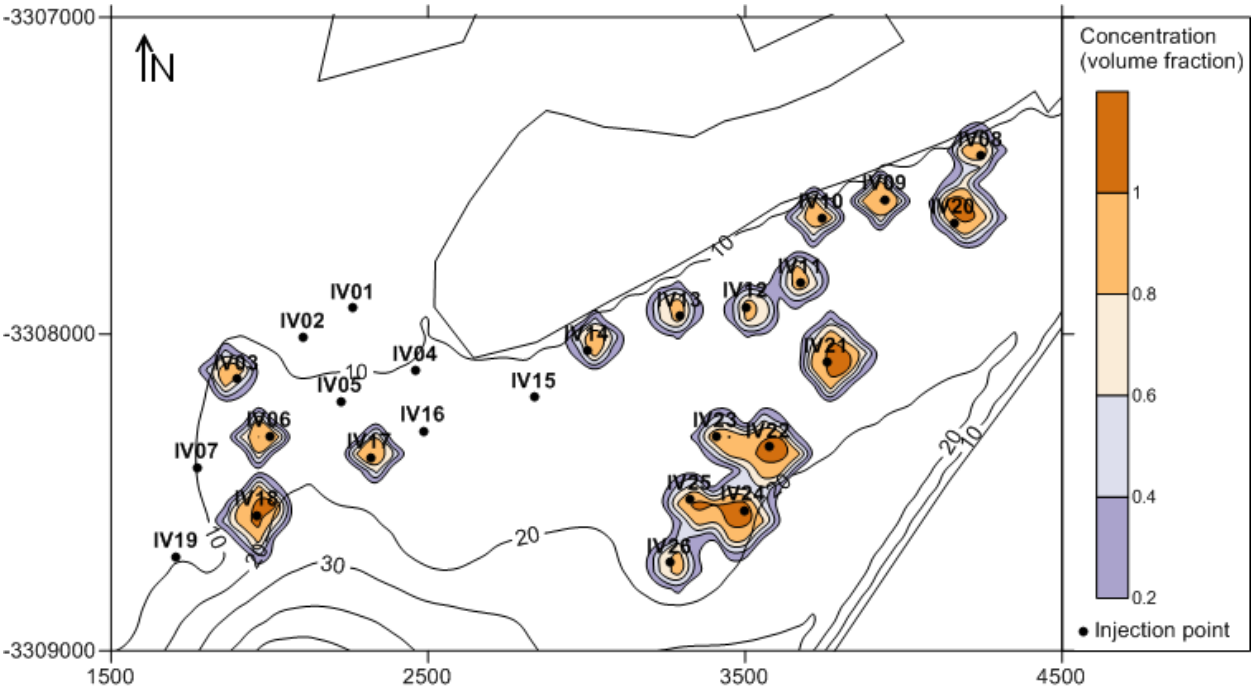

G26: Map illustrating the simulation results for the remediation of non-aqueous phase PCE with undiluted surfactant SDS and ethanol at a high infiltration rate in the bottom layer.

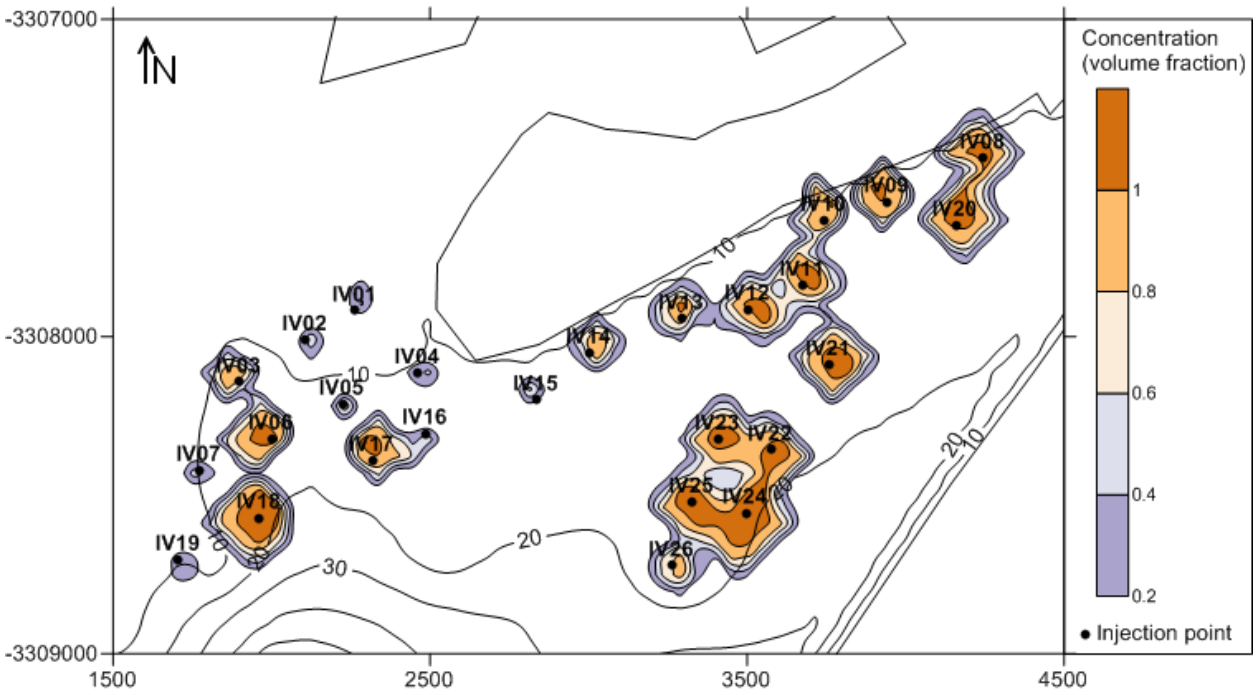

G27: Map illustrating the simulation results for the remediation of non-aqueous phase PCE with diluted ethanol at a low infiltration rate in the top layer.

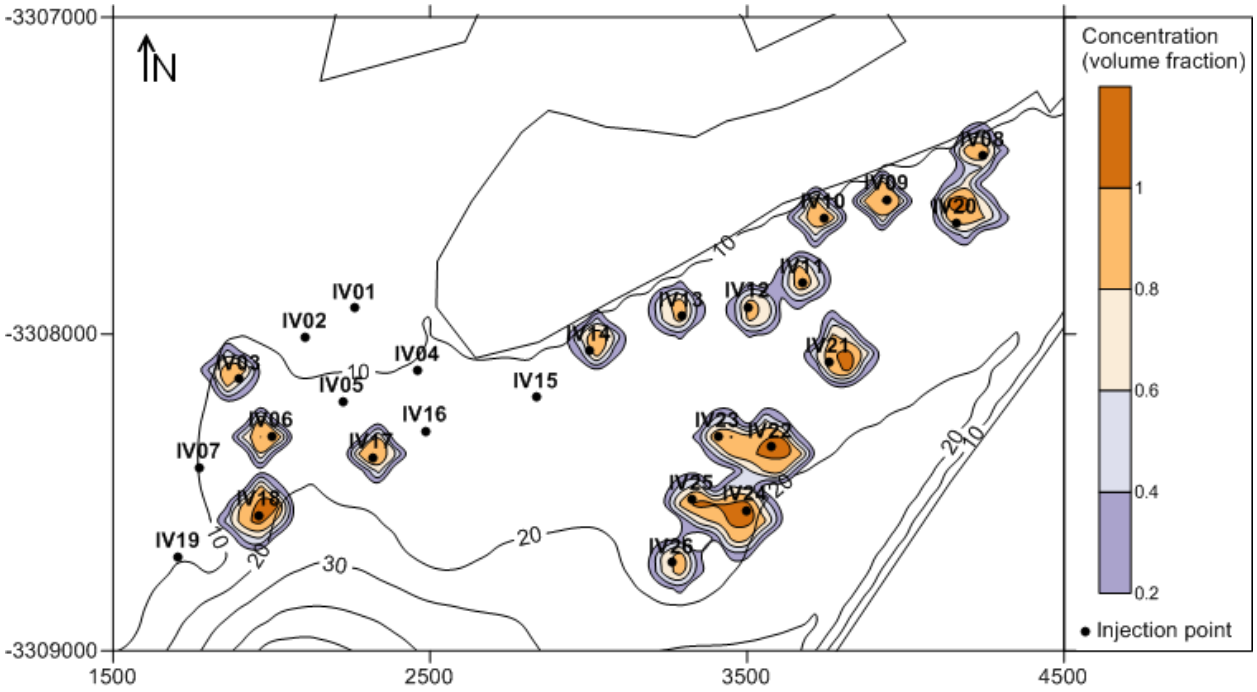

G28: Map illustrating the simulation results for the remediation of non-aqueous phase PCE with diluted ethanol at a low infiltration rate in the bottom layer.

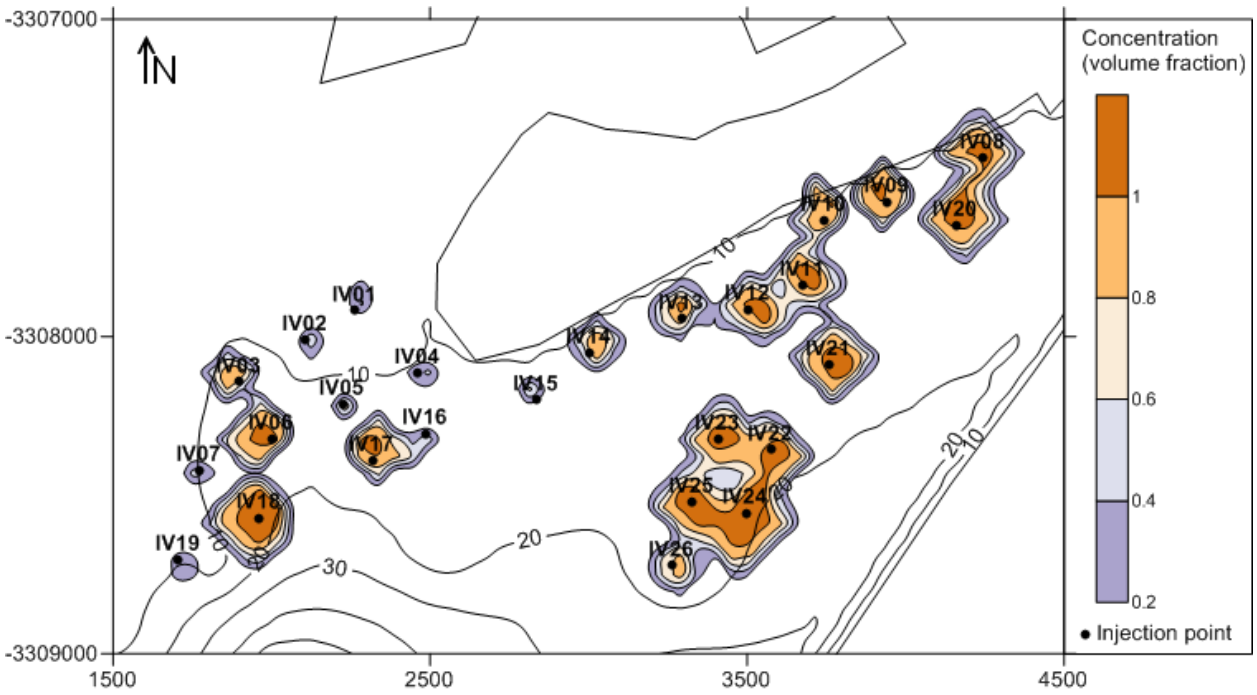

G29: Map illustrating the simulation results for the remediation of non-aqueous phase PCE with undiluted ethanol at a low infiltration rate in the top layer.

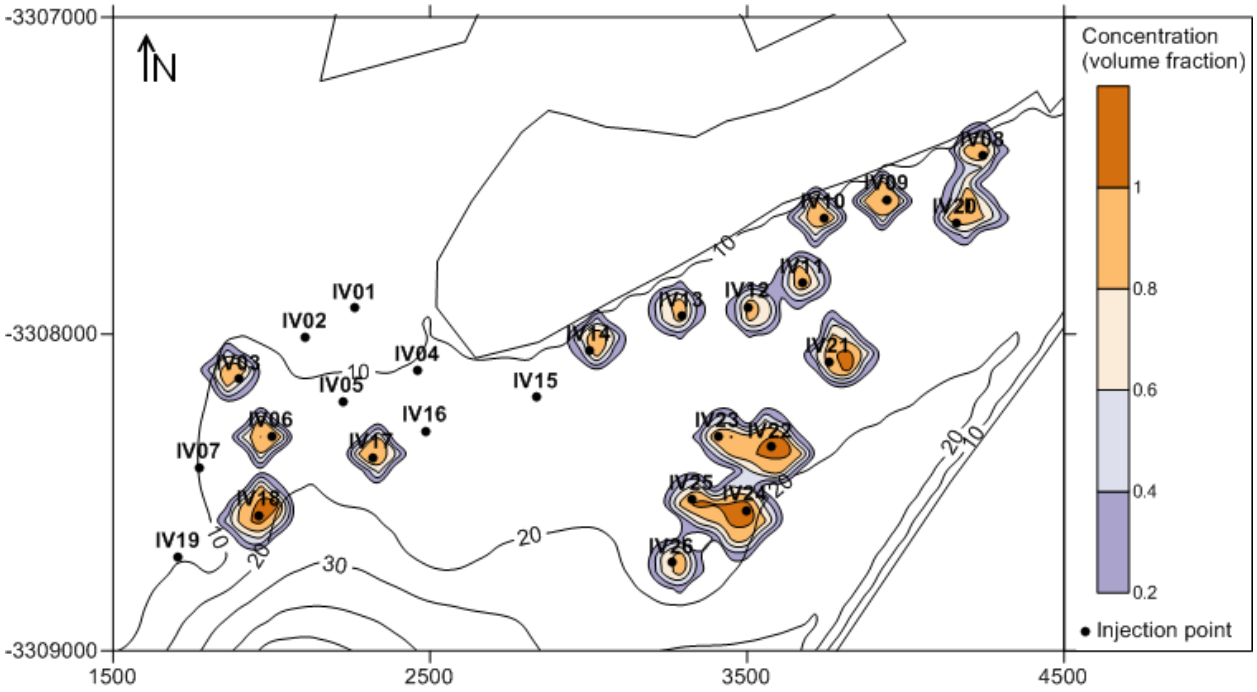

G30: Map illustrating the simulation results for the remediation of non-aqueous phase PCE with undiluted ethanol at a low infiltration rate in the bottom layer.

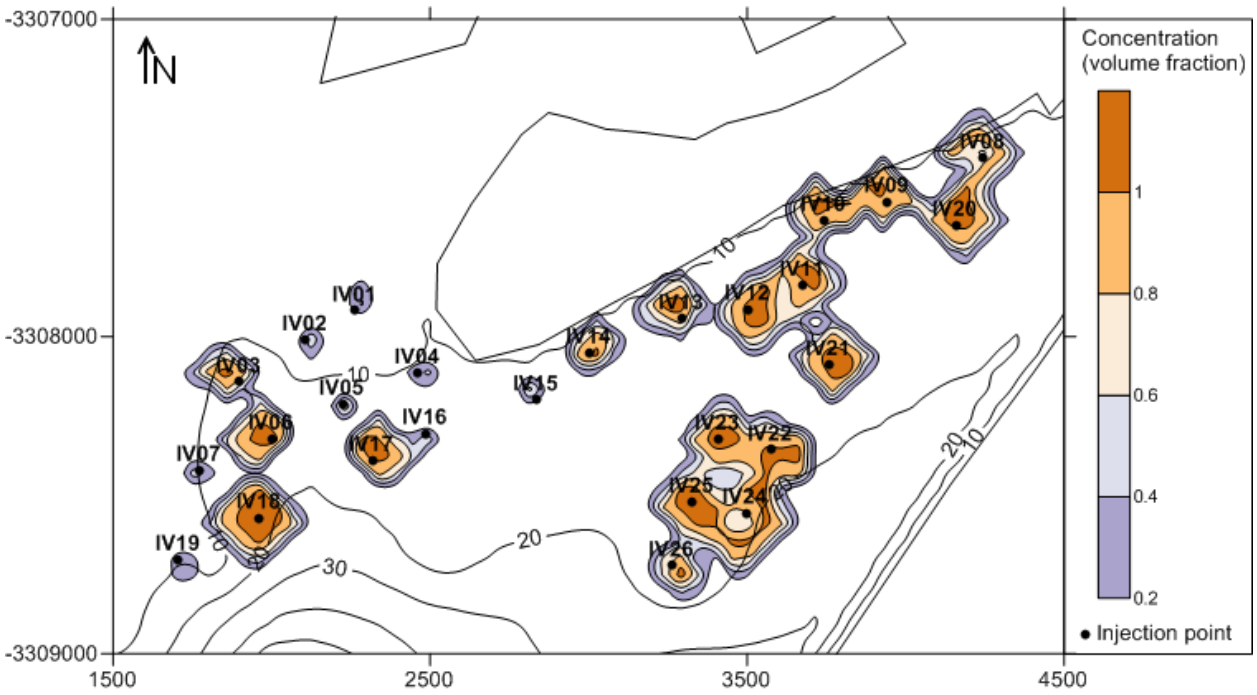

G31: Map illustrating the simulation results for the remediation of non-aqueous phase PCE with undiluted ethanol at a high infiltration rate in the top layer.

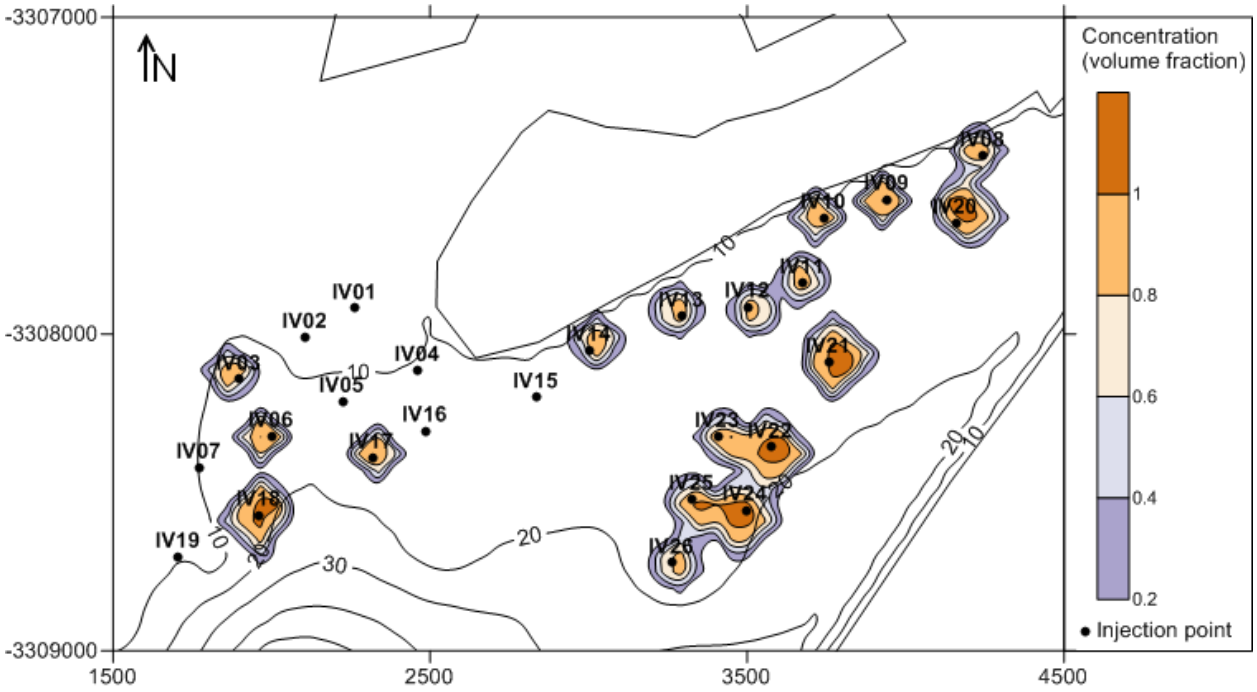

G32: Map illustrating the simulation results for the remediation of non-aqueous phase PCE with undiluted ethanol at a high infiltration rate in the bottom layer.

Appendix H: Appendix G: Maps illustrating the simulation results for the infiltration and migration of aqueous PCE

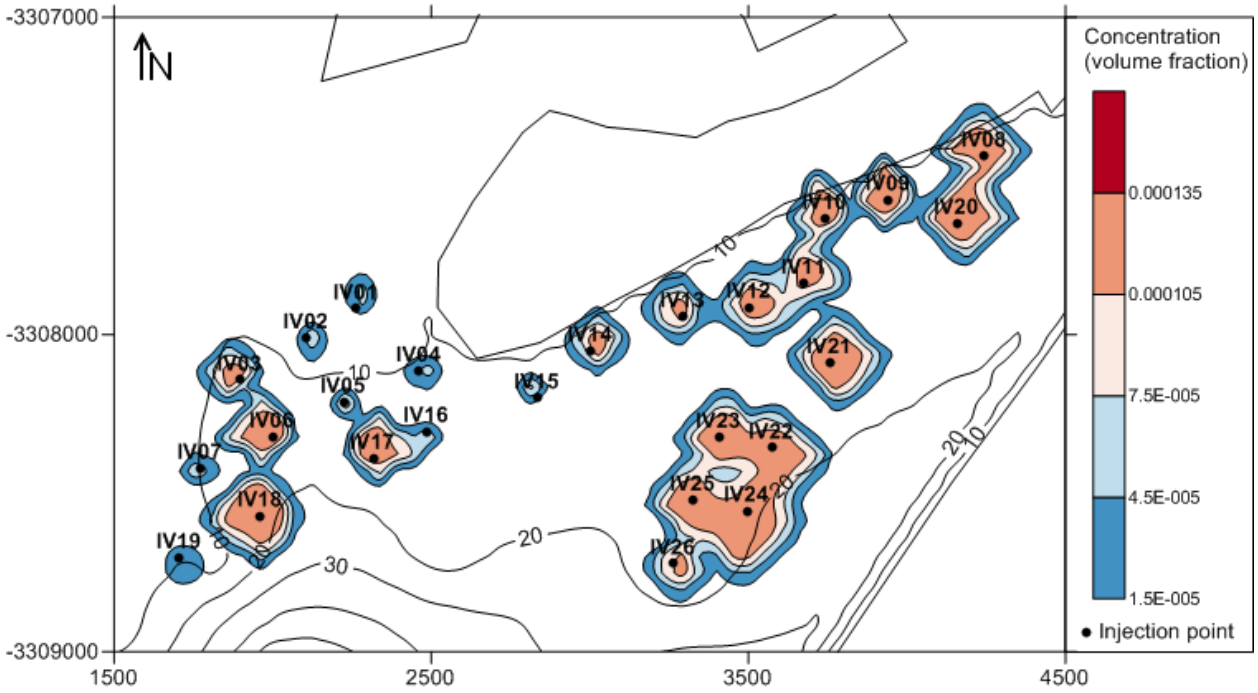

H1: Map illustrating the simulation results for the infiltration and migration of aqueous phase PCE in the top layer.

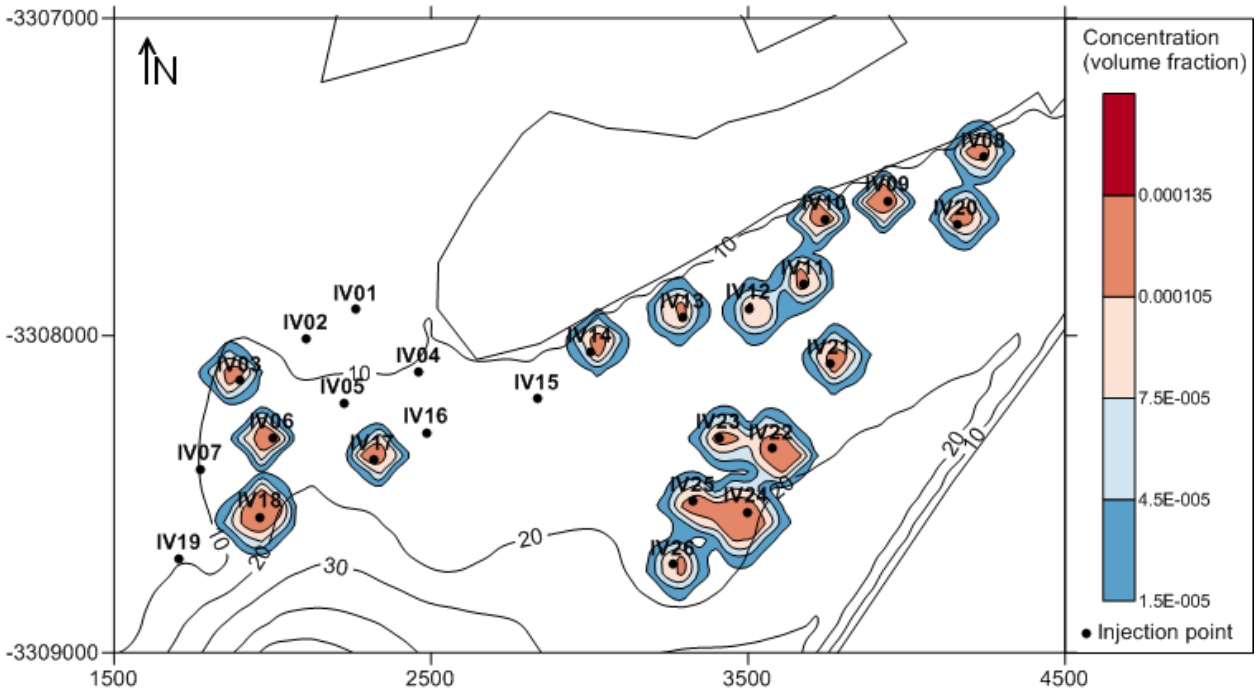

H2: Map illustrating the simulation results for the infiltration and migration of aqueous phase PCE in the bottom layer.

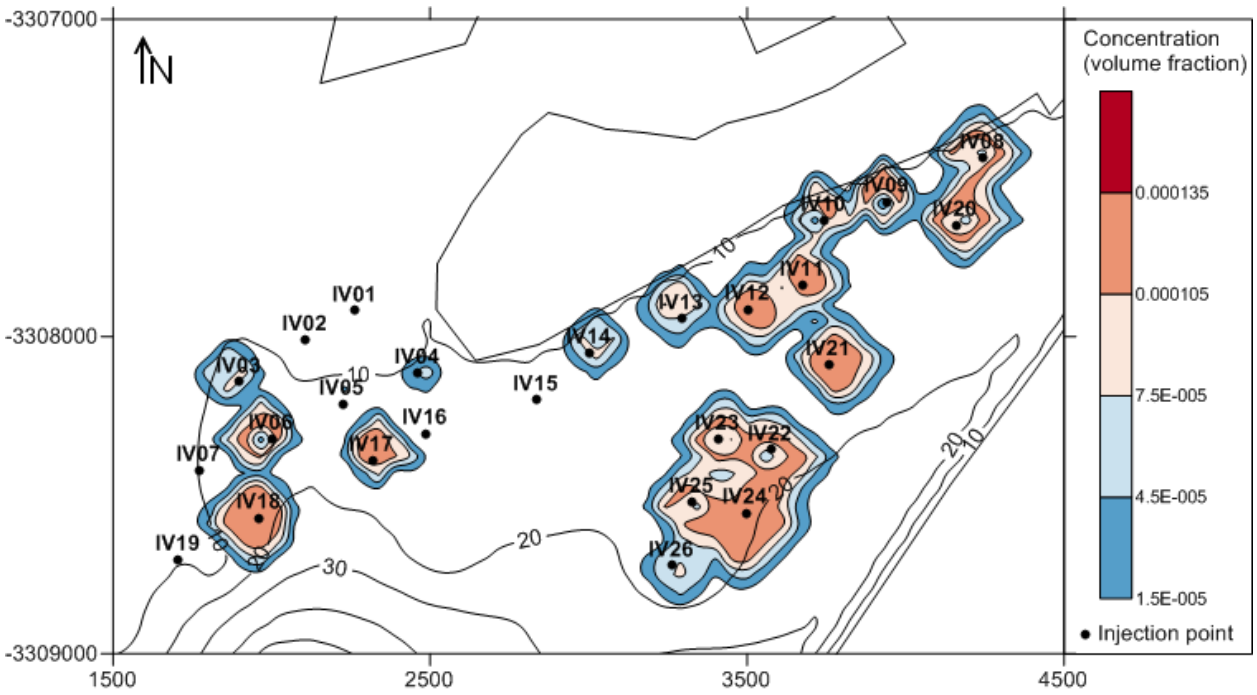

H3: Map illustrating the simulation results for the remediation of aqueous phase PCE with diluted surfactant SDS and polymer xanthan gum at a low infiltration rate in the top layer.

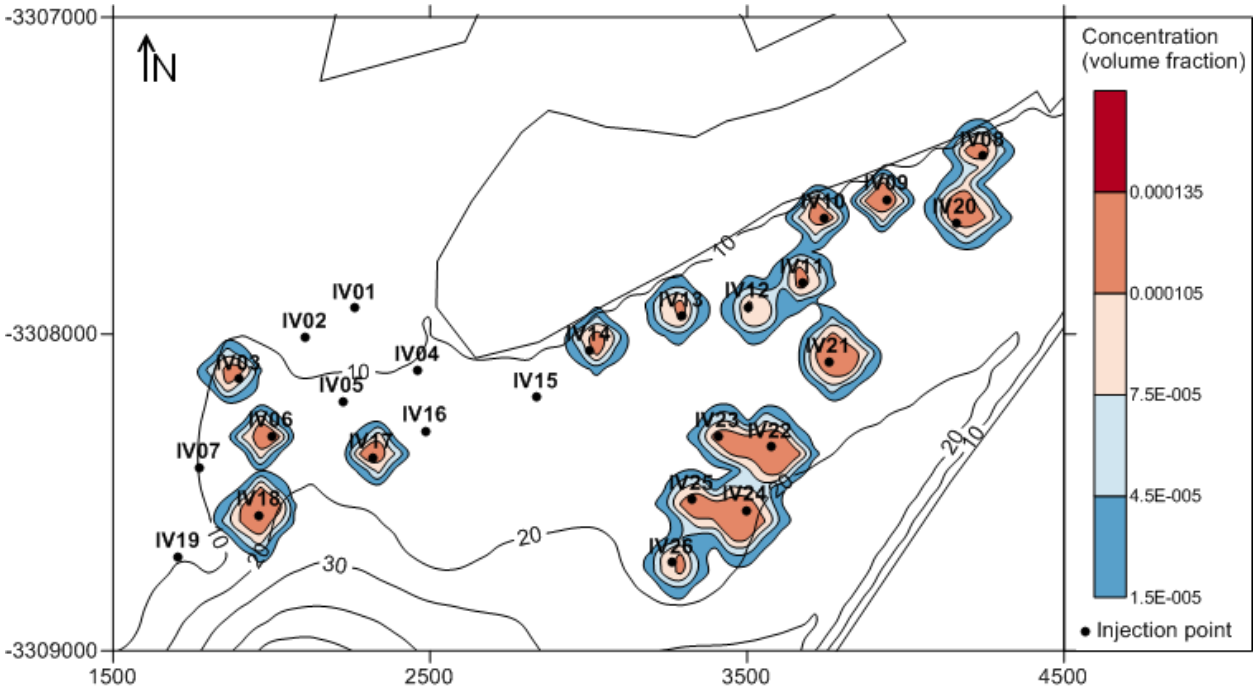

H4: Map illustrating the simulation results for the remediation of aqueous phase PCE with diluted surfactant SDS and polymer xanthan gum at a low infiltration rate in the bottom layer.

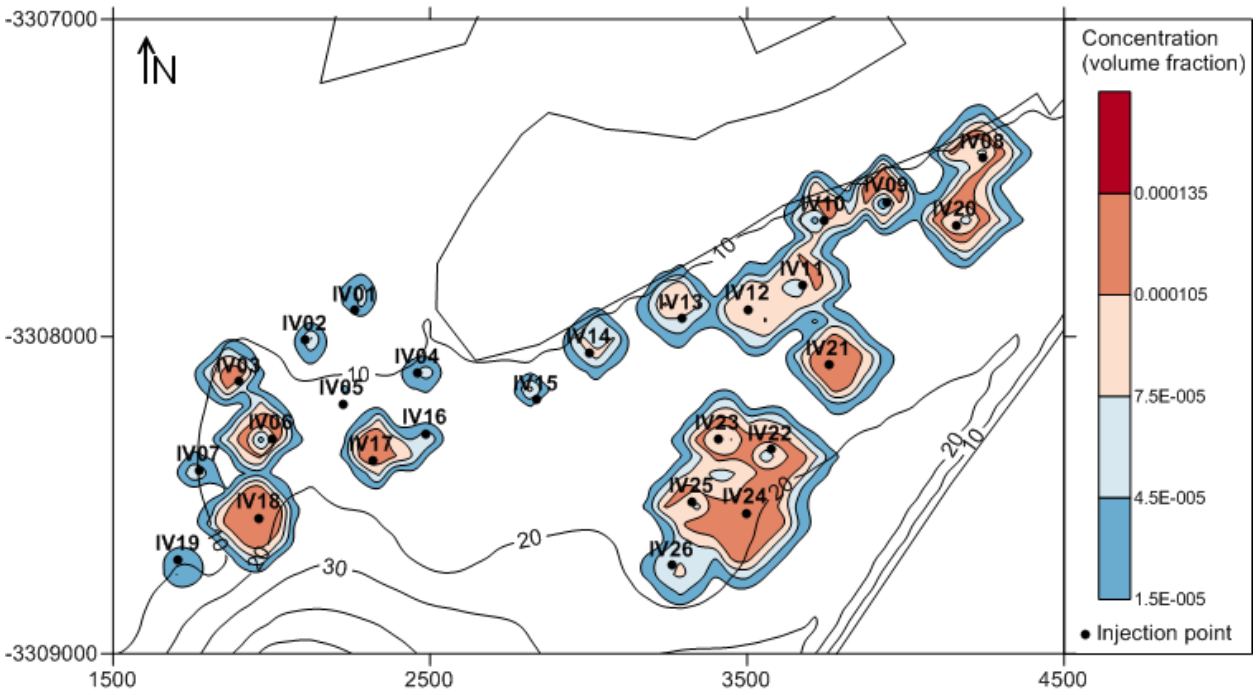

H5: Map illustrating the simulation results for the remediation of aqueous phase PCE with undiluted surfactant SDS and polymer xanthan gum at a low infiltration rate in the top layer.

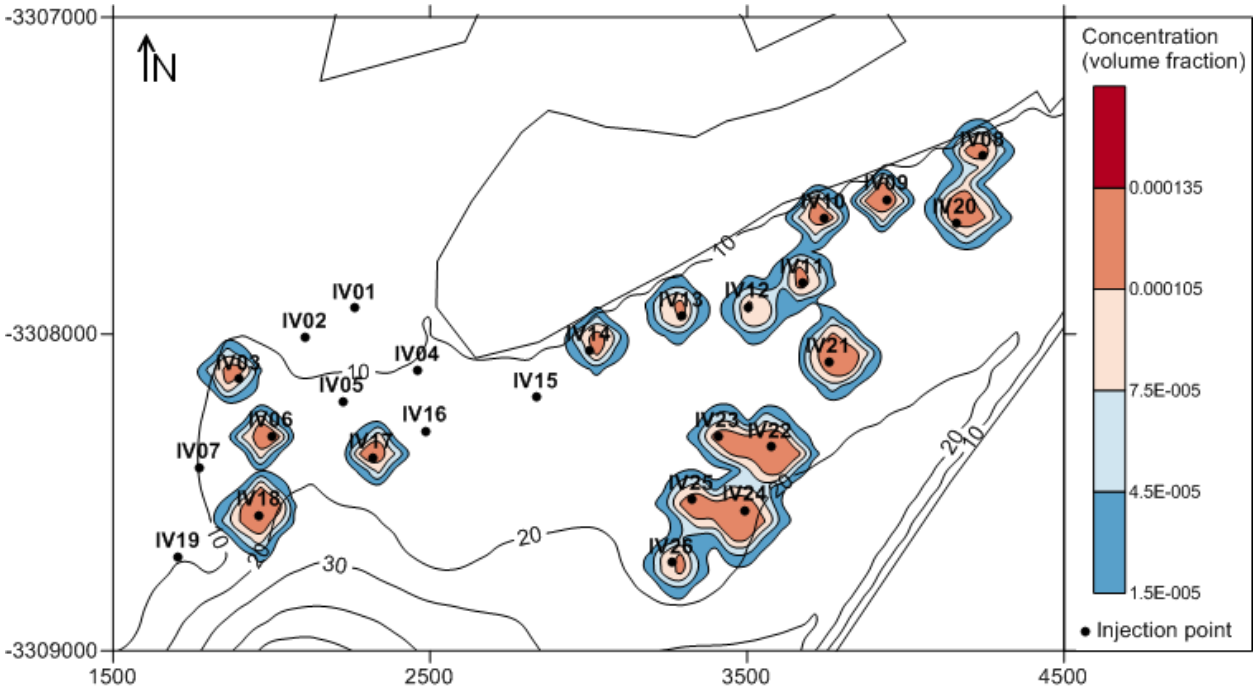

H6: Map illustrating the simulation results for the remediation of aqueous phase PCE with undiluted surfactant SDS and polymer xanthan gum at a low infiltration rate in the bottom layer.

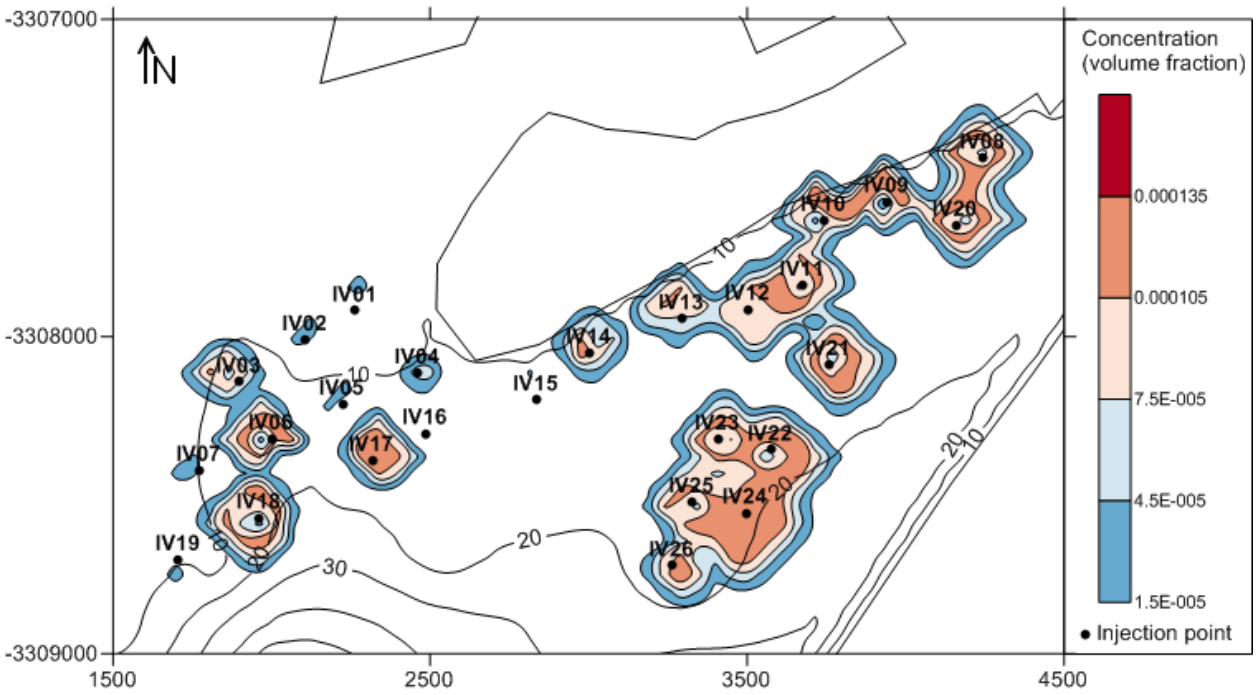

H7: Map illustrating the simulation results for the remediation of aqueous phase PCE with undiluted surfactant SDS and polymer xanthan gum at a high infiltration rate in the top layer.

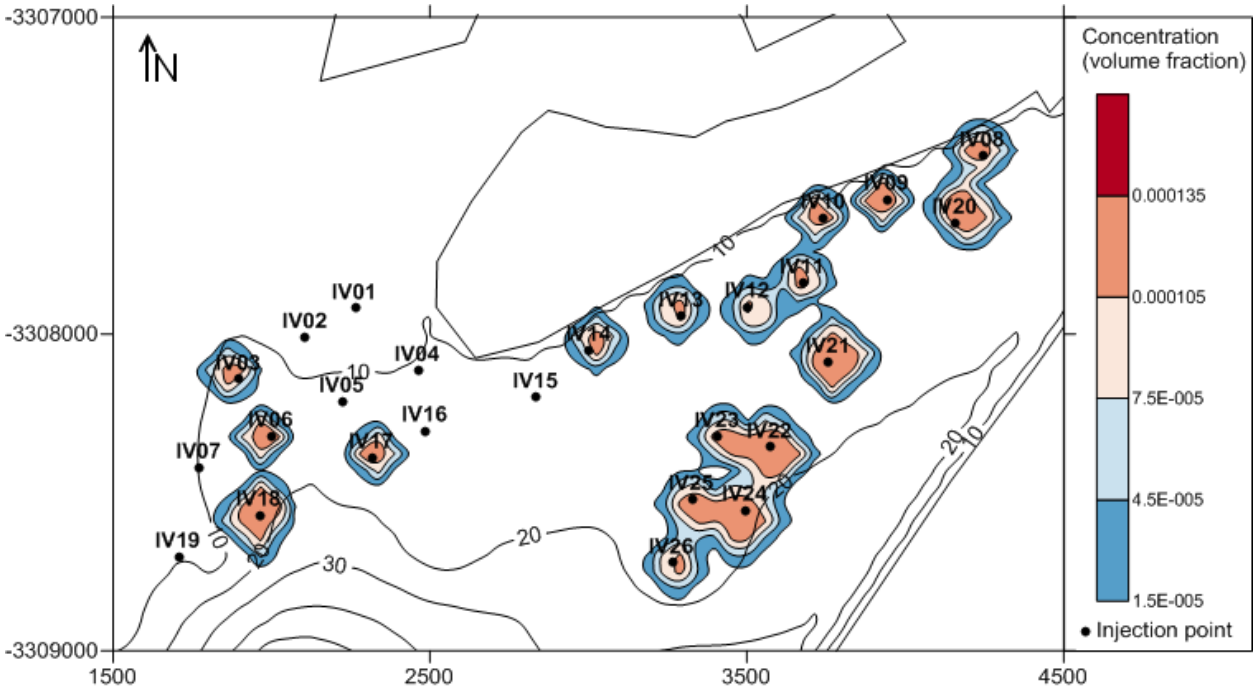

H8: Map illustrating the simulation results for the remediation of aqueous phase PCE with undiluted surfactant SDS and polymer xanthan gum at a high infiltration rate in the bottom layer.

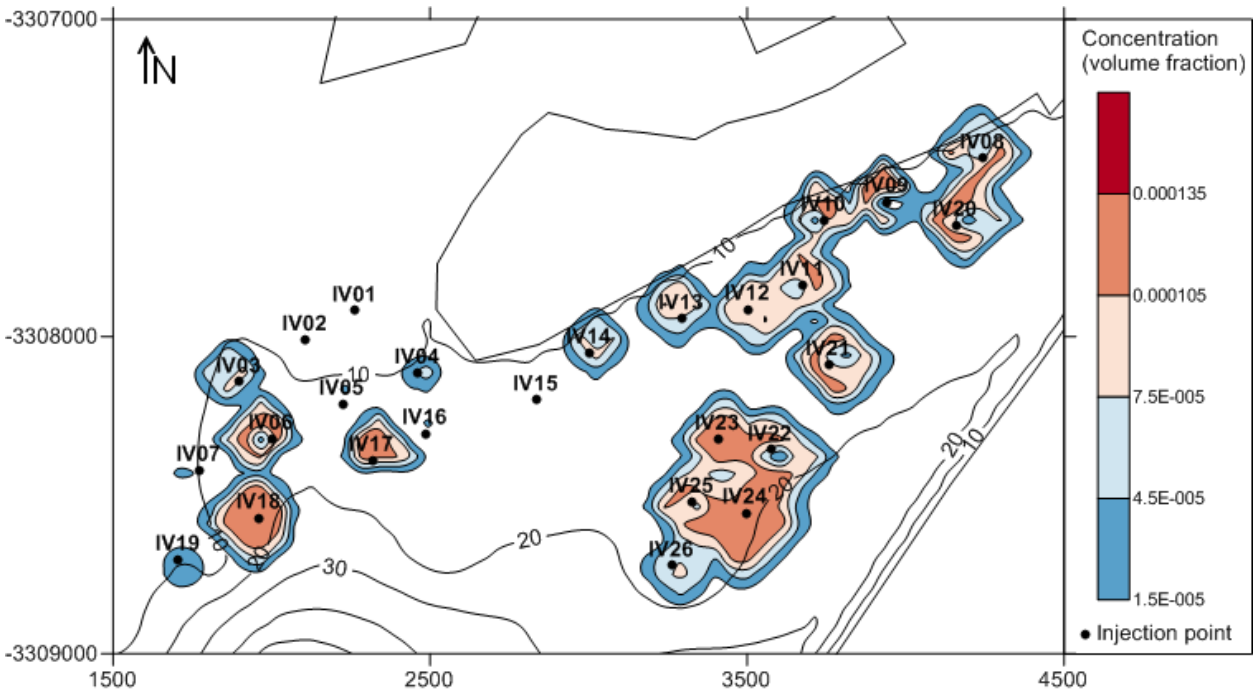

H9: Map illustrating the simulation results for the remediation of aqueous phase PCE with diluted surfactant SDS at a low infiltration rate in the top layer.

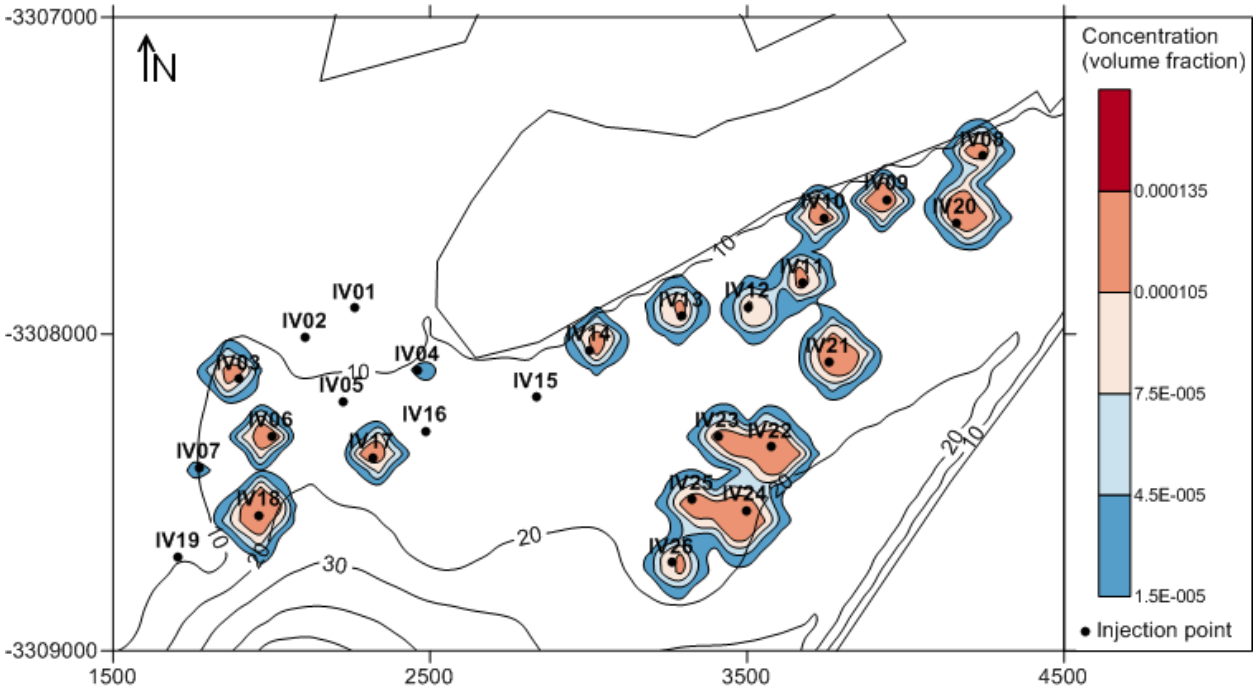

H10: Map illustrating the simulation results for the remediation of aqueous phase PCE with diluted surfactant SDS at a low infiltration rate in the bottom layer.

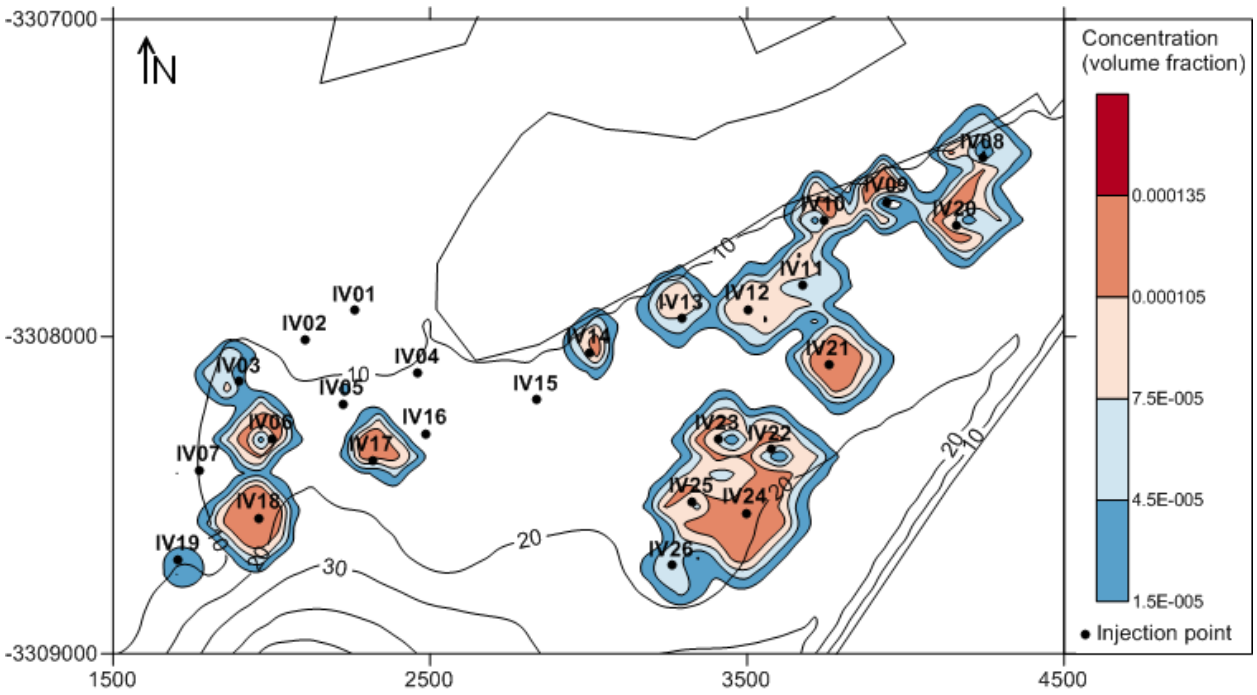

H11: Map illustrating the simulation results for the remediation of aqueous phase PCE with undiluted surfactant SDS at a low infiltration rate in the top layer.

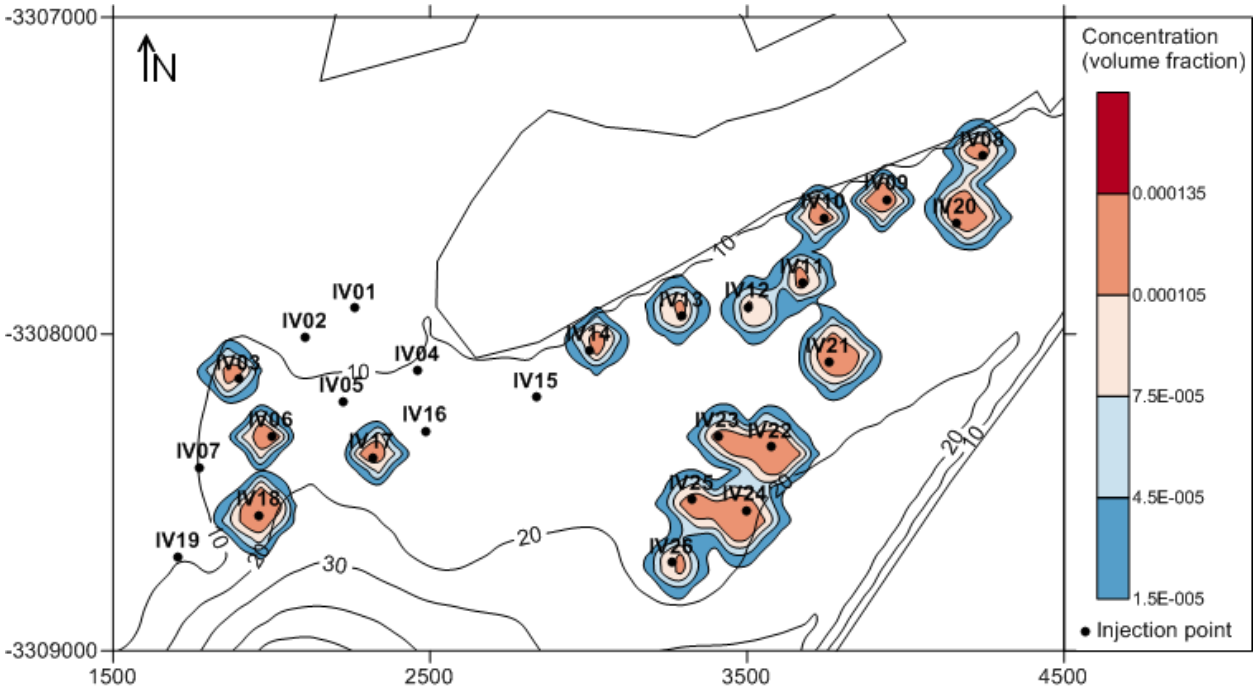

H12: Map illustrating the simulation results for the remediation of aqueous phase PCE with undiluted surfactant SDS at a low infiltration rate in the bottom layer.

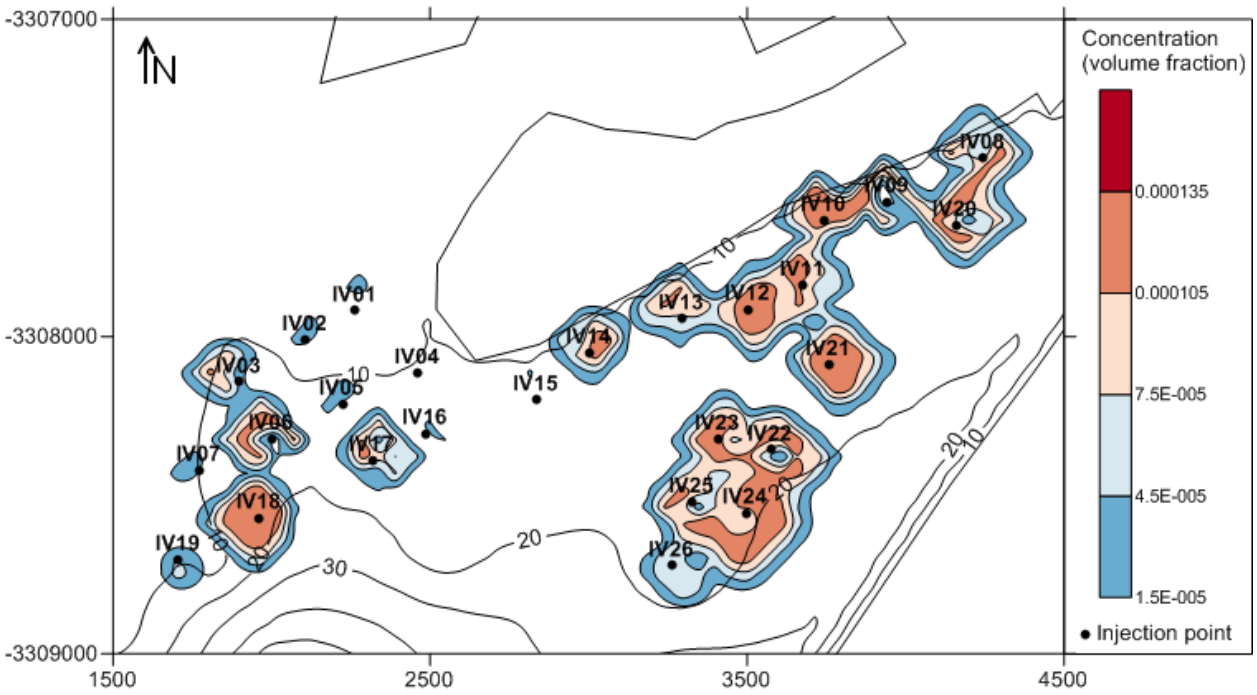

H13: Map illustrating the simulation results for the remediation of aqueous phase PCE with undiluted surfactant SDS at a high infiltration rate in the top layer.

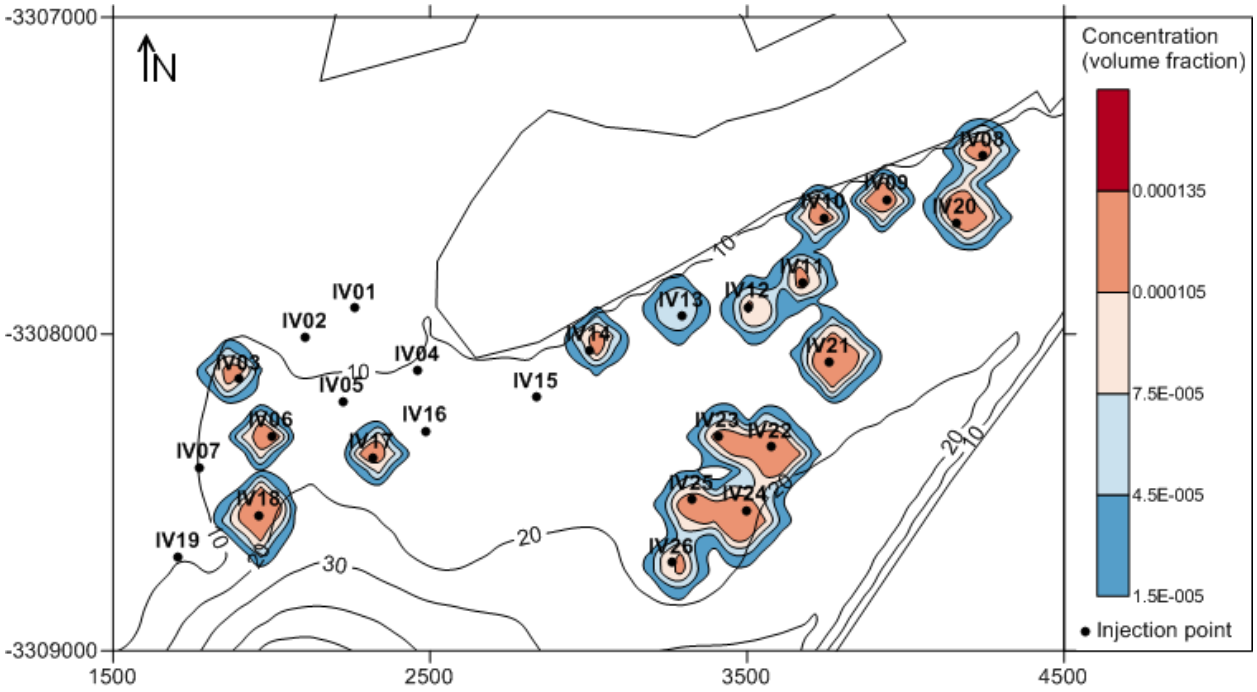

H14: Map illustrating the simulation results for the remediation of aqueous phase PCE with undiluted surfactant SDS at a high infiltration rate in the bottom layer.

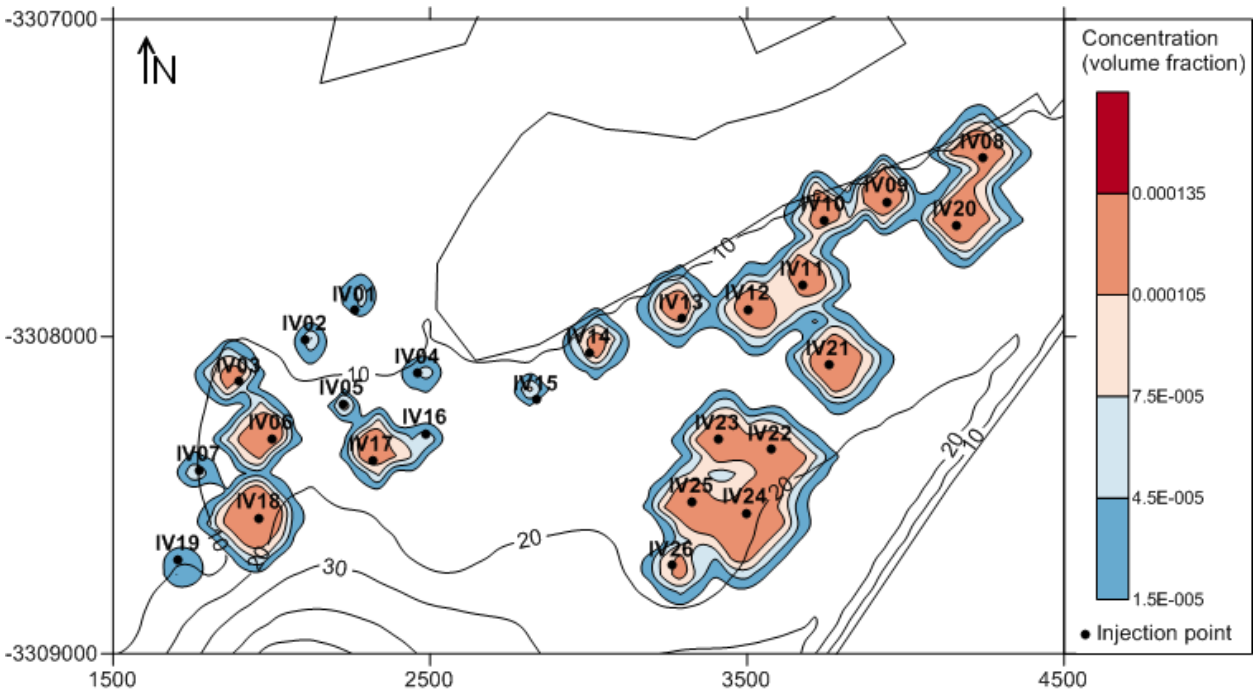

H15: Map illustrating the simulation results for the remediation of aqueous phase PCE with diluted polymer xanthan gum at a low infiltration rate in the top layer.

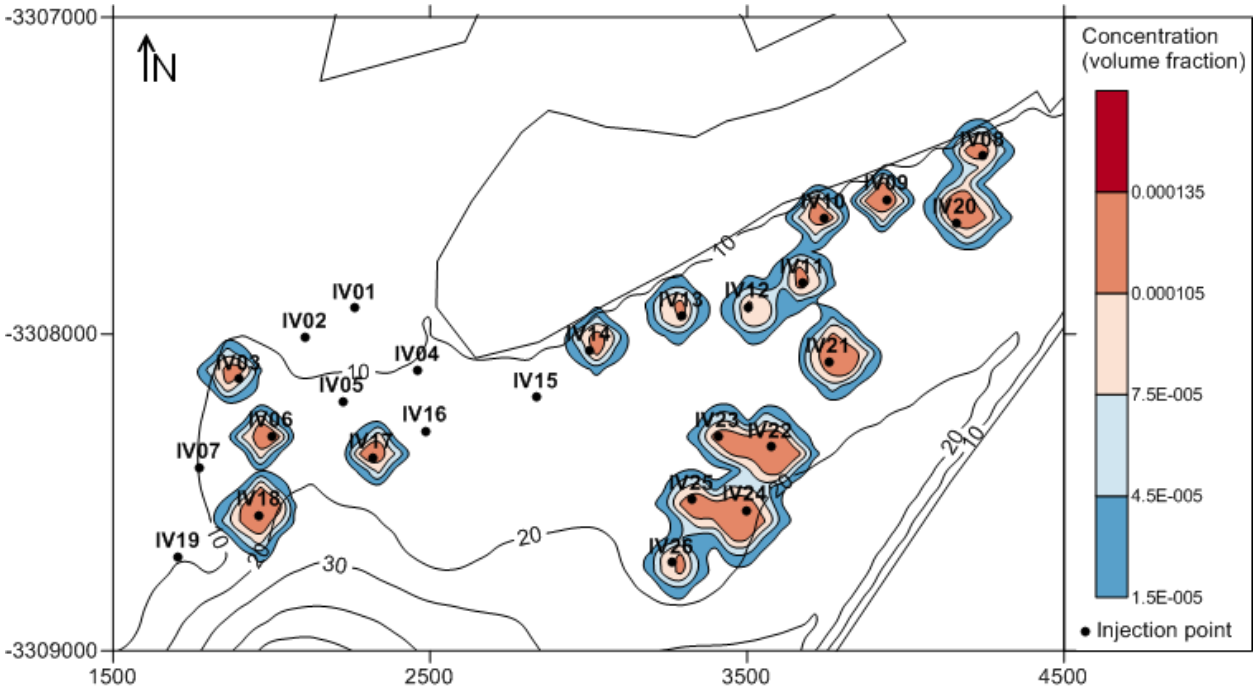

H16: Map illustrating the simulation results for the remediation of aqueous phase PCE with diluted polymer xanthan gum at a low infiltration rate in the bottom layer.

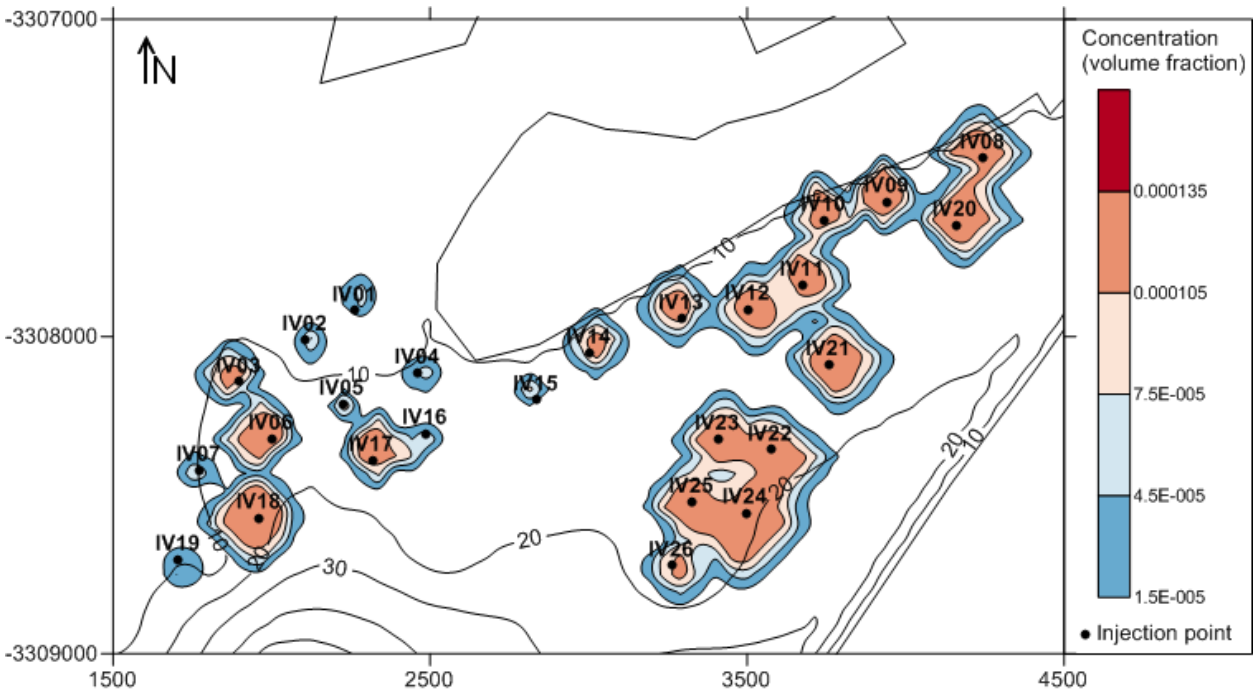

H17: Map illustrating the simulation results for the remediation of aqueous phase PCE with undiluted polymer xanthan gum at a low infiltration rate in the top layer.

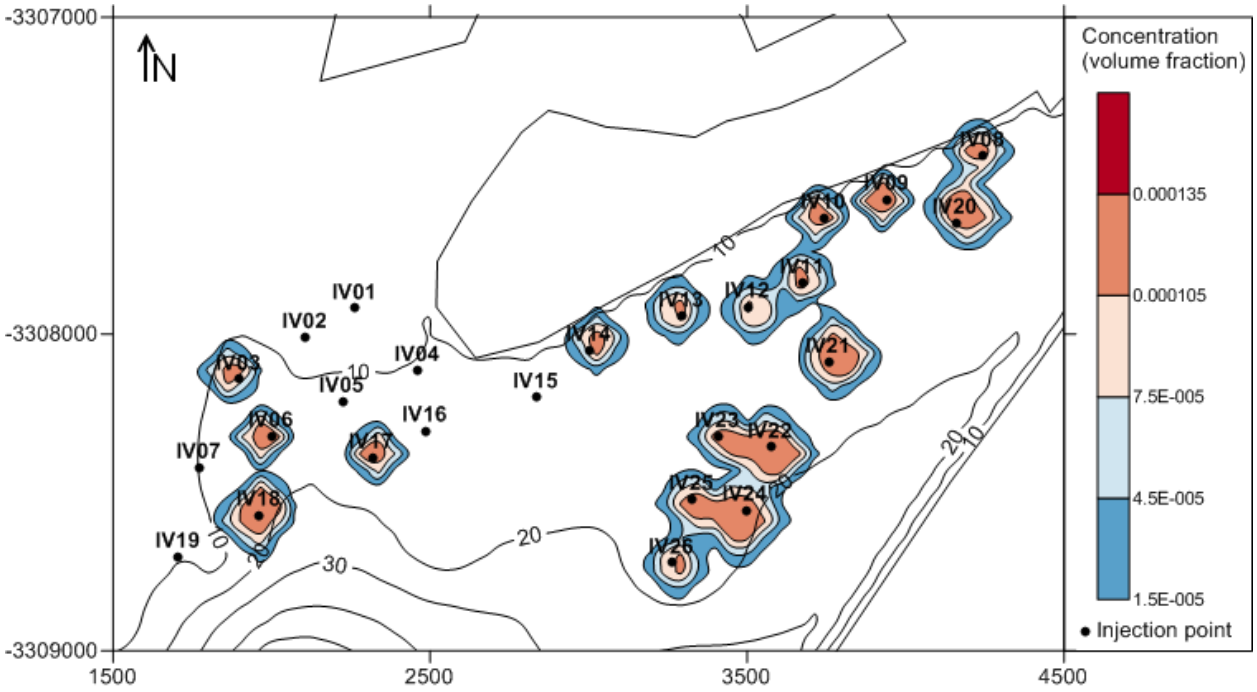

H18: Map illustrating the simulation results for the remediation of aqueous phase PCE with undiluted polymer xanthan gum at a low infiltration rate in the bottom layer.

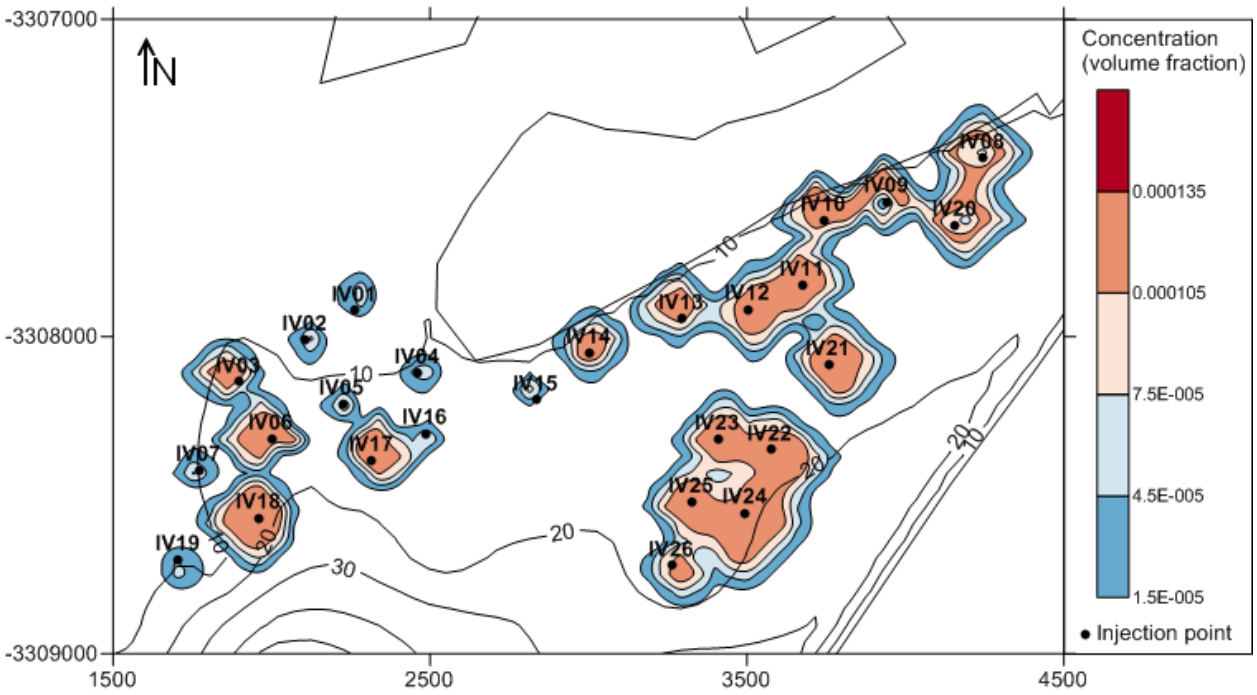

H19: Map illustrating the simulation results for the remediation of aqueous phase PCE with undiluted polymer xanthan gum at a high infiltration rate in the top layer.

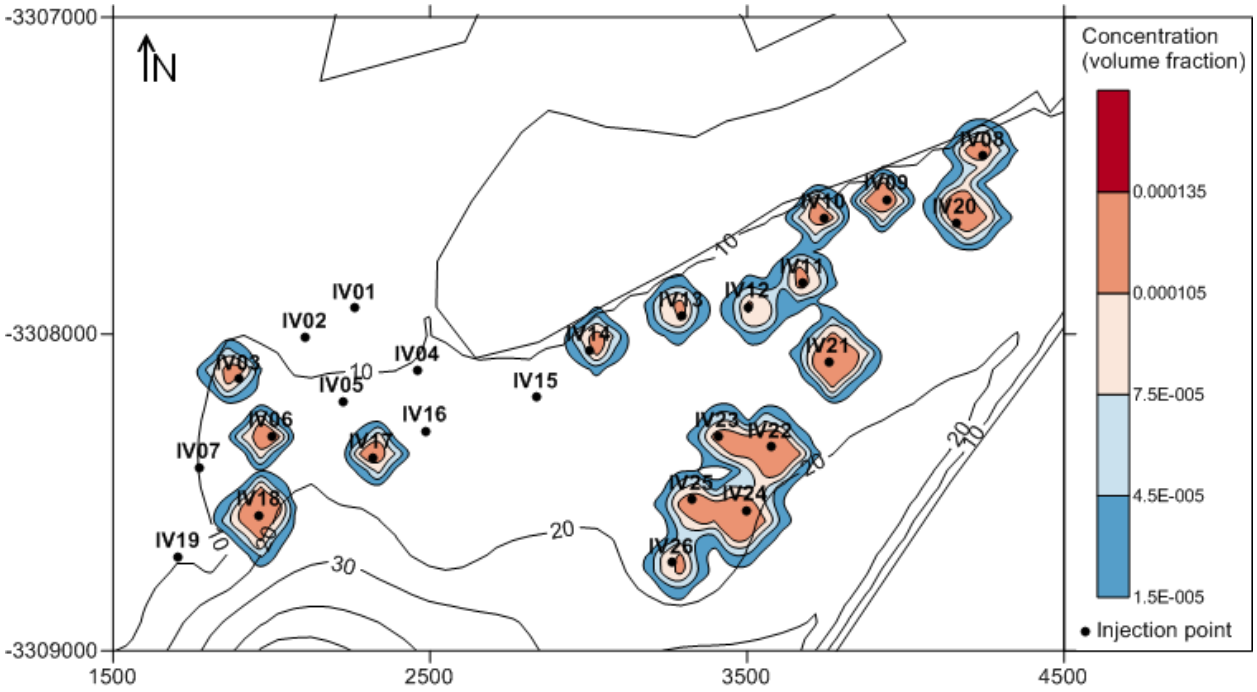

H20: Map illustrating the simulation results for the remediation of aqueous phase PCE with undiluted polymer xanthan gum at a high infiltration rate in the bottom layer.

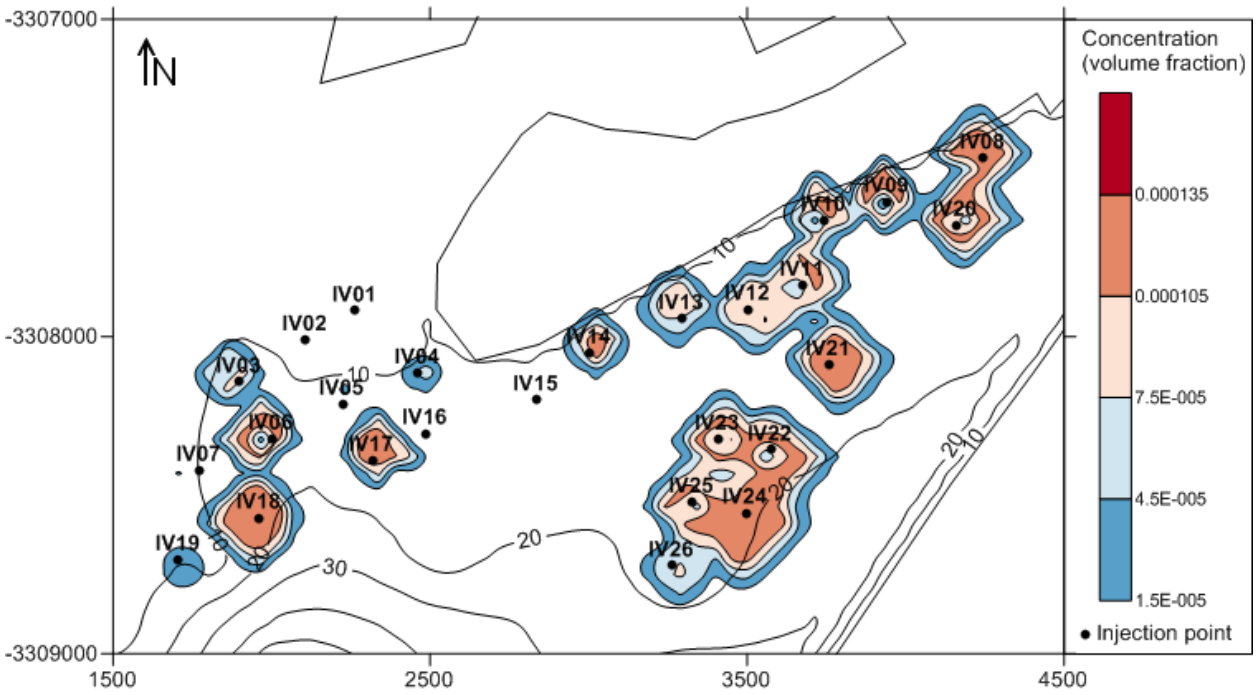

H21: Map illustrating the simulation results for the remediation of aqueous phase PCE with diluted surfactant SDS and ethanol at a low infiltration rate in the top layer.

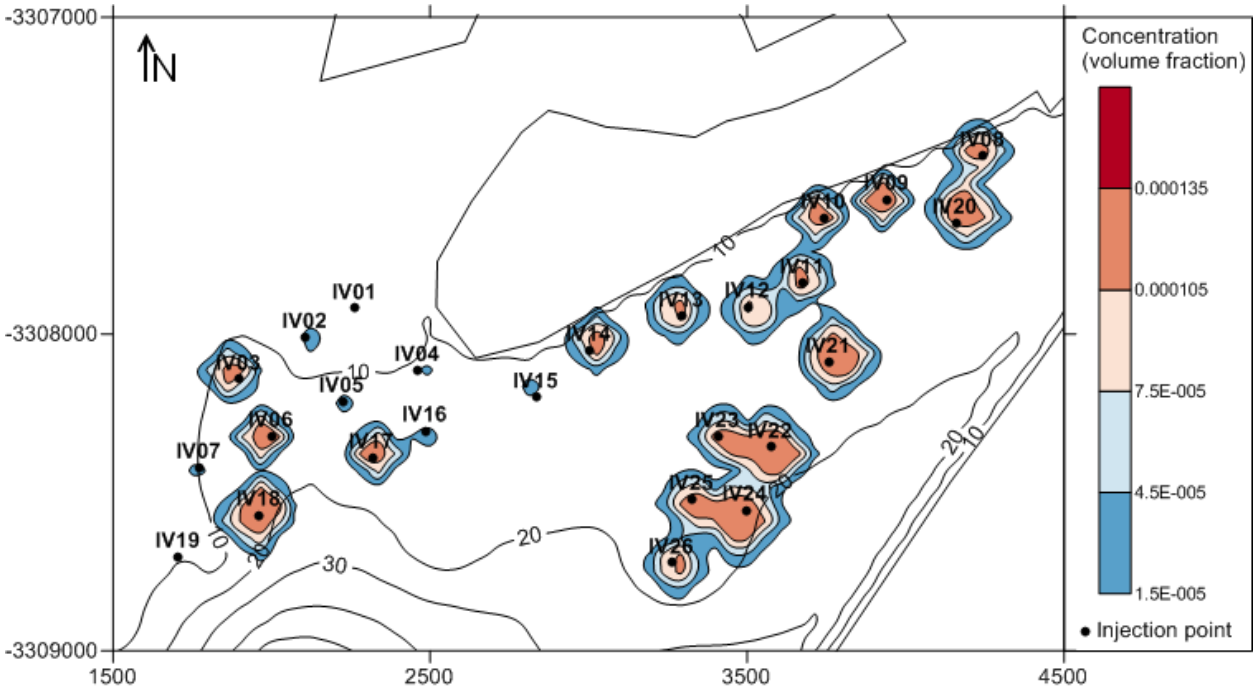

H22: Map illustrating the simulation results for the remediation of aqueous phase PCE with diluted surfactant SDS and ethanol at a low infiltration rate in the bottom layer.

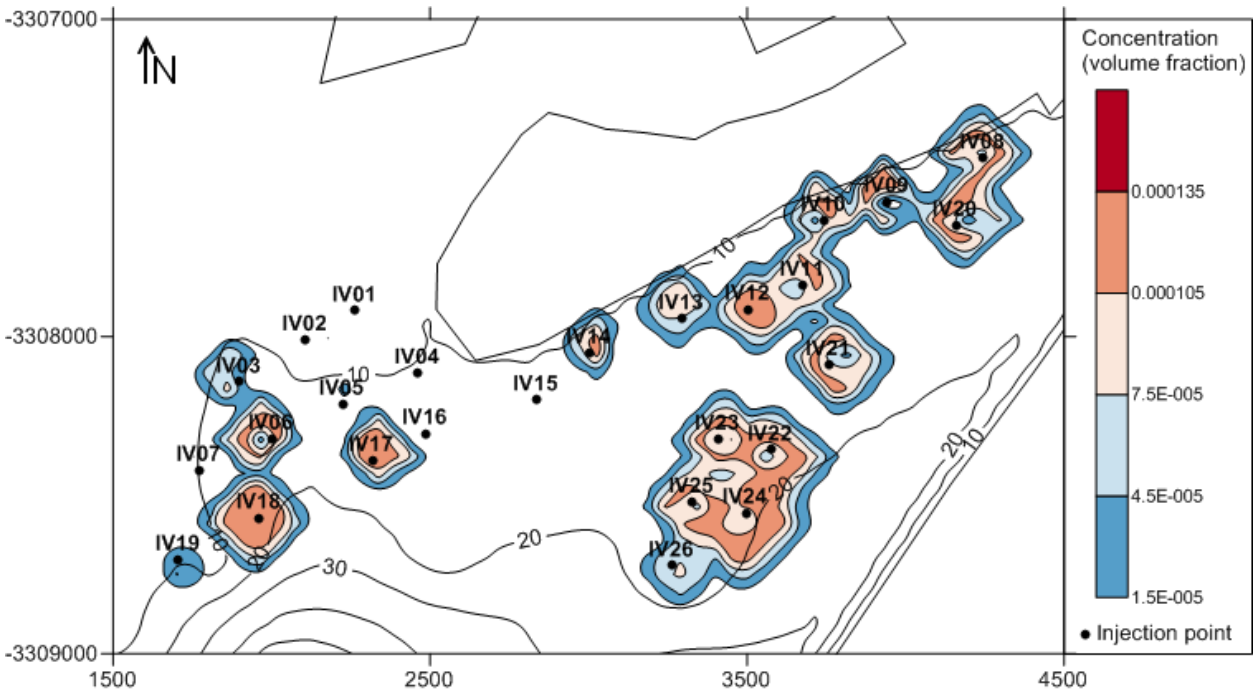

H23: Map illustrating the simulation results for the remediation of aqueous phase PCE with undiluted surfactant SDS and ethanol at a low infiltration rate in the top layer.

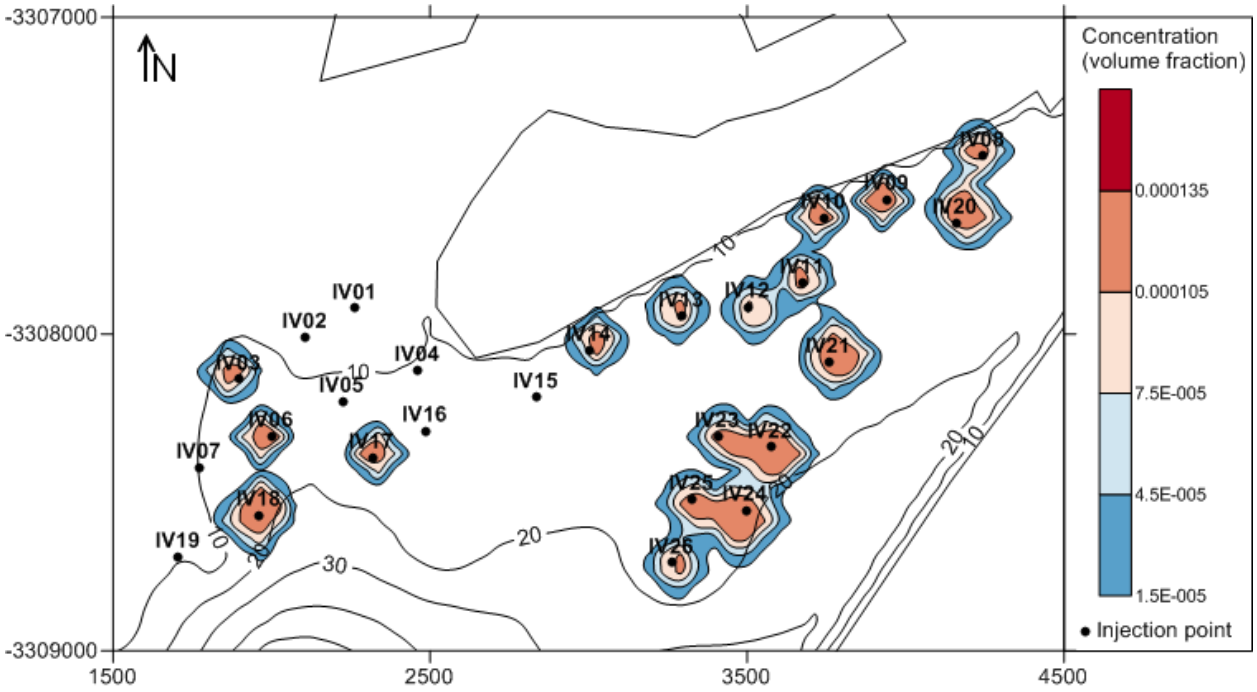

H24: Map illustrating the simulation results for the remediation of aqueous phase PCE with undiluted surfactant SDS and ethanol at a low infiltration rate in the bottom layer.

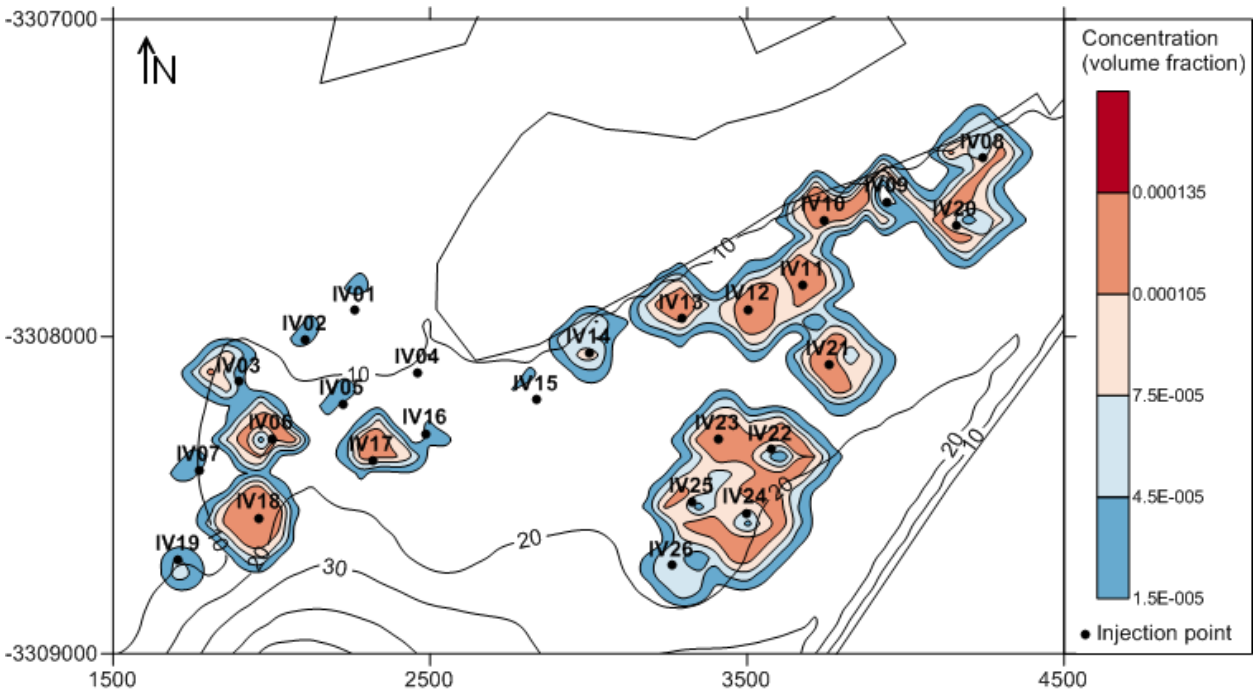

H25: Map illustrating the simulation results for the remediation of aqueous phase PCE with undiluted surfactant SDS and ethanol at a high infiltration rate in the top layer.

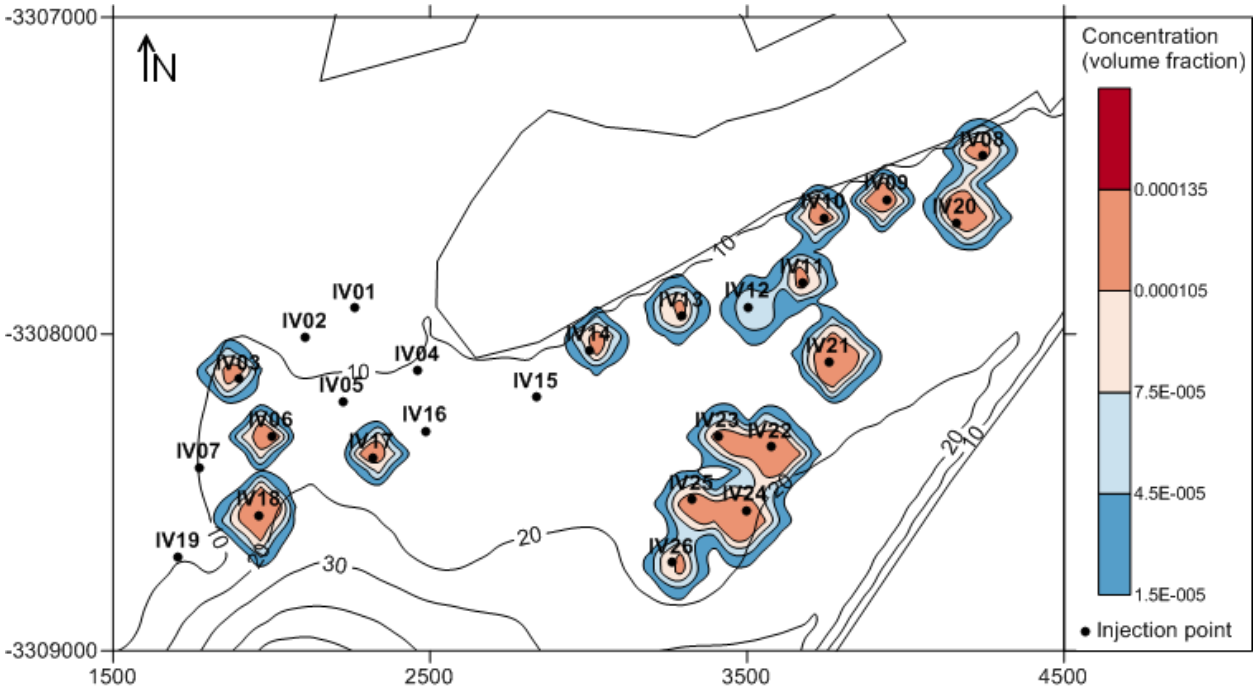

H26: Map illustrating the simulation results for the remediation of aqueous phase PCE with undiluted surfactant SDS and ethanol at a high infiltration rate in the bottom layer.

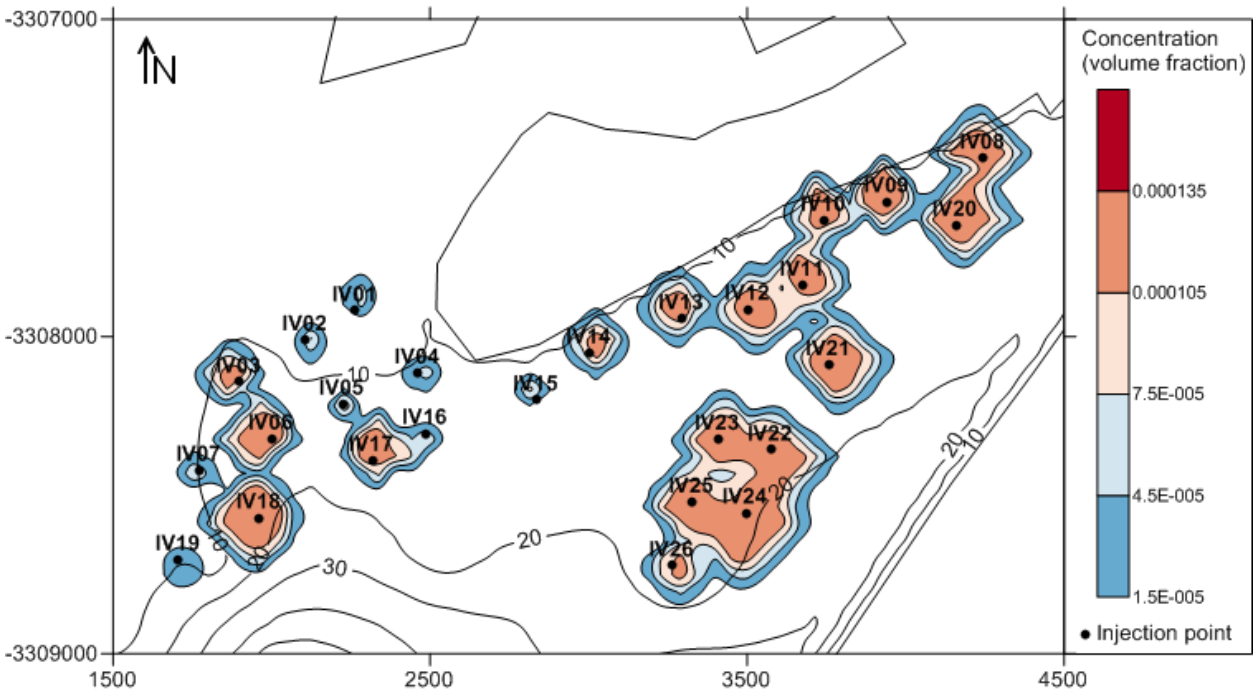

H27: Map illustrating the simulation results for the remediation of aqueous phase PCE with diluted ethanol at a low infiltration rate in the top layer.

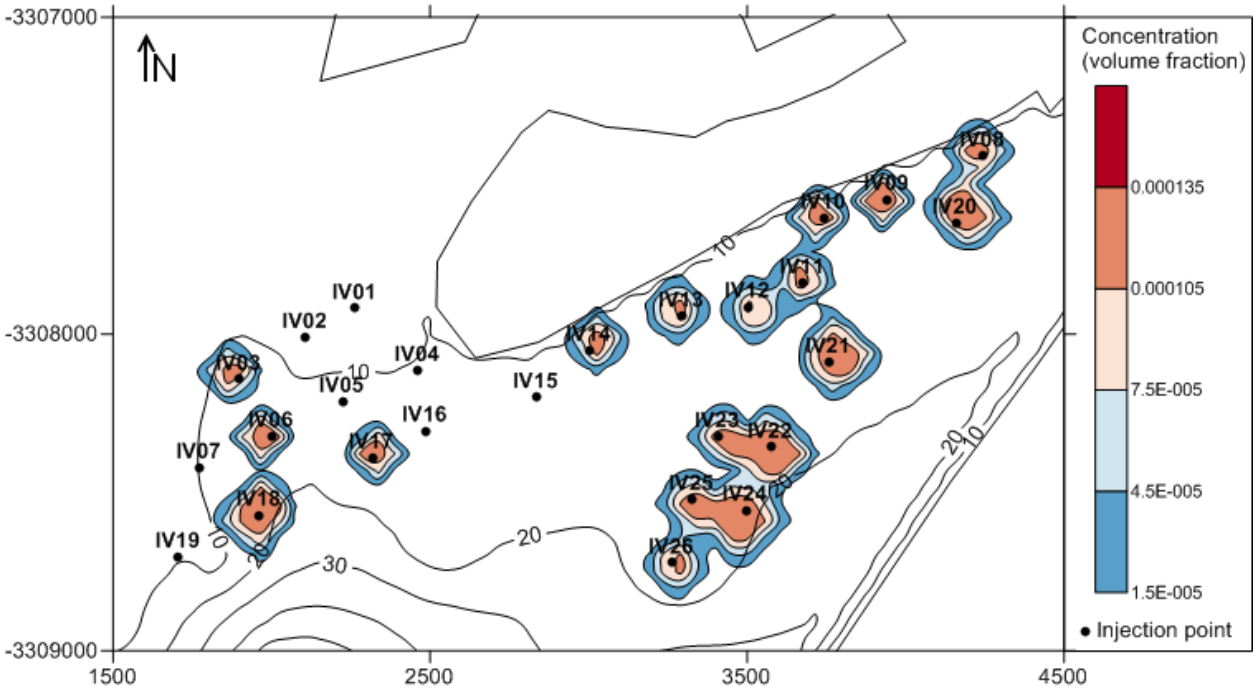

H28: Map illustrating the simulation results for the remediation of aqueous phase PCE with diluted ethanol at a low infiltration rate in the bottom layer.

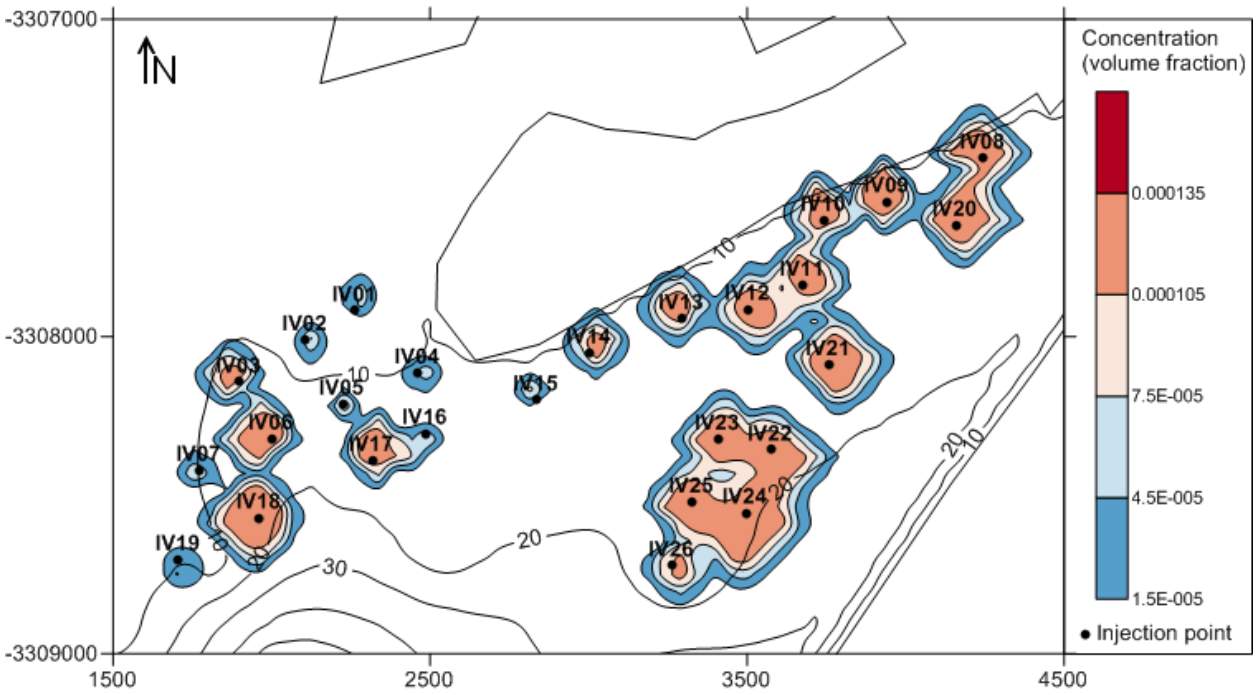

H29: Map illustrating the simulation results for the remediation of aqueous phase PCE with undiluted ethanol at a low infiltration rate in the top layer.

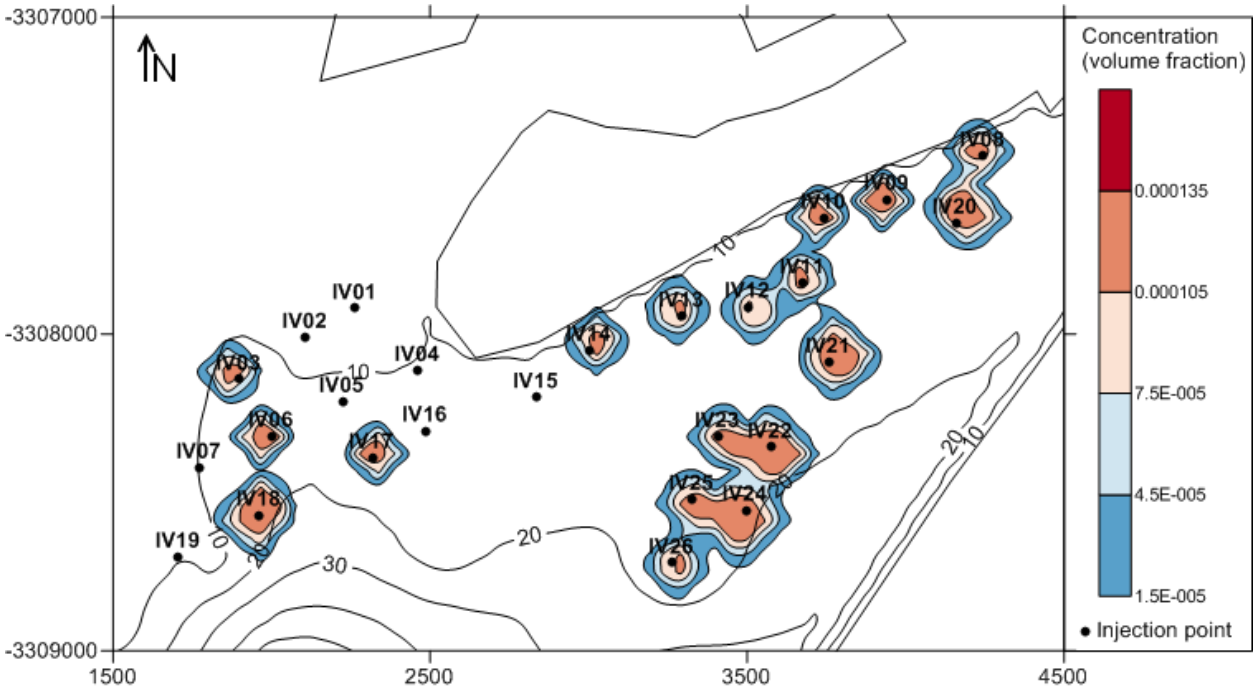

H30: Map illustrating the simulation results for the remediation of aqueous phase PCE with undiluted ethanol at a low infiltration rate in the bottom layer.

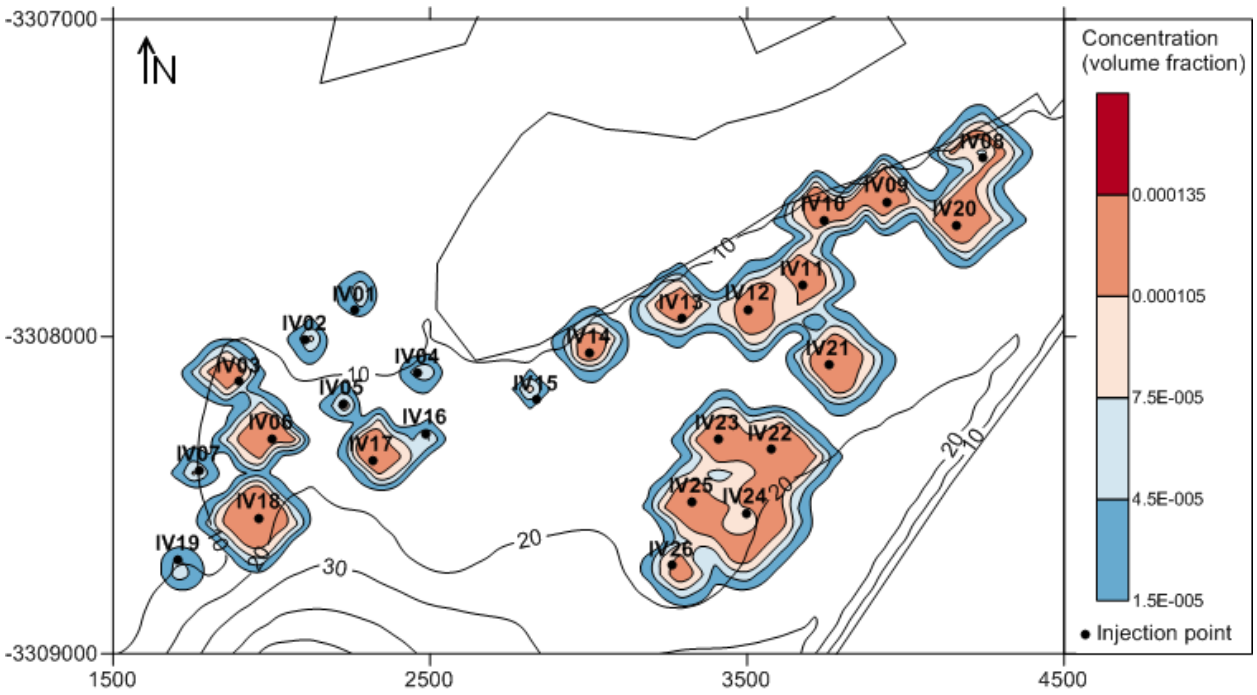

H31: Map illustrating the simulation results for the remediation of aqueous phase PCE with undiluted ethanol at a high infiltration rate in the top layer.

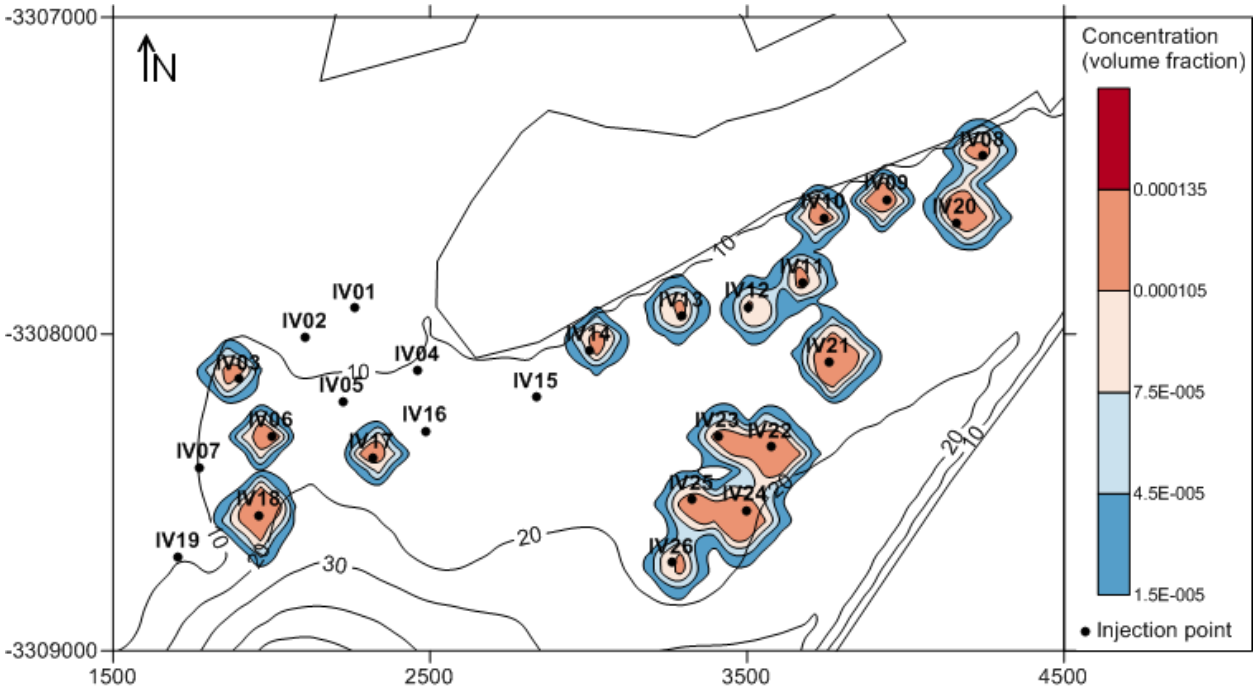

H32: Map illustrating the simulation results for the remediation of aqueous phase PCE with undiluted ethanol at a high infiltration rate in the bottom layer.

Appendix I: Risk Characteristics of the BTEX hydrocarbons

BTEX hydrocarbons	**Health effects in humans**	**Health effects in animal**	**RfD (Reference dose) (mg/kg/d)**	**CPF (cancer potency factor) (mg/kg/d)**
Benzene	-Carcinogenic causing leukaemia -Oxidises and accumulates in bone marrow. -Bone marrow depression causing a decrease of white and red blood cells. -Produce neurotoxic effects such as dizziness, headaches, tremors and loss of consciousness. -Destroys red blood cells and cell of the immune system.	-Toxic to genes and living cells. -Oxidises and accumulates in bone marrow. -Bone marrow depression causing a decrease of white and red blood cells. -Destroys progenitor cells needed to produce new blood cells and replace aging blood cells. -Produce neurotoxic effects such as dizziness, headaches, tremors and loss of consciousness. -Reduction in lymphocytes count	0.004	0.015-0.055

Appendix H (continues): Risk Characteristics of the BTEX hydrocarbons

Toluene	-Neurological effects with resect to inhalation.	-Decrease in size and damage of liver and kidneys (Nephrosis – loss of protein in the kidney). -Death -Immunosuppressive effects. Reduces antibody forming cells. -Neurobehavioral changes. -Mammary cancer and leukaemia.	0.08	inadequate evidence of carcinogenic effects
Ethylbenzene	-Kills cells in tissue and organs. -Toxic to respiratory system. -Carcinogenic	-Reduce the number of live births. -Increase in weight of kidneys, liver and spleen. -Skeletal retardation.	0.1	No carcinogen data
Xylenes	-Temporary neurological impairment. -Irritation of eyes and throat.	-Decrease in body weight -Death	0.2	Inadequate evidence of carcinogenic effects